UNIVERSITÀ DI PARMA

UNIVERSITA' DEGLI STUDI DI PARMA

DOTTORATO DI RICERCA IN

"SCIENZE DEGLI ALIMENTI"

CICLO XXXV

Strategies for extraction, characterization and enzymatic modification of dietary fibre

Coordinatore:

Chiar.ma Prof.ssa Chiara Dall'Asta

Tutore:

Chiar.ma Prof.ssa Augusta Caligiani

Co-tutori:

Dr. Franco Rosso, Dr.ssa Ginevra Rosso

Dottorando:

Andrea Fuso

Anni Accademici 2019/2020 – 2021/2022

Table of content

Abstract and outline..... 6

CHAPTER 1

General introduction..... 10

CHAPTER 2

An enzymatic approach for isolation and quantification of soluble polysaccharides from complex matrices: extraction and characterization of exopolysaccharides from LAB fed with different sugars..... 29

CHAPTER 3

Protease-assisted mild extraction of soluble fibre and protein from fruit by-products: a biorefinery perspective..... 48

CHAPTER 4

A multiplatform "reactomics" approach as a powerful strategy to identify reaction compounds generated during hemicellulose hydrothermal extraction from agro-food biomasses..... 65

CHAPTER 5

Hydrothermal treatment of hazelnut shells: impact of temperature on degradation compounds and fibre's structure 93

CHAPTER 6

Production of xylo-oligosaccharides (XOS) of tailored degree of polymerization from acetylated xylans through modelling of enzymatic hydrolysis 117

CHAPTER 7

Antioxidant and prebiotic activities of xylo-oligosaccharides mixtures of controlled composition: a step forward in understanding structure-activity relationship 144

CHAPTER 8

Conclusions and future perspectives..... 172

Supplementary material..... 177

Acknowledgements..... 191

About the author..... 193

I the undersigned Andrea Fuso, author of this Ph.D. dissertation, declare that I prepared the drafting of this thesis giving the following contribution, according to Elsevier's CRediT (Contributor Roles Taxonomy):

- Formal analysis
- Investigation
- Writing – Original Draft
- Software
- Conceptualization
- Methodology
- Visualization

Abstract and outline

In recent times, a twofold trend is taking hold: on the one hand, the ethical, environmental and economic need to manage wastes and by-products originating from the food supply chain differently and better, and on the other hand the will of consumers to direct their choices toward healthier foods. An intelligent and logical consequence for meeting both needs is the reuse of dietary fibre from unexplored and undervalued biomasses. When it comes to isolating dietary fibre, there are several extraction methods that may be more or less suitable depending on the matrix considered, and that may have as a consequence an impact on dietary fibre's chemical structure, with the latter which in turn is closely related to the techno/bio-functional properties. This Ph.D. thesis explores the feasibility of reusing dietary fibre from various matrices by employing different approaches, in terms of extraction, characterization, enzymatic modification, evaluation of functional properties, and investigation of the chemical compounds inevitably produced during certain extraction methods.

Chapter 1 gives a general overview of dietary fibre, briefly describing some of the most common types and their chemical structures, covering the main extraction methods, the use of enzymes to modify their structure, and the most popular analytical techniques for determining structural information on extracts and hydrolysates. The limitations that all these processes still have are here critically discussed, analysing what will be necessary to be done in the future steps. In particular, a special focus is made on lignocellulosic materials and xylo-oligosaccharides (XOS), which are topics particularly central to this thesis.

Chapters 2 and 3 deal with the mild enzymatic assisted extraction and characterization of two types of dietary fibre from very different sources, namely bacterial culture broths and fruit wastes, respectively. **Chapter 2**, in particular, concerns the use of an official method for dietary fibre quantification (AOAC 991.43) that has been here adapted for the extraction of bacterial exopolysaccharides (EPS), namely from *Lactobacillus* strains previously isolated from food products. The method is proposed as a universal methodology for the isolation and purification of EPS from complex matrices, allowing the detailed characterization of their molecular structure, extremely variable depending on both the strain and the substrate. **Chapter 3** used a similar approach, namely, isolating dietary fibre through a protease-based enzymatic assisted extraction on kernels, seeds, and peels derived from fruits. The purpose was to evaluate whether it was possible, under mild conditions in terms of temperature and pH, to extract at the same time not only a mixture of proteins and peptides, but also a fraction of soluble fibre. The results showed, for some by-products, high extraction yields for both protein and soluble fibres, suggesting the possibility to integrate the recovery of these important plant components. Molecular characterization of isolated fibre showed in most cases the presence of arabinogalactans, with potential technological applications.

Chapters 4 and 5 focused on hydrothermal treatment, a harsh extraction method needed to extract hemicellulose from lignocellulosic biomasses, studying in detail its effects on hazelnut shells' fibre composition. **Chapter 4** deals with the evaluation of three analytical techniques, namely ^{1}H NMR, GC-MS, and UHPLC-IM-Q-TOF-MS, to investigate the wide range of degradation compounds, mostly still unknown, that originate following such thermal treatment. NMR analysis identified the main chemical classes present, allowing their quantification. GC-MS detected in more detail the presence of small molecules, while the LC method coupled with ion mobility separation allowed to identify more than 200 compounds belonging to numerous different chemical classes, becoming a candidate as one of the most dominant techniques in the near future for a comprehensive characterization of these extracts. In **Chapter 5**, the impact of temperature in hydrothermal treatments was evaluated both on the fibre extracted from hazelnut shells and on the pattern of degradation compounds. It was found that lower temperatures yield high molecular weight pectin, while when they get higher xylans and xylo-oligosaccharides gradually become predominant, suggesting the potential for a fractionation approach by means of consecutive treatments. In addition, the formation of degradation compounds was investigated, showing how the total number of molecules is generally positively correlated with temperature, but also how a strong variability occurs at different temperatures in terms of type of compounds belonging to different chemical classes.

Chapters 6 and 7 have in common the focus on the enzymatic hydrolysis of xylans, one of the main types of hemicellulose, for the production of XOS. In **Chapter 6**, in particular, the modelling of this enzymatic hydrolysis was studied by using commercial acetylated xylan as substrates and different enzymes, namely, endo-xylanase and acetylxylan esterase, and evaluating through the application of a Design of Experiments how hydrolysis parameters could influence the product outcome in terms of the degree of polymerization (DP). XOS with DP 2-6 were always present, but some experiments led to mixtures with higher DP, up to 10, expanding the possibility to test specific bioactivities related to the degree of polymerization. The method was also tested on acetylated xylan previously extracted from grape stalks, suggesting the feasibility of the approach even on non-pure agro-industrial samples. **Chapter 7** exploited the results of the previous one for the production of XOS mixtures having variegate structures, in terms of DP and degree of acetylation. Tangential ultrafiltration was here performed together with the xylanolytic hydrolysis, enhancing the conversion yield of xylan into XOS, while a purification by preparative gel permeation chromatography allowed to obtain for the first time a highly pure mixture of XOS having DP 6-9. The various XOS mixtures were subsequently tested in terms of *in-vitro* antioxidant activity and prebiotic properties by testing *Lactobacillus brevis* and *Escherichia coli* strains. The results showed a clear influence of XOS' chemical structure in both tests, suggesting that a higher DP and low substitution degree could have improved functionalities in many cases.

Finally, the relevance of this research and its implication for future applications is discussed in **Chapter 8.**

CHAPTER 1

General introduction

Part of this chapter has also been published as:

Andrea Fuso, Davide Risso, Ginevra Rosso, Franco Rosso, Federica Manini, Ileana Manera, Augusta Caligiani (**2021**). Potential valorization of hazelnut shells through extraction, purification and structural characterization of prebiotic compounds: A critical review. *Foods*, 10(6), 1197.

1.1. Dietary fibre: definition and classification

Dietary fibre has been defined in many different ways throughout history. Botanists, chemists or consumers can intend dietary fibre differently, but nowadays the most commonly used definition is from Trowell, who defined it as “the skeletal of plant cells which resists to hydrolysis (digestion) by enzymes of men” [1]. From a chemical point of view, the term “dietary fibre” includes in its definition a mixture of complex molecules, mainly polysaccharides such as cellulose, hemicellulose, oligosaccharides, inulin, pectin, gums and mucilages, but also the non-carbohydrate lignin [2]. Many classifications of dietary fibres have been proposed over the years, for instance according to their sources, composition, fermentability or physiological effects. The most common one concerns their distinction in soluble and insoluble fibres, based on their capacity to form or not a dispersion when added to water [3]. Among soluble fibres one can commonly find pectin, inulin, gums and mucilages, while cellulose, hemicellulose and lignin are generally classified as insoluble [4,5]. Actually, it is important to specify that the solubility of a certain type of fibre may be quite variable [6]: indeed, each of these molecules includes in its definition a wide range of chemical structures, for instance in terms of monosaccharide composition, configuration of glycosidic bonds, molecular weight and side chains. Regarding the matter of solubility, for example, on the one hand there are some clear examples of soluble and insoluble fibres, such as low molecular weight oligosaccharides and lignocellulose, respectively, but on the other hand some fibres can exhibit variability in this feature. Hemicellulose, for example, is a category including different types of polysaccharides, namely xylans, xyloglucans, mannans, glucomannans, β-glucans and others [7,8], and they can be either soluble or insoluble depending on various features (eg, substituents along the main chain, intermolecular cross-links) [9]. Despite this variability in the structures, some of the main features of the most common dietary fibres are briefly summarized and listed in Table 1.1.

Table 1.1: *Main chemical structure features of some of the principal dietary fibres. "glu" = glucose; "xyl"= xylose; "man" = mannose; "gal" = galactose; "fru" = fructose; "fuc" = fucose; "ara" = arabinose; "rha" = rhamnose; "rib" = ribose; "gluAc" = glucuronic acid; "galAc" = galacturonic acid; "ag" = acetyl group; "cou" = p-coumaryl alcohol; "con" = coniferyl alcohol; "syn" = sinapyl alcohol.*

	Main monomers	Main chain's glycosidic bond	Side chain	Degree of polymerization (DP)	Reference
Pectin	galAc	α-1,4	ara, glu, rha, gal, man, xyl, rib, fuc, ag	150 – 500	[10,11]
Inulin	fru (+ terminal glu)	β-2,1	-	11 – 60	[12]
Arabinogalactan	gal	β-1,4 / β-1,3 / β-1,6	ara	40 - 600	[13]
Lignin	cou, con, syn	-	-	Mw 1440-78400 Da	[14]
Cellulose	glu	β-1,4	-	10000 - 15000	[15,16]
Hemicelluloses					
Xyloglucan	glu	β-1,4	xyl, gal, fuc, ag	300 – 3000	[8,17]
β-glucan	glu	β-1,4 ; β-1,3	-	360 – 16000	[8,18]
Xylan	xyl	β-1,4	gluAc, ag	70 – 200	[8,19]
Arabinoxylan	xyl	β-1,4	ara	30 - 280	[20]
Mannan	man	β-1,4	-	20 - 10000	[21]
Galactomannan	man	β-1,4	gal, ag	average 1700	[8,22]
Glucomannan	man, glu	β-1,4	-	1000 – 10000	[8,23]
Galactoglucomannan	man, glu	β-1,4	gal	40 - 100	[8,24]
Oligosaccharides					
FOS	fru	β-2,1	-	3 - 10	[25,26]
GOS	gal (+ terminal glu)	β-1,4 / β-1,3 / β-1,6	-	2 - 10	
XOS	xyl	β-1,4	gluAc, ag	3 - 20	
AXOS	xyl	β-1,4	ara, gluAc, ag	2 - 40	
IMOS	glu	α-1,6	-	10 - 60	
MOS	man	β-1,4	-	2 - 4	

As can be seen from the table, most of the indigestible polysaccharides commonly found in nature present a main backbone containing various monomers linked to each other through β-1,4 glycosidic bonds. These backbones often show side chains which are bound to the main chain through different glycosidic linkages and make the polysaccharide to result in more or less extended branched structures. Neutral monosaccharides are most commonly found within the side chains, but other substituents such as uronic sugars, acetyl groups and even phenylpropenoic acids may also be present [26]. The degree of polymerization of dietary fibres can be enormously variable, depending on the type of fibre, the source it is obtained from, and the extraction method.

Apart from the fibres listed in Table 1.1, others from non-vegetable origin are also catching attention, such as chitin, chitosan and microbial polysaccharides. The former two are mainly present in crustaceans but even in insects [27] and are composed of glucosamine and N-acetyl glucosamine monomers, bound together with β-1-4-glycosidic bonds [28], while the last can be produced by many different bacterial strains, and especially those produced by lactic acid bacteria have the potential to be used in the food supply chain. They are called exopolysaccharides or extracellular polymeric substances (EPS) and their chemical structure can be diversified depending on the strains and the environment the latter grow in [29].

In general, it is important to underline how this information about dietary fibre's structures has just to be considered as a general guidance, and that every type of fibre can be obtained from different sources with different methods, leading to even more variable chemical structures.

1.2. Extraction of dietary fibre

The first step for the obtainment of dietary fibres is obviously their extraction. Recently, several studies have focused their work on the development of a method to optimize the extraction yield starting from different matrices. Different chemical structures of raw materials and different process conditions may however affect the composition, the structure and therefore the functional properties of the poly- or oligosaccharides obtained [30], thus it is essential to evaluate case-by-case the best process conditions possible. Depending on the type of fibre and on the starting material it is considered, many extraction methods have been proposed over the years.

As discussed in Paragraph 1.1, the distinction of dietary fibres in soluble and insoluble is commonly taken into account, but within the same classification fibres can differ greatly from one another, and thus no common extraction method exists. For example, pectin is among the most interesting soluble polysaccharides, and its valorization and reutilization has been studied for a long time. Pectin conventional extraction methods generally include the use of mineral or organic acids, such as citric, sulphuric or acetic acid, but even hydrochloric or nitric acid. Acid concentration is commonly around 0.5-2 M, temperatures range between 80 and 100 °C and extraction times are around 60 minutes [31]. However, "hard" extractions methods involving the use of acids, bases and high temperatures often lead to changes in the chemical structure of fibres, thus impacting on their functional properties. If on the one hand these hard extractions are necessary in order to get some fibres solubilised, as in the case of hemicelluloses from lignocellulosic complexes, on the other hand other possibilities exist for more soluble polysaccharides, such as pectin or other types of soluble fibres, in order to extract them as intact as possible. Among them, enzyme-assisted extraction (EAE) is taking hold as one of the most employed techniques. It consists in using enzymes with

various activities, either added alone or in mixtures, aiming to hydrolyse the matrix of the plant cell wall releasing the compounds of interest into the external environment [32]. Generally, the plant cell wall is made of cellulose, hemicellulose, lignin, pectin and starch [32], but their intermolecular interactions can be different, making the whole structure more or less complex. For example, some polysaccharides similar to hemicelluloses (i.e., some xylogulcans) can be solubilised with hot neutral water when they are not hydrogen-bonded to cellulose, whereas others can be covalently bound to pectins, originating hybrid polysaccharides [33]. For this reason, EAE exploits the action of different enzymes that are able to hydrolyse different cell wall components: this method is efficient and sustanaible, but the extraction yields totally depend on which enzymes one chooses to use. In this sense, cellulase is one of the most employed enzymes, since cellulose is major portion of plant cell walls, but it is often accompanied by xylanase, ligninase, pectinase and amylase, aiming to disrupt hemicellulose, lignin, pectin and starch, respectively [32]. EAE often showed an increase in extraction yields compared to conventional processes and has the advantage that is used under low temperatures, allowing a reduction of energy consumption. This technique has been used with good results for extraction of many bioactive compounds in general, such as carotenoids [34], oils [35], and phenolics [36], but also for polysaccharides, like starch [37], pectin [38,39] and other soluble fibres [40,41] from different by-products. Despite this, this technique is still too much unexplored and needs further studies. Its drawbacks are mainly related to the high costs of enzymes, even if some techniques, like the immobilization of enzymes and their *in-situ* production by fermentation, are emerging tools to stem this problem.

Among the most difficult fibres to be extracted with good yields through the application of mild methods one can surely found hemicellulose. The latter is recently gaining a lot of interest because of the high amounts of available lignocellulosic by-products. Also in this case, there are different extraction methods which exploit the use of chemicals: they involve acids, bases, ionic liquids, or organic solvents [42]. Despite this, the most used methods on an industrial scale are the physico-chemical ones, mainly steam explosion and hydrothermal treatment. The first consists in subjecting the matrix to heating by using pressurized steam (150–300 °C, 1–5 MPa) for a few seconds or minutes; then, the reaction is stopped and there is an immediate return to atmospheric pressure [42,43]. This method causes structural degradation of lignin, making hemicellulose available for extraction. In particular, xylans (the most abundant hemicellulose polysaccharides) are in part hydrolysed in xylo-oligosaccharides (XOS) and xylose by organic acids, such as acetic acid, which in turn are formed due to the hydrolysis of functional groups (such as acetyl groups) linked to xylans [44]; for this reason, this technique is also called “autohydrolysis”. Time of pre-treatment, temperature, pH and moisture content are the parameters that most affect the efficiency of steam explosion treatments [45,46]. This is an advantageous technique thanks to the non-use of chemicals with high environmental impact and to the low energy costs [43]. An even more commonly used technique is hydrothermal treatment. This is an operation in which the biomass is simply treated with water at high temperature. Generally, temperatures varying between 160 and 220 °C are used, in combination with high

pressures for maintaining water at liquid state, for a period of 5-60 minutes [47]. This technique leads to the hydrolysis of the hemicellulosic backbone, to its consequent depolymerization and therefore solubilization in the form of smaller fragments. Here too, one can speak of autohydrolysis, because the hydrolysis of acetyl groups along the backbone (with consequent acetic acid formation) is responsible for subsequent hydrolysis of glycosidic bonds. At the end of the treatment, cellulose and lignin will instead be found in the solid phase with few chemical modifications [30,48] and can be separated and reused for other applications in a perspective of biorefinery [49]. When xylan-rich lignocellulosic biomasses are used, autohydrolysis conditions (time and temperature) have a great influence on xylan depolymerization, therefore on the solubilization and on the extraction yield. By increasing treatment severity, in fact, it is possible to obtain such a strong hydrolysis that it can lead to xylan decomposition in xylose and its dehydration products [48]. Vice versa, when lignocellulosic biomass is subjected to hydrothermal treatment in milder conditions, bigger fragments are found in liquid phase [49]. To report an example, in the study conducted by Surek and Buyukkileci the greater extraction yield from hazelnut shells was obtained through a hydrothermal treatment at 190 °C for 5 min. With these conditions, less than half of extracted XOS had a low degree of polymerization (DP 2–6), that was desired; though, by increasing the temperature, a great extraction yield was obtained, but xylans were mainly degraded to xylose, furfural, and acetic acid. Authors in this study have stressed that the time-temperature combination is fundamental and should be studied on a case-by-case basis, also because holding time does not have the same effect on the extraction yield at all temperatures. Hence, it is necessary to also regulate autohydrolysis conditions in relation to desired DP [30]. In choosing the conditions of the process to be applied, the substituents on the xylan backbone, like acetyl and uronic groups, must also be considered. In fact, they have an influence on the solubility of XOS and their prebiotic effect [50] and therefore the sensibility of different functional groups to autohydrolysis must also be assessed. Arabinose, an essential constituent of arabino-xylooligosaccharides (AXOS), seems to degrade earlier than xylose [30], and acetyl groups, if hydrolysed, can lead to the formation of acetic acid in solution with consequent lowering pH, promoting further hydrolysis of xylan backbone [51]. Ultimately, there are many factors that may influence the chemical composition of the raw material, such as genetics, growth area, or storage conditions [52], and consequently also the autohydrolysis conditions must be regulated time after time. However, there is no doubt that hydrothermal treatment is a very valuable method for the extraction of hemicellulose. Indeed, this is a green technique, with relatively low costs and, unlike acid or alkaline based methods, it does not require specific corrosion-resistant materials [42,43]. However, autohydrolysis treatments have a limit. Indeed, when hemicellulose is extracted through hot liquid water or steam explosion, beside oligosaccharides, there is the appearance of numerous other compounds in the reaction media, in more or less large quantities: monosaccharides, furfural or hydroxymethylfurfural, acetic acid, protein-derived products, inorganic compounds, or other products derived from the extractive and acid-soluble lignin fractions of the feedstock [48]. The mechanism of formation of these compounds is very complicated, being

related to the time/temperature conditions, to the pH and to the matrix. For instance, cellulose-deriving glucose can be converted into 5-(hydroxymethyl)-2-furaldehyde (HMF) and/or levulinic acid, formic acid and various phenolics at high temperatures, depending on the reaction conditions, while xylose can follow different reaction mechanisms originating furan-2-carbaldehyde (furfural) and/or various C-1 and C-4 compounds. Then, monosaccharides can further react to form pseudo-lignin, humine, aldehydes, ketones, organic acids or aromatic compounds [53]. It is important to highlight that although some of these mechanisms are to date well understood, many other reaction pathways still remain unknown [54]. Therefore, since one of the main aims of reusing hemicellulose from lignocellulosic biomasses is its transformation into healthy ingredients for the food supply chain, it is of enormous importance to further study the presence of all these compounds that originate following autohydrolysis treatments, to understand their formation and especially to evaluate them in terms of potential toxicity. This investigation should be done both through the study and understanding of the reaction mechanisms, but also through the improvement of analytical techniques able to allow their identification and quantification.

1.3. Enzymatic modification of fibre extracts to obtain bioactive oligosaccharides

Consumers are increasingly aware of the relationship between diet and health [55]. With onsets of chronic obesity, gastrointestinal diseases, diabetes, coronary diseases, cancers, and degenerative diseases on the rise, the trend in consumer choices is increasingly moving towards prebiotics, probiotics, and functional foods more in general, with the market for these products constantly expanding [56]. Among all the functional foods and supplements, a lot of attention has been paid over the time to various types of oligosaccharides, which can be obtained from polysaccharides through hydrolysis and which have been reported to have applications in food, feed and pharmaceuticals, claiming innumerable biological and functional properties [57]. Among the oligosaccharides that are more commonly obtained, studied and in some cases even commercialized there are fructo-oligosaccharides (FOS), galacto-oligosaccharides (GOS), manno-oligosaccharides (MOS), isomalto-oligosaccharides (IMOS), xylo-oligosaccharides (XOS), arabino-xylooligosaccharides (AXOS), human milk oligosaccharides (HMOS), chito-oligosaccharides (COS) but also many others. Different oligosaccharides have shown over the years to have many diverse functional benefits, depending on their physico-chemical features, such as solubility, monosaccharide composition, degree of polymerization, reducing sugar content, amount and type of sobstituents in the side chains, etc. [58]. In general, however, the use of functional oligosaccharides improves the balance of the intestinal microflora preventing intestinal diseases, helps in the regulation of sugar and lipid content in blood, prevents obesity and has been reported to play a role in another huge quantity of biological processes, accurately reviewed in literature over the time [59,60]. If on the one hand especially FOS and GOS have been dominating the market in the last years, nowadays XOS are catching the attention, mainly due to their apparent better resistance to

gastric acidity and thanks to the abundant presence of xylan (i.e., the polysaccharide they could potentially be originated from) in agro-industrial leftovers. For this reason, this dissertation especially focus on XOS. They are oligosaccharides constituted by a linear β-(1→4)-D-xylopyranan backbone. In general, the oligomers that contain from 2 to 10 molecules of xylose are considered XOS, even if some authors include in this category also molecules with DP ≤ 20 [61]. In spite of XOS can be easily obtained from main-chain-xylan compounds, their precise chemical structure (and therefore their biological functions) varies once again according to the extraction process and to the source they are obtained from. XOS may contain different substituents bonded to the xylose-based backbone, such as acetyl groups, phenylpropenoic acids (like hydroxycinnamic acids, mainly ferulic acid, and to a lesser extent dehydrodiferulic acid, p-coumaric acid, and sinapic acid), uronic acids (like α-D-glucopyranosyl uronic acid or its 4-O-methyl derivative), other xylopyranose units and so on, and this makes their structure branched [48,61,62]. An example of XOS structure is reported in Figure 1.1.

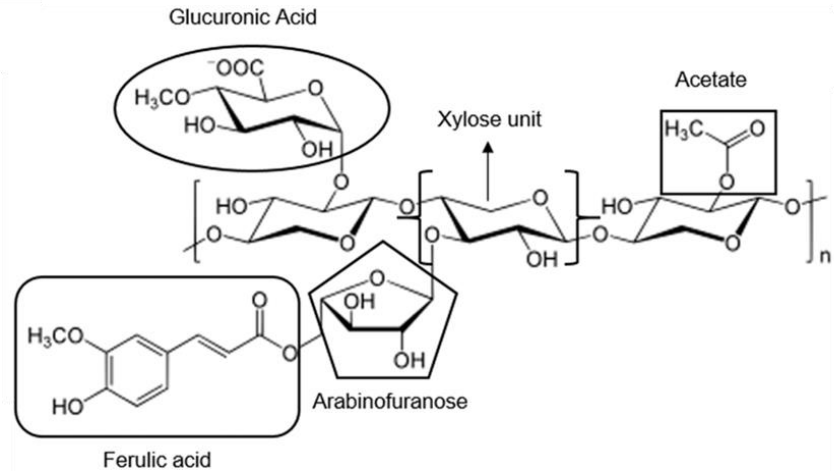

Figure 1.1: *Xylo-oligosaccharide showing different bonds and substitutions. Source: De Freitas et al., 2019* [63]. *Reproduced with permission from De Freitas et al., Bioactive Carbohydrates and Dietary Fibre; published by Elsevier, 2019.*

The consumption of XOS has been associated with many beneficial effects, after *in vivo* trials both on animals and humans, such as immunomodulatory, antioxidant and prebiotic properties, but also positive effects on diabetes prevention, lipid metabolism, colon inflammation, and stool frequency and consistence. Then, also non-cariogenicity has been associated with XOS, together with antiallergic activities and beneficial effects on the skin [26,64].

For all these reasons, after hemicellulose extraction, a very common step is its modification through enzymatic hydrolysis. It is important to clarify that when lignocellulosic biomasses are considered, the addition of the enzyme should always take place after another initial chemical treatment (often acid or alkaline solutions are employed) or autohydrolysis treatment. This is because it seems that lignin presence is the main factor which limits the hydrolysis by cellulolytic and hemicellulolytic enzymes, and for this reason its partial degradation with a pre-treatment is necessary [65]. Indeed, when an enzymatic hydrolysis is carried

out directly on lignocellulosic native biomass, less than 20% of cellulose-deriving glucose is released [66] and the same result is predictable as regards hemicellulose. However, as regards the process, the enzyme can be added directly to the reaction medium, immobilized, produced in situ via microbial fermentation, or immobilized inside the biomass [49]. Many enzymatic tests have been performed with different lignocellulosic materials, such as corncobs [67,68], almond shell [69], oil palm frond fibres [70], and wheat bran [71], with variable XOS yields and variable DP, although most obtained XOS had a good percentage of DP 2–4. In the study conducted by Mathew et al., arabinoxylan extracted from wheat bran have been subjected to enzymatic hydrolysis with four different xylanases; all of them have been able to originate XOS and AXOS, with different DP and substitutions [72]. Despite this, it seems that GH10 family xylanases are generally more efficient in producing shorter and more substituted XOS than GH11 family [72,73] and therefore are better for the production of low-DP XOS. The degree of substitution of arabinose on the xylan backbone (A/X ratio) also has a strong influence on enzyme activity and thus on (arabino)-xylooligosaccharides ((A)XOS) production. In fact, it has been reported that a lower A/X ratio favours hydrolytic activity of the enzymes, whether they belong to the GH10 or to GH11 family [74].

Despite these recent findings, it is essential to highlight that enzymatic hydrolyses are in general not sufficiently optimized for the production of tailored oligosaccharides, having a well defined structure. In fact, all the products originated by a xylanase from a given substrate depend on the substrate specificity, which in turn depends on the structure of the xylanase [75]. In addition to this, other factors may affect the yield and the structure of the hydrolysis products, such as temperature, pH, reaction time and synergy between xylanase and other auxiliary enzymes able to hydrolyse the substituent groups present in the polymer chain (including, in particular, acetylxylan esterase, glucuronidase or arabinofuranosidase). As a consequence, the production of XOS with a well-defined structure is not a foregone conclusion, when it should be of great importance, since as previously mentioned the structure is strictly related to the functional properties of carbohydrates in general [63]. For example, some studies have shown that XOS with a low DP and without substitutions have higher prebiotic activity [59,76–78] and that therefore these are more suitable to be used as prebiotic ingredients. At the same time, XOS with higher DP have been presented elsewhere as better antioxidants compared to the low-DP ones [79], and the degree of substitution also play a very important role in affecting this property [80–82]. And besides, if on the one hand quite a lot of research has been done with XOS with DP 2-6, very little is known about the properties of XOS having a DP comprised between 7 and 10, or higher: in fact, the availability of analytical XOS standards in the market is limited to DP 2-6, and furthermore it is quite complex to hydrolyse the xylan polymer obtaining oligosaccharides with specific and precise DPs to be able to study their properties. In a 2010 study, Mäkeläinen and colleagues tested four different XOS mixtures having different DPs, showing how every mixture favoured in a different way the growth of different *Bifidobacterium* and *Lactobacillus* strains and hence demonstrating their variable prebiotic effectiveness [83]. Numerous authors have obtained medium-DP XOS from a multitude of

agricultural by-products, but mostly through the use of chemical or autohydrolysis methods [84–86], leading the formation of all the undesired compounds previously discussed. For these reasons it is fundamental to further study the enzymatic hydrolyses and in particular how to tailor them in order to obtain different products having different features, depending on the specific need. Obviously, the following step that we would need to do is to in depth characterize their chemical structure and to test their properties, aiming to build, over time, a well-defined and clear structure-activity relationship.

1.4. Chemical structure characterization of fibres extracted and of degrading compounds

If the optimization of the fibre extraction and the eventual production of functional oligosaccharides are challenging operations, perhaps their characterization in terms of chemical structure is even more so. The development of high throughput methods of analysis allowing fibre detailed characterization is essential, since as repeatedly mentioned the nutritional and technological properties are strictly related to the structure. In this sense, the most influential factors are the degree of polymerization and the molecular weight, the stereochemistry of monosaccharides, the configuration of their bonds, the more or less extensive branching, and the type of substituents on the backbone [87]. Because of the need to determine all these aspects, it is clear that the structural analysis of carbohydrates turns out to be much more complex than that of other macromolecules, such as nucleic acids or proteins [60]. Despite the importance of carbohydrates, the current tools for their detailed structural characterization are still not well codified in universally applied protocols. In most cases, the first characterization step involves a depolymerization leading to monosaccharides, that is followed by a chromatographic separation and identification. Over the years, many different techniques have been developed, of varying efficiency, however they have low reproducibility, low sensibility and specificity, and lack speed [87]. To date, in fact, there is no official method for analysing and quantifying oligosaccharides (OS) or polysaccharides through their monosaccharides composition. Polysaccharide hydrolysis is a delicate phase: although several depolymerization methods have been found, such as acid hydrolysis, enzymatic hydrolysis or methanolysis, it seems that each polysaccharide requires different optimized conditions [88]. When neutral monosaccharides are present, an acid hydrolysis is probably the more efficient method: in a three-method comparative study, this has been the one that has allowed the release of the greatest quantity [89]. Different acids can be used, but the most common are trifluoroacetic acid (TFA), hydrochloric acid (HCl) and sulfuric acid (H_2SO_4). TFA is one of the most used, but it shows weak hydrolysis when for instance cellulose polymers, glycosaminoglycans or other polymers containing uronic acids (e.g. pectin) or amino sugars (e.g. chitin/chitosan) are present [90] and therefore the hydrolysis conditions must be regulated depending on the monomers expected. In the last case, an analytical method based on liquid chromatography has been proposed for the quantification of chitin in insects [91].

Regarding separative analysis of originated monosaccharides, one of the most employed techniques has been gas chromatography coupled with mass spectrometry detector (GC-MS) or flame ionization detector (GC-FID). Current platforms however have limited scope and GC method requires analytes with high volatility, which is why derivatization techniques are needed, for example using methylation, acetylation or trimethylsilylation [92,93]. This additional phase is not welcome because of the costs associated with the purchase of reagents and because it lengthens the analysis time. This does not generally happen when techniques based on liquid chromatography (LC) are employed. Different types of LC methods have been developed over time: anion exchange chromatography coupled with pulsed amperometric detector (HPAEC-PAD) is a technique especially used in OS characterization and it offers specific and sensitive detection, as well as good OS separation [94], however it has some limits, such as the progressive loss of detector signal during the analysis, the expensive replacement of disposable electrodes, and the difficulty in separating and characterizing branched OS [94]. In particular, in AXOS analysis, it has been observed that the position of substituent arabinose affects the retention time, and that some of these AXOS can elute simultaneously, which complicates their identification [95]. Furthermore, according to some scholars, HPAEC-PAD could perhaps lead to epimerization and OS degradation when an aqueous solution with a high concentration of sodium hydroxide is used as the mobile phase [96]. Several studies have also tried to establish a method for the identification of oligosaccharides and polysaccharides by relying on other liquid chromatography techniques, coupled with different detectors. UV-vis detector has been employed in some cases, but it has the limit of needing a chromophore-based derivatization step, since monosaccharides do not have UV activity [87]. By contrast, HPLC-RID has permitted a good identification in some studies, even though limited to OS with a low DP (2–4) [97,98]. RID is commonly used for the detection of polysaccharides when it is coupled with size-exclusion chromatography (HPSEC). The latter is widely employed because it provides information on molecular weight distribution and is particularly advantageous since it needs aqueous solvents, allowing for quick and easy sample preparation [99]. Actually, HPSEC separation principle is based on the hydrodynamic volume of molecules, which can be strongly influenced by the number and the length of any eventually present branch: therefore, molecules with the same hydrodynamic volume can have different molecular weights and, despite this, coelute. For this reason, although sometimes this problem can be solved through the use of HPSEC with multiple-detection (by two independent methods, viscometry and light scattering), this technique can yield molecular weights with highly variable accuracy [100]. Liquid chromatography coupled with mass spectrometry is also commonly employed for mono/oligosaccharides characterization. However, one limitation of MS is that it alone cannot discriminate between hexose isomers or pentose isomers, since they all have the same molecular formula and therefore the same mass [101]. Reverse phase-high pressure liquid chromatography coupled with tandem mass spectrometry (RP-HPLC/MS-MS) has been very useful to characterize oligosaccharides (also in terms of linkage position and monosaccharides sequence after enzymatic hydrolysis, even though other complementary techniques were

also necessary) [102], however it can cause problems when there are same-type monomers, as in the case of (A)XOS [73]. In this sense, in fact, a derivatization step or a labelling step at the non-reducing end is necessary [103]. Pu et al. proposed another method to characterize XOS, based on hydrophilic interaction liquid chromatography with evaporative light scattering detection (HILIC-ELSD), without the need for derivatization [96]. The coupling of HILIC with ELSD and with the MSn detector can give important structural information, such as the presence of acetyl groups, and allows the characterization and quantification of many OS with different structures; however, isomeric structures tend to coelute, leading to overlapping peaks [104]. In another study, neutral deprotonated AXOS structure was characterized through negative electrospray with quadrupole and time of flight coupled with mass spectrometer (ESI-Q-TOFMS) and through negative electrospray associated with ion trap and MS (ESI-ITMS): these techniques have proven to be particularly efficient for structural analysis of AXOS up to DP 9, including isomer differentiation. In reality, the interpretation of the spectra obtained by ESI-Q-TOFMS was successful also thanks to the knowledge gained from previous characterization through ^{1}H NMR [105]. Nuclear magnetic resonance (NMR) is indeed an effective tool for determining carbohydrates structures, especially monosaccharides composition, their configuration and sequence and the characteristics of the bond. Providing complementary information, NMR has often been coupled with negative ESI-MS/MS and methylation analysis [60]. In a recent study, Xiao and colleagues have extracted XOS from bamboo by autohydrolysis, then they separated and purified them by gel permeation chromatography (GPC) and finally characterized them by combining ESI-MS, NMR and HPAEC-PAD; the combination of ^{1}H, ^{13}C, and 2D HSQC NMR has given important structural information, especially on the sites where substitutions took place [106]. The degree of branching of polysaccharides have been sometimes determined by 1D/2D NMR combined with GC–MS analysis, whereas the α and β configurations for sugar residues in polysaccharides are commonly detected in FT-IR and 1D NMR [107]. Another technology that has taken hold to study polysaccharide structure is matrix-assisted laser desorption/ionization coupled with mass spectrometry (MALDI-MS). It has proven to be an effective tool for determining (A)XOS molecular weights [73], and thanks to the ease in sample preparation and high speed of analysis, it is often used for offline MS analysis to identify DPs and the composition of separate oligomers [108]. Moreover, it has low fragmentation, large mass range and tolerance to impurities, and does not require derivatization [60], as shown in a study conducted on XOS from olive pulp [109]. More recently, however, more advanced techniques have been developed, such as MALDI-TOF-MS and MALDI post-source decay TOF/MS, which are up to ten times more sensitive [60]. Despite the fact that this technique allows a good determination of molecular masses, it is limited by not directly distinguishing the anomers and OS branched configurations [60]. More in general, complete structural elucidation may not be possible with mass spectrometry alone, but may require other tools, such as NMR and chemical and enzymatic methods [110]. Finally, ion mobility (IM) is a very promising technique in contributing to OS identification; it is often coupled with MS and allows ion separation based on their mass, charge, size, and shape, thus also allowing differentiation of isomers

[111]. The principle on which IM is based is the separation of the analytes in a long drift tube, in which an electric field is applied and in which an inert gas passes, before they reach the detector for mass analysis; drift times, which vary according to the size and shape of the analytes, can be combined with MS spectra and integrated into databases for future structural identification. The major advantages given by this technique are the high-resolution power, the high sensitivity, and the very low time required for the analysis. On the other hand, IM-MS is not yet powerful enough to separate almost identical structures: overlaps between species with similar drift time can in fact still occur [112]. Moreover, there are few studies in literature about carbohydrates structural characterization by IM-MS, but it is very likely that this technique will be in the foreground in the near future. Indeed, some studies have already shown a very high potential on the separation and discrimination between different OS [113].

Another very relevant point connected to the extraction of dietary fibres and hemicellulose in particular is, as previously mentioned, the formation of a myriad of other compounds when thermal treatments are applied. These compounds mainly come from lignin and sugars degradation and several studies have shown how it was possible to vary the composition of the autohydrolysis liquor after hydrothermal treatment in different conditions, but mainly in terms of quantity of furfural, HMF, acetic, formic and lactic acid content [114–116]. Actually, not many studies have deeply investigated the composition of these liquors, and some authors highlighted how some reaction mechanisms are to date still unknown [54]. Hence, since one of the main final aims of extracting and modifying hemicellulose from agro-industrial by-products is the obtainment of functional ingredients for food companies, it is of enormous importance to further investigate the presence and the formation of all these compounds. To understand all the mechanisms of reaction would be difficult but also of great interest, as well as to develop rapid techniques that are able to simultaneously identify and quantify all the molecules that can originate in a certain process. Indeed, as previously mentioned, many autohydrolysis treatments can be regulated time after time depending on the products one wants to obtain, on the matrix undergoing the extraction and on several other factors. Therefore, temperature, holding time, liquid/solid ratio, etc., might be changed and as a consequence also the degradation compounds can do the same. In short, the formation of these compounds that today look like “unpredictable” can no longer be overlooked, especially for a matter of potential toxicity.

REFERENCES

1. Trowell, H. Ischemic heart disease and dietary fiber. *Am. J. Clin. Nutr.* 1972, 926–932.
2. Dhingra, D.; Michael, M.; Rajput, H.; Patil, R.T. Dietary fibre in foods: A review. *J. Food Sci. Technol.* **2012**, *49*, 255–266, doi:10.1007/s13197-011-0365-5.
3. Jiménez-Escrig, A.; Sánchez-Muniz, F.J. Dietary fibre from edible seaweeds: Chemical structure, physicochemical properties and effects on cholesterol metabolism. *Nutr. Res.* **2000**, *20*, 585–598, doi:10.1016/S0271-5317(00)00149-4.
4. Williams, B.A.; Mikkelsen, D.; Flanagan, B.M.; Gidley, M.J. "Dietary fibre": Moving beyond the "soluble/insoluble" classification for monogastric nutrition, with an emphasis on humans and pigs. *J. Anim. Sci. Biotechnol.* **2019**, *10*, 45, doi:10.1186/s40104-019-0350-9.
5. Mudgil, D.; Barak, S. Classification, technological properties, and sustainable sources. In *Dietary Fiber: Properties, Recovery, and Applications - Chapter 2*; 2019; pp. 27–58 ISBN 9780128164952.
6. Lovegrove, A.; Edwards, C.H.; De Noni, I.; Patel, H.; El, S.N.; Grassby, T.; Zielke, C.; Ulmius, M.; Nilsson, L.; Butterworth, P.J.; et al. Role of polysaccharides in food, digestion, and health. *Crit. Rev. Food Sci. Nutr.* **2017**, *57*, 237–253, doi:10.1080/10408398.2014.939263.
7. Nirmala Prasadi, V.P.; Joye, I.J. Dietary fibre from whole grains and their benefits on metabolic health. *Nutrients* **2020**, *12*, 3045, doi:10.3390/nu12103045.
8. Scheller, H.V.; Ulvskov, P. Hemicelluloses. *Annu. Rev. Plant Biol.* **2010**, *61*, 263–289, doi:10.1146/annurev-arplant-042809-112315.
9. Sharma, P.; Bhandari, C.; Kumar, S.; Sharma, B.; Bhadwal, P.; Agnihotri, N. Chapter 11 - Dietary fibers: A way to a healthy microbiome. In *Diet, Microbiome and Health*; 2018; pp. 299–345 ISBN 9780128114407.
10. Chen, L.; Yang, Z.; McClements, D.J.; Jin, Z.; Miao, M. Chapter 20 - Biological macromolecules for nutrients delivery. In *Biological Macromolecules*; 2022; pp. 455–477.
11. Müller-Maatsch, J.; Bencivenni, M.; Caligiani, A.; Tedeschi, T.; Bruggeman, G.; Bosch, M.; Petrusan, J.; Van Droogenbroeck, B.; Elst, K.; Sforza, S. Pectin content and composition from different food waste streams. *Food Chem.* **2016**, *201*, 37–45, doi:10.1016/j.foodchem.2016.01.012.
12. Meyer, D.; Blaauwhoed, J.P. Inulin. In *Handbook of Hydrocolloids: Second Edition*; 2009; pp. 829–848 ISBN 9781845695873.
13. López-Franco, Y.; Higuera-Ciapara, I.; Goycoolea, F.M.; Wang, W. 18 - Other exudates: tragancanth, karaya, mesquite gum and larchwood arabinogalactan BT - Handbook of Hydrocolloids (Second edition). In *Woodhead Publishing Series in Food Science, Technology and Nutrition*; 2009; pp. 495–534 ISBN 978-1-84569-414-2.
14. Tolbert, A.; Akinosho, H.; Khunsupat, R.; Naskar, A.K.; Ragauskas, A.J. Characterization and analysis of the molecular weight of lignin for biorefining studies. *Biofuels, Bioprod. Biorefining* **2014**, *8*, 836–856, doi:10.1002/bbb.1500.
15. Heinze, T. Cellulose: Structure and properties. *Adv. Polym. Sci.* **2015**, *271*, 1–52, doi:10.1007/12_2015_319.
16. Blanco, A.; Monte, M.C.; Campano, C.; Balea, A.; Merayo, N.; Negro, C. Chapter 5 - Nanocellulose for industrial use: Cellulose nanofibers (CNF), cellulose nanocrystals (CNC), and bacterial cellulose (BC). In *Handbook of Nanomaterials for Industrial Applications*; 2018; pp. 74–126 ISBN 9780128133514.
17. Fry, S.C. The structure and functions of xyloglucan. *J. Exp. Bot.* **1989**, *40*, 1–11, doi:10.1093/jxb/40.1.1.
18. Gidley, M.J.; Nishinari, K. Chapter 2.2 - Physico-chemistry of (1,3)-β-glucans. In *Chemistry, Biochemistry, and Biology of 1-3 Beta Glucans and Related Polysaccharides*; 2009; pp. 47–118 ISBN 9780123739711.
19. Saka, S.; Bae, H.J. Chapter 11 - Secondary Xylem for Bioconversion. In *Secondary Xylem Biology: Origins, Functions, and Applications*; 2016; pp. 213–231 ISBN 9780128021859.
20. Chen, Z.; Li, S.; Fu, Y.; Li, C.; Chen, D.; Chen, H. Arabinoxylan structural characteristics, interaction with gut microbiota and potential health functions. *J. Funct. Foods* **2019**, *54*, 536–551, doi:10.1016/j.jff.2019.02.007.
21. Hägglund, P. *Mannan-hydrolysis by hemicellulases: Enzyme-polysaccharide interaction of a modular β-mannanase*; 2002; ISBN 9162852035.
22. Wielinga, W.C.; Meyhall, A.G. Chapter 10 - Galactomannans. In *Handbook of Hydrocolloids: Second Edition*; 2009; pp. 228–251 ISBN 9781845695873.

23. Zhang, H.; Zhang, F.; Yuan, R. Chapter 13 - Applications of natural polymer-based hydrogels in the food industry. In *Hydrogels Based on Natural Polymers*; 2019; pp. 357–410 ISBN 9780128164211.

24. Deshavath, N.N.; Veeranki, V.D.; Goud, V. V. Chapter 1 - Lignocellulosic feedstocks for the production of bioethanol: Availability, structure, and composition. In *Sustainable Bioenergy: Advances and Impacts*; 2019; pp. 1–19 ISBN 9780128176542.

25. A. Saville, B.; H. Saville, S. Functional Attributes and Health Benefits of Novel Prebiotic Oligosaccharides Derived from Xylan, Arabinan, and Mannan. In *Prebiotics and Probiotics - Potential Benefits in Nutrition and Health*; 2020.

26. Fuso, A.; Risso, D.; Rosso, G.; Rosso, F.; Manini, F.; Manera, I.; Caligiani, A. Potential valorization of hazelnut shells through extraction, purification and structural characterization of prebiotic compounds: A critical review. *Foods* **2021**, *10*, 1197, doi:10.3390/foods10061197.

27. Caligiani, A.; Marseglia, A.; Leni, G.; Baldassarre, S.; Maistrello, L.; Dossena, A.; Sforza, S. Composition of black soldier fly prepupae and systematic approaches for extraction and fractionation of proteins, lipids and chitin. *Food Res. Int.* **2018**, *105*, 812–820, doi:10.1016/j.foodres.2017.12.012.

28. Hamed, I.; Özogul, F.; Regenstein, J.M. Industrial applications of crustacean by-products (chitin, chitosan, and chitooligosaccharides): A review. *Trends Food Sci. Technol.* **2016**, *48*, 40–50, doi:10.1016/j.tifs.2015.11.007.

29. Korcz, E.; Kerényi, Z.; Varga, L. Dietary fibers, prebiotics, and exopolysaccharides produced by lactic acid bacteria: Potential health benefits with special regard to cholesterol-lowering effects. *Food Funct.* **2018**, *9*, 3057–3068, doi:10.1039/c8fo00118a.

30. Surek, E.; Buyukkileci, A.O. Production of xylooligosaccharides by autohydrolysis of hazelnut (Corylus avellana L.) shell. *Carbohydr. Polym.* **2017**, *174*, 565–571, doi:10.1016/j.carbpol.2017.06.109.

31. Marić, M.; Grassino, A.N.; Zhu, Z.; Barba, F.J.; Brnčić, M.; Rimac Brnčić, S. An overview of the traditional and innovative approaches for pectin extraction from plant food wastes and by-products: Ultrasound-, microwaves-, and enzyme-assisted extraction. *Trends Food Sci. Technol.* **2018**, *76*, 28–37, doi:10.1016/j.tifs.2018.03.022.

32. Das, S.; Nadar, S.S.; Rathod, V.K. Integrated strategies for enzyme assisted extraction of bioactive molecules: A review. *Int. J. Biol. Macromol.* **2021**, *191*, 899–917, doi:10.1016/j.ijbiomac.2021.09.060.

33. Fry, S.C. Chapter 1 - Cell Wall Polysaccharide Composition and Covalent Crosslinking. In *Annual Plant Reviews, Plant Polysaccharides: Biosynthesis and Bioengineering*; 2010; pp. 1–42 ISBN 9781444391015.

34. Prokopov, T.; Nikolova, M.; Dobrev, G.; Taneva, D. Enzyme-assisted extraction of carotenoids from Bulgarian tomato peels. *Acta Aliment.* **2017**, *46*, 84–91, doi:10.1556/066.2017.46.1.11.

35. Passos, C.P.; Yilmaz, S.; Silva, C.M.; Coimbra, M.A. Enhancement of grape seed oil extraction using a cell wall degrading enzyme cocktail. *Food Chem.* **2009**, *115*, 48–53, doi:10.1016/j.foodchem.2008.11.064.

36. Li, B.B.; Smith, B.; Hossain, M.M. Extraction of phenolics from citrus peels: II. Enzyme-assisted extraction method. *Sep. Purif. Technol.* **2006**, *48*, 189–196, doi:10.1016/j.seppur.2005.07.019.

37. Dzogbefia, V.P.; Ofosu, G.A.; Oldham, J.H. Evaluation of locally produced Saccharomyces cerevisiae pectinase enzyme for industrial extraction of starch from cassava in Ghana. *Sci. Res. Essays* **2008**, *3*, 365–369.

38. Wikiera, A.; Mika, M.; Grabacka, M. Multicatalytic enzyme preparations as effective alternative to acid in pectin extraction. *Food Hydrocoll.* **2015**, *44*, 156–161, doi:10.1016/j.foodhyd.2014.09.018.

39. Dominiak, M.; Søndergaard, K.M.; Wichmann, J.; Vidal-Melgosa, S.; Willats, W.G.T.; Meyer, A.S.; Mikkelsen, J.D. Application of enzymes for efficient extraction, modification, and development of functional properties of lime pectin. *Food Hydrocoll.* **2014**, *40*, 273–282, doi:10.1016/j.foodhyd.2014.03.009.

40. Cheng, L.; Zhang, X.; Hong, Y.; Li, Z.; Li, C.; Gu, Z. Characterisation of physicochemical and functional properties of soluble dietary fibre from potato pulp obtained by enzyme-assisted extraction. *Int. J. Biol. Macromol.* **2017**, *101*, 1004–1011, doi:10.1016/j.ijbiomac.2017.03.156.

41. Chiang, C.F.; Lai, L.S. Effect of enzyme-assisted extraction on the physicochemical properties of mucilage from the fronds of Asplenium australasicum (J. Sm.) Hook. *Int. J. Biol. Macromol.* **2019**, *124*, 346–353, doi:10.1016/j.ijbiomac.2018.11.181.

42. Haldar, D.; Purkait, M.K. Lignocellulosic conversion into value-added products: A review. *Process Biochem.* **2020**, *89*, 110–133, doi:10.1016/j.procbio.2019.10.001.

43. Kumari, D.; Singh, R. Pretreatment of lignocellulosic wastes for biofuel production: A critical review. *Renew. Sustain. Energy Rev.* **2018**, *90*, 877–891, doi:10.1016/j.rser.2018.03.111.

44. Singh, J.; Suhag, M.; Dhaka, A. Augmented digestion of lignocellulose by steam explosion, acid and alkaline pretreatment methods: A review. *Carbohydr. Polym.* **2015**, *7*, 19–27, doi:10.1016/j.carbpol.2014.10.012.

45. Negro, M.J.; Manzanares, P.; Oliva, J.M.; Ballesteros, I.; Ballesteros, M. Changes in various physical/chemical parameters of Pinus pinaster wood after steam explosion pretreatment. *Biomass and Bioenergy* **2003**, *25*, 301–308, doi:10.1016/S0961-9534(03)00017-5.

46. Talebnia, F.; Karakashev, D.; Angelidaki, I. Production of bioethanol from wheat straw: An overview on pretreatment, hydrolysis and fermentation. *Bioresour. Technol.* **2010**, *101*, 4744–4753, doi:10.1016/j.biortech.2009.11.080.

47. Ruiz, H.A.; Galbe, M.; Garrote, G.; Ramirez-Gutierrez, D.M.; Ximenes, E.; Sun, S.N.; Lachos-Perez, D.; Rodríguez-Jasso, R.M.; Sun, R.C.; Yang, B.; et al. Severity factor kinetic model as a strategic parameter of hydrothermal processing (steam explosion and liquid hot water) for biomass fractionation under biorefinery concept. *Bioresour. Technol.* **2021**, *342*, 125961, doi:10.1016/j.biortech.2021.125961.

48. Aachary, A.A.; Prapulla, S.G. Xylooligosaccharides (XOS) as an Emerging Prebiotic: Microbial Synthesis, Utilization, Structural Characterization, Bioactive Properties, and Applications. *Compr. Rev. Food Sci. Food Saf.* **2011**, *10*, 2–16, doi:10.1111/j.1541-4337.2010.00135.x.

49. Carvalho, A.F.A.; Neto, P. de O.; da Silva, D.F.; Pastore, G.M. Xylo-oligosaccharides from lignocellulosic materials: Chemical structure, health benefits and production by chemical and enzymatic hydrolysis. *Food Res. Int.* **2013**, *51*, 75–85, doi:10.1016/j.foodres.2012.11.021.

50. Kabel, M.A.; Kortenoeven, L.; Schols, H.A.; Voragen, A.G.J. In vitro fermentability of differently substituted xylo-oligosaccharides. *J. Agric. Food Chem.* **2002**, *50*, 6205–10, doi:10.1021/jf020220r.

51. Nabarlatz, D.; Ebringerová, A.; Montané, D. Autohydrolysis of agricultural by-products for the production of xylo-oligosaccharides. *Carbohydr. Polym.* **2007**, *69*, 20–28, doi:10.1016/j.carbpol.2006.08.020.

52. Hames, B.R.; Thomas, S.R.; Sluiter, A.D.; Roth, C.J.; Templeton, D.W. Rapid Biomass Analysis. In *Biotechnology for Fuels and Chemicals*; 2003; pp. 5–16.

53. Rasmussen, H.; Sørensen, H.R.; Meyer, A.S. Formation of degradation compounds from lignocellulosic biomass in the biorefinery: Sugar reaction mechanisms. *Carbohydr. Res.* **2014**, *385*, 45–57, doi:10.1016/j.carres.2013.08.029.

54. Gao, Y.; Wang, H.; Guo, J.; Peng, P.; Zhai, M.; She, D. Hydrothermal degradation of hemicelluloses from triploid poplar in hot compressed water at 180-340 °c. *Polym. Degrad. Stab.* **2016**, *126*, 179–187, doi:10.1016/j.polymdegradstab.2016.02.003.

55. Dixit, Y.; Wagle, A.; Vakil, B. Patents in the Field of Probiotics, Prebiotics, Synbiotics: A Review. *J. Food Microbiol. Saf. Hyg.* **2016**, *1*, 1–13, doi:10.4172/2476-2059.1000111.

56. Farias, D. de P.; de Araújo, F.F.; Neri-Numa, I.A.; Pastore, G.M. Prebiotics: Trends in food, health and technological applications. *Trends Food Sci. Technol.* **2019**, *93*, 23–35, doi:10.1016/j.tifs.2019.09.004.

57. Pereira, M.A.F.; Cesca, K.; Poletto, P.; de Oliveira, D. New perspectives for banana peel polysaccharides and their conversion to oligosaccharides. *Food Res. Int.* **2021**, *149*, 110706, doi:10.1016/j.foodres.2021.110706.

58. Vieira, T.F.; Corrêa, R.C.G.; Peralta, R.A.; Peralta-Muniz-Moreira, R.F.; Bracht, A.; Peralta, R.M. An Overview of Structural Aspects and Health Beneficial Effects of Antioxidant Oligosaccharides. *Curr. Pharm. Des.* **2018**, *26*, 1759–1777, doi:10.2174/1381612824666180517120642.

59. Wu, Y.; Chen, Y.; Lu, Y.; Hao, H.; Liu, J.; Huang, R. Structural features, interaction with the gut microbiota and anti-tumor activity of oligosaccharides. *RSC Adv.* **2020**, *10*, 16339–16348, doi:10.1039/d0ra00344a.

60. Zhao, C.; Wu, Y.; Liu, X.; Liu, B.; Cao, H.; Yu, H.; Sarker, S.D.; Nahar, L.; Xiao, J. Functional properties, structural studies and chemo-enzymatic synthesis of oligosaccharides. *Trends Food Sci. Technol.* **2017**, *66*, 135–145, doi:10.1016/j.tifs.2017.06.008.

61. Singh, R.D.; Banerjee, J.; Arora, A. Prebiotic potential of oligosaccharides: A focus on xylan derived oligosaccharides. *Bioact. Carbohydrates Diet. Fibre* **2015**, *5*, 19–30, doi:10.1016/j.bcdf.2014.11.003.

62. Rennie, E.A.; Scheller, H.V. Xylan biosynthesis. *Curr. Opin. Biotechnol.* 2014.

63. de Freitas, C.; Carmona, E.; Brienzo, M. Xylooligosaccharides production process from lignocellulosic biomass and bioactive effects. *Bioact. Carbohydrates Diet. Fibre* **2019**, *18*, 100184, doi:10.1016/j.bcdf.2019.100184.

64. Chen, Y.; Xie, Y.; Ajuwon, K.M.; Zhong, R.; Li, T.; Chen, L.; Zhang, H.; Beckers, Y.; Everaert, N. Xylo-Oligosaccharides, Preparation and Application to Human and Animal Health: A Review. *Front. Nutr.* **2021**, *8*, 731930, doi:10.3389/fnut.2021.731930.

65. Van Dyk, J.S.; Pletschke, B.I. A review of lignocellulose bioconversion using enzymatic hydrolysis and synergistic cooperation

between enzymes-Factors affecting enzymes, conversion and synergy. *Biotechnol. Adv.* **2012**, *30*, 1458–1480, doi:10.1016/j.biotechadv.2012.03.002.

66. Zhang, Y.H.P.; Lynd, L.R. Toward an aggregated understanding of enzymatic hydrolysis of cellulose: Noncomplexed cellulase systems. *Biotechnol. Bioeng.* **2004**, *88*, 797–824, doi:10.1002/bit.20282.

67. Aachary, A.A.; Prapulla, S.G. Value addition to corncob: Production and characterization of xylooligosaccharides from alkali pretreated lignin-saccharide complex using Aspergillus oryzae MTCC 5154. *Bioresour. Technol.* **2009**, *100*, 991–995, doi:10.1016/j.biortech.2008.06.050.

68. Chapla, D.; Pandit, P.; Shah, A. Production of xylooligosaccharides from corncob xylan by fungal xylanase and their utilization by probiotics. *Bioresour. Technol.* **2012**, *115*, 215–221, doi:10.1016/j.biortech.2011.10.083.

69. Singh, R.D.; Nadar, C.G.; Muir, J.; Arora, A. Green and clean process to obtain low degree of polymerisation xylooligosaccharides from almond shell. *J. Clean. Prod.* **2019**, *241*, 118237, doi:10.1016/j.jclepro.2019.118237.

70. Sabiha-Hanim, S.; Noor, M.A.M.; Rosma, A. Effect of autohydrolysis and enzymatic treatment on oil palm (Elaeis guineensis Jacq.) frond fibres for xylose and xylooligosaccharides production. *Bioresour. Technol.* **2011**, *102*, 1234–1239, doi:10.1016/j.biortech.2010.08.017.

71. Immerzeel, P.; Falck, P.; Galbe, M.; Adlercreutz, P.; Nordberg Karlsson, E.; Stålbrand, H. Extraction of water-soluble xylan from wheat bran and utilization of enzymatically produced xylooligosaccharides by Lactobacillus, Bifidobacterium and Weissella spp. *LWT - Food Sci. Technol.* **2014**, *56*, 321–327, doi:10.1016/j.lwt.2013.12.013.

72. Mathew, S.; Karlsson, E.N.; Adlercreutz, P. Extraction of soluble arabinoxylan from enzymatically pretreated wheat bran and production of short xylo-oligosaccharides and arabinoxylo-oligosaccharides from arabinoxylan by glycoside hydrolase family 10 and 11 endoxylanases. *J. Biotechnol.* **2017**, doi:10.1016/j.jbiotec.2017.09.006.

73. Juvonen, M.; Kotiranta, M.; Jokela, J.; Tuomainen, P.; Tenkanen, M. Identification and structural analysis of cereal arabinoxylan-derived oligosaccharides by negative ionization HILIC-MS/MS. *Food Chem.* **2019**, *275*, 176–185, doi:10.1016/j.foodchem.2018.09.074.

74. Falck, P.; Aronsson, A.; Grey, C.; Stålbrand, H.; Nordberg Karlsson, E.; Adlercreutz, P. Production of arabinoxylan-oligosaccharide mixtures of varying composition from rye bran by a combination of process conditions and type of xylanase. *Bioresour. Technol.* **2014**, *174*, 118–125, doi:10.1016/j.biortech.2014.09.139.

75. Linares-Pasten, J.A.; Aronsson, A.; Karlsson, E.N. Structural Considerations on the Use of Endo-Xylanases for the Production of prebiotic Xylooligosaccharides from Biomass. *Curr. Protein Pept. Sci.* **2018**, *19*, 48–67, doi:10.2174/1389203717666160923155209.

76. Ho, A.L.; Kosik, O.; Lovegrove, A.; Charalampopoulos, D.; Rastall, R.A. In vitro fermentability of xylo-oligosaccharide and xylo-polysaccharide fractions with different molecular weights by human faecal bacteria. *Carbohydr. Polym.* **2018**, *179*, 50–58, doi:10.1016/j.carbpol.2017.08.077.

77. Gullón, P.; Moura, P.; Esteves, M.P.; Girio, F.M.; Domínguez, H.; Parajó, J.C. Assessment on the fermentability of xylooligosaccharides from rice husks by probiotic bacteria. *J. Agric. Food Chem.* **2008**, *56*, 7482–7487, doi:10.1021/jf800715b.

78. Mendis, M.; Martens, E.C.; Simsek, S. How Fine Structural Differences of Xylooligosaccharides and Arabinoxylooligosaccharides Regulate Differential Growth of Bacteroides Species. *J. Agric. Food Chem.* **2018**, *66*, 8398–8405, doi:10.1021/acs.jafc.8b01263.

79. Valls, C.; Pastor, F.I.J.; Vidal, T.; Roncero, M.B.; Díaz, P.; Martínez, J.; Valenzuela, S. V. Antioxidant activity of xylooligosaccharides produced from glucuronoxylan by Xyn10A and Xyn30D xylanases and eucalyptus autohydrolysates. *Carbohydr. Polym.* **2018**, *194*, 43–50, doi:10.1016/j.carbpol.2018.04.028.

80. Bouiche, C.; Boucherba, N.; Benallaoua, S.; Martinez, J.; Diaz, P.; Pastor, F.I.J.; Valenzuela, S. V. Differential antioxidant activity of glucuronoxylooligosaccharides (UXOS) and arabinoxylooligosaccharides (AXOS) produced by two novel xylanases. *Int. J. Biol. Macromol.* **2020**, *155*, 1075–1083, doi:10.1016/J.IJBIOMAC.2019.11.073.

81. Rao, R.S.P.; Muralikrishna, G. Water soluble feruloyl arabinoxylans from rice and ragi: Changes upon malting and their consequence on antioxidant activity. *Phytochemistry* **2006**, *67*, 91–99, doi:10.1016/j.phytochem.2005.09.036.

82. Mengíbar, M.; Mateos-Aparicio, I.; Miralles, B.; Heras, Á. Influence of the physico-chemical characteristics of chito-oligosaccharides (COS) on antioxidant activity. *Carbohydr. Polym.* **2013**, *97*, 776–782, doi:10.1016/j.carbpol.2013.05.035.

83. Mäkeläinen, H.; Forssten, S.; Saarinen, M.; Stowell, J.; Rautonen, N.; Ouwehand, A.C. Xylo-oligosaccharides enhance the growth of bifidobacteria and Bifidobacterium lactis in a simulated colon model. *Benef. Microbes* **2010**, *1*, 81–91, doi:10.3920/BM2009.0025.

84. Han, J.; Cao, R.; Zhou, X.; Xu, Y. An integrated biorefinery process for adding values to corncob in co-production of xylooligosaccharides and glucose starting from pretreatment with gluconic acid. *Bioresour. Technol.* **2020**, *307*, 123200, doi:10.1016/j.biortech.2020.123200.

85. Otieno, D.O.; Ahring, B.K. A thermochemical pretreatment process to produce xylooligosaccharides (XOS), arabinooligosaccharides (AOS) and mannooligosaccharides (MOS) from lignocellulosic biomasses. *Bioresour. Technol.* **2012**, *112*, 285–292, doi:10.1016/j.biortech.2012.01.162.

86. Zhou, X.; Xu, Y. Eco-friendly consolidated process for co-production of xylooligosaccharides and fermentable sugars using self-providing xylonic acid as key pretreatment catalyst. *Biotechnol. Biofuels* **2019**, *12*, 272, doi:10.1186/s13068-019-1614-5.

87. Amicucci, M.J.; Galermo, A.G.; Nandita, E.; Vo, T.T.T.; Liu, Y.; Lee, M.; Xu, G.; Lebrilla, C.B. A rapid-throughput adaptable method for determining the monosaccharide composition of polysaccharides. *Int. J. Mass Spectrom.* **2019**, *438*, 22–28, doi:10.1016/j.ijms.2018.12.009.

88. Wang, Q.C.; Zhao, X.; Pu, J.H.; Luan, X.H. Influences of acidic reaction and hydrolytic conditions on monosaccharide composition analysis of acidic, neutral and basic polysaccharides. *Carbohydr. Polym.* **2016**, *143*, 296–300, doi:10.1016/j.carbpol.2016.02.023.

89. Willför, S.; Pranovich, A.; Tamminen, T.; Puls, J.; Laine, C.; Suurnäkki, A.; Saake, B.; Uotila, K.; Simolin, H.; Hemming, J.; et al. Carbohydrate analysis of plant materials with uronic acid-containing polysaccharides-A comparison between different hydrolysis and subsequent chromatographic analytical techniques. *Ind. Crops Prod.* **2009**, doi:10.1016/j.indcrop.2008.11.003.

90. Liu, D.; Tang, W.; Yin, J.Y.; Nie, S.P.; Xie, M.Y. Monosaccharide composition analysis of polysaccharides from natural sources: Hydrolysis condition and detection method development. *Food Hydrocoll.* **2021**, *116*, 106641, doi:10.1016/j.foodhyd.2021.106641.

91. Luparelli, A.V.; Leni, G.; Fuso, A.; Pedrazzani, C.; Palini, S.; Sforza, S.; Caligiani, A. Development of a Quantitative UPLC-ESI/MS Method for the Simultaneous Determination of the Chitin and Protein Content in Insects. *Food Anal. Methods* **2022**, doi:https://doi.org/10.1007/s12161-022-02411-2.

92. Zhu, H.; Liu, C.; Hou, J.; Long, H.; Wang, B.; Guo, D. an; Lei, M.; Wu, W. Gastrodia elata blume polysaccharides: A review of their acquisition, analysis, modification, and pharmacological activities. *Molecules* **2019**, *24*, 2436, doi:10.3390/molecules24132436.

93. Amicucci, M.J.; Nandita, E.; Lebrilla, C.B. Function without Structures: The Need for In-Depth Analysis of Dietary Carbohydrates. *J. Agric. Food Chem.* **2019**, *67*, 4418–4424, doi:10.1021/acs.jafc.9b00720.

94. Mechelke, M.; Herlet, J.; Benz, J.P.; Schwarz, W.H.; Zverlov, V. V.; Liebl, W.; Kornberger, P. HPAEC-PAD for oligosaccharide analysis—novel insights into analyte sensitivity and response stability. *Anal. Bioanal. Chem.* **2017**, *409*, 7169–7181, doi:10.1007/s00216-017-0678-y.

95. Pastell, H.; Tuomainen, P.; Virkki, L.; Tenkanen, M. Step-wise enzymatic preparation and structural characterization of singly and doubly substituted arabinoxylo-oligosaccharides with non-reducing end terminal branches. *Carbohydr. Res.* **2008**, *343*, 3049–3057, doi:10.1016/j.carres.2008.09.013.

96. Pu, J.; Zhao, X.; Xiao, L.; Zhao, H. Development and validation of a HILIC-ELSD method for simultaneous analysis of non-substituted and acetylated xylo-oligosaccharides. *J. Pharm. Biomed. Anal.* **2017**, *139*, 232–237, doi:10.1016/j.jpba.2017.03.007.

97. Mafei, T.D.T.; Neto, F.S.P.P.; Peixoto, G.; de Baptista Neto, Á.; Monti, R.; Masarin, F. Extraction and Characterization of Hemicellulose from Eucalyptus By-product: Assessment of Enzymatic Hydrolysis to Produce Xylooligosaccharides. *Appl. Biochem. Biotechnol.* **2020**, *190*, 197–217, doi:10.1007/s12010-019-03076-0.

98. Ding, C.; Li, M.; Hu, Y. High-activity production of xylanase by Pichia stipitis: Purification, characterization, kinetic evaluation and xylooligosaccharides production. *Int. J. Biol. Macromol.* **2018**, *117*, 72–77, doi:10.1016/j.ijbiomac.2018.05.128.

99. Gómez-Ordóñez, E.; Jiménez-Escrig, A.; Rupérez, P. Molecular weight distribution of polysaccharides from edible seaweeds by high-performance size-exclusion chromatography (HPSEC). *Talanta* **2012**, *93*, 153–159, doi:10.1016/j.talanta.2012.01.067.

100. Gaborieau, M.; Castignolles, P. Size-exclusion chromatography (SEC) of branched polymers and polysaccharides. *Anal. Bioanal. Chem.* **2011**, *399*, 1413–1423, doi:10.1007/s00216-010-4221-7.

101. Tian, T.; Freeman, S.; Corey, M.; German, J.B.; Barile, D. Chemical Characterization of Potentially Prebiotic Oligosaccharides in Brewed Coffee and Spent Coffee Grounds. *J. Agric. Food Chem.* **2017**, *65*, 2784–2792, doi:10.1021/acs.jafc.6b04716.

102. Bowman, M.J.; Dien, B.S.; Vermillion, K.E.; Mertens, J.A. Structural characterization of (1→2)-β-xylose-(1→3)-α-arabinose-containing oligosaccharide products of extracted switchgrass (Panicum virgatum, L.) xylan after exhaustive enzymatic treatment with α-arabinofuranosidase and β-endo-xylanase. *Carbohydr. Res.* **2014**, doi:10.1016/j.carres.2014.08.006.

103. Suzuki, S. Recent developments in liquid chromatography and capillary electrophoresis for the analysis of glycoprotein glycans. *Anal. Sci.* **2013**, *29*, 1117–1128, doi:10.2116/analsci.29.1117.

104. Leijdekkers, A.G.M.; Sanders, M.G.; Schols, H.A.; Gruppen, H. Characterizing plant cell wall derived oligosaccharides using hydrophilic interaction chromatography with mass spectrometry detection. *J. Chromatogr. A* **2011**, *1218*, 9227–9235, doi:10.1016/j.chroma.2011.10.068.

105. Quéméner, B.; Ordaz-Ortiz, J.J.; Saulnier, L. Structural characterization of underivatized arabino-xylo-oligosaccharides by negative-ion electrospray mass spectrometry. *Carbohydr. Res.* **2006**, *341*, 1834–1847, doi:10.1016/j.carres.2006.04.039.

106. Xiao, X.; Wen, J.Y.; Wang, Y.Y.; Bian, J.; Li, M.F.; Peng, F.; Sun, R.C. NMR and ESI–MS spectrometry characterization of autohydrolysis xylo-oligosaccharides separated by gel permeation chromatography. *Carbohydr. Polym.* **2018**, *195*, 303–310, doi:10.1016/j.carbpol.2018.04.088.

107. Huang, Y.; Chen, H.; Zhang, K.; Lu, Y.; Wu, Q.; Chen, J.; Li, Y.; Wu, Q.; Chen, Y. Extraction, purification, structural characterization, and gut microbiota relationship of polysaccharides: A review. *Int. J. Biol. Macromol.* **2022**, *213*, 967–986, doi:10.1016/J.IJBIOMAC.2022.06.049.

108. Babbar, N.; Dejonghe, W.; Gatti, M.; Sforza, S.; Elst, K. Pectic oligosaccharides from agricultural by-products: production, characterization and health benefits. *Crit. Rev. Biotechnol.* **2016**, *36*, 594–606, doi:10.3109/07388551.2014.996732.

109. Reis, A.; Coimbra, M.A.; Domingues, P.; Ferrer-Correia, A.J.; Rosário, M.; Domingues, M. Structural characterisation of underivatised olive pulp xylo-oligosaccharides by mass spectrometry using matrix-assisted laser desorption/ionisation and electrospray ionisation. *Rapid Commun. Mass Spectrom.* **2002**, *16*, 2124–2132, doi:10.1002/rcm.839.

110. Park, Y.; Lebrilla, C.B. Application of Fourier transform ion cyclotron resonance mass spectrometry to oligosaccharides. *Mass Spectrom. Rev.* **2005**, *24*, 232–264, doi:10.1002/mas.20010.

111. Hofmann, J.; Hahm, H.S.; Seeberger, P.H.; Pagel, K. Identification of carbohydrate anomers using ion mobility-mass spectrometry. *Nature* **2015**, *526*, 241–244, doi:10.1038/nature15388.

112. Mu, Y.; Schulz, B.L.; Ferro, V. Applications of ion mobility-mass spectrometry in carbohydrate chemistry and glycobiology. *Molecules* **2018**, *23*, 2557, doi:10.3390/molecules23102557.

113. Both, P.; Green, A.P.; Gray, C.J.; Šardzík, R.; Voglmeir, J.; Fontana, C.; Austeri, M.; Rejzek, M.; Richardson, D.; Field, R.A.; et al. Discrimination of epimeric glycans and glycopeptides using IM-MS and its potential for carbohydrate sequencing. *Nat. Chem.* **2014**, *6*, 65–74, doi:10.1038/nchem.1817.

114. Wang, Z.W.; Zhu, M.Q.; Li, M.F.; Wang, J.Q.; Wei, Q.; Sun, R.C. Comprehensive evaluation of the liquid fraction during the hydrothermal treatment of rapeseed straw. *Biotechnol. Biofuels* **2016**, *9*, 142, doi:10.1186/s13068-016-0552-8.

115. Negahdar, L.; Delidovich, I.; Palkovits, R. Aqueous-phase hydrolysis of cellulose and hemicelluloses over molecular acidic catalysts: Insights into the kinetics and reaction mechanism. *Appl. Catal. B Environ.* **2016**, *184*, 285–298, doi:10.1016/j.apcatb.2015.11.039.

116. Luo, Y.; Li, Z.; Li, X.; Liu, X.; Fan, J.; Clark, J.H.; Hu, C. The production of furfural directly from hemicellulose in lignocellulosic biomass: A review. Catal. Today 2019, 319, 14–24, doi:10.1016/j.cattod.2018.06.042.la

CHAPTER 2

An enzymatic approach for isolation and quantification of soluble polysaccharides from complex matrices: extraction and characterization of exopolysaccharides from LAB fed with different sugars

Part of this chapter has also been published as:

Andrea Fuso, Elena Bancalari, Vincenzo Castellone, Augusta Caligiani, Monica Gatti, Benedetta Bottari (**2023**). Feeding Lactic Acid Bacteria with different sugars: effect on exopolysaccharides (EPS) production and their molecular characteristics. *Foods*, 12(1), 215.

ABSTRACT

Exopolysaccharides (EPS) are complex molecules produced by some microorganisms which can be employed in food as texturizers and stabilizers, and an association between their consumption and some positive effects on human health has also been reported. However, these properties attributed to EPS are strictly dependent on their chemical structure, in terms of monosaccharides composition, molecular weight, branching and charge. In this work, three different strains of wild lactic acid bacteria isolated from dairy products were tested for their ability to produce EPS by using different sugars (glucose, galactose, fructose, maltose and lactose) as the only carbon source. A method for EPS extraction and quantification was developed, based on AOAC 991.43 official method for dietary fibres quantification. Monosaccharides composition was performed after acid hydrolysis by GC-MS, whereas HPSEC-RID was used for determining the molecular weight. EPS amount significantly differenced both among different strains and when the same strain was fed with different sugars. A variability in sugars compositions and molecular weights of EPS was found depending on the strain and on the carbon source too. A significant co-precipitation of nitrogen containing compounds with EPS during extraction was observed.

1. Introduction

Lactic Acid Bacteria (LAB) are closely associated with humans since ancient times and all throughout history [1]. Nowadays LAB are receiving increasing attention due to their ability to ferment different matrices and to produce valuable compounds with an increased value. Among these, exopolysaccharides (EPS) are gaining interest due to their technological properties, such as the improvement of rheology and of mouth feel of food [2], and to their multiple effects on health, thanks to their immunoregulatory [3], cholesterol-lowering [4], antioxidant and antihypertensive functions [5]. For these reasons, EPS can be exploited in improving foods' technological characteristics but also to increase their nutritional value. To date, about 30 different LAB species are recognized as EPS-producers, the most known are: *Lacticaseibacillus paracasei, Lacticaseibacillus rhamnosus*, *Lactobacillus helveticus*, *Lactobacillus delbrueckii*, *Lactobacillus acidophilus*, *Latilactobacillus sakei* and *Lactiplantibacillus plantarum*, and many of them were isolated from traditional food matrices [6–13]. However, when it comes to the structure, the EPS produced by LAB can be very different from each other. First, EPS can be divided in two macro-categories, depending on the composition of the saccharidic chain, namely homo-polysaccharides (HoPS) and hetero-polysaccharides (HePS). The former are made of the same monosaccharide repeating unit, show a linear and bigger structure (> 10^6 Da), do not present charge and are primarily associated with prebiotic effects [4,14,15], while HePS are smaller (10^4-10^6 Da), they present two or more sugar moieties in a linear or branched chain and may have non-carbohydrates residues in their composition, including charged groups. Therefore, it is widely recognized that different LAB species are able to produce a wide variety of structurally different EPS, having different structure, size or functional groups and thus with diverse functions and multiple possible applications [16,17]. Nowadays the production of EPS is mainly achieved by feeding LAB with industrial by-products and media rich in sucrose [18]. Despite it is generally accepted that for bacteria EPS production and composition is gene-driven and not affected by cultural factors [19], recently many studies have proven the ability of LAB of adapting to different media and change their behaviors according to the medium characteristics, resulting also in a modification of the quantity and quality of the polymeric substances produced [20–23]. Glucose seemed to be the best solution to increase the production for different microorganisms, while on the other hand fructose has been reported to reduce EPS' production with respect to control media [24]. As an example, *L. delbrueckii* subsp. *bulgaricus* NCFB 2722 has proven to produce higher amounts of EPS when grown in media containing glucose or lactose with respect to media containing fructose [25]. Cheng et al. [26] measured the EPS production of *L. plantarum* LPC-1 on media containing glucose, sucrose or a mix of both sugars and their results suggest the effect of sucrose in increasing EPS' production and in modifying the molecular structure, leading to a higher level of antioxidant activity [26]. These findings seem to suggest that it is possible to modulate the EPS production and structure and therefore their properties by feeding different sugars to specific LAB strains. However, more data are needed to better elucidate the complex relationship

among LAB strain, carbon source, EPS structure and activity. Moreover, once the combination strain-medium composition has been chosen, it is also necessary to evaluate an appropriate extraction technique in order to isolate the polysaccharide fraction as pure as possible for molecular characterization. To date, many different protocols have been proposed for EPS extraction and among these are physical methods, such centrifugation, sonication and heating, and chemical methods, employing sodium hydroxide, EDTA or ion exchange resin [27]. The most efficient methods are those involving the use of centrifugation, in order to remove bacterial cells, followed by organic solvent precipitation, in most cases ethanol [28]. Sometimes, precipitation with ethanol is preceded by another step, useful to remove proteins and enhance the purity degree, that is the employment of trichloroacetic acid, but sometimes also EDTA or trypsin [29] or again the purification step may be performed on the pellet, with different techniques such dialysis [30], enzymes employment or reprecipitation of the polymer from diluted aqueous solution [31]. Finally, also tangential ultrafiltration has been often used as an alternative to conventional extraction of EPS, especially those produced by microalgae, but some drawbacks has been attributed to this technique because of the high viscosity of solutions resulting in the clogging of membranes [32]. However, most of the methods result in low-purity or modification of EPS structure, especially when thermal or chemical treatments are applied.

To contribute in this field, in the present study an extraction method based on AOAC 991.43 was applied for EPS extraction from LAB strains, in the optic to develop a method applicable to any food matrix containing EPS, limiting as much as possible the modification of the polysaccharide extracted. EPS were obtained from three LAB strains belonging to the EPS's producer species and commonly found in dairy products. In particular, *L. delbrueckii* represents one of the most commonly used starter species in cheese and yoghurt [33], while *L. paracasei and L. rhamnosus* are known for their importance as non-starter strains in ripened cheeses and their potential health benefits [34,35]. Each LAB was fed with five different individual sugars (sucrose, glucose, lactose, fructose and maltose), representative of the main simple sugars that can be found in different food matrices as vegetables, dairy, cereals etc., with the aim to understand how and whether the strain and the variation of the carbon source may affect EPS yield and its chemical structures.

2. Material and methods

2.1. Bacterial strains, growth conditions and media

Three wild LAB strains, namely *L. bulgaricus* 1932, *L. rhamnosus* 1019, and *L. paracasei* 2333, previously isolated from dairy matrices and belonging to the microbial collection of the Department of Food and Drug of the University of Parma (UPCC), were tested. Modified MRS medium (mMRS) was used as basic EPS production medium. mMRS was prepared according to Degeest et al. [36]. The carbon sources consisting of fructose (FRU), glucose (GLU), lactose (LAC), maltose (MAL), and sucrose (SUC) (Merck, Darmstadt, Germany)

were prepared as a concentrated water solution, sterilized separately from the medium, and then properly added to each bottle of mMRS to a final concentration of 5%. Cells were inoculated in 6 mL of the five different aliquots of mMRS broths prepared with the five different sugars and cultured at 37 °C in anaerobiosis. After 20 hours of incubation the cells were diluted to a final concentration of $1x10^7$ CFU/ml and used to inoculate 200 mL of media that were incubated in anaerobiosis at 37 °C, then used for EPS extraction and chemical analysis.

2.2. EPS extraction and quantification

The total EPS content produced by the strains in the five different mMRS was determined by the AOAC 991.43 official enzymatic-gravimetric method for dietary fibres [37]. The analysis was carried out in 20 mL of sample in triplicate. Residual ash in extracted fibres was determined through mineralization at 550 °C for 5 h, while residual nitrogen was determined using a Kjeldahl system (DKL heating digestor and UDK 139 semiautomatic distillation unit, VELP SCIENTIFICA).

The same enzymatic-gravimetric method, with few modifications, was also used for the EPS extraction, in order to enable further analysis on their chemical structure. After letting 20 mL of culture broth to react with heat-stable α-amylase, protease and amyloglucosidase in the quantities reported by the aforementioned official method, EPS were precipitated by adding four volumes of 96% ethanol. Then, the solution was centrifuged at 3900 rpm, at 4 °C for 30 minutes and the pellet was washed twice with ethanol and finally dried overnight at 40 °C in an oven.

2.3. EPS monosaccharide composition and quantification analysis through Gas Chromatography-Mass Spectrometry (GC-MS)

The EPS monosaccharide composition was investigated following two different protocols. The first was employed in order to detect neutral and acid sugars, following a method previously proposed by Xia et al. with some modifications [38]. Here, 10 mg of EPS sample were dissolved in 3 mL of 2N trifluoroacetic acid (TFA) and hydrolysed at 110 °C for 2 hours. Then, an aliquot of the solution was withdrawn and put together with 125 µL of 1190 ppm phenyl-β-D-glucopyranoside, used as internal standard, and then evaporated by rotavapor. The obtained dried hydrolysate was washed with 1 mL of methanol to remove the residue of TFA and evaporated again. 1 mL of 0.5 M NH_4OH was subsequently added to delactonize the eventually present acid sugar lactones in the sample, and again evaporated by rotavapor. Finally, the dried hydrolysate was dissolved in 800 µL of dimethylformamide (DMF) and 200 µL of N,O-Bis(trimethylsilyl)trifluoroacetamide (BSTFA), the latter used as derivatizing agent. The reaction was held for 1 hour at 60 °C and then the derivatized sample was injected in gaschromatography.

The second protocol was used with the aim of detecting amino sugars by acid hydrolysis with hydrochloric acid. Briefly, 10 mg of sample were dissolved in 6 mL of 7 N HCl and kept for 4 hours at 110 °C. Later, an aliquot was added to 125 µL of 1190 ppm phenyl-β-D-glucopyranoside and they were together evaporated. As in the first method, 800 µL of DMF and 200 µL of BSTFA were subsequently added, the reaction was held at 60 °C for 1 h and the solution was ready to be injected.

GC-MS analysis of monosaccharides was performed with a 6890 N gas chromatograph coupled to a 5973 N mass selective detector (Agilent technologies, Santa Clara, CA). A SLB-5ms, 30 m × 0.25 mm, 0.25 µm thickness column (Supelco, Bellafonte, PA, USA) was used. The chromatogram was recorded in the scan mode (40–500 m/z) with a programmed temperature from 60 °C to 270 °C. The initial temperature was 60 °C, held for 2 minutes, then increased to 160 °C at a rate of 10 °C/min, held isothermal for 5 minutes, increased to 220 °C at a rate of 10 °C/min, kept for 5 minutes, increased to 270 °C at a rate of 20 °C/min and maintained for 5 minutes. Quantification was performed with a response factor, considering the area and concentration ratios between the internal standard (phenyl-β-D-glucopyranoside), and the following monosaccharides: D-glucose, D-fructose, D-galactose, D-mannose, D-rhamnose, D-ribose, D-xylose, D-fucose, D-galacturonic acid, D-glucuronic acid, D-glucosamine and D-galactosamine.

2.4. Evaluation of EPS molecular weight through HPSEC-RID

The molecular weight of EPS produced by the selected strains was investigated through high-performance size-exclusion chromatography (HPSEC), with an Agilent 1260 Infinity II LC system equipped with a refractive index detector (RID) (Agilent, Santa Clara, CA, USA). The EPS extracted from the culture broth (Paragraph 2.4), were dissolved in ultrapure water at a concentration of 10 mg/mL. Later, the solutions were filtered through a 0.45 µm membrane. A 50 mM NaCl aqueous solution was used as mobile phase at a flow rate of 1 mL/min and a PL aquagel-OH MIXED-M column, 7.5 x 300 mm, 8 µm (Agilent, Santa Clara, CA, USA) was employed to separate the different molecular weight fractions. The injection sample volume was set at 100 µL, column temperature 30 °C and RID temperature 35 °C. Standard pullulans having known molecular weight were purchased from Agilent (Santa Clara, CA, USA) and used for the calibration curve.

2.5. Determination of EPS amino acid profile through UPLC/ESI-MS

The total amino acid profile was evaluated in a representative EPS sample in triplicate, following the protocol proposed by Caligiani et al. with some modifications [39]. An amount of 40 mg of EPS previously extracted from culture broth was hydrolysed with 6 mL of 6 M HCl for 23 hours at 110 °C, then the internal standard (7.5 mL of 5 mM Norleucine in 0.1 M HCl) was added. The solution was subsequently filtered through filter paper and diluted to a final volume 250 mL. Finally, the amino acids contained in the solution were

derivatized with 6-aminoquinolyl-N-hydroxysuccinimidyl carbamate (AQC) and analysed by ultra-performance liquid chromatography with electrospray ionization and mass spectrometry detector (UPLC/ESI-MS, WATERS ACQUITY). In detail, UPLC/ESI-MS analysis was performed with an ACQUITYUPLC separation system with an Acquity BEH C18 column (1.7 µm, 2.1 × 150 mm). The mobile phase was composed of H2O + 0.2% CH3CN +0.1% HCOOH (eluent A) and CH3CN + 0.1% HCOOH (eluent B). Gradient elution was performed as follows: isocratic 100% A for 7 min, from 100% A to 75.6% A and 24.4% B by linear gradient from 8 to 28 min, isocratic 100% B from 29 to 32 min, isocratic 100% A from 33 to 45 min. The flow rate was set at 0.25 mL/min, injection volume 2 µL, column temperature 35 °C and sample temperature 18 °C. Detection was performed by using Waters SQ mass spectrometer: the ESI source was in positive ionization mode, capillary voltage 3.2 kV, cone voltage 30 V, source temperature 150 °C, desolvation temperature 300 °C, cone gasflow (N2) 100 L/h, desolvation gas flow (N2) 650 L/h, full scan acquisition (270–518 m/z) and scan duration 1 s. Calibration was performed with standard solutions prepared mixing norleucine, amino acids hydrolysate standard mixture and deionized water.

2.6. Statistical analysis

All the calculated parameters (amount of EPS produced, relative percentage of monosaccharides and percentage of various EPS fractions with different molecular weights) were compared each other through Pearson correlation by employing IBM SPSS software version 21.0 (SPSS Inc., Chicago, IL, USA). Significant correlations were considered for values > 0.6 and < -0.6. Moreover, a one-way analysis of variance (ANOVA) with Tukey's post-hoc test was applied with the same software at a confidence level of 95 % (p-value = 0.05) in order to determine significant differences among the amounts of EPS produced in the various experiments.

3. Results and discussion

3.1. EPS isolation, quantification and evaluation of the degree of purity

The ability of the strains to produce EPS was assessed by quantifying EPS through an enzymatic-gravimetric method, that is the official method for dietary fibers quantification in complex samples (Paragraph 2.2). This method, thanks to the employment of enzymes able to hydrolyze both starch and proteins and thanks to the fact that considers residual nitrogen and ash, allows to obtain a more accurate quantification respect to others that are based on only weighing after the precipitation with ethanol. To the best of our knowledge, this method is not commonly employed for the quantification and isolation of EPS from complex matrices,

despite its undoubtful advantages also in terms of purity of the fraction extracted. Results of the quantification of EPS produced from each strain using different sugars (Table 2.1) showed that all the strains were able to produce EPS with any sugar, but interestingly the maximum quantity of EPS was not always achieved by using sucrose as unique carbon source. Up to nowadays, most of the literature has reported the addition of sucrose to the growth media as an effective method to maximize the EPS production by LAB [40], however our results seem not supporting the correlation sucrose-EPS formation [41].

Table 2.1: *Amount of EPS produced by tested microorganisms with different carbon sources, expressed as g l^{-1} culture broth, and percentage of residual nitrogen within EPS. Different letters indicate significant differences in the EPS amount ($p < 0,05$).*

Strain	**Sugar added**	EPS amount (g/L, ash and protein free)	Residual Nitrogen in the crude extract (%)
***L. paracasei* 2333**	fru	1.51 ± 0.24 bc	9.7
	mal	2.38 ± 0.13 d	7.5
	suc	0.71 ± 0.01 a	9.5
	lac	1.76 ± 0.15 bcd	10.4
	glu	1.52 ± 0.23 bc	10.2
***L. rhamnosus* 1019**	fru	1.77 ± 0.59 bcd	7.6
	mal	1.50 ± 0.38 bc	8.5
	suc	1.21 ± 0.21 ab	10.3
	lac	2.05 ± 0.14 cd	10.1
	glu	1.49 ± 0.08 bc	9.2
***L. delbrueckii bulgaricus* 1932**	fru	1.80 ± 0.24 bcd	9.3
	mal	1.32 ± 0.08 ab	9.7
	suc	1.75 ± 0.08 bcd	9
	lac	1.80 ± 0.09 bcd	9.1
	glu	1.28 ± 0.18 ab	10.2

Furthermore, it has been possible to observe a great variability both in terms of amount of EPS produced by the different strains, but also at strain level. From Table 2.1 it is possible to observe that by employing maltose, *L. paracasei* 2333 turned out to be the best EPS producer in terms of quantity as compared to the other two strains in the same conditions. It is interesting to note, as highlighted above, that this strain showed the lowest EPS production when sucrose was the only carbon source used, compared to the other four sugars. A similar behavior was observed for the strain *L. rhamnosus* 1019, that produced a low amount of EPS when grown in mMRS with sucrose, though non significantly different compared to the growth in mMRS with fructose, maltose and glucose. On the contrary, this quantity was found to be significantly lower than the one found when *L. rhamnosus* 1019 was grown in mMrs with lactose. Finally, *L. delbrueckii bulgaricus* 1932 led to the obtaining of non-significantly different amounts of EPS starting from all the feeding sugars.

Globally, these results show that different strains may have different behaviors when are fed with different sugars also in EPS production, underlining the importance to apply also for exopolysaccharides a robust method of quantification.

An interesting aspect, however, concerns the high residual amount of nitrogen in isolated EPS, indicating a low degree of purity, despite the use of the official method for soluble fiber quantification. The percentage of nitrogen in the crude extract came out to be variable in the range between 7.5 and 10.4% (Table 2.1). In the official method for the quantification of total dietary fiber [42], that has been used in this work, the use of a bacterial protease is foreseen, among other enzymes, in order to hydrolyse proteins present in the sample. Because of this, it is not very plausible that this nitrogen value was attributable exclusively to the non-hydrolysed proteins and/or peptides co-precipitated together with the polysaccharide fraction. For this reason, to better clarify the residual protein amount, the amino acid analysis was carried out on a representative EPS sample, in triplicate. The results are reported in Table 2.2.

Table 2.2: *Amino acid profile and total protein content of EPS produced by L. paracasei 2333 grown with glucose as the only carbon source.*

	mg anhydrous AA/100 mg EPS	Relative distribution (g/100g protein)
ala	1.02 ± 0.01	6.36 ± 0.05
asp+asn	2.01 ± 0.06	12.52 ± 0.56
arg	1.19 ± 0.06	7.38 ± 0.30
gly	0.84 ± 0.01	5.21 ± 0.06
his	1.01 ± 0.01	6.32 ± 0.13
ile	0.69 ± 0.01	4.32 ± 0.01
leu	0.88 ± 0.04	5.50 ± 0.17
met	0.48 ± 0.01	3.01 ± 0.12
phe	0.91 ± 0.03	5.65 ± 0.28
pro	0.71 ± 0.01	4.43 ± 0.15
ser	0.80 ± 0.05	4.98 ± 0.36
thr	0.85 ± 0.02	5.30 ± 0.20
val	0.73 ± 0.02	4.55 ± 0.05
lys	1.01 ± 0.34	6.27 ± 2.06
tyr	0.72 ± 0.01	4.51 ± 0.07
glu+gln	2.20 ± 0.07	13.69 ± 0.61
Total protein content (%)	16.06 ± 0.14	-
Total amino acids (%)	18.70 ± 0.16	-

As can be seen from Table 2.2, the total protein content was quite high, probably indicating an incomplete hydrolysis by the protease. This could be due to some structural interactions between proteins and EPS [43], which make the action of the enzyme partially ineffective. In any case, if we consider the classic nitrogen-to-protein conversion factor, namely 6.25, the sum of proteins and amino acid in the sample of the EPS analysed

(equal to 18.70 %, Table 2.2) would correspond to a percentage of nitrogen equal to 3%, which is rather far from the actual nitrogen quantity in the crude extract (Table 2.1). A more accurate result can be obtained by using as conversion factor 5.43, calculated on the specific amino acid composition reported in Table 2.2, corresponding to a percentage of nitrogen approximately equal to 3.5%. This still means that a large portion of nitrogen of a non-protein nature is present, which is probably partially due to the triammonium citrate present as an ingredient in the broth, which could co-precipitate together with the EPS after the addition of ethanol. Furthermore, other nitrogenous compounds could be present, such as phospholipids or nucleic acids [44], and within the polysaccharide chain also amino sugars give their contribution, even if partial (Paragraph 3.2). Therefore, for a more accurate quantification of EPS, it would be appropriate to identify and quantify each of these individual nitrogen compounds, calculate each nitrogen conversion factor and then subtract proportionally. In this case, it was decided to keep 6.25 as the average conversion factor, but this specific case is quite illustrative of how approximate it is to use this value, as has already been reported in the literature for a long time [45]. This is true not only for protein quantification, but the uncertainty can be also extended to dietary fiber quantification, especially when the co-precipitated nitrogen amount is high and of unpredictable origin.

Moreover, this result highlights the complete inaccuracy of the methods for EPS quantification and isolation based only on physical treatments or ethanol precipitation, due to the strong link between EPS and proteins or other nitrogen containing compounds.

3.2. EPS monosaccharide composition

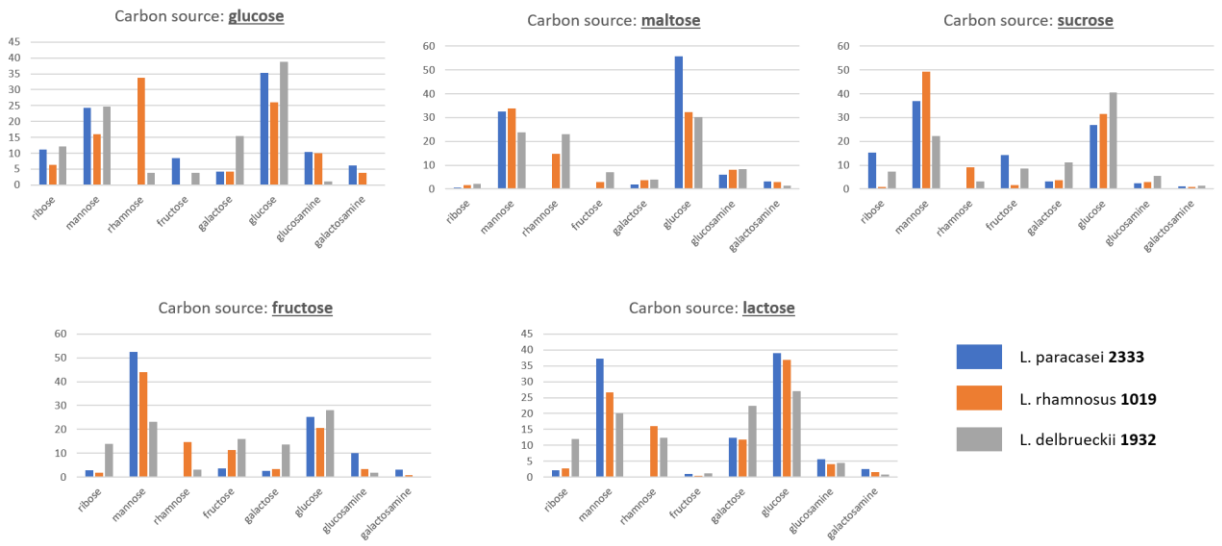

***Figure 2.1**: Monosaccharide composition (expressed as relative percentages) of EPS produced by three LAB strains fed with five different sugars.*

The monosaccharide composition (Figure 2.1) of EPS produced by the three selected strains fed with the five sugars was also determined on the fraction isolated according to the enzymatic method as reported in Paragraph 2.2. All the EPS contained glucose, mannose, galactose, fructose, ribose, glucosamine and galactosamine as principal sugars. *L. rhamnosus* 1019 and *L. bulgaricus* 1932 produced EPS containing also rhamnose, with *L. rhamnosus* 1019 being able to include this sugar in the EPS chain with average quantities that are twice as much as those found in the EPS made by *L. bulgaricus* 1932 (17.6% and 9%, respectively), when fed with all the sugars but maltose. On the contrary, *L. paracasei* 2333, regardless of the carbon source it was fed with, was unable to include rhamnose within the polysaccharide chain, probably due to the lack of gene clusters encoding for the production of this sugar [46]. Rhamnose was observed to be uncommon in EPS produced by lactobacilli in Zeidan et al. [8] that reports the presence of this sugar only for some strains of *L. bulgaricus* and *L. rhamnosus,* in agreement with our results. Except for this clear difference, the other sugars were inserted in all the EPS chains in similar, albeit variable, quantities. All the three strains produced EPS consisting mostly of glucose and mannose, regardless of the carbon source added to the growth medium. The sum of mannose and glucose, expressed as a relative percentage of total sugars, was found to range between 42 % and 88 %, with an average of 64 %, suggesting that despite the presence of other hexoses and pentoses, the EPS produced were mainly classifiable as glucomannans [47–49]. In particular, mannose was found to be present in greater quantities when fructose was present as a carbon source, both as it is and when present within sucrose. This correlation is supported by the fact that mannose and fructose are metabolically close, with only one metabolic step between them [50]. These results are quite in agreement with the literature, where glucose, galactose, mannose, rhamnose, glucosamine and galactosamine are reported to be always the most frequent monosaccharides in LAB's EPS [51]. However, in some cases, fructose [52] and ribose [53] have also been found as monosaccharides constituting the LAB-produced EPS chain. As concerns ribose, in the present study, it showed considerable variations within the EPS produced by the same strain that have been fed with different carbon sources: *L. paracasei* 2333 originated amounts of ribose varying between 0.5 and 15.3%, *L. rhamnosus* 1019 between 0.9 and 6.3% and *L. bulgaricus* 1932 between 2.1 and 13.8%. The highest concentrations were almost always found when glucose was used as feed. Fructose, on the other hand, was variable between 0 and 14.3%, between 0 and 11.3% and between 1.1 and 16.1% within the EPS produced by *L. paracasei* 2333, *L. rhamnosus* 1019 and *L. bulgaricus* 1932 respectively, depending on the fed carbon source. Generally, fructose showed the highest concentrations when fructose itself was used as a carbon source. Galactose also showed considerable variability. It was particularly abundant in the EPS produced by *L. bulgaricus* 1932, with an average amount 2.5 times higher than that produced by the other two strains. Furthermore, also the carbon source influenced the quantities again: in fact, the largest amount was found when the three strains were grown on lactose, which is the only galactose-containing carbon source among the selected ones, and the lowest quantities have been found

when maltose was employed as feed. Finally, glucosamine and galactosamine were always found but in relatively low quantities, ranging between 1.2 and 10.4% and between 0.1 and 6.1%, respectively. The presence of amino sugars in the EPS chain is actually of great importance, because of their characteristic electric charge. In fact, when this latter is present on the EPS it may cause, depending on the ionic strength, an increase in the intramolecular repulsion forces and therefore a consequent increase in the hydrodynamic volume and intrinsic viscosity [54].

3.3. EPS molecular weight (Mw)

The molecular weight of EPS produced in the various experiments was investigated by size-exclusion chromatography coupled with a refractive index detector (HPSEC-RID). Results are reported in Table 2.3.

***Table 2.3**: Molecular weight profile (expressed as relative percentages of total chromatographic area) of EPS produced by three LAB strains, fed with five different carbon sources.*

		Area (%)				
Strain	**Carbon source**	Fraction 1 (> 500 kDa)	Fraction 2 (130–200 kDa)	Fraction 3 (40 – 65 kDa)	Fraction 4 (8 – 25 kDa)	Fraction 5 (< 10 kDa)
***L. paracasei* 2333**	Fructose	-	7	38	56	-
	Glucose	-	9	37	54	-
	Lactose	-	6	41	52	-
	Maltose	-	5	42	53	-
	Sucrose	-	4	44	40	12
***L. rhamnosus* 1019**	Fructose	-	10	42	47	-
	Glucose	-	8	34	57	-
	Lactose	5	17	36	42	-
	Maltose	-	6	36	57	-
	Sucrose	4	10	25	29	32
***L. bulgaricus* 1932**	Fructose	16	4	61	19	-
	Glucose	15	3	29	23	30
	Lactose	18	3	24	20	36
	Maltose	-	11	32	48	9
	Sucrose	15	5	47	32	-

First, it can be noted that all the selected strains gave rise to HePS having different fractions of different Mw, as often happens for LAB-deriving HePS [55]. *L. paracasei* 2333 produced EPS that are always very similar to each other, regardless of the carbon source used. In particular, three different fractions having Mw between 10 and 200 kDa emerged in all the experiments, and always in very similar proportions. The highest Mw fraction (130 - 200 kDa) was produced in relatively small amounts, corresponding to 4-9% of the total EPS. On the contrary, the two most abundant fractions were the third and the fourth one, having smaller Mw variable in the range 10 - 65 kDa, which constituted 84-95% of the total. When sucrose was used as a carbon

source, another very small fraction with Mw lower than 10 kDa was detected, and it was equal to 12% of the total EPS.

L. *rhamnosus* 1019, as well as *L. paracasei* 2333, produced EPS which were mainly represented by medium-Mw fractions, which together represent 78-94% of the total EPS for four out of five sugars. The most peculiar case was found again when *L*. *rhamnosus* 1019 was fed with sucrose, since an abundant low-Mw fraction equal to 4 kDa was detected, representing 32% of the total. Furthermore, in two experiments, when sucrose and lactose were added as the only carbon source, even a high-Mw fraction (> 500 kDa) was detected, albeit in low quantities.

L. bulgaricus 1932 was the strain that behaved in the most different way compared to the others: although it also always produced EPS with abundant medium-Mw fractions, they were less abundant, and their sum was 43-80%. The presence of the high-Mw fraction was also detected, in quantities ranging between 15 and 18%, when the strain was grown on all the carbon source except maltose. Furthermore, when maltose, glucose and lactose were added to the growth medium, EPS produced by *L. bulgaricus* 1932 were characterized also by the smallest fraction (< 10 kDa) which represented 9, 30 or 36% of the total EPS.

From these results, it appears that the Mw profile of the EPS is mainly dependent on the bacterial strain. However, in several cases, it was found out that the carbon source has an influence on this feature too, although not always predictable and constant. This agrees with a study by Polak-Berecka and colleagues, where a *L*. *rhamnosus* strain, fed with five different carbon sources, produced EPS having different Mw [56]. On the other hand, in that study, the absolute values of EPS molecular fractions were very far from those obtained in our work, confirming that this structural peculiarity is mainly related to the selected strain. In general, the Mw of LAB's He-EPS that are reported in the literature vary from 10^4 to 10^6 Da [20]. Our values fall within this range, with the only exception of fraction 5, having Mw < 10 kDa. Actually, it must be specified that many authors perform an ultrafiltration step (10 kDa cut-off) before analysing the Mw of the considered EPS [57], thus preventing the detection of that fraction. However, the presence of low-Mw EPS can be considered an element of further valorization for the producing strains because these EPS have been reported to be more effective in terms of antioxidant activity [58]. Conversely, the high-Mw fractions detected in some samples (and originated especially by *L*. *bulgaricus* 1932) may have an interesting potential for technological and functional activities related to viscosity. In fact, the positive correlation between Mw of EPS and induced viscosity is now well known [59], so as it is for the relation between an increase in viscosity and better cholesterol-lowering and antimicrobial properties [51].

3.4. Correlation analysis among EPS molecular characteristics

With the aim to gain more information on the different EPS structure, a correlation analysis among all the molecular data collected in this study was performed. In Table 2.4 the correlation matrix among EPS chemical characteristics (yield, monosaccharides composition and molecular weight distribution), is presented, independently from the feeding sugars. Colored cells represent data with a negative (red) or positive (green) correlation score higher than 0.6, indicating a strong link between the examined variables.

No significant correlation was found among monosaccharide composition, except for the positive correlation found between glucosamine and galactosamine, indicating that the inclusion of positively charged sugars in the EPS chain is made utilizing both amino sugar epimers.

The most interesting data emerged from this correlation analysis is the link between some specific molecular weight EPS fractions and the presence of some monosaccharides. These significant correlations permit to infer more information about the distribution of monosaccharides in the EPS of different molecular weights. More in detail, fraction 1 is positively correlated with galactose, meaning that EPS > 500 kDa contained this monosaccharide. The presence of galactose was the highest in the EPS produced by *L. bulgaricus* 1932 (Figure 2.1), that were also the EPS with the highest Mw. It can therefore be speculated that *L. bulgaricus* is characterized by the ability to produce EPS with a larger molecular size and that these EPS contain galactose. Positive correlation can be observed between EPS' fraction 3 and fructose, which in turn is abundant in EPS when fructose sources are present in the feeding sugars. As that fraction includes Mw ranging between 40 and 65 kDa, this result suggest that LAB produce medium to small size EPS when fructose is the available carbon source. EPS' fraction 4 is negatively correlated with galactose and positively correlated with glucosamine and galactosamine. This fraction comprises EPS with a Mw between 8 and 25 kDa. These correlations suggest the presence of charged HePS in this Mw range.

Table 2.4: *Correlation matrix of factors involved in EPS production and composition. "Fraction" represents different groups of EPS at different molecular mass: Fraction 1 (> 500 kDa), Fraction 2 (130 - 200 kDa), Fraction 3 (40 - 65 kDa), Fraction 4 (8 - 25 kDa), Fraction 5 (< 10 kDa).*

** Correlation is significant at a 0,05 level.*

*** Correlation is significant at a 0,01 level.*

Correlations	EPS g/L	Ribose	Mannose	Rhamnose	Fructose	Galactose	Glucose	Glucosamine	Galactosamine	Fraction1	Fraction2	Fraction3	Fraction4	Fraction5
EPS g/L	1	-0.382	-0.180	-0.032	-0.346	0.230	0.503	0.076	0.126	0.145	0.151	0.229	0.084	-0.369
Ribose	-0.382	1	-0.468	-0.268	,549*	0.464	-0.218	-0.340	-0.191	,555*	-,534*	0.229	-,560*	0.294
Mannose	-0.180	-0.468	1	-0.371	0.002	-0.489	-0.168	-0.071	-0.038	-0.463	0.127	-0.038	0.243	-0.009
Rhamnose	-0.032	-0.268	-0.371	1	-0.286	-0.088	-0.395	0.279	-0.022	-0.155	0.440	-0.368	0.193	-0.003
Fructose	-0.346	,549*	0.002	-0.286	1	-0.084	-0.388	-0.325	-0.291	0.152	-0.210	,672**	-0.283	-0.195
Galactose	0.230	0.464	-0.489	-0.088	-0.084	1	0.031	-0.457	-0.474	,850**	-0.311	-0.081	-,726**	0.457
Glucose	0.503	-0.218	-0.168	-0.395	-0.388	0.031	1	-0.024	0.215	0.034	-0.105	0.057	0.079	-0.115
Glucosamine	0.076	-0.340	-0.071	0.279	-0.325	-0.457	-0.024	1	,848**	-,541*	0.219	-0.165	,778**	-0.472
Galactosamine	0.126	-0.191	-0.038	-0.022	-0.291	-0.474	0.215	,848**	1	-,585*	0.161	-0.070	,762**	-0.484
Fraction1	0.145	,555*	-0.463	-0.155	0.152	,850**	0.034	-,541*	-,585*	1	-0.431	0.069	-,893**	0.483
Fraction2	0.151	-,534*	0.127	0.440	-0.210	-0.311	-0.105	0.219	0.161	-0.431	1	-0.203	0.342	-0.272
Fraction3	0.229	0.229	-0.038	-0.368	,672**	-0.081	0.057	-0.165	-0.070	0.069	-0.203	1	-0.015	-,669**
Fraction4	0.084	-,560*	0.243	0.193	-0.283	-,726**	0.079	,778**	,762**	-,893**	0.342	-0.015	1	-,667**
Fraction5	-0.369	0.294	-0.009	-0.003	-0.195	0.457	-0.115	-0.472	-0.484	0.483	-0.272	-,669**	-,667**	1

4. Conclusions

The enzymatic method for dietary fibre quantification was adapted and proposed as universal methodology for the isolation and purification of EPS from complex matrices. By analysing the isolated EPS produced by three different LAB strains fed with five different sugars, we concluded that EPS amount significantly differed both among different strains and when the same strain was fed with different sugars.

An important point emerged from this work, related to the methodology used for extraction and quantification of EPS. Despite the use of the official method for dietary fibres quantification to isolate EPS, an unusual amount of residual co-precipitating nitrogen compounds was observed. A big portion of nitrogen comes from proteins, highlighting their strict interaction with exopolysaccharides and the need of using proteases to better purify EPS fraction. The use of amylolytic enzymes could be instead of particular relevance to purify EPS released by LAB in cereal-based products, as for example in sourdough fermentation.

Finally, an extreme variability in sugars compositions and molecular weights of EPS was also observed, depending on the strain and the carbon source too. These strong differences suggest that is of outmost importance to determine the molecular structure of EPS, because differences in terms of monosaccharide composition and Mw fraction could in turn differently impact on their nutritional and technological properties.

REFERENCES

1. Lynch, K.M.; Zannini, E.; Coffey, A.; Arendt, E.K. Lactic Acid Bacteria Exopolysaccharides in Foods and Beverages: Isolation, Properties, Characterization, and Health Benefits. *Annu. Rev. Food Sci. Technol.* **2018**, *9*, 155–176, doi:10.1146/annurev-food-030117-012537.

2. Patel, S.; Majumder, A.; Goyal, A. Potentials of Exopolysaccharides from Lactic Acid Bacteria. *Indian J. Microbiol.* **2012**, *52*, 3–12, doi:10.1007/s12088-011-0148-8.

3. Zhu, Y.; Wang, X.; Pan, W.; Shen, X.; He, Y.; Yin, H.; Zhou, K.; Zou, L.; Chen, S.; Liu, S. Exopolysaccharides produced by yogurt-texture improving Lactobacillus plantarum RS20D and the immunoregulatory activity. *Int. J. Biol. Macromol.* **2019**, *121*, 342–349, doi:10.1016/j.ijbiomac.2018.09.201.

4. Korcz, E.; Kerényi, Z.; Varga, L. Dietary fibers, prebiotics, and exopolysaccharides produced by lactic acid bacteria: Potential health benefits with special regard to cholesterol-lowering effects. *Food Funct.* **2018**, *9*, 3057–3068, doi:10.1039/c8fo00118a.

5. Saadat, Y.R.; Khosroushahi, A.Y.; Gargari, B.P. A comprehensive review of anticancer, immunomodulatory and health beneficial effects of the lactic acid bacteria exopolysaccharides. *Carbohydr. Polym.* **2019**, *217*, 79–89.

6. Slattery, C.; Cotter, P.D.; O'Toole, P.W. Analysis of health benefits conferred by Lactobacillus species from kefir. *Nutrients* **2019**, *11*, 1–24, doi:10.3390/nu11061252.

7. Xiao, L.; Xu, D.; Tang, N.; Rui, X.; Zhang, Q.; Chen, X.; Dong, M.; Li, W. Biosynthesis of exopolysaccharide and structural characterization by Lacticaseibacillus paracasei ZY-1 isolated from Tibetan kefir. *Food Chem. Mol. Sci.* **2021**, *3*, 100054, doi:10.1016/j.fochms.2021.100054.

8. Zeidan, A.A.; Poulsen, V.K.; Janzen, T.; Buldo, P.; Derkx, P.M.F.; Øregaard, G.; Neves, A.R. Polysaccharide production by lactic acid bacteria: from genes to industrial applications. *FEMS Microbiol. Rev.* **2017**, *41*, S168–S200, doi:10.1093/femsre/fux017.

9. Nowak, B.; Śróttek, M.; Ciszek-Lenda, M.; Skałkowska, A.; Gamian, A.; Górska, S.; Marcinkiewicz, J. Exopolysaccharide from Lactobacillus rhamnosus KL37 Inhibits T Cell-dependent Immune Response in Mice. *Arch. Immunol. Ther. Exp. (Warsz).* **2020**, *68*, 1–11, doi:10.1007/s00005-020-00581-7.

10. Li, B.; Du, P.; Smith, E.E.; Wang, S.; Jiao, Y.; Guo, L.; Huo, G.; Liu, F. In vitro and in vivo evaluation of an exopolysaccharide produced by Lactobacillus helveticus KLDS1.8701 for the alleviative effect on oxidative stress. *Food Funct.* **2019**, *10*, 1707–1717, doi:10.1039/c8fo01920g.

11. Tang, W.; Zhou, J.; Xu, Q.; Dong, M.; Fan, X.; Rui, X.; Zhang, Q.; Chen, X.; Jiang, M.; Wu, J.; et al. In vitro digestion and fermentation of released exopolysaccharides (r-EPS) from Lactobacillus delbrueckii ssp. bulgaricus SRFM-1. *Carbohydr. Polym.* **2020**, *230*, 115593, doi:10.1016/j.carbpol.2019.115593.

12. Wang, B.; Song, Q.; Zhao, F.; Han, Y.; Zhou, Z. Production optimization, partial characterization and properties of an exopolysaccharide from Lactobacillus sakei L3. *Int. J. Biol. Macromol.* **2019**, *141*, 21–28, doi:10.1016/j.ijbiomac.2019.08.241.

13. Xu, Y.; Cui, Y.; Wang, X.; Yue, F.; Shan, Y.; Liu, B.; Zhou, Y.; Yi, Y.; Lü, X. Purification, characterization and bioactivity of exopolysaccharides produced by Lactobacillus plantarum KX041. *Int. J. Biol. Macromol.* **2019**, *128*, 480–492, doi:10.1016/j.ijbiomac.2019.01.117.

14. Demirbas, F. Glucan type exopolysaccharide (EPS) shows prebiotic effect and reduces syneresis in chocolate pudding. **2018**, *55*, 3821–3826, doi:10.1007/s13197-018-3181-3.

15. Pan, L.; Han, Y.; Zhou, Z. In vitro prebiotic activities of exopolysaccharide from Leuconostoc pseudomesenteroides XG5 and its e ff ect on the gut microbiota of mice. *J. Funct. Foods* **2020**, *67*, 103853, doi:10.1016/j.jff.2020.103853.

16. Dertli, E.; Mercan, E.; Ar, M.; Tahsin, M. LWT - Food Science and Technology Characterisation of lactic acid bacteria from Turkish sourdough and determination of their exopolysaccharide (EPS) production characteristics Osman Sa g. **2016**, *71*, 116–124, doi:10.1016/j.lwt.2016.03.030.

17. Nachtigall, C.; Surber, G.; Herbi, F.; Wefers, D.; Jaros, D.; Rohm, H. Production and molecular structure of heteropolysaccharides from two lactic acid bacteria. *Carbohydr. Polym.* **2020**, *236*, 116019, doi:10.1016/j.carbpol.2020.116019.

18. Wolter, A.; Hager, A.S.; Zannini, E.; Galle, S.; Gänzle, M.G.; Waters, D.M.; Arendt, E.K. Evaluation of exopolysaccharide producing Weissella cibaria MG1 strain for the production of sourdough from various flours. *Food Microbiol.* **2014**, *37*, 44–50, doi:10.1016/j.fm.2013.06.009.

19. Roca, C.; Alves, V.D.; Freitas, F.; Reis, M.A.M. Exopolysaccharides enriched in rare sugars: Bacterial sources, production, and

applications. *Front. Microbiol.* **2015**, *6*, 1–7, doi:10.3389/fmicb.2015.00288.

20. Torino, M.I.; de Valdez, G.F.; Mozzi, F. Biopolymers from lactic acid bacteria. Novel applications in foods and beverages. *Front. Microbiol.* 2015, 834.

21. Haj-Mustafa, M.; Abdi, R.; Sheikh-Zeinoddin, M.; Soleimanian-Zad, S. Statistical study on fermentation conditions in the optimization of exopolysaccharide production by Lactobacillus rhamnosus 519 in skimmed milk base media. *Biocatal. Agric. Biotechnol.* **2015**, *4*, 521–527, doi:10.1016/j.bcab.2015.08.013.

22. Polak-Berecka, M.; Waśko, A.; Szwajgier, D.; Choma, A. Bifidogenic and antioxidant activity of exopolysaccharides produced by Lactobacillus rhamnosus E/N cultivated on different carbon sources. *Polish J. Microbiol.* **2013**, *62*, 181–188, doi:10.33073/pjm-2013-023.

23. Degeest, B.; De Vuyst, L. Indication that the nitrogen source influences both amount and size of exopolysaccharides produced by Streptococcus thermophilus LY03 and modelling of the bacterial growth and exopolysaccharide production in a complex medium. *Appl. Environ. Microbiol.* **1999**, *65*, 2863–2870, doi:10.1128/aem.65.7.2863-2870.1999.

24. Mıdık, F.; Tokatlı, M.; Bağder Elmacı, S.; Özçelik, F. Influence of different culture conditions on exopolysaccharide production by indigenous lactic acid bacteria isolated from pickles. *Arch. Microbiol.* **2020**, *202*, 875–885, doi:10.1007/s00203-019-01799-6.

25. De Vuyst, L.; Degeest, B. Heteropolysaccharides from lactic acid bacteria. *FEMS Microbiol. Rev.* **1999**, *23*, 153–177, doi:10.1016/S0168-6445(98)00042-4.

26. Cheng, X.; Huang, L.; Li, K. tai Antioxidant activity changes of exopolysaccharides with different carbon sources from Lactobacillus plantarum LPC-1 and its metabolomic analysis. *World J. Microbiol. Biotechnol.* **2019**, *35*, 1–13, doi:10.1007/s11274-019-2645-6.

27. Bibi, A.; Xiong, Y.; Rajoka, M.S.R.; Mehwish, H.M.; Radicetti, E.; Umair, M.; Shoukat, M.; Khan, M.K.I.; Aadil, R.M. Recent advances in the production of exopolysaccharide (EPS) from lactobacillus spp. and its application in the food industry: A review. *Sustain.* **2021**, *13*, 12429, doi:10.3390/su132212429.

28. Buksa, K.; Kowalczyk, M.; Boreczek, J. Extraction, purification and characterisation of exopolysaccharides produced by newly isolated lactic acid bacteria strains and the examination of their influence on resistant starch formation. *Food Chem.* **2021**, *362*, 130221, doi:10.1016/j.foodchem.2021.130221.

29. Hooshdar, P.; Kermanshahi, R.K.; Ghadam, P.; Khosravi-Darani, K. A review on production of exopolysaccharide and biofilm in probiotics like lactobacilli and methods of analysis. *Biointerface Res. Appl. Chem.* **2020**, *10*, 6058–6075, doi:10.33263/BRIAC105.60586075.

30. Li, Y.; Liu, Y.; Cao, C.; Zhu, X.Y.; Wang, C.; Wu, R.; Wu, J. Extraction and biological activity of exopolysaccharide produced by Leuconostoc mesenteroides SN-8. *Int. J. Biol. Macromol.* **2020**, *157*, 36–44, doi:10.1016/j.ijbiomac.2020.04.150.

31. Freitas, F.; Alves, V.D.; Reis, M.A.M. Advances in bacterial exopolysaccharides: From production to biotechnological applications. *Trends Biotechnol.* **2011**, *29*, 388–398, doi:10.1016/j.tibtech.2011.03.008.

32. Delattre, C.; Pierre, G.; Laroche, C.; Michaud, P. Production, extraction and characterization of microalgal and cyanobacterial exopolysaccharides. *Biotechnol. Adv.* **2016**, *34*, 1159–1179, doi:10.1016/j.biotechadv.2016.08.001.

33. Hebert, E.M.; Raya, R.R.; Brown, L.; de Valdez, G.F.; de Giori, G.S.; Taranto, M.P. Genome sequence of the cheese-starter strain Lactobacillus delbrueckii subsp. lactis CRL 581. *Genome Announc.* **2013**, *1*, 1–2, doi:10.1128/genomeA.00602-13.

34. Vinderola, C.G.; Costa, G.A.; Regenhardt, S.; Reinheimer, J.A. Influence of compounds associated with fermented dairy products on the growth of lactic acid starter and probiotic bacteria. *Int. Dairy J.* **2002**, *12*, 579–589, doi:10.1016/S0958-6946(02)00046-8.

35. Bottari, B.; Felis, G.E.; Salvetti, E.; Castioni, A.; Campedelli, I.; Torriani, S.; Bernini, V.; Gatti, M. Effective identification of Lactobacillus casei group species: Genome-based selection of the gene mutL as the target of a novel multiplex PCR assay. *Microbiol. (United Kingdom)* **2017**, *163*, 950–960, doi:10.1099/mic.0.000497.

36. Degeest, B.; Mozzi, F.; De Vuyst, L. Effect of medium composition and temperature and pH changes on exopolysaccharide yields and stability during Streptococcus thermophilus LY03 fermentations. *Int. J. Food Microbiol.* **2002**, *79*, 161–174, doi:10.1016/S0168-1605(02)00116-2.

37. Lee, S.C.; Prosky, L.; Vries, J.W. De Determination of Total, Soluble, and Insoluble Dietary Fiber in Foods—Enzymatic-Gravimetric Method, MES-TRIS Buffer: Collaborative Study. *J. AOAC Int.* **1992**, *75*, 395–416, doi:10.1093/jaoac/75.3.395.

38. Xia, Y.G.; Wang, T.L.; Sun, H.M.; Liang, J.; Kuang, H.X. Gas chromatography–mass spectrometry-based trimethylsilyl-alditol derivatives for quantitation and fingerprint analysis of Anemarrhena asphodeloides Bunge polysaccharides. *Carbohydr.*

Polym. **2018**, doi:10.1016/j.carbpol.2018.06.066.

39. Caligiani, A.; Marseglia, A.; Leni, G.; Baldassarre, S.; Maistrello, L.; Dossena, A.; Sforza, S. Composition of black soldier fly prepupae and systematic approaches for extraction and fractionation of proteins, lipids and chitin. *Food Res. Int.* **2018**, *105*, 812–820, doi:10.1016/j.foodres.2017.12.012.

40. Nouha, K.; Kumar, R.S.; Balasubramanian, S.; Tyagi, R.D. Critical review of EPS production, synthesis and composition for sludge flocculation. *J. Environ. Sci. (China)* **2018**, *66*, 225–245, doi:10.1016/j.jes.2017.05.020.

41. Chintana Tayuan Growth and exopolysaccharide production by Weissella sp. from low-cost substitutes for sucrose. *African J. Microbiol. Res.* **2011**, *5*, 3693–3701, doi:10.5897/ajmr11.486.

42. AOAC AOAC Official Method 991.43 Total, Soluble, and Insoluble Dietary Fibre in Foods. *J. AOAC Int.* **2012**, doi:10.5740/jaoacint.CS2011_25.

43. Badel, S.; Bernardi, T.; Michaud, P. New perspectives for Lactobacilli exopolysaccharides. *Biotechnol. Adv.* **2011**, *29*, 54–66, doi:10.1016/j.biotechadv.2010.08.011.

44. Mariotti, F.; Tomé, D.; Mirand, P.P. Converting nitrogen into protein - Beyond 6.25 and Jones' factors. *Crit. Rev. Food Sci. Nutr.* **2008**, *48*, 177–184, doi:10.1080/10408390701279749.

45. Jones, D.B. Factors for converting percentages of nitrogen in foods and feeds into percentages of protein. *Br. Food J.* 1932.

46. Zhang, Y.; Dai, X.; Jin, H.; Man, C.; Jiang, Y. The effect of optimized carbon source on the synthesis and composition of exopolysaccharides produced by Lactobacillus paracasei. *J. Dairy Sci.* **2021**, *104*, 4023–4032, doi:10.3168/jds.2020-19448.

47. Joulak, I.; Finore, I.; Nicolaus, B.; Leone, L.; Moriello, A.S.; Attia, H.; Poli, A.; Azabou, S. Evaluation of the production of exopolysaccharides by newly isolated Halomonas strains from Tunisian hypersaline environments. *Int. J. Biol. Macromol.* **2019**, *138*, 658–666, doi:10.1016/j.ijbiomac.2019.07.128.

48. Vaningelgem, F.; Zamfir, M.; Mozzi, F.; Adriany, T.; Vancanneyt, M.; Swings, J.; De Vuyst, L. Biodiversity of Exopolysaccharides Produced by Streptococcus thermophilus Strains Is Reflected in Their Production and Their Molecular and Functional Characteristics. *Appl. Environ. Microbiol.* **2004**, *70*, 900–912, doi:10.1128/AEM.70.2.900-912.2004.

49. Bomfim, V.B.; Pereira Lopes Neto, J.H.; Leite, K.S.; de Andrade Vieira, É.; Iacomini, M.; Silva, C.M.; Olbrich dos Santos, K.M.; Cardarelli, H.R. Partial characterization and antioxidant activity of exopolysaccharides produced by Lactobacillus plantarum CNPC003. *Lwt* **2020**, *127*, doi:10.1016/j.lwt.2020.109349.

50. Wu, H.; Zhang, W.; Mu, W. Recent studies on the biological production of D-mannose. *Appl. Microbiol. Biotechnol.* **2019**, *103*, 8753–8761, doi:10.1007/s00253-019-10151-3.

51. Zhou, Y.; Cui, Y.; Qu, X. Exopolysaccharides of lactic acid bacteria: Structure, bioactivity and associations: A review. *Carbohydr. Polym.* **2019**, *207*, 317–332, doi:10.1016/j.carbpol.2018.11.093.

52. Kansandee, W.; Moonmangmee, D.; Moonmangmee, S.; Itsaranuwat, P. Characterization and Bifidobacterium sp. growth stimulation of exopolysaccharide produced by Enterococcus faecalis EJRM152 isolated from human breast milk. *Carbohydr. Polym.* **2019**, *206*, 102–109, doi:10.1016/j.carbpol.2018.10.117.

53. Pradeepa; Shetty, A.D.; Matthews, K.; Hegde, A.R.; Akshatha, B.; Mathias, A.B.; Mutalik, S.; Vidya, S.M. Multidrug resistant pathogenic bacterial biofilm inhibition by Lactobacillus plantarum exopolysaccharide. *Bioact. Carbohydrates Diet. Fibre* **2016**, *8*, 7–14, doi:10.1016/j.bcdf.2016.06.002.

54. Ruas-Madiedo, P.; Hugenholtz, J.; Zoon, P. An overview of the functionality of exopolysaccharides produced by lactic acid bacteria. *Int. Dairy J.* **2002**, *12*, 163–171, doi:10.1016/S0958-6946(01)00160-1.

55. Salazar, N.; Prieto, A.; Leal, J.A.; Mayo, B.; Bada-Gancedo, J.C.; de los Reyes-Gavilán, C.G.; Ruas-Madiedo, P. Production of exopolysaccharides by Lactobacillus and Bifidobacterium strains of human origin, and metabolic activity of the producing bacteria in milk. *J. Dairy Sci.* **2009**, *92*, 4158–4168, doi:10.3168/jds.2009-2126.

56. Polak-Berecka, M.; Choma, A.; Waśko, A.; Górska, S.; Gamian, A.; Cybulska, J. Physicochemical characterization of exopolysaccharides produced by Lactobacillus rhamnosus on various carbon sources. *Carbohydr. Polym.* **2015**, *117*, 501–509, doi:10.1016/j.carbpol.2014.10.006.

57. Ziadi, M.; Bouzaiene, T.; M'Hir, S.; Zaafouri, K.; Mokhtar, F.; Hamdi, M.; Boisset-Helbert, C. Evaluation of the efficiency of ethanol precipitation and ultrafiltration on the purification and characteristics of exopolysaccharides produced by three lactic acid bacteria. *Biomed Res. Int.* **2018**, doi:https://doi.org/10.1155/2018/1896240.

58. Min, W.H.; Fang, X. Bin; Wu, T.; Fang, L.; Liu, C.L.; Wang, J. Characterization and antioxidant activity of an acidic exopolysaccharide from Lactobacillus plantarum JLAU103. *J. Biosci. Bioeng.* **2019**, *127*, 758–766,

doi:10.1016/j.jbiosc.2018.12.004.

59. Du, R.; Xing, H.; Yang, Y.; Jiang, H.; Zhou, Z.; Han, Y. Optimization, purification and structural characterization of a dextran produced by L. mesenteroides isolated from Chinese sauerkraut. Carbohydr. Polym. 2017, 174, 409–416, doi:10.1016/j.carbpol.2017.06.084.

CHAPTER 3

Protease-assisted mild extraction of soluble fibre and protein from fruit by-products: a biorefinery perspective

Part of this chapter has also been published as:

Andrea Fuso, Pio Viscusi, Susanna Larocca, Francesco Saverio Sangari, Veronica Lolli, Augusta Caligiani (**2022**). Protease-assisted mild extraction of soluble fibre and protein from fruit by-products: a biorefinery perspective. *Foods*, 12(1), 148.

ABSTRACT

By-products from the fruit supply chain have shown great potential to be valorised, due to their high content of macronutrients, such as lipids, protein, and fibre. A mild enzymatic assisted extraction (EAE) involving the use of a protease was tested to evaluate the feasibility of a cascade approach to fractionate the main fruit by-products components. Protease from *Bacillus licheniformis* (the enzyme used in the AOAC 991.43 official method for dietary fibre quantification) was used and, besides protein, the conditions of hydrolysis (60°C, neutral pH, overnight) allowed to dissolve a portion of soluble fibres, which was then separated from the solubilized peptide fraction through ethanol precipitation. Protein extraction yields were in the range 35-93%, while soluble fibre extraction yield ranged from 0.6% to 71% depending on the by-product, suggesting its applicability only for certain substrates, and was found negatively correlated with the molecular weight of the fibre. The monosaccharide composition of the soluble fibres extracted was also diverse. Galacturonic acid was present in low amount, indicating that pectin were not efficiently extracted. On the other hand, a predominance of arabinose and galactose monomers was detected in many fractions, indicating the isolation of a fruit soluble fibre portion with potential similarity with arabinogalactans and gum arabic, opening perspectives for technological applications. The residual solid pellet obtained after protease assisted extraction was characterized aiming to understand its further potential uses, and it was found to still be an excellent fibre-rich substrate, suitable for being subjected to more “hard” processing (e.g. sequential pectin and hemicellulose extraction) with the objective to derive other fractions with potential great added economic value.

1. Introduction

The global food waste generation, estimated at 1.3 billion tons/year by FAO [1], and the limited availability of natural resources have led to investigate on more sustainable strategies to recover valuable products from different waste streams such as agri-food residues [2]. Among these, fruit processing waste (FPW) (e.g., peels, pods, seeds, skins, etc.) accounts till 45% of the total fresh weight, generating around 3.3 billion tons of carbon dioxide each year, due to decomposition inside landfills or incinerators [3,4]. Also, this incorrect waste management represents a loss of valuable biomass and nutrients. Various compositional studies on FPW [5] indeed suggested its potential utilization as substrate for biorefinery in the production of high-value compounds. In particular, fruit seeds and kernels represent an ideal substrate to be valorised, being naturally rich in nutrients (e.g., lipids, proteins, dietary fibres) and secondary metabolites (phytochemicals, phytosterols) [6], in some cases, in concentrations potentially higher than those of other edible parts of the fruit [7,8]. The application of cascade sustainable biorefinery processes to recover the most of these compounds could meet two important challenges: from one side to give added value to the whole fruit processing value chain, justifying the additional investment related to the new technologies, and from the other side to face the increasing market request of valuable nutrients to formulate innovative products for different high value applications. Despite this, development of fruit waste biorefineries is limited, mainly due to the lack of information on feedstock availability, process design, and scale-up. Moreover, the presence of potentially toxic substances in some kernels, as for example the cyanogenic glycoside amygdalin (D-mandelonitrile-β-D-gentiobioside) naturally present in some fruits of *Prunus* genus (i.e., apricot, peach, cherry, plum), have prevented until now the re-use of the whole kernel cake in the food industry [9].

Dietary fibres are certainly one of the most promising compounds to be extracted from fruit by-products, because of their high quantity [10] and their beneficial effects on health. In particular fibres emerged as the leading product segment in the Europe bioactive ingredients market and accounted for over 20% of the total industry in 2015 [11]. Fibres, beside their fundamental role as technological additives, are also recognized as an important part of healthy diet (by preventing cardiovascular diseases, obesity and diabetes) and the global market for high fibre content foods has been estimated to be continuously growing, driven by the consumer focus on health, wellbeing and increasing awareness on the benefits of fibre-rich diets [12].

At the same time, there is a growing need to study and develop more sustainable and innovative technologies of extraction and fractionation, with lower environmental impact, energy consumption, waste production and process contaminants. Among recent promising environmentally friendly methods, enzyme-assisted extraction (EAE) is a green extraction method often performed at laboratory scale to disrupt the structural integrity of the plant cell wall [3], thus enhancing the extraction of valuable nutrients, minimizing the use of solvents and heat and preserving functional properties of the extracted biomolecules. Moreover, the lower

total thermal impact on the biomass is expected to reduce the presence of other emerging process contaminants, obtaining safer products. Hence, adapting the biorefinery strategy with integrated approaches based on green (enzyme-assisted) methods would lead to products with significantly higher values compared to the current applications of the fruit residual biomass.

In this context, this chapter is a part of a bigger research project financed by University of Parma (Research Grant Azione C, 2020 and 2021), focusing on the valorisation through biorefinery approach of underexploited fruit biomass streams, namely seeds, peels and kernels. The general aim was to investigate the molecular composition of fruit by-products and to test mild EAE by using protease for the cascade recovery of nutrients (especially protein and fibres), evaluating yields and chemical compositions of the various macromolecules resulting from extraction and purification processes. In particular, this chapter deals with the purification and chemical characterization of soluble dietary fibres simultaneously extracted with protein through EAE with protease and with the investigation of the residual biomass composition obtained after this process, in a total biorefinery perspective.

A plant-based diet and plant proteins are becoming more and more important to meet the nutritional requirements of the growing human population, as well as to reduce the negative impact of food production on the environment. On the other hand, eating more fibres is currently considered mandatory for a healthy diet, despite the use of fibre rich integral plant foods pose technological and organoleptic problems, often requiring fibre extraction and modification. This work is in the direction of giving a contribution to tackle this current need of shifting food products and diets towards higher intakes of both plant protein and fibres.

2. Materials and methods

2.1. Reagents

D-glucose, D-fructose, D-arabinose, D-galactose, D-mannose, D-rhamnose, D-ribose, D-xylose, D-fucose, D-galacturonic acid, D-glucuronic acid, phenyl β-D-glucopyranoside, dimethylformamide (DMF), trifluoroacetic acid (TFA), ammonium hydroxyde and N,O-Bis(trimethylsilyl)trifluoroacetamide (BSTFA) were purchased from Sigma-Aldrich (Taufkirchen, Germany); ethanol was purchased from Carlo Erba (Milan, Italy); bidistilled water was obtained using Milli-Q System (Millipore, Bedford, MA, USA), while methanol from VWR International (Milan, Italy).

2.2. Fruit by-products collection and characterization

The analyses were carried out on fruit-derived by-products samples. The latter were either purchased or supplied by fruit and vegetable processing companies. In detail, samples comprised different fruit by-product covering different species and characteristics: stone fruits of the *Prunus* genus as apricot kernel (*Prunus Armeniaca*), cherry kernel (*Prunus Avium*), peach Kernel (*Prunus persica)* and mango seeds (*Mangifera indica L.*), citrus fruits as orange peel and seed (*Citrus X sinensis*), lemon seeds and lemon peels (*Citrus limon*), and finally a less common specie of the Rosaceae family, namely loquar kernel (*Eriobtria japonica*).

Samples were treated with liquid nitrogen and milled through laboratory blenders and then characterized in terms of proximate composition according to official methods of analysis [13]. Moisture was determined in an oven at 105 °C for 24 h. Total ash was determined through mineralization at 550 °C for 5 h. Proteins were determined with a Kjeldahl system (DKL heating digestor and UDK 139 semiautomatic distillation unit, VELP SCIENTIFICA) by using 6.25 as nitrogen-to-protein conversion factor. Total and soluble fibre content were determined by the AOAC 991.43 official enzymatic-gravimetric method for dietary fibres [14].

2.3. Protease assisted extraction

20 g of each sample underwent enzymatic assisted extraction (EAE) with the employment of an alcalase of microbial origin, namely protease from *Bacillus licheniformis* (EC 3.4.21.62). The EAE was performed for each fruit by-product at the optimal conditions of temperature and pH for the enzyme (60°C and pH 7.5, respectively). An enzyme/substrate ratio of 1:100 (w/w) was mixed with a phosphate buffer solution (10 mM Na_2HPO4/NaH_2PO4) and hydrolysed overnight (12 hours), then heated at 90 °C for 10 min to inactivate the enzyme. The hydrolysed substrate was centrifuged at 3900 rpm at 4 °C for 40 min and three fractions were obtained: an insoluble precipitate (pellet), an aqueous supernatant and a portion of lipid fraction on the surface. The top surfaced oil (when present) was directly recovered. The solid residue (pellet) was recovered and characterized in terms of proximate composition (oil, protein and total dietary fibre) as described in paragraph 2.5. Ethanol (95% v/v) was then added to the supernatant in a 4:1 ratio in order to get the precipitation of soluble fibre that had been simultaneously extracted from the matrices along with proteins/peptides. Proteins were then purified from the precipitated soluble fibres by centrifugation (3900 rpm, 4 °C, 30 min). Then, the supernatant was recovered to determine total nitrogen and the pellet constituted by the alcohol insoluble residue was recovered, washed again with ethanol and characterized according to paragraph 2.4. The process workflow is represented in Figure 3.1.

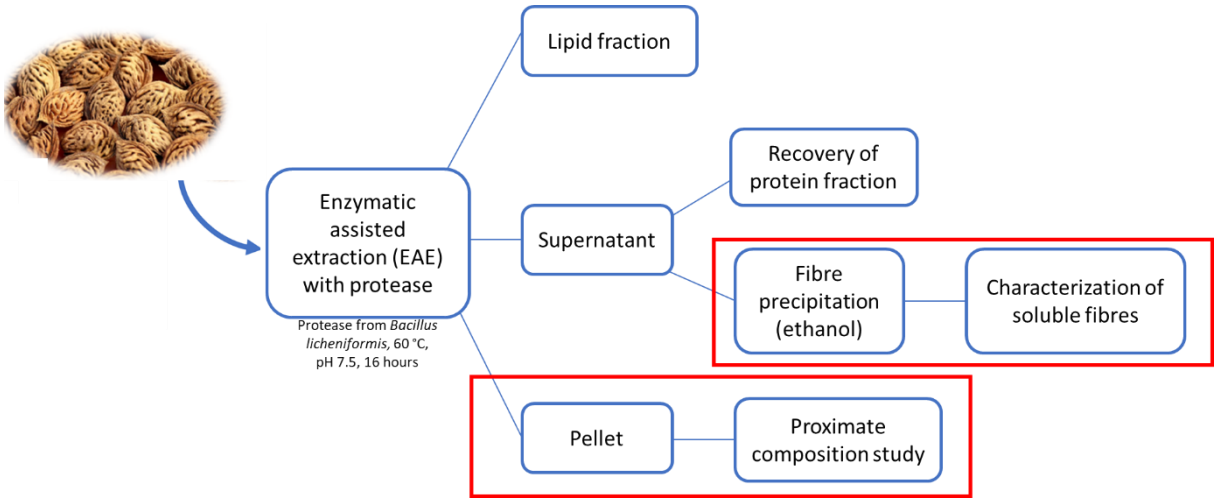

Figure 3.1: *Representation of the whole fractionation process. Red rectangles highlight the parts of it that are treated in the present chapter.*

2.4. Characterization of soluble fibre

2.4.1. Residual ash and protein

The soluble fibres extracted were characterized in terms of purity by quantifying the total protein and ash content. Official methods were used, according to paragraph 2.2.

2.4.2. Monosaccharide composition

The total quantity of soluble fibres obtained after precipitation through ethanol addition to the supernatant, as well as their monosaccharide composition, was investigated for every sample. The analysis was performed following a method proposed in literature with some modifications [15], as already reported in Chapter 2, paragraph 2.3 of this dissertation.

2.4.3. Molecular weight

The molecular weight of soluble fibres was also evaluated, in order to understand their potential use in the food supply chain, through High-Performance Size-Exclusion Chromatography coupled with Refractive Index Detector (HPSEC-RID). The samples were dissolved in ultrapure water at a concentration of 10000 ppm, then centrifuged at 7000 rpm for 20 minutes at 4 °C and finally filtered through a 0.45 µm nylon membrane. An Agilent 1260 Infinity II LC system equipped with a refractive index detector (RID) (Agilent, Santa Clara, CA, USA) was used. Ultrapure water was also used as eluent, at a flow rate equal to 0.7 mL/min, and a PL aquagel-OH mixed-M column, 7.5 x 300 mm, 8 µm was employed for the separation (Agilent, Santa Clara, CA, USA). The injection sample volume was set at 10 µL, column temperature 30 °C and RID temperature 35 °C.

Standard pullulans having known molecular weight ranging from 6,000 to 200,000 Da were used for the calibration curve.

2.5. Proximate composition of residual pellet after EAE

A residual pellet was obtained on the bottom of the tube after EAE (Figure 3.1). This pellet was characterized in terms of proximate composition, namely dry weight, residual proteins, lipids, ash, and total dietary fibre. Official methods were used to quantify all the components, as already reported in paragraph 2.2.

2.6. Determination of extractions yields

The total yield of soluble fibre obtained after ethanol precipitation was determined as percentage (%) which was calculated by dividing the sum of monosaccharides determined in paragraph 2.4.2 by the absolute amount of soluble fibre of the starting material determined by AOAC gravimetric method.

The enzymatic extraction yields (%) of proteins were calculated by comparing the total nitrogen after the enzymatic hydrolysis in the supernatant and the total nitrogen determined before the proteolysis in the raw materials.

3. Results and discussion

3.1. Proximate composition of the raw materials (fruit by-products)

The fruit by-products compositional analysis is of great importance for their further exploitation. As reported in Table 3.1, the proximate composition (ash, protein, lipids, soluble, insoluble, and total fibres) of the different raw materials (seeds, kernels, and peels) considered in this study revealed different nutritional contents based on the fruit type/category.

The protein fraction accounted for about 3-15 % on dry matter basis, and especially lemon seeds resulted as a good source of protein (15.3 ± 0.2), whereas peach kernels had the lowest content (< 3%). Fruit seeds/kernels mainly turned out to be good sources of dietary fibre, as previously documented [10]. Stone fruits of *Prunus* genus as peach, cherry and apricot were found to be the richest in total dietary fibre (ranging between 76.9% and 88.9%), and among them cherry kernels also contained good quantities of soluble fibre (6.5%). Lemon seeds resulted on par with stone fruit with a percentage of 75.9% of total fibre (of which about 4% was represented by soluble fibre). Citrus peels contained very high amount of soluble fibre (around 20%) likely due to the contribute of pectin fraction. Compared to these percentages, total fibre was lower in mango

seeds and loquar kernels, but the latter had a well-balance proportion between soluble and insoluble fractions.

Digestible carbohydrates (of which percentage values were obtained by difference) represented the major nutrients in mango seeds and loquar kernels, thus being potential energy food sources. On the other hand, the potential presence of starch could interfere with soluble fibre purification after protease assisted extraction. In mango seeds, the presence of starch has been confirmed by Patiño-Rodríguez and colleagues, who determined a concentration close to 30% within the same by-products [16]. No studies were found in literature regarding the presence of starch in the other seeds and kernels considered in this work.

Table 3.1: Proximate composition of fruit by-products as such, namely ground seeds, kernels and peels, expressed as percentage on dry matter (%DM). "Others" = obtained by difference, comprising digestible carbohydrates. Results are the mean of two replicate analyses, CV%<8%.

	Ash	Proteins	Lipids	Total fibre (TDF)	Insoluble fibre (IDF)	Soluble fibre (SDF)	Others
Lemon peels	4.29	7.26	1.62	58.42	37.70	20.72	28.40
Lemon seeds	2.45	15.27	6.37	75.91	75.43	3.92	trace
Mango seeds	1.91	5.11	7.32	37.07	35.97	1.11	48.57
Peach kernels	1.39	2.95	4.29	76.90	76.46	0.44	13.46
Loquar kernels	2.74	6.08	1.12	27.01	14.89	12.11	63.04
Cherry kernels	1.48	4.54	7.42	80.90	74.38	6.54	5.64
Apricot kernels	0.95	5.03	5.04	88.90	4.64	0.41	trace
Orange peels/seeds	5.56	4.84	1.91	59.68	26.65	33.03	28.01

3.2. Yield determination for soluble fibre and protein after protease assisted extraction

As already mentioned, one of the purposes of this chapter was to simultaneously recover through a mild process (namely EAE with protease from *Bacillus licheniformis* at 60 °C) fruit protein as a novel potential source of plant protein, and if possible even a portion of the soluble fibre. Ethanol was then added to the supernatant obtained in order to precipitate soluble fibres eventually present in the solution, with the double aim to purify protein fraction and simultaneously recover the soluble fibre portion. After protease reaction and ethanol addition, the fruit proteins were recovered in the form of protein hydrolysates in the hydro-alcoholic supernatant. Ethanol may cause the co-precipitation together with fibres of starch, when present in the starting material [17]. The use of amylolytic enzymes, resembling conditions used for gravimetric quantification of soluble fibres [14] could be therefore appropriate, but was excluded in this study due to the

need to have a protein fraction as pure as possible. Amylase and amyloglucosidase could be used, if needed, directly on the soluble fibre extract.

Table 3.2 shows the extraction yields, expressed as a percentage, of protein and soluble fibres in the eight samples considered. Regarding protein fraction, yields were on average high (60%), suggesting the good activity of the protease employed also on recalcitrant residues as lignocellulosic seeds/kernels. The maximum values were obtained for citrus fruit peels (80 and 93% for orange and lemon peels, respectively), whereas the minimum yield (35 ± 2 %) was determined for loquar kernels.

The quantity of soluble fibre in the ethanol precipitates was determined by the sum of the single monosaccharides freed up following acid hydrolysis (see paragraph 2.4.2). It was found that the protease assisted extraction had excellent extraction yields not only for protein but also for soluble fibres in some samples, namely cherry kernels (71%), peach kernels (54%), mango seeds (33%) and orange peels (30%). On the contrary, in other samples significantly lower extraction yields were obtained, as in the case of loquar (1.7%) and apricot kernels (1.2%), suggesting different characteristics of the soluble fibres or likely their different interactions and bond with the lignocellulosic structures. De Albuquerque and colleagues performed a similar experiment, evaluating the effectiveness of "mild" extractions in various tropical fruits by-products. After carrying out a "mild" extraction, using distilled water as a solvent at a temperature of 90-95 °C, at atmospheric pressure and pH around neutrality, the authors quantified the soluble fibre content in the extract, and also in that case the quantity of fibres extracted from mango by-products was significantly greater than in other samples examined, followed by orange, while for passion fruit and acerola these quantities were found to be very low [18]. The extraction yields obtained by De Albuquerque's group are on average higher than the ones in the present work, but this is not surprising since different extraction temperatures were used (90 °C against 60 °C); indeed, the primary objective of our process was the extraction of proteins.

***Table 3.2**: Extraction yields, expressed in percentage, of soluble fibres (determined from total monosaccharide composition) and solubilized protein (determined by Kjeldahl method on the supernatant). Values are mean ± SD of replicates of independent extraction.*

	Extraction yield of protein (% respect to the total protein in the raw sample)	**Extraction yield of soluble fibres (% respect to the total soluble fibre in the raw sample)**
Lemon peels	93 ± 7	6 ± 1
Lemon seeds	50 ± 2	9 ± 1
Mango seeds	42 ± 6	33 ± 2
Peach kernels	64 ± 1	54 ± 2
Loquar kernels	35 ± 2	1.6 ± 0.3
Cherry kernels	70 ± 2	71 ± 5

Apricot kernels	47 ± 1	1.3 ± 0.4
Orange peels and seeds	80 ± 2	29.8 ± 0.2

However, since the potential re-use of soluble fibres strictly depends on the chemical structure which affects their functional properties, their structural features were further investigated in terms of molecular weight and monosaccharide composition.

3.3. Molecular weight of soluble fibres

The molecular weight of soluble fibre extracted from fruit by-products through EAE was investigated by High-Performance Size-Exclusion Chromatography coupled with a Refractive Index Detector (HPSEC-RID). The results are shown in Table 3.3.

Table 3.3: *Molecular weight distribution of soluble fibre extracted by EAE from different fruit by-products.*

	Molecular weight (kDa)			
	< 6	**15– 20**	**96– 100**	**> 200**
		Peak area (%)		
Lemon peels	2	8	-	90
Lemon seeds	5	-	19	76
Mango seeds	70	-	-	30
Peach kernels	96	-	-	4
Loquar kernels	21	-	-	79
Cherry kernels	3	-	-	97
Apricot kernels	32	-	-	68
Orange peels and seeds	72	-	-	28

From Table 3.3, it can be seen that all the samples were composed mainly of low molecular weight polysaccharides, lower than 6 kDa, or high molecular weight polysaccharides, higher than 200 kDa. Mango, peach, and orange by-products turned out to consist mainly of low molecular weight molecules, which could explain the higher extraction yield obtained for these matrices. In contrast, loquar and cherry kernels and lemon peels and seeds turn out to be composed mainly of high molecular weight polymers.

Fractions with intermediate molecular weights were detected only in the samples derived from lemon peels and seeds. The soluble fibre extracted from lemon seeds turned out to be composed for 19% of polymers with a molecular weight in the range of 95 to 100 KDa, while the precipitate obtained from the peels was made of molecules with a molecular weight ranging from 15 to 20 kDa for 8% of the total area.

It is well known that the molecular weight of polysaccharides has consequences for their physicochemical, physiological and biological properties. In particular, molecular weight is strictly related to viscosity, which

increases as the chain length. Therefore, biological and physiological activities positively associated with viscosity, such as antimicrobial and cholesterol-lowering activity [19], improve in a directly proportional manner with chain length. In addition, it has been proposed that the antioxidant property might be related to the molecular weight of polymers, being possibly influenced by the number of hydroxyl and hemiacetal groups of the polymer [19]. Molecular weight also affects the technological properties of carbohydrates: to report an example, β-glucans of different sizes affected breadmaking ability, increasing water binding capacity, and modified the texture and the ability to stabilize emulsions [20]. The presence of molecules with different molecular weights could be the starting point of possible future strategies for the preparative separation of polymers on the basis of this feature, in order to be able to exploit them according to their functional properties.

3.4. Monosaccharide composition

The characterization of soluble fibre was also carried out in terms of their monosaccharide profile by GC-MS. Although this technique does not provide a full understanding of the chemical structure of the molecule, it gives important information about which monomers make up the polysaccharide, both in qualitative and quantitative terms. Histograms in Figure 3.2 and Figure 3.3 show this composition for the eight fruit by-products considered in this study. The determination of monosaccharide composition for each sample was performed in duplicate, and the results are reported as mean ± standard deviation.

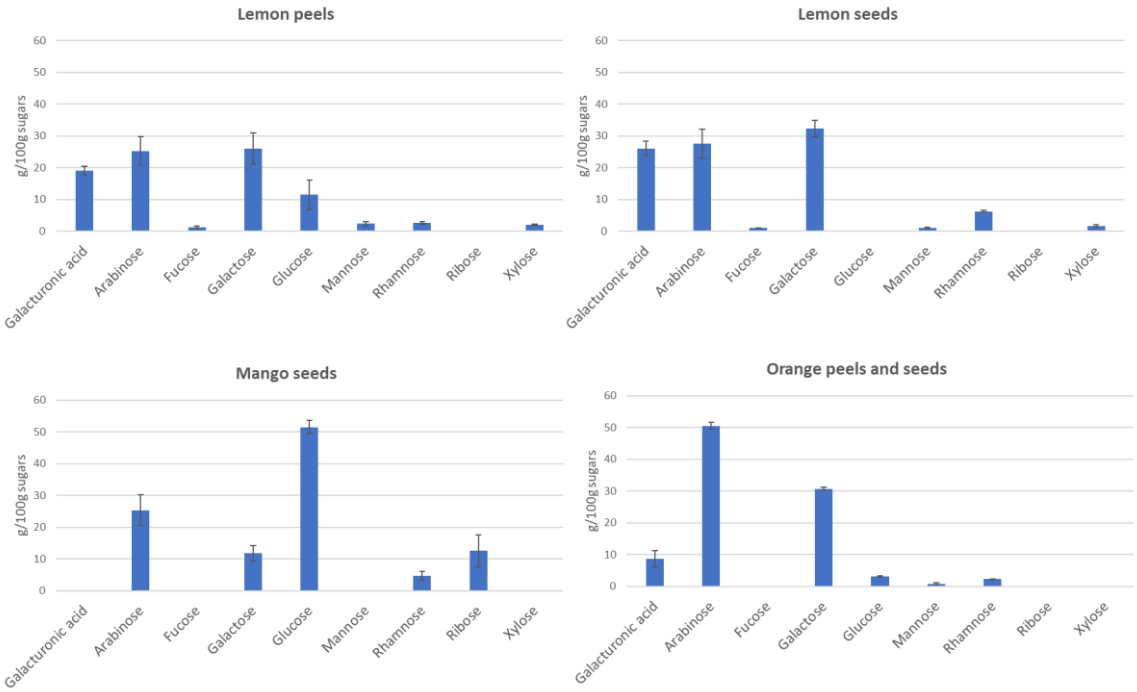

Figure 3.2: *Sugar composition (expressed as g sugar/100 g total sugars) of four fruit by-products, namely lemon and orange seeds and peels, and mango seeds.*

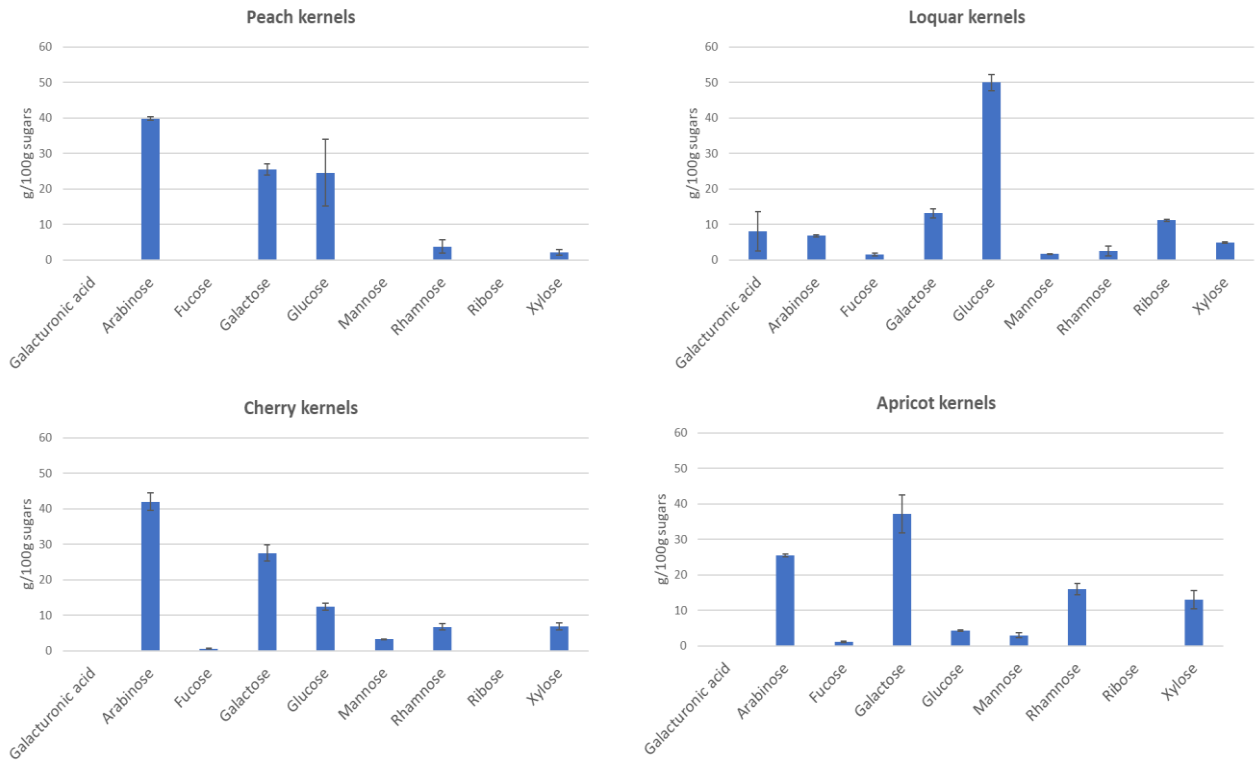

***Figure 3.3**: Sugar composition (expressed as g sugar/100 g total sugars) of four fruit by-products, namely peach, loquar, cherry and apricot kernels.*

Soluble fibre of loquar kernels and mango seeds were the only ones containing glucose as main monosaccharides, suggesting a potential significant presence of starch that needs to be further evaluated in terms of purification process, as highlighted in paragraph 3.1. In Citrus fruit samples (Figure 3.2), namely orange by-products and lemon peels and seeds, the most present monosaccharides were arabinose (25-50%) and galactose (25-35%), followed by galacturonic acid (10-25%). A higher concentration of uronic acids was expected. The latter, in fact, accounts for about 65% of the monosaccharides present in citrus peels [21], as it is the main constituent of pectin, a polysaccharide known to be present in high concentration in these by-products. However, it is important to underline that the methods generally used for pectin extraction involve diverse temperature and pH conditions, namely 80 °C and pH 2 [22], quite far from those used during the EAE used in our work. So, it is evident that the "mild" extraction methodology tested here is not totally suitable for pectin extraction. On the other hand, the protease assisted extraction allowed to isolate from citrus fruits by-products a specific fraction of soluble fibre that is rich in arabinose and galactose, with possible specific applications.

More in general, arabinose and galactose were the two main monomers in almost every sample, excluding mango seeds and loquar kernels. In fact, their sum accounted for 82% of total sugars in orange by-products, for 65% in peach kernels, for 60% in lemon seeds and for 51% in lemon peels, suggesting the presence of

arabinogalactans as the main soluble fibre extracted in the conditions used. It has been indeed reported that arabinogalactans, unlike pectin, have better extraction yields at low temperatures and neutral pH, as obtained by Hamed and colleagues [23]. According to literature, the presence of arabinogalactans has been shown in the pulp of peach [24], in pistachio shells [23], and in general in different fruit parts, such as apples [25], prickly pear peels [26], and carambola (starfruit) [27]. Arabinogalactans are polysaccharides having molecular weight of about 58 kDa [28], composed mainly of galactose and arabinose and sometimes with lower amount of rhamnose and glucose units [23]. The presence of high molecular weight molecules within all the analysed samples (Table 3.3) could be associated with the presence of polymers similar to gum arabic, which have been reported to have molecular weights in the range of 312-950 kDa and arabinose and galactose as prevalent monosaccharides [29]. In plants, arabinogalactans are often bound to proteins and represent the major proteoglycans within plant cell walls, and gum arabic is indeed made of arabinogalactans (AG) and arabinogalactan-protein (AGP) complexes [30]. The proximate composition of the soluble fruit fibre fractions extracted in this work was also investigated and turned out, on average and respect to the dry matter, to be made of 50% fibres, 30% proteins and 20% ash, indeed demonstrating a significant amount of protein in the soluble fibre fraction as for gum arabic. However, the percentage of residual protein is quite high and it cannot be exclusively attributed to glycoproteins, also suggesting a small percentage of non-hydrolysed proteins that co-precipitates with fibres after ethanol addition.

Although a lot of unusual new sources of arabinogalactans, including plant seeds, have been recently found and summarized in a recent review [31], not many reports about their presence in fruit by-products are present, especially when fruit kernels are considered. This work lays the foundation for future studies, which could focus more on these by-products as a potential matrix for the recovery with good yields of this polysaccharide, which in recent years has also attracted attention for its immunostimulatory activity [32].

3.5. Proximate composition of residual pellet

After the employment of EAE, a significant amount of residual solid fraction (from now on named as “pellet”) remained (Figure 3.1). In order to understand the possibility to further valorise it, in a perspective of circular economy and complete fractionation, a characterization of its components was performed in terms of dry matter, lipids, proteins, ash and total fibres. The pie charts below (Figure 3.4) report the results obtained.

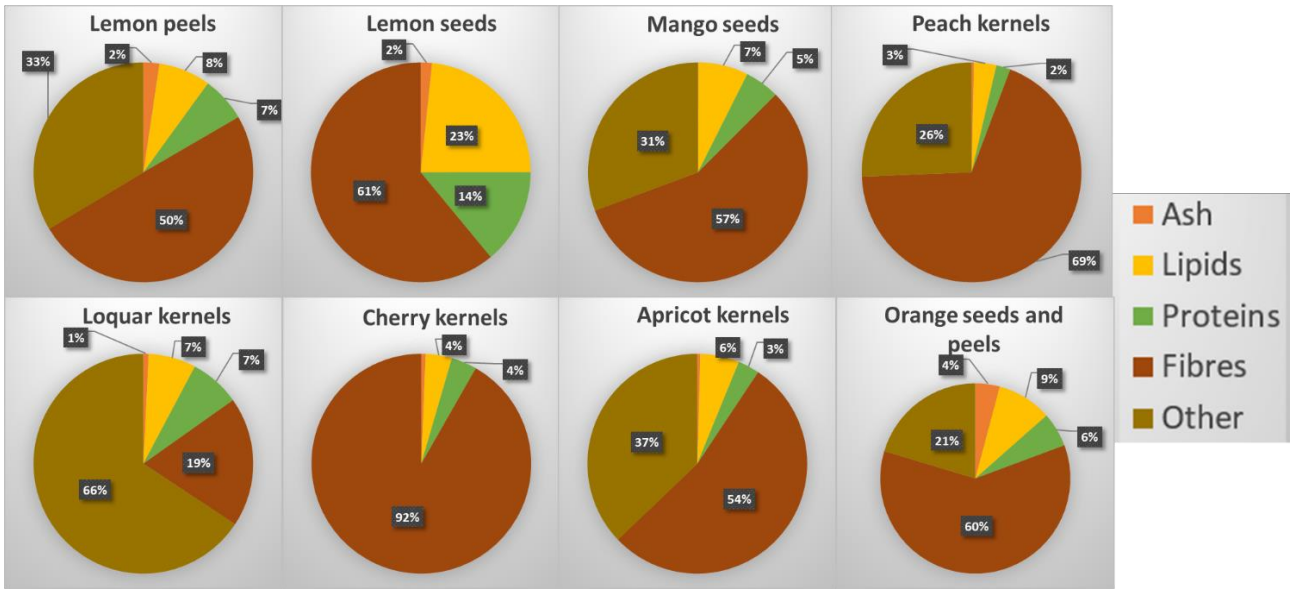

Figure 3.4: *Proximate composition of the residual pellets remained after EAE. Each analysis was performed in duplicate and the results are expressed as their mean and as percentage on dry matter (%DM). The percentage of "other" was calculated by difference from 100.*

Results showed that all the residual pellets, with the exception of loquar kernels, were composed mainly of fibre. On average, seven samples out of eight presented a quantity of dietary fibre in the range 50-90%. These fibres are mainly insoluble (see Table 3.1), and since not the whole amount of soluble fibres was extracted during EAE (see Table 3.2), some residual soluble fibres are certainly also included in this portion. Since most of the samples examined are definable as lignocellulosic materials, it is assumed that most of this residual fibre consists of hemicellulose, cellulose and lignin as major fractions, which certainly cannot be extracted through a "mild" extraction like the EAE performed in the present work. These findings represent an interesting starting point for future works: in fact, through the use of "harder" extractions, such as extractions at higher temperatures and acid pH, it would be possible to recover pectin eventually present, and through autohydrolysis treatments the extraction of hemicelluloses could be also carried out. Therefore, it would be possible to further valorise these fruit and vegetable by-products, completing their fractionation and satisfying the circular economy concept.

Regarding other compounds, the relative amount of protein present within the pellet still appears to be significant, especially for lemon seeds, and for this reason further studies are needed to understand whether the proteins are “free” and easily extractable in other media or complexed with other molecules. The lipid fraction remained almost totally within the pellets: this is not surprising, since they are sometimes bound to the matrix, and for a total extraction from seeds they should be treated with organic solvent, in some cases also after acid treatment of the matrix, as for lipid extraction from raw cocoa beans [33].

4. Conclusions

This work fits into the context of agri-food by-products valorisation, in the perspective of trying to contribute to address issues regarding increased waste generation, environmental pollution and resource consumption. Some scraps from the fruit and vegetable supply chain, namely peels, seeds, and kernels, were subjected to enzymatic assisted extraction (EAE) with a protease aiming to simultaneously obtain proteins, lipids and fibres.

As promising results, the enzymatic process based on the use of protease allowed to: i) recover proteins as protein hydrolysates; ii) preserve the structural integrity of the soluble fibre, which was recovered from the aqueous solution by ethanol precipitation, and the insoluble fibres, which mainly constituted the residual pellet.

Soluble fibres were quantified aiming to calculate the extraction yield, and for cherry and peach kernels, mango seeds and orange by-products very good yields were obtained (71%, 54%, 33% and 30%, respectively), while scarce yields were gained from the others. These soluble fibres were characterized in their monosaccharide composition, and in many samples a dominant presence of arabinose and galactose moieties was detected, suggesting a potential similarity with arabinogalactans. High molecular weight polymers (> 201 kDa) were present in all samples, particularly in cherry, loquar, and apricot kernels and in lemon seeds and peels; the high molecular weights together with the monosaccharide composition might suggest the hypothesis of technological similarity of the obtained fibres with gum arabic. The presence of low molecular weight polymers (< 6kDa) was also revealed, especially in mango seeds, peach kernels and orange scraps. Since it is known how molecular weight affects certain technological and nutritional properties of polymers, a future approach based on the separation of these fractions may be considered. Finally, the study on the proximate composition of the residual pellets after EAE showed that even though they still contained decent quantities of proteins and lipids, the main portion was constituted by fibres, namely presumably cellulose, hemicellulose and lignin, but also the soluble fibres portion that was not extracted by the mild enzymatic treatment employed. These results suggest the potentiality to further exploit the residual pellet, employing harder treatment to extract more valuable compounds, in order to fully valorise a very precious by-product that is today too much undervalued.

REFERENCES

1. FAO *Food wastage footprint: Impacts on natural resources - Summary report*; 2013;
2. Moreno-González, M.; Ottens, M. A Structured Approach to Recover Valuable Compounds from Agri-food Side Streams. *Food Bioprocess Technol.* **2021**, *14*, 1387–1406, doi:10.1007/s11947-021-02647-6.
3. Banerjee, J.; Singh, R.; Vijayaraghavan, R.; MacFarlane, D.; Patti, A.F.; Arora, A. Bioactives from fruit processing wastes: Green approaches to valuable chemicals. *Food Chem.* **2017**, *225*, 10–22, doi:10.1016/j.foodchem.2016.12.093.
4. Manhongo, T.T.; Chimphango, A.F.A.; Thornley, P.; Röder, M. Current status and opportunities for fruit processing waste biorefineries. *Renew. Sustain. Energy Rev.* **2022**, *155*, 111823, doi:10.1016/j.rser.2021.111823.
5. Kosseva, M.R.; Webb, C. *Food Industry Wastes*; 2013; ISBN 9780123919212.
6. Cherubini, F. The biorefinery concept: Using biomass instead of oil for producing energy and chemicals. *Energy Convers. Manag.* **2010**, *51*, 1412–1421, doi:10.1016/j.enconman.2010.01.015.
7. Henríquez, C.; Speisky, H.; Chiffelle, I.; Valenzuela, T.; Araya, M.; Simpson, R.; Almonacid, S. Development of an ingredient containing apple peel, as a source of polyphenols and dietary fiber. *J. Food Sci.* **2010**, *75*, H172–H181, doi:10.1111/j.1750-3841.2010.01700.x.
8. Matsusaka, Y.; Kawabata, J. Evaluation of antioxidant capacity of non-edible parts of some selected tropical fruits. *Food Sci. Technol. Res.* **2010**, *16*, 467–472, doi:10.3136/fstr.16.467.
9. Bolarinwa, I.F.; Orfila, C.; Morgan, M.R.A. Amygdalin content of seeds, kernels and food products commercially- available in the UK. *Food Chem.* **2014**, *152*, 133–139, doi:10.1016/j.foodchem.2013.11.002.
10. Kumoro, A.C.; Alhanif, M.; Wardhani, D.H. A Critical Review on Tropical Fruits Seeds as Prospective Sources of Nutritional and Bioactive Compounds for Functional Foods Development: A Case of Indonesian Exotic Fruits. *Int. J. Food Sci.* **2020**, *2020*, 1–15, doi:10.1155/2020/4051475.
11. market data forecast.
12. Global Industry Analysts Research Reports - MarketResearch.com.
13. AOAC Official Method of Analysis. 16th Edition. Association of official analytical, Washington DC. **2002**.
14. AOAC AOAC Official Method 991.43 Total, Soluble, and Insoluble Dietary Fibre in Foods. *J. AOAC Int.* **2012**, doi:10.5740/jaoacint.CS2011_25.
15. Xia, Y.G.; Wang, T.L.; Sun, H.M.; Liang, J.; Kuang, H.X. Gas chromatography–mass spectrometry-based trimethylsilyl-alditol derivatives for quantitation and fingerprint analysis of Anemarrhena asphodeloides Bunge polysaccharides. *Carbohydr. Polym.* **2018**, doi:10.1016/j.carbpol.2018.06.066.
16. Patiño-Rodríguez, O.; Agama-Acevedo, E.; Ramos-Lopez, G.; Bello-Pérez, L.A. Unripe mango kernel starch: Partial characterization. *Food Hydrocoll.* **2020**, *101*, 105512, doi:10.1016/j.foodhyd.2019.105512.
17. Mañas, E.; Saura-Calixto, F. Ethanolic precipitation: A source of error in dietary fibre determination. *Food Chem.* **1993**, *47*, 351–355, doi:10.1016/0308-8146(93)90176-G.
18. de Albuquerque, M.A.C.; Levit, R.; Beres, C.; Bedani, R.; de Moreno de LeBlanc, A.; Saad, S.M.I.; LeBlanc, J.G. Tropical fruit by-products water extracts of tropical fruit by-products as sources of soluble fibres and phenolic compounds with potential antioxidant, anti-inflammatory, and functional properties. *J. Funct. Foods* **2019**, *52*, 724–733, doi:10.1016/j.jff.2018.12.002.
19. Zhou, Y.; Cui, Y.; Qu, X. Exopolysaccharides of lactic acid bacteria: Structure, bioactivity and associations: A review. *Carbohydr. Polym.* **2019**, *207*, 317–332, doi:10.1016/j.carbpol.2018.11.093.
20. Lazaridou, A.; Biliaderis, C.G. Molecular aspects of cereal β-glucan functionality: Physical properties, technological applications and physiological effects. *J. Cereal Sci.* **2007**, *46*, 101–118, doi:10.1016/j.jcs.2007.05.003.
21. Hosseini, S.S.; Khodaiyan, F.; Kazemi, M.; Najari, Z. Optimization and characterization of pectin extracted from sour orange peel by ultrasound assisted method. *Int. J. Biol. Macromol.* **2019**, *125*, 621–629, doi:10.1016/j.ijbiomac.2018.12.096.
22. Thu Dao, T.A.; Webb, H.K.; Malherbe, F. Optimization of pectin extraction from fruit peels by response surface method: Conventional versus microwave-assisted heating. *Food Hydrocoll.* **2021**, *113*, 106475, doi:10.1016/j.foodhyd.2020.106475.
23. Hamed, M.; Coelho, E.; Bastos, R.; Evtuguin, D. V.; Ferreira, S.S.; Lima, T.; Vilanova, M.; Sila, A.; Coimbra, M.A.; Bougatef, A. Isolation and identification of an arabinogalactan extracted from pistachio external hull: Assessment of immunostimulatory

activity. *Food Chem.* **2022**, *373*, 131416, doi:10.1016/j.foodchem.2021.131416.

24. Simas-Tosin, F.F.; Abud, A.P.R.; De Oliveira, C.C.; Gorin, P.A.J.; Sassaki, G.L.; Bucchi, D.F.; Iacomini, M. Polysaccharides from peach pulp: Structure and effects on mouse peritoneal macrophages. *Food Chem.* **2012**, *134*, 2257–2260, doi:10.1016/j.foodchem.2012.04.041.

25. Leszczuk, A.; Szczuka, E.; Wydrych, J.; Zdunek, A. Changes in arabinogalactan proteins (AGPs) distribution in apple (Malus x domestica) fruit during senescence. *Postharvest Biol. Technol.* **2018**, *138*, 99–106, doi:10.1016/j.postharvbio.2018.01.004.

26. Habibi, Y.; Mahrouz, M.; Marais, M.F.; Vignon, M.R. An arabinogalactan from the skin of Opuntia ficus-indica prickly pear fruits. *Carbohydr. Res.* **2004**, *339*, 1201–1205, doi:10.1016/j.carres.2004.02.004.

27. Leivas, C.L.; Iacomini, M.; Cordeiro, L.M.C. Structural characterization of a rhamnogalacturonan I-arabinan-type I arabinogalactan macromolecule from starfruit (Averrhoa carambola L.). *Carbohydr. Polym.* **2015**, *121*, 224–230, doi:10.1016/j.carbpol.2014.12.034.

28. Li, H.; Xie, W.; Qiao, X.; Cui, H.; Yang, X.; Xue, C. Structural characterization of arabinogalactan extracted from Ixeris chinensis (Thunb.) Nakai and its immunomodulatory effect on RAW264.7 macrophages. *Int. J. Biol. Macromol.* **2020**, *143*, 977–983, doi:10.1016/j.ijbiomac.2019.09.158.

29. Islam, A.M.; Phillips, G.O.; Sljivo, A.; Snowden, M.J.; Williams, P.A. A review of recent developments on the regulatory, structural and functional aspects of gum arabic. *Food Hydrocoll.* **1997**, *11*, 493–505, doi:10.1016/S0268-005X(97)80048-3.

30. Han, L.; Hu, B.; Ma, R.; Gao, Z.; Nishinari, K.; Phillips, G.O.; Yang, J.; Fang, Y. Effect of arabinogalactan protein complex content on emulsification performance of gum arabic. *Carbohydr. Polym.* **2019**, *224*, 115170, doi:10.1016/j.carbpol.2019.115170.

31. Saeidy, S.; Petera, B.; Pierre, G.; Fenoradosoa, T.A.; Djomdi, D.; Michaud, P.; Delattre, C. Plants arabinogalactans: From structures to physico-chemical and biological properties. *Biotechnol. Adv.* **2021**, *53*, 107771, doi:10.1016/j.biotechadv.2021.107771.

32. Ferreira, S.S.; Passos, C.P.; Cepeda, M.R.; Lopes, G.R.; Teixeira-Coelho, M.; Madureira, P.; Nunes, F.M.; Vilanova, M.; Coimbra, M.A. Structural polymeric features that contribute to in vitro immunostimulatory activity of instant coffee. *Food Chem.* **2018**, *242*, 548–554, doi:10.1016/j.foodchem.2017.09.059.

33. Parsons, J.G.; Keeney, P.G.; Patton, S. Identification and Quantitative Analysis of Phospholipids in Cocoa Beans. J. Food Sci. 1969, 34, 497– 499, doi:10.1111/j.1365-2621.1969.tb12069.x.

CHAPTER 4

A multiplatform “reactomics” approach as a powerful strategy to identify reaction compounds generated during hemicellulose hydrothermal extraction from agro-food biomasses

The content of this chapter has also been submitted as:

Andrea Fuso, Laura Righetti, Franco Rosso, Ginevra Rosso, Ileana Manera, Augusta Caligiani. A multiplatform metabolomics/reactomics approach as a powerful strategy to identify reaction compounds generated during hemicellulose hydrothermal extraction from agro-food biomasses.

ABSTRACT

Hydrothermal treatment is commonly used for hemicelluloses extraction from lignocellulosic materials. In this study, we thoroughly investigated with a novel approach the metabolomics of degradation compounds formed when hazelnut shells are subjected to this type of treatment. Three different techniques were combined, namely GC-MS, ^{1}H NMR, and UHPLC-IM-Q-TOF-MS. Organic acids, modified sugars and aromatic compounds, likely to be the most abundant chemical classes, were detected by all techniques, while many other molecules, like furans, polyols, N-heterocyclic compounds, aldehydes, ketones, and esters appeared only when the chromatographic methods were employed. Ion mobility-based LC-MS method, in particular, was innovatively used for this purpose and could allow in the near future to create potentially useful datasets for building specific databases relating to the formation of these compounds in different process conditions and employing different matrices. This could be a very intelligent approach especially in a risk assessment perspective.

1. Introduction

In the last decades much attention has been paid in combatting the phenomenon of food waste, which represents a big issue for ethical, environmental and economic reasons [1,2]. Among all foodstuffs, products of vegetable origin, such as cereals, tubers, roots, fruit and vegetables, are those connected to the greatest quantity of waste [3]. The composition of these wastes can be disparate, but according to a recent study about 90% of plant biomass is represented by lignocellulosic material [4], which means that it is mainly composed of lignin, hemicellulose and cellulose, in variable proportions. The valorization of these by-products, due to the extraordinary structural complexity of the polymers present within them, cannot disregard the principle of biorefinery, i.e., the separation of the individual biomass fractions for the production of different components, such as biomolecules, biomaterials, bioenergy and biofuels [5]. In a historical period in which consumer's food choices are changing, moving towards healthier foods [6], dietary fibres naturally play a fundamental role. For this reason, hemicelluloses in particular acquire an even greater global interest, as also demonstrated by the exponential growth of studies on the subject over the years [7]. Indeed, hemicelluloses have a wide variety of applications: for instance, they can be easily transformed into oligosaccharides with interesting bio-functional properties or further depolymerized into pentoses and hexoses for subsequent conversion into bioethanol and chemical substances [8]. Hemicelluloses are relatively small heteropolysaccharides (degree of polymerization 100-200 units), branched and made of five- and six-carbon monosaccharide units, of which the most frequent are xylose, mannose, arabinose, galactose, glucose and glucuronic acid, as well as acetyl groups [9,10]. These complex polymers were found to be linked by hydrogen bonds and van der Waals interactions with cellulose, forming highly resistant networks [10], and at the same time they interact with lignin through complex interactions, which are radical coupling of ferulate substitutions and incorporation of hemicellulosic glycosyl residues by re-aromatization of lignification intermediates [11]. Hence, to extract and isolate hemicelluloses, "strong" methods are needed, and the most used combine high temperatures and high pressures. The most common in this sense is the hydrothermal treatment (HT), also called autohydrolysis treatment, which consists in subjecting the matrix of interest to extraction at 160 - 220 °C in water, kept in the liquid state thanks to the high pressures [12]. When such treatment is applied, however, it is very likely to get the formation in the reaction medium of innumerable undesired compounds, such as degradation products derived from lignin, sugars or proteins, as well as monosaccharides, furans and organic acids [13]. The mechanism of formation of these compounds is extremely complicated, since it is strictly related to the time/temperature conditions set, to the pH and to the matrix. Depending on the reaction conditions, for example, glucose can be converted into 5-(hydroxymethyl)-2-furaldehyde (HMF) and/or levulinic acid, formic acid and various phenolics at high temperatures, while xylose can follow different reaction mechanisms originating furan-2-carbaldehyde

(furfural) and/or various C-1 and C-4 compounds. Furthermore, monosaccharides can further react to form pseudo-lignin, humine, aldehydes, ketones, organic acids or aromatic compounds [14]. Several studies have shown how it was possible to vary the composition of the autohydrolysis liquor after HT in different conditions, mainly in terms of furfural, HMF, acetic, formic and lactic acid content [8,15,16]. At the same time, other research has shown that although some mechanisms are to date well understood, many other metabolic pathways still remain unknown [17]. Therefore, since one of the main aims of reusing hemicellulose from vegetable by-products is its transformation into healthy ingredients for food companies, it is of enormous importance to further investigate the presence and the formation of all these compounds that originate following HT, especially to evaluate them in terms of potential toxicity. This investigation must be done both through the study and understanding of the reaction mechanisms, and through the improvement of analytical techniques that allow their identification and quantification. In this complex scenario, where multiple reaction pathways not fully understood led to very complicated mixtures of neo-formed compounds, there is the need of combining different and complementary analytical approaches, to further unravelling the reaction mechanisms and better characterize the composition of lignocellulose hydrothermal extracts. To this aim, in the present work the molecular composition of the hydrothermal extracts of hazelnut shells (HS) was studied using different metabolomics platform, namely ^{1}H NMR, GC-MS and UHPLC-IM-Q-TOF-MS.

2. Materials and methods

2.1. Chemicals and reagents

HPLC-grade acetonitrile, ammonium formiate, trifluoroacetic acid (TFA), N,O-Bis(trimethylsilyl)trifluoroacetamide (BSTFA), 3-(trimethylsilyl)propionate-*d4* (TSP), D-glucose, D-fructose, D-galactose, D-mannose, D-rhamnose, D-ribose, D-xylose, D-fucose, D-galacturonic acid, D-glucuronic acid, D-glucosamine, D-galactosamine and phenyl-β-D-glucopyranoside were purchased from Sigma-Aldrich (Taufkirchen, Germany); bidistilled water was obtained using Milli-Q System (Millipore, Bedford, MA, USA); diethyl ether, hydrochloric acid and ethanol were purchased from Carlo Erba (Milan, Italy); D_2O was bought from VWR (Radnor, PA, USA); MS-grade formic acid from Fisher Chemical (Thermo Fisher Scientific Inc., San Jose, CA, USA) was also used.

2.2. Hydrothermal treatment of hazelnut shells

Hazelnut shells (HS) were kindly provided by Ferrero S.p.A. (Cuneo, Italy), finely ground and sieved with grain size <500 µm. The hydrothermal treatment (HT) was performed in a stainless-steel Parr reactor 4566 (Parr Instrument Company, Moline, Illinois, USA) with an internal volume of 300 mL and internal cooling loop,

equipped with Parr PDI for temperature control (model 4848). 5 g of ground sample were extracted with 125 mL of bidistilled water, and HT was carried out under isothermal conditions for 60 minutes at 175 °C. The time to reach the working temperature was 30 min and the final relative pressure was 8.1 bar. After treatment, the obtained solid and liquid phases were separated by centrifugation at 3900 rpm for 30 minutes at 4 °C. Finally, the supernatant was collected and freeze-dried. All the following analyses described in the next sections were performed on this sample.

2.3. Proximate composition of HS extract

Proximate composition of HS extract was investigated using standard procedures [18]. Moisture was determined by drying in oven at 105 °C for 24 h. Total ash was determined through mineralization at 550 °C in two steps, each one lasting 5 h. Total nitrogen was determined with a Kjeldahl system (DKL heating digester and UDK 139 semiautomatic distillation unit, VELP SCIENTIFICA) using 6.25 as a nitrogen-to-protein conversion factor. Lipid content was determined using a Soxhlet extractor (SER 148/3 VELP SCIENTIFICA, Usmate Velate, Italy) employing diethyl ether as extracting solvent.

Total sugars and monosaccharide distribution were investigated following a protocol previously proposed by Xia et al. with some modifications [19]. Briefly, 10 mg of sample were dissolved in 3 mL of 2N trifluoroacetic acid (TFA) and hydrolysed at 110 °C for 2 hours under stirring. Then, 900 µL of the solution were withdrawn and put together with 150 µL of 1000 ppm phenyl-β-D-glucopyranoside, used as internal standard, and then evaporated by rotavapor. The obtained dried hydrolysate was washed with 1 mL of methanol to remove the residue of TFA and evaporated again. 1 mL of 0.5 M NH_4OH was subsequently added to delactonize the eventually present acid sugar lactones in the sample, and again evaporated by rotavapor. Finally, the dried hydrolysate was dissolved in 800 µL of dimethylformamide (DMF) and 200 µL of N,O-Bis(trimethylsilyl)trifluoroacetamide (BSTFA), the latter used as derivatizing agent. The reaction was held for 1 hour at 60 °C and finally the derivatized sample was injected in gaschromatography. GC-MS analysis of monosaccharides was performed with a 6890 N gas chromatograph coupled to a 5973 N mass selective detector (Agilent technologies, Santa Clara, CA). A SLB-5ms, 30 m × 0.25 mm, 0.25 µm thickness column (Supelco, Bellafonte, PA, USA) was used. The chromatogram was recorded in the scan mode (40–500 m/z) with a programmed temperature from 60 °C to 270 °C. The initial temperature was 60 °C, held for 2 minutes, then increased to 160 °C at a rate of 10 °C/min, held isothermal for 5 minutes, increased to 220 °C at a rate of 10 °C/min, kept for 5 minutes, increased to 270 °C at a rate of 20 °C/min and maintained for 5 minutes. Quantification was performed with a response factor, considering the area and concentration ratios between the internal standard (phenyl-β-D-glucopyranoside), and the following monosaccharides: D-glucose, D-fructose, D-galactose, D-mannose, D-rhamnose, D-ribose, D-xylose, D-fucose, D-galacturonic acid, D-glucuronic acid, D-glucosamine and D-galactosamine.

2.4. Gaschromatography-mass spectrometry (GC-MS) analysis

The protocol for samples preparation before GC-MS analysis is represented in Figure 4.1. Briefly, 300 mg of sample were weighted and added to 6 mL of water and the extraction was carried out at 50 °C for 2 hours. Later, the sample was split in three different 2 mL aliquots: the first ("H_2O") was simply analyzed after putting 200 µL in a round-bottomed flask containing 65 µL of 1160 ppm phenyl-β-glucopyranoside, used as standard. In both the second and third aliquot, 8 mL of ethanol were firstly added to make the fibres to precipitate. The solutions were thoroughly mixed and centrifuged at 4 °C and 3900 rpm for 25 minutes. Later, in the second aliquot ("EtOH") about 1700 µL of the supernatant were withdrawn and put together with 65 µL of 1160 ppm phenyl-β-glucopyranoside in a new round-bottomed flask. In the third aliquot ("HCl"), 3 mL of the supernatant obtained after centrifugation were withdrawn, put in a new round-bottomed flask and dried by rotavapor, then here 2 mL of 4N HCl were added, and the solution was allowed to stand at 100 °C for 3 hours under stirring. At the end of the reaction, the same amount of phenyl-β-glucopyranoside used in the other experiments was added. Finally, the three solutions were dried by rotavapor, then derivatized by adding 800 µL of DMF and 200 µL of N,O-Bis(trimethylsilyl)trifluoroacetamide (BSTFA), the latter used as derivatizing agent, and allowing the reaction to stand for 1 h at 60 °C before being injected in GC-MS.

GC-MS analysis of the degradation products originated from the HT was performed with a 6890 N gas chromatograph coupled to a 5973 N mass selective detector (Agilent technologies, Santa Clara, CA). A SLB-5ms, 30 m × 0.25 mm, 0.25 µm thickness column (Supelco, Bellafonte, PA, USA) was used. The mass spectrometer operated in the electron impact (EI) ionization mode (70 eV) and the ion source temperature was set at 230 °C. The chromatogram was recorded in the scan mode (50–800 m/z) with a programmed temperature from 60 °C to 270 °C. The initial temperature was 60 °C, held for 2 minutes, then increased to 160 °C at a rate of 10 °C/min, held isothermal for 10 minutes, increased to 220 °C at a rate of 10 °C/min, kept for 5 minutes, increased to 270 °C at a rate of 20 °C/min and maintained for 15 minutes. A semi-quantification of each analyte identified was performed, according to the following formula:

$$\text{ppm}_{\text{analyte}} = \frac{\text{Area}_{\text{analyte}} * \text{ppm}_{\text{phenyl-β-D-glucopyranoside}}}{\text{Area}_{\text{phenyl-β-D-glucopyranoside}}}$$

The identification of the various compounds was performed comparing mass spectra with WILEY library data.

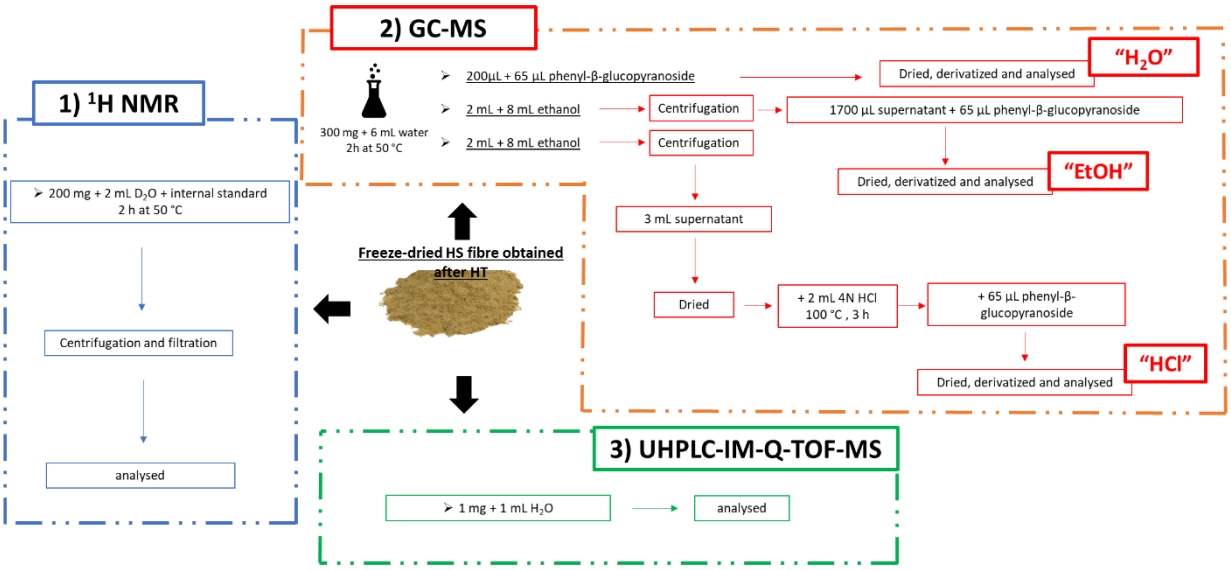

Figure 4.1: *Representation of samples preparation before ^{1}H NMR, GC-MS and UHPLC-IM-Q-TOF-MS analysis.*

2.5. ^{1}H NMR analysis

An aqueous extract of the freeze-dried extract obtained after hydrothermal treatment of HS was analysed through ^{1}H NMR. Briefly, 200 mg of sample were added to 2 mL D_2O together with 100 µL of 2210 ppm TSP dissolved in D_2O, and the extraction was performed under stirring at 50 °C for 2 hours. Then, the solution was centrifuged at 4 °C and 3900 rpm for 25 minutes and subsequently filtered through a 0.45 µm nylon membrane in a 5 mm NMR tube (Figure 4.1).

^{1}H NMR spectra were recorded on a Bruker Avance III 400 MHz NMR Spectrometer (Bruker BioSpin, Rheinstetten, Karlsruhe, Germany) operating at a magnetic field-strength of 9.4T. A 1D 1H NOESY sequence, previously optimized to remove the residual water signal with minimal affection of the baseline, was utilized for water suppression [20]. Spectra were acquired at 298 K, with 32 K complex points, using a 90° pulse length and 5 s of relaxation delay (d1). 128 scans were acquired with a spectral width of 20 ppm, an acquisition time of 1.707 s, 8 dummy scans and a mixing time of 0.010 s. The complete relaxation of the protons obtained during acquisition time and relaxation delay allowed to use integrals for quantitative purposes. Figure 4.2 reports the main spectral zones assigned to different classes of compounds found in hydrothermal extracts of hazelnut shells. The same zones were integrated and used for a preliminary crude quantification of the different compounds. Acetyl groups deriving from free acetate and substituted sugars (mainly acetylated xylans) were quantified integrating the spectral zone 1.92-2.34 ppm. Total aromatic compounds were determined from the integration of the whole zone 5.97-7.78 and expressed as phenylpropanoids. The signal

of formic acid at 8.45 was integrated as determinant indicative of a part of degraded sugars according to the mechanism of levulinic acid formation [21].

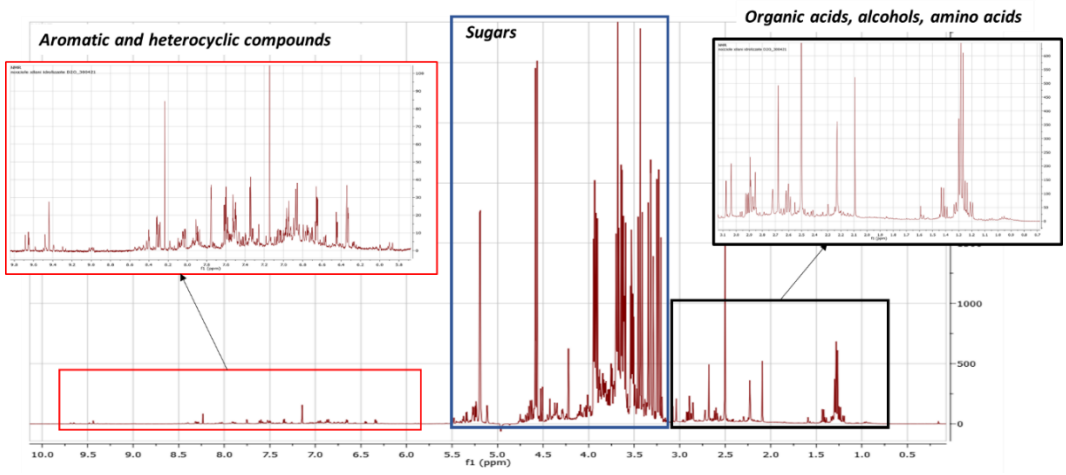

***Figure 4.2**: 1D ^{1}H-NOESY NMR spectrum (400 MHz, D_2O) of the HS fibre solubilized in D_2O.*

2.6. Ultra-high-performance liquid chromatography - Ion mobility – quadrupole time-of-flight – mass spectrometry (UHPLC-IM-Q-TOF-MS) analysis

The reaction products originated from hydrothermal treatment of HS were further identified through UHPLC-IM-Q-TOF-MS. The sample was simply dissolved in water and analysed (Figure 4.1). Specifically, 1 mg of the freeze-dried extract obtained after HT was dissolved in 1 mL of MilliQ water.

2.6.1. UHPLC- TWIMS-QTOF analysis

ACQUITY I-Class UHPLC separation system coupled to a VION IMS QTOF mass spectrometer (Waters, Wilmslow, UK) equipped with an electrospray ionization (ESI) interface was employed. Samples were injected (2 µL) and chromatographically separated using a reversed-phase ACQUITY Premier HSS T3 column 2.1 × 100 mm, 1.8 µm particle size (Waters, Milford, MA, USA). A gradient profile was applied using water 5mM ammonium formiate (eluent A) and acetonitrile (eluent B) both acidified with 0.1% formic acid as mobile phases. Initial conditions were set at 2% B, after 3 min of isocratic step, a linear change to 100% B was achieved in 12 min and holding for 5 min to allow for column washing before returning to initial conditions. Column recondition was achieved over 3 min, providing a total run time of 23 min. The column was maintained at 45 °C and a flow rate of 0.35 mL/min used.

Mass spectrometry data were collected in positive and negative electrospray mode over the mass range of *m/z* 50−1100. Source settings were maintained using a capillary voltage, 2.5 kV and 2 kV for positive and negative ESI modes, respectively; source temperature, 150 °C; desolvation temperature, 500 °C and desolvation gas flow, 950 L/h. The TOF analyzer was operated in sensitivity mode and data acquired using

HDMSE, which is a data independent approach (DIA) coupled with ion mobility. The optimized ion mobility settings included: nitrogen flow rate, 90 mL/min (3.2 mbar); wave velocity 650 m/s and wave height, 40 V. Device within the Vion was calibrated using the Major Mix IMS calibration kit (Waters, Wilmslow, UK) to allow for collisional cross section (CCS) values to be determined in nitrogen. The calibration covered the CCS range from 130-306 Å2. The TOF was also calibrated prior to data acquisition and covered the mass range from 151 Da to 1013 Da. TOF and CCS calibrations were performed for both positive and negative ion mode. Data acquisition was conducted using UNIFI 1.8 (Waters, Wilmslow, UK).

2.6.2. Data Processing

Data processing and compound identification were conducted using Progenesis QI Informatics (Nonlinear Dynamics, Newcastle, UK). Each UHPLC-MS run was imported as an ion-intensity map, including *m/z* and retention time, that were then aligned in the retention-time direction (0–20 min). From the aligned runs, an aggregate run representing the compounds in all samples was used for peak picking. This aggregate was then compared with all runs, so that the same ions were detected in every run. Isotope and adduct deconvolution were applied, to reduce the number of features detected. Metabolites were identified by publicly available database searches including Lipid Metabolites and Pathways Strategy (LIPID MAPS) [22], Human Metabolome database (HMDB) [23], and METLIN [24], as well as by fragmentation patterns, retention times, and CCS.

3. Results and discussion

3.1. Proximate composition of HS extract

After undergoing the HT and before studying the degradation compounds originated from it, both proximate composition and monosaccharide distribution of the freeze-dried extract was investigated. Results are reported in Table 4.1.

Table 4.1*: Proximate composition and fibre's monosaccharide distribution of the freeze-dried extract obtained following HT of HS.*

	Proximate composition (g/100 g of freeze-dried HT extract)	Method
Moisture	2.4 ± 0.1	AOAC official method [18]
Lipids	1.0 ± 0.4	
Proteins	3.0 ± 0.5	
Ash	9.3 ± 0.2	
Total monosaccharides	49.3 ± 3.1	GC-MS and ^{1}H NMR
Total acetyl groups	8.0 ± 0.7	
Total aromatic compounds (expressed as phenylpropanoids)	5.0 ± 0.7	^{1}H NMR

Degraded sugars	1.1 ± 0.1	
	Monosaccharide distribution (g/100 g monosaccharides)	
Arabinose	8.1 ± 1.2	GC-MS
Rhamnose	6.0 ± 0.8	
Xylose	63.4 ± 1.3	
Galactose	4.4 ± 0.4	
Glucose	1.4 ± 0.3	
Galacturonic acid	8.0 ± 1.6	
Glucuronic acid + 4-O-methylglucuronic acid	8.7 ± 1.5	

As expected, this sample was predominantly made of sugars, which accounted for half of its fresh weight (see Table 4.1). As concerns monosaccharide distribution of the fibres extracted, they were mainly made of xylose (63%). Other sugars, such as arabinose and glucuronic acid, were also present probably as substituents along the xylose-based chain, as often happens in xylans extracted from lignocellulosic matrices [25]. Finally, galacturonic acid and glucose could be derived from pectin and cellulose fractions, while rhamnose and galactose could derive from pectin as well [26].

A relevant amount of ash, equal to 9%, was also found, while proteins and lipids were quite lower (3% and 1%, respectively). Interestingly, the sum of moisture, proteins, lipids, ash and total sugars accounted for only 65%. By ^{1}H NMR analysis it was also possible to investigate the amount of acetyl groups attached to the xylan backbone, and to estimate both the aromatic compounds, derived from lignin and calculated as phenylpropanoids, as well as the sugars chemically modified by thermal degradation, overall reaching a total sum of about 80%. However, about one-fifth of the percentage by weight of the gross composition remained uncharacterized and most likely constituted by neo-formation compounds risen from polysaccharides and lignin during the thermal process. In the effort of characterizing as much as possible these process-derived compounds, different analytical methods have been applied, as reported in the following paragraphs.

3.2. GC-MS analysis

Following GC-MS analysis carried out on the sample treated in three different ways (Figure 4.1), compounds identification was carried out by comparing the mass spectra of the trimethylsilyl (TMS) derivatives with Wiley275 library. A total of 54 compounds were selected and integrated as they are likely to be derived from HT (Table 4.2).

Table 4.2: List of compounds originated after HT, identified and semi-quantified by GC-MS.

Peak number	RT (min)	Compound	Main MS peaks of TMS derivatives (*m/z*)	Identification score	Pathway	Semi-quantitative amount (g/100 g initial sample)		
						Water Extract ("H_2O")	*Water Extract after Fibre Precipitation ("EtOH")*	*Acid Hydrolysed-Water Extract after Fibre Precipitation ("HCl")*
Organic acids								
1	6.88	Lactic acid	73,117,147,219,190	74	Glucose oxidation/ raw material	0.054	0.029	0.136
2	7.15	Glycolic acid	73,147,177,205	78	From sugars	0.045	0.004	0.113
3	8.02	2-ketogluconic acid	73,103,117,147,189,204	59	From sugar oxidation	0.019	0.013	ND
4	8.11	Levulinic acid	73,75,131,145,173	93	From sugars	ND	ND	0.012
6	8.24	3-hydroxypropionic acid	73,147,177,219	59	Aromatic compounds oxidation	ND	0.007	ND
10	10.74	5-hydroxyvaleric acid	73,75,147,172,247,	86	From sugars	0.011	ND	0.020
11	10.94	2,3-dihydroxypropanoic acid	73,103,147,189,205,292,307	83	Glycerol derivative	ND	ND	0.008
12	11.02	2-hydroxyhexanoic acid	73,147,159,190,233,261	78	From sugars	ND	ND	0.011
Total organic acids						**0.129**	**0.053**	**0.300**
Aromatic compounds								
7	9.83	Benzoic acid	51,77,105,135,179,194	86	Lignin	0.320	0.420	0.161
24	23.56	3-Vanillyl propanol	73,179,192,206,221,236,311,326	83	Lignin	0.010	0.024	0.011
25	23.67	3,4-dihydroxybenzoic acid	73,193,223,267,281,311,355,370	99	Lignin	ND	ND	0.062

28	26.27	4-hydroxy mandelic acid	73,147,179,193,237,251,267	59	Lignin	0.001	0.002	0.001
32	26.88	Gallic acid	73,179,281,311,355,399,443,458	99	Raw material?-released after acid hydrolysis	0.022	0.006	0.091
34	27.70	Vanilethanediol	73,147,223,267,297	90	Lignin	0.179	0.237	ND
37	28.73	trans-diethylstilbestrol	73,217,368,383,397,412	47	Lignin	ND	ND	0.043
41	30.07	7,8-dihydroxyflavone	73,208,281,310,383,398	68	Lignin	ND	ND	0.010
49	36.26	Vanillyl derivate	73,193,225,297,355		Lignin	0.007	ND	ND
50	36.37	Hydroferulic acid	73,192,209,297	74	Lignin	0.104	0.215	ND
51	36.53	Vanillyl mandelic acid	73,192,209,297	56	Lignin	0.120	0.215	ND
Total aromatic compounds						**0.763**	**1.122**	**0.379**
			Polyols					
9	10.14	Glycerol	73,103,117,147,205,218	93	Raw material/ lipolysis	0.191	0.197	0.267
17	13.47	Erythritol	73,103,129,147,189,205	60		0.006	0.008	0.000
21	17.91	Arabitol	73,103,147,205,217,307	74	Raw material	ND	0.010	0.000
22	19.26	Xylitol	73,103,147,205,217,307,319	89	Raw material	ND	0.035	0.022
23	19.28	Ribitol	73,103,147,189,205,217,243,307,319	74	Raw material	0.035	ND	ND
29	26.30	Sorbitol	73,103,147,205,217,319	59	Sugar	0.008	0.014	0.011
31	26.75	Inositol1	73,147,191,217,265,291,305,318	98	Raw material	0.035	0.042	0.080
38	28.84	Inositol2	73,103,147,191,204,217,265,291,305,318,367	87	Raw material	0.050	0.055	0.158
Total polyols						**0.325**	**0.361**	**0.538**
			Fatty acids					
8	10.05	Octanoic acid	73,75,117,132,145,201,216	96	Triglycerides hydrolysis	ND	ND	0.006
13	11.41	Nonanoic acid	73,75,117,129,132,215,230	59	Triglycerides hydrolysis	ND	ND	0.007
35	28.29	Palmitic acid	73,117,129,145,313	98	Triglycerides hydrolysis	ND	ND	0.449

40	29.93	Eptadecanoic acid	73,117,132,145,327,342	90	Triglycerides hydrolysis	ND	ND	0.007
42	31.96	Stearic acid	73,117,132,145,341,356	58	Triglycerides hydrolysis	ND	ND	0.027
Total fatty acids						**ND**	**ND**	**0.496**
			Modified sugars					
18	14.66	2-O-methyl-xylose	73,89,131,146,159,191,204	83	Pectin	ND	ND	0.019
19	14.97	2-O-Methyl glucose	73,89,146,159,191,204	64		ND	ND	0.018
26	24.10	Glucuronic acid lactone	73,129,147,230	83	Glucuronic acid	ND	ND	0.019
43	34.08	Pentose derivative	73,191, 217,259,281,341,356,428	-	Disaccharide?	0.018	0.032	ND
44	34.24	Pentose derivative	73,103,147,191,217,243,259	-	Disaccharide?	0.009	0.021	ND
45	34.31	Pentose derivative	73,103,147,191,217,230,259	-	Arabinose disaccharide?	0.032	0.057	ND
46	34.74	Hexose derivative	73,131,204,217,246,273,363	-	Disaccharide?	0.025	ND	ND
47	34.97	Pentose derivative	73,191, 217,259,281,341	-	Disaccharide?	0.005	0.011	ND
48	35.13	Pentose derivative	73,103,147,191,217,230,259	-	Arabinose disaccharide?	0.011	0.018	ND
52	36.93	Hexose derivative	73,131,204,217,259,283,341	-	Disaccharide?	0.013	0.099	ND
53	38.27	Disaccharide	73,103,147,191,217,243,271,361		Sucrose-like disaccharide	ND	ND	0.021
54	34.00 -> 38.00	Sugar derivatives	73,103,129,147,191,204,217,259,349	-		ND	0.460	3.899
Total modified sugars						**0.113**	**0.698**	**3.976**
			Other					
5	8.14	3-hydroxy-pyridine	73,152,167	57	Maillard reaction	ND	0.008	0.013
14	12.47	Unknown1	73,243,258	-		ND	ND	0.034
15	12.71	2,4(1H,3H)-Pyrimidinedione, dihyro-1,3-dimethyl	73,99,147,243,258	52	Maillard reaction	0.020	ND	ND

16	13.20	Unknown2	73,147,243,258	-		0.006	ND	ND
20	17.19	Unknown3	73,159, 204		Sugar	0.026	0.014	ND
27	26.07	Unknown4	73,223,297,307,323,338	-	Lignin	ND	ND	0.077
30	26.54	Unknown5	73,235,267,293,309,324	-	Lignin	0.018	0.037	ND
33	27.51	Unknown6	73,103,192,236,325,428	-		ND	ND	0.006
36	28.45	Unknown7	73,103,129,147,175,205,217	-	Sugars	ND	ND	0.098
39	28.98	Unknown8	73,117,147,208,282,327	-		0.002	0.008	ND
	Total "other"					**0.072**	**0.067**	**0.228**
	Total					**1.402**	**2.301**	**5.917**

As reported in table 4.2, the set of identified and semi-quantified compounds constituted 1.4%, 2.3% and 5.9% of the initial sample when semi-quantified in the simple aqueous extract (H_2O), in the aqueous extract followed by precipitation of the fibre by ethanol (EtOH), and in the aqueous extract followed by fibre precipitation and acid hydrolysis (HCl), respectively. It is important to emphasize how the acid hydrolysis carried out on the supernatant after fibre precipitation allows to quantify a total content of metabolites much higher than that obtained with a simple aqueous extract. This indicates the complex nature of the compounds extracted from the raw material or originated after the hydrothermal treatment, which are probably present conjugated to other compounds and not directly detectable by GC-MS due to the high molecular weight (Mw). The compounds were putatively identified comparing their mass spectra with Wiley 275 library and are reported in Table 4.2. They can be categorized into 5 main classes, namely organic acids, aromatic compounds, modified sugars (these three are the classes identified with ^{1}H NMR technique as well), fatty acids and polyols. Then, other compounds were also detected, including a couple of N-heterocyclic compounds and various unidentified signals. Organic acids constituted, in terms of percentage of the initial sample, a rather small quantity, varying between 0.05% and 0.3%. In all three extracts, the most abundant ones were found to be lactic acid and glycolic acid, originating from glucose or xylose as a result of high temperatures [27]. 2-ketogluconic acid is mainly produced by glucose fermentation [28] but may be also formed from oxidation of D-gluconic acid, which is commonly found in plants, hence it was likely degraded and therefore not detected in "HCl" sample. Levulinic acid, that has been classified as one of the top 12 promising bio-based building blocks for the synthesis of fuels and chemicals, was found in very small concentrations, and this is not surprising since it is formed from hexoses or directly from cellulose [21], which are quite scarce in our extract. On the other hand, the higher amount of formic acid quantified by ^{1}H NMR could indicate the formation of a larger amount of levulinic acid which is further degraded during thermal treatment. 3-hydroxypropionic (3-HP) acid was found in very low concentrations too, and although its main

origin is from glucose fermentation, in this case the formation is likely attributable to the oxidation of aromatic compounds [29]. Finally, 5-hydroxyvaleric acid has been reported to derive from oxidation of furfural derivatives, such as cyclopentanone or 1,5-pentanediol, and therefore from xylose [30], while 2,3-dihydroxypropanoic acid (glyceric acid) is derived from glycerol oxidation [31] and 2-hydroxyhexanoic acid from sugar degradation in acid condition [32]. Even not detected by GC-MS, acetic and formic acids were also present, as evidenced by ^{1}H NMR, originating from autohydrolysis of acetylated xylans and degradation of hexose, respectively. As a whole, the majority of organic acids detected, originated from sugar modification pathways.

Aromatic compounds as a class constituted a significant fraction of the extract, if compared to organic acids: their total quantity was indeed semi-quantified with values ranging from 0.4% to 1.1%. These compounds are formed from the aromatic residues of lignin and are degraded to many types of phenolic structures, depending on the monomeric units in the native lignin [33]. In fact, lignin is a polymer made of various amounts of three different monolignols, that are p-coumaryl alcohol, coniferyl alcohol, and sinapyl alcohol [34] (Figure 4.3).

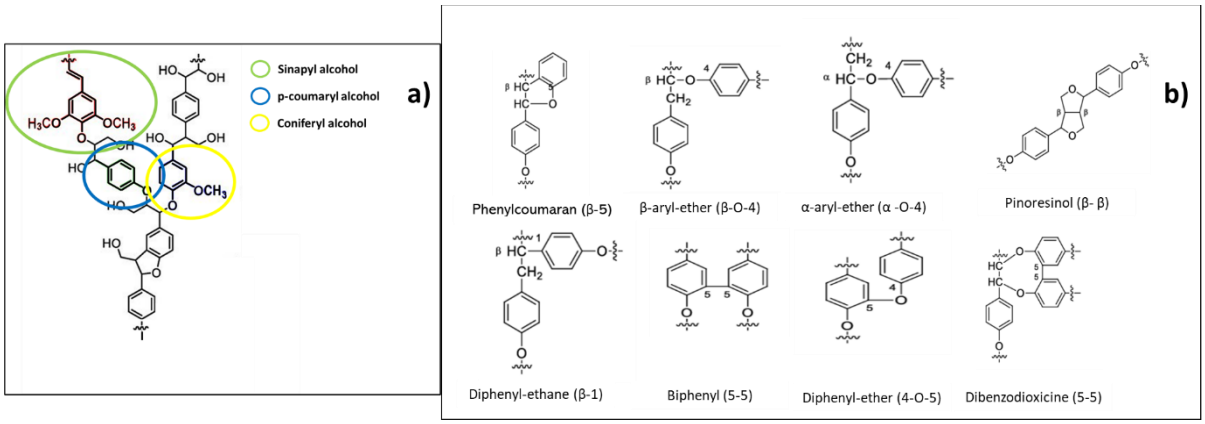

Figure 4.3: *(a) Example of lignin structure with focus on its monomers and (b) different chemical bonds which can occur between them.*

For this reason, most of the identified aromatic compounds might be divided in three subclasses, namely p-coumaryl, coniferyl, or sinapyl alcohol derivatives.

Previous studies showed how the increase in temperature during HT leads to methoxy group (-O-CH_3) hydrolysis with the consequent increase in p-coumaryl derivatives, making it harder to identify the mechanism of formation [35]. Among the compounds identified in our work by GC-MS, four of them were classifiable as coniferyl alcohol derivatives: 3-vanilyl propanol, vanilethanediol, hydroferulic acid and vanillylmandelic acid. The latter two were always found to be among the compounds present in the highest amount, even though not detected in "HCl" sample. The most abundant aromatic compound turned out to be benzoic acid, one of the most known lignin-derived molecules, and this may be explained by its great

stability to high temperatures in liquid water [36], while gallic acid, 7,8-dihydroxyflavone and diethylstilbestrol are likely derived from the raw material and were found only or especially in “HCl” sample, suggesting their presence in a complex with other structures.

Polyols were always found, as sum, in rather similar quantities in the three samples and varied between 0.3% and 0.5% of the initial sample, indicating their presence mainly as free form in the extract. An exception was glycerol, the most abundant one, its presence could be due to the thermal hydrolysis of triacylglycerols in HS [37] and it is not surprising that the highest amount has been found in “HCl” sample, being even easier to release it following acid hydrolysis. Sorbitol probably derived from the reduction of glucose [38], while the pentitols xylitol, arabitol and ribitol from the reduction of xylose and arabinose [39,40] in the pentose and glucuronate interconversions pathway in the raw material. Erythritol has been reported as a compound mainly produced from glucose through yeast fermentation [41] while inositol, on the other hand, may be produced from the hydrolysis of phytic acid, and it has been recently demonstrated how its degradation through HT is effective already with low temperatures [42]. Then, many fatty acids were found, only in HCl sample because deriving from hydrolysis of triglycerides present in the raw material, and among them the most abundant was palmitic acid. Their total amount correspond to about 0.5% of the initial sample and adding up this value to glycerol’s one the result turns out to be in accordance with the total lipid content reported in Table 4.1. One of the most numerous classes was that of modified sugars, that was the greatest in terms of abundance as well, reaching 4% of the initial sample in “HCl”, showing again the complex nature of these compounds, likely bound to each other and detectable only after acid hydrolysis. Some rare sugars, namely 2-O-methyl xylose and 2-O-methyl glucose were also found: the first may have been obtained as a result of a simultaneous extraction of pectin fraction present in HS, because it has been reported as a rhamnogalacturonan-II component [43,44]. Glucuronic acid lactone can be obtained from degradation of D-glucuronic acid when subcritical water is used [45], while a lot of sugar-derivative peaks appeared especially in “HCl” sample, in the last part of the chromatographic run, but without being able to identify them. These can be released from the matrix after hydrolysis, but it is not excluded their ex-novo formation during acid treatment. Finally, regarding “other” compounds, not classifiable in any of the previous classes, different abundant compounds were found. The maximum quantity of this substances peaked to 0.2% of the freeze-dried extract obtained from HT of HS. Both 3-hydroxy-pyridine and 2,4(1H,3H)-Pyrimidinedione, dihydro-1,3-dimethyl can be originated from Maillard reaction [46].

Despite gas chromatographic methods are very often used for the characterization of HT degradation compounds [14,16,17,47–51], their indisputable limits related to the necessity of matrix hydrolysis and analyte derivatization hinder a complete molecular characterization of the hydrothermal extract. As a consequence, the same sample was also submitted as it is to UHPLC-IM-Q-TOF-MS analysis.

3.3. UHPLC-IM-Q-TOF-MS analysis

The freeze-dried extract obtained after HT was also analysed by UHPLC-IM-Q-TOF-MS, dissolving it in water (see Figure 4.1). This approach was applied to characterize in detail various degradation products with higher Mw that may originate from the thermal process. To the best of our knowledge, this is the first time that such a technique is used for this purpose. The sample was analysed in triplicate both in positive and in negative ion modes to enlarge the metabolite coverage. At first, 4852 and 3941 features were aligned in ESI+ and ESI- modes, respectively, and among these features a total of 212 compounds were putatively annotated. The selection of the compounds of interest was carried out at first checking their abundance and their fragmentation score. Then, were retained only those compounds whose experimental fragmentation pattern matched with the theoretical and/or with the one present in the online databases. Finally, duplicate metabolites such as those ionizing in both polarities were checked. Some features with even good abundance but low fragmentation score have therefore not been considered, even though they could constitute compounds with relevance for bioactivity or risk assessment. The workflow applied is represented in Figure 4.4.

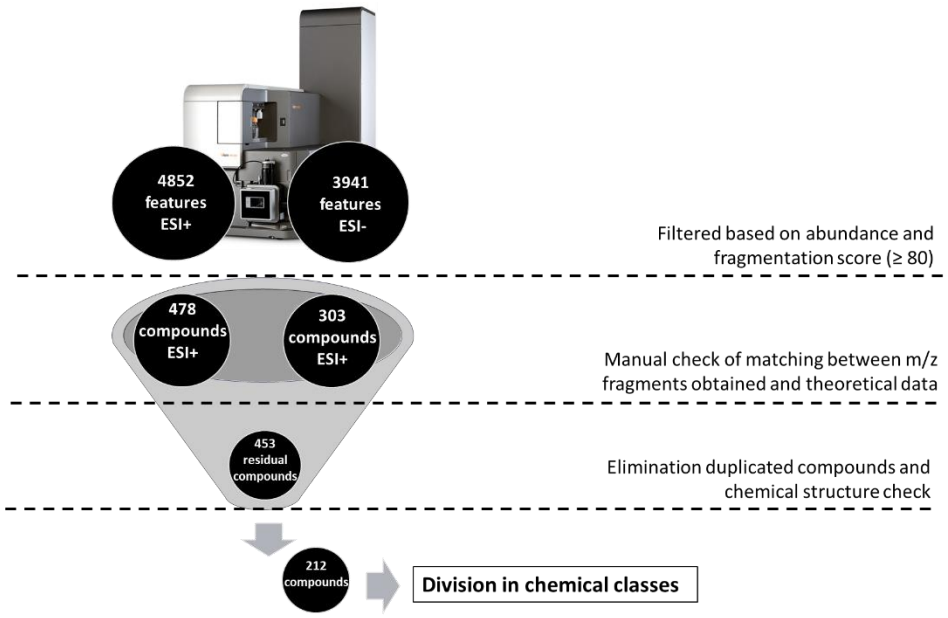

Figure 4.4: *Representation of funnel filtration of the compounds identified by UHPLC-IM-Q-TOF-MS.*

It is of great importance to underline that Progenesis QI software automatically proposes, for every compound, many different options of identification, based on the mass fragments detected. Among these options, one may select different structures even with very close fragmentation scores. Actually, the molecules chosen by the software are often belonging to the same chemical class. For the sake of clarity, an example of identification confirmation is reported in Figure 4.5. In this case, the compound CSID9358110 was

chosen because of the best spectra matching, but other options corresponding to other compounds were also possible.

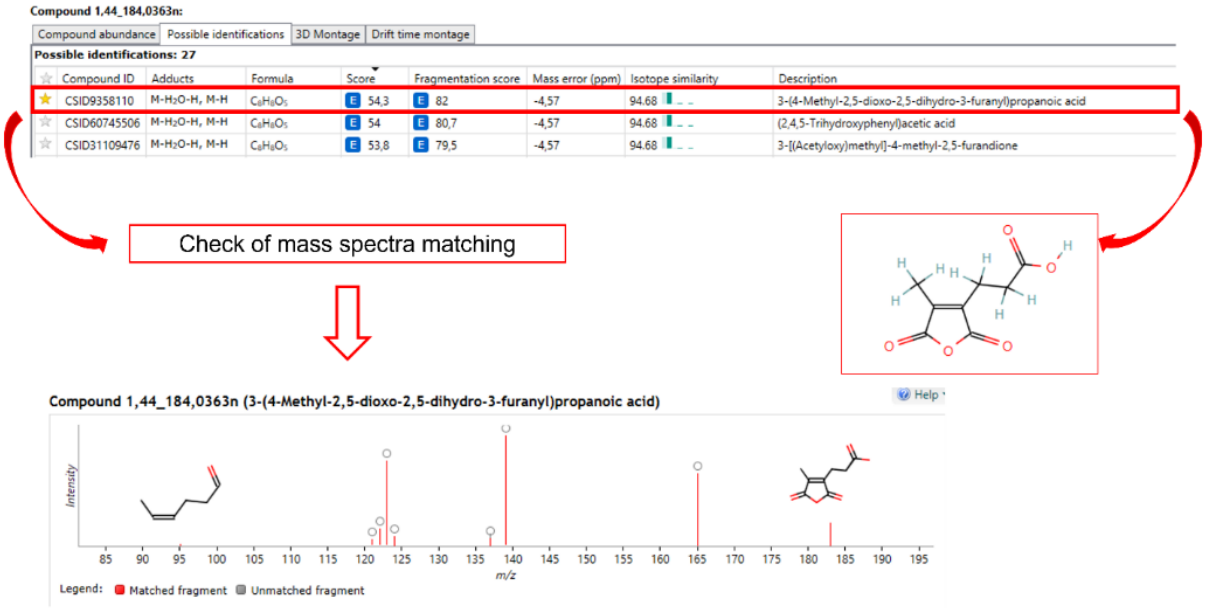

Figure 4.5: *Example of metabolite annotation, relative to 3-(4-Methyl-2,5-dioxo-2,5-dihydro-3-furanyl)propanoic acid.*

The whole list of putatively identified compounds and their respective chemical structures are available in Table S1 of the supplementary material. All the selected compounds were finally classified in chemical classes, according to the main functional group. The inclusion of a compound in a specific class was in some cases arbitrary, being many molecules complex structures with more than one functional group. However, the secondary functional groups have been specified in Table S1.

Overall, all the compounds were classified into twenty-two classes, as reported in the pie chart in Figure 4.6.

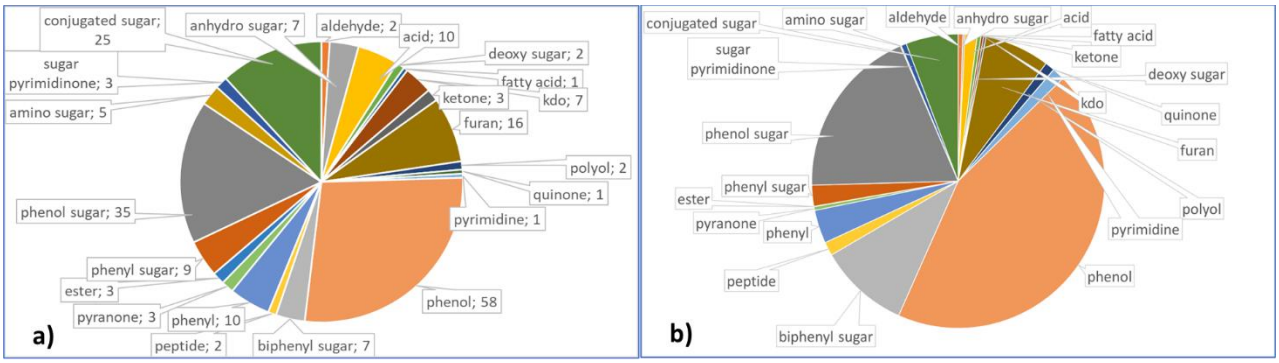

Figure 4.6: *Distribution of the compounds identified in different chemical classes, in terms of number of compounds per class (a) and relative abundance (b).*

Some classes of compounds ionized both in ESI- and ESI+, and they are anhydro oligosaccharides, kdos, deoxy oligosaccharides, sugars conjugated with a large range of phenols, sugar conjugated with phenyl/diphenyl

groups, sugars conjugated with various compounds (as for example pyran, fatty acid, polyol, ketone, purine), then organic acids, aldehydes, phenols, benzene-containing compounds, peptides, ketones and furans. Then, in ESI- analysis one fatty acid and some pyran-derivatives were also detected, whilst carrying out ESI+ analysis even some sugar pyrimidinones, amino sugars, polyols and esters were comprised in the list. It is important to specify that many oligosaccharides and acetylated sugars were also putatively identified, but not selected nor reported in the list because not definable as degradation compounds. Indeed, both acetylated or unsubstituted sugars and oligosaccharides are formed from the hydrothermal extraction of hemicellulose, and they usually are the target compounds that one wants to obtain. Specifically, xylans are hydrolysed into XOS and xylose by the acetic acid, which in turn is in part originated following the hydrolysis of acetyl groups linked to xylans [52].

However, it can be noted that the main classes of molecules previously identified by GC-MS (i.e., organic acids, phenols, polyols, fatty acids and modified sugars) came out with UHPLC-IM-Q-TOF-MS as well. As expected, many different types of sugars were detected, each of them with degrees of polymerization ranging from 2 to a maximum of 8 (Table S1). Each of the seven anhydro oligosaccharides was identified to be built up by agarobiose residues, and therefore they can be classified as agaro-oligosaccharides (AOS). Here, different DPs were detected, ranging from 2 (neoagarobiose) to 6. Agar/agarose is usually extracted from red seaweeds and basing on our knowledge no reports of its presence within lignocellulosic biomasses are present in literature. For this reason, their origin may need to be found from galactose degradation following the high temperatures employed in the HT. A recent work has proposed the mechanism of formation of levoglucosan and cellobiosan (i.e., glucose-based anhydro sugars) starting from cellulose by pyrolysis through hydrolysis and transglycosylation reactions [53], thus this may suggest the presence of galactose in HS in the form of galactan polymers. On the other hand, Harris and Richards proposed a mechanism of formation of sucrose-oligosaccharides containing anhydro glucose and fructose just undergoing acidified sucrose to thermal treatment at 170 °C for 80 minutes [54].

Seven compounds were also found and classified as Kdo sugars, which means that contain at least one 3-deoxy-d-manno-oct-2-ulosonic acid (or ketodeoxyoctonic acid, Kdo) molecule. Although Kdo is often just considered a characteristic component of bacterial lipopolysaccharide [55], it was also found to be a component of the cell walls of higher plants and in particular it is present only in the rhamnogalacturonan II structure [56]. This may suggest the formation of these compounds starting from pectin fractions, and this may be confirmed by the presence in decent amounts of galacturonic acid among the total monosaccharides of HS (Table 4.1). Indeed, the UHPLC-IM-Q-TOF-MS analysis revealed the presence of Kdo sugars with different structures and degrees of polymerization, in some cases bound to each other, in others linked to monosaccharides or sometimes even to deoxy-sugars or dehydro-sugars (Figure 4.7).

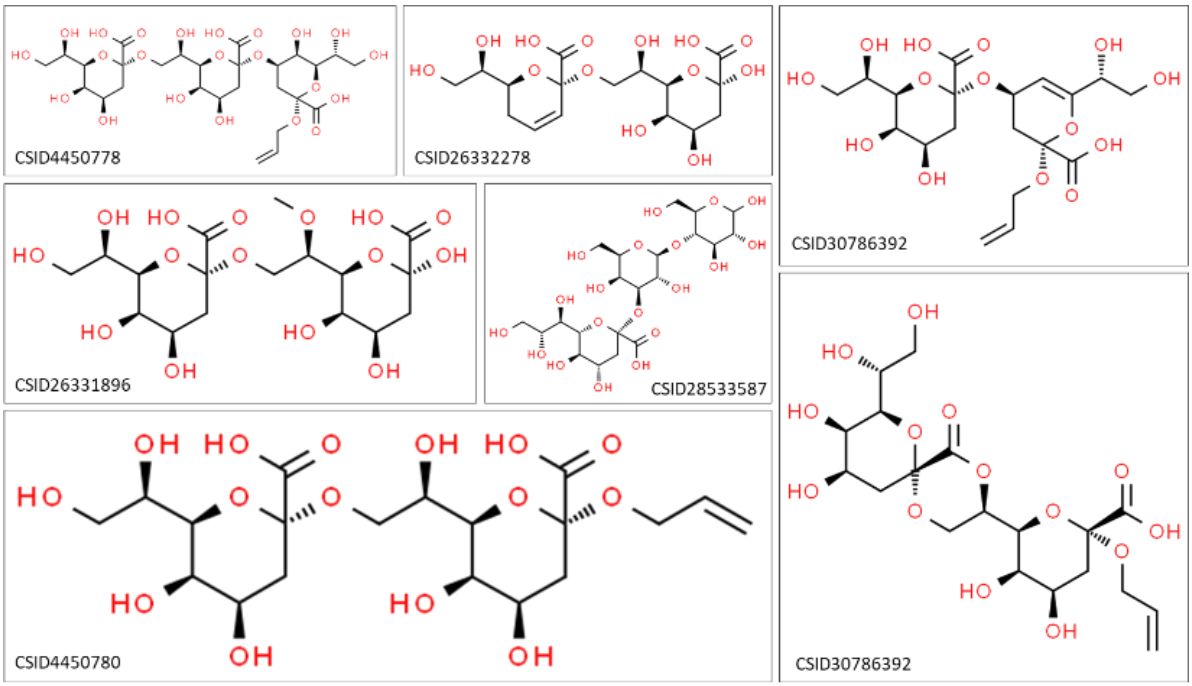

Figure 4.7: *Chemical structures of the putatively identified Kdo sugars. Molecule ID is reported according to ChemSpider database.*

In general, all these compounds (Kdos, anhydro oligosaccharides, deoxy oligosaccharides) accounted for about 8% of the total compounds identified (Figure 4.6). Among them, deoxy sugars were the most abundant in terms of ion intensity, albeit numerically less. Although this value cannot be considered totally accurate from a quantitative point of view, it gives an indication that it is likely that other classes of molecules are more present in the hydrolysate. In fact, apart from the aforementioned compounds, coming from hydrolysis and modification of cellulose and hemicellulose, many other molecules were detected. Among them, organic acids, which represented almost 5% of the total number and only 1.3% in terms of relative abundance. Within this group, it can be noted that none of the molecules detected by GC-MS or ^{1}H NMR were found here, and this could be ascribable to the difference in their molecular weights. Indeed, all the organic acids identified by GC-MS or ^{1}H NMR had a low Mw, with a maximum of 132 g/mol, while the ones detected by UHPLC-IM-Q-TOF-MS had Mw in the range 188 – 290 g/mol. Within this class, monocarboxylic (e.g. 2-deoxypentonic acid, quinic acid), dicarboxylic (e.g. 3-oxoheptanedioic acid) and tri-carboxylic acids (1-Butene-1,2,4-tricarboxylic acid and 1-Hexene-1,2,6-tricarboxylic acid), but also more complex structures have been putatively identified. For example, the carboxylic group was also found in complex molecules, containing other functional groups and cyclic structures in the carbon skeleton, as a propanoic acid containing an indene-dioxol group, a methyl-butenoic acid substituted with and epoxycyclohexenoic acid, a 4-oxo-pentanoic acid containing a cyclopentane ring. The complexity of these structures makes any hypothesis about their formation speculative, also considering the lack of analytical standards. However, their presence

in the hydrothermal extract suggests the need to reach a better level of understanding about the complex molecular profile of thermally treated biomasses.

Another class of compounds which confirms the result obtained with GC-MS and ^{1}H NMR involves lignin-derived aromatic molecules. Several sub-classes can be identified in it, depending on the functional groups and the molecular residues present bound together. Specifically, these sub-classes were: phenols, sugar phenols (i.e., phenols conjugated with mono-/oligosaccharides), phenyls, phenyls/diphenyls sugars (i.e., phenyls or diphenyls conjugated with mono-/oligosaccharides). The most present in this sense were by far phenols and sugar-phenols, comprising in total 93 compounds out of 212, corresponding to 44% of the total number of compounds and to 63% of the total relative ion abundance. These compounds come from complex mechanisms involving lignin. Compared to the aromatic molecules identified through GC-MS analysis, the ones found here were once again of greater complexity and with a Mw on average greater, also because constituted by complexes between phenols and other molecules. In fact, as reported in Table S1, very different molecules were found within the phenolic class, for instance containing functional groups typical of anthraquinones, naphtalenones, anthracenes, benzoquinones, stilbenes, tetraphenes, and again sulphate groups, furans and so on, depending on the number of rings that were present in the structure and on how they were bound together. Most of the features identified have never been previously reported for hydrothermal extracts of lignocellulosic materials, therefore it is difficult to extract information about their mechanism of formation, potential toxicity or, on the other hand, beneficial effects. Only few molecules among the identified ones were previously discussed in the literature, and the presence of these compounds mainly in natural sources suggests that they (or some analogues) probably derive from the raw material. For example, a good relative abundance was detected for C-2'-decoumaroyl-aloeresin G, a phenolic glycoside previously isolated from Aloe vera [57]. Then, 6,8-Dihydroxy-3,4-bis(hydroxymethyl)-1H-isochromen-1-one is an isocoumarin previously obtained from a sponge-derived fungus on the genus *Penicillium* [58], and in the same way (2R,3S,4aS,9aR,10R)-2,3,5,8-Tetrahydroxy-6,10-dimethoxy-3-methyl-1,3,4,4a,9a,10-hexahydro-9(2H)-anthracenone and methyl (1S,2S,3S)-2,3,8-trihydroxy-3-methyl-9-oxo-2,3,4,9-tetrahydro-1H-xanthene-1-carboxylate were associated with fungi in literature as well [59,60]. Chlorogenic acid butyl ester was previously isolated from the leaves of a species of tree and flowering plant in the family *Anacardiaceae* [61]. 5,7-Dihydroxy-2-(4-methoxyphenyl)-8-(3-methyl-2-buten-1-yl)-4-oxo-4H-chromen-3-yl-6-deoxy-β-D-mannopyranoside, better known as icariside II, is a prenylated flavonoid glycoside generally found in *Epimedii* herbs [62]. On the other hand, Figure 4.8 reports as an example the chemical structures of two putatively identified phenolic compounds not found in natural sources. They correspond to complex cyclic molecules, having Mw ranging from 328 to 468 g/mol and despite no specific information about their mechanism of formation is reported, the presence of coumaryl and sinapyl alcohols' skeletons suggest their direct formation from lignin cleavage and intramolecular recondensation. At the same time, some of these structures seem distantly reminiscent of the skeleton of some diarylheptanoids. These molecules are

frequently found in plants belonging to the *Betulaceae* family and have been described in depth in a recent review about hazelnut's phytochemicals [63].

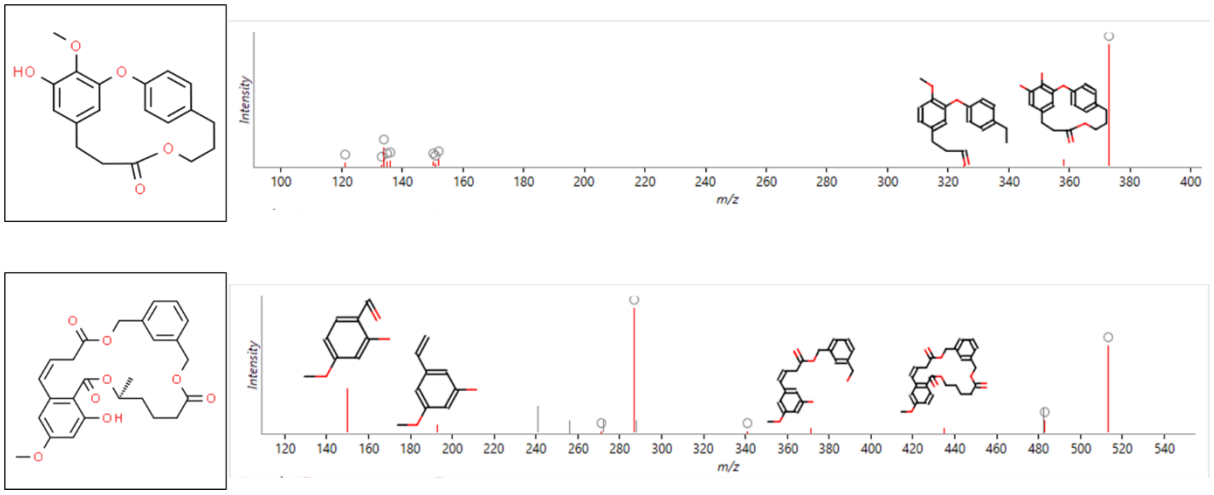

Figure 4.8: *Chemical structures of two putatively identified phenolic compounds and matching of their mass spectra.*

On the other hand, compounds carrying simple phenyl groups were numerically much less, and this is in line with the lignin origin of the most of these neo-formed compounds. Nineteen compounds were detected and classified as phenyls or phenyl sugars, depending on the eventual presence of sugars residues. One of the most abundant was putatively identified as 10-Ethoxy-9-hydroxy-8,8-dimethyl-9,10-dihydropyrano(2,3-f)chromen-2(8H)-one, a pyranocoumarine compound previously reported as a synthetic compound obtained starting from an epoxide through ethanol addition and InCl3 catalysis [64], a condition very far from ours. Even some biphenyl sugars were putatively identified in the extract: this is not surprising, since it is a typical bond that can be found in lignin structure (Figure 4.3).

As in the other classes of compounds, it can be noted how different combinations of chemical structures were present again, such as furan-containing or acetic acid-containing molecules, and how different sugar moieties can occur. In general, the aromatic compounds detected showed extraordinary structural complexity. In a recent study, Kim and colleagues evaluated which are the main reactions lignin undergoes during a heat treatment. The authors concluded that these reactions concerned a methoxyl groups cleavage in C3 and C5, a propane side chain cleavage, a cleavage of the β-O-4 bond (depolymerization) and some simultaneous condensation reactions between released fragments, causing high molecular weight lignin (Figure 4.9) [65].

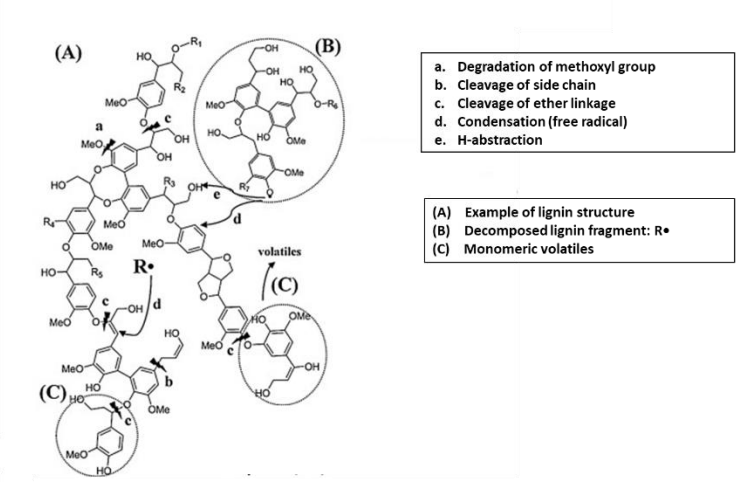

Figure 4.9: *Reactions that may occur in thermal treatment of lignin. Source: Kim et al., 2012* [65]. *Reproduced with permission from Kim et al., International Journal of Biological Macromolecules—; published by Elsevier, 2014.*

Although in our study the temperature of the HT was a little bit lower, our findings suggest that most of these condensation reactions may have taken place. Moreover, in the aforementioned work the lignin was extracted and thermally treated as it was, while in our case many other compounds, mainly derived from hemicellulose, had the chance to interact with lignin fragments, making even more complex the reaction pathways.

Another very important class of compounds both in terms of total number of compounds identified and of their relative abundance corresponds to furans. Sixteen molecules containing a furan functional group were detected. The most abundant one in negative ion mode was found to be a furan complexed with a hydrocarbon and containing a thio group, namely 5-(Tetradecylsulfanyl)-2-furoic acid. Some furancarboxylic acids have been reported to derive from oxidation of HMF [66] and the presence of sulfate may therefore be due to some previous Maillard reactions with sulfur-containing amino acids. A derivative of maleic anhydride, namely 3-(4-Methyl-2,5-dioxo-2,5-dihydro-3-furanyl)propanoic acid was also found, and despite the reported toxicity of maleic anhydride itself, this derivate could be of interest for its biological and pharmacological potential, such as antibiotic activity and enzymatic inhibition [67]. In general, the putatively identified furans were once again found within very complex molecular structures, namely linked to other fragments of molecules containing other functional groups, such as phenols, phenyls, organic acids and fatty acids (Figure 4.10). Interestingly, simple furans as HMF or furanoic acids have not been detected with any of the analytical techniques used in this work, likely due to a loss in the most volatile molecules during HT extract freeze-drying process. The basic mechanism of formation of these furan-based molecules starts from sugars dehydratation, both starting from hexoses to form 5-HMF and/or from pentoses to form furfural, also depending on temperature and pH. Then, they may react in different ways, as dienes in the Diels–Alder

reaction, but also through radical, electrophilic or polymerization reactions. A recent interesting review has been published about furans mechanisms of reaction [68].

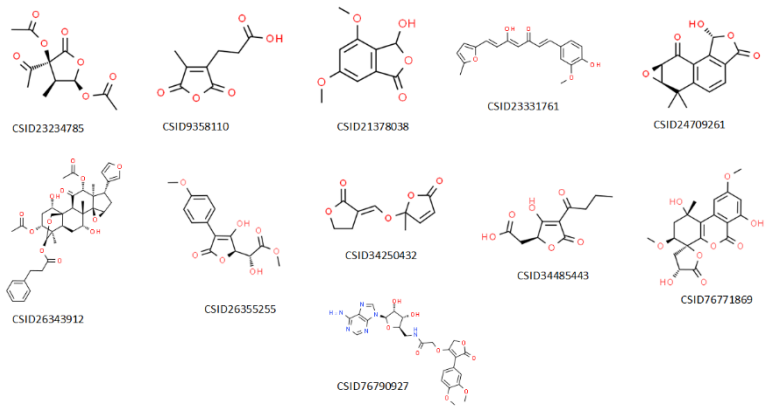

Figure 4.10: *Representation of some of the putatively identified furan-based molecules, in complexes with other functional groups. Molecule ID is reported according to ChemSpider database.*

4. Conclusions

Since hydrothermal treatment is a very commonly used method to extract hemicellulose from lignocellulosic biomasses, it is essential to deeply investigate which are the degradation compounds that are simultaneously formed. The majority of literature available so far employed GC-MS analysis to identify the molecules originated from this kind of extraction. However, this technique presents some limitations in detecting high molecular weight and more complex compounds that may result from the degradation, hydrolysis and condensation reactions between lignin, hemicellulose and other constituents of the matrix. In this work, three different techniques, namely ^{1}H NMR, GC-MS and UHPLC-IM-Q-TOF-MS have been employed to investigate and identify the degradation compounds after hydrothermal treatment of hazelnut shells. These approaches led to the detection of some common chemical classes of compounds, likely the most abundant, such as organic acids, degraded/modified sugars and aromatic compounds. The two chromatographic-MS based techniques also allowed to detect different classes of furans, polyols, N-heterocyclic compounds, aldehydes, ketones, esters, among others. However, deciphering the chemical mechanism involved in the formation of all these compounds is still a major challenge. On the one hand several variables, primarily the HT severity, in terms of time and temperature, strongly influence their formation. On the other hand, also the initial matrix plays a fundamental role, since the proportion and the structure of the various polymers within the lignocellulosic complex can have a huge impact on the reaction mechanisms and products. However, sophisticated techniques such as UHPLC-IM-Q-TOF-MS are emerging and enabling to bridge this gap, allowing researchers to create datasets like ours, which can hopefully be used for the construction of specific ”reactomics” databases, so that more light can be shed for the understanding of the formation of all these compounds and also for the building of predictive models.

REFERENCES

1. Lombardi, M.; Costantino, M. A hierarchical pyramid for food waste based on a social innovation perspective. *Sustain.* **2021**, *13*, 4661, doi:10.3390/su13094661.

2. Mirabella, N.; Castellani, V.; Sala, S. Current options for the valorization of food manufacturing waste: A review. *J. Clean. Prod.* **2014**, *65*, 28–41, doi:10.1016/j.jclepro.2013.10.051.

3. Gustavsson, J.; Cederberg, C.; Sonesson, U. Global Food Losses and Food Waste-FAO Report. *Food Agric. Organ. United Nations* 2011.

4. Saini, J.K.; Saini, R.; Tewari, L. Lignocellulosic agriculture wastes as biomass feedstocks for second-generation bioethanol production: concepts and recent developments. *3 Biotech* **2015**, *5*, 337–353, doi:10.1007/s13205-014-0246-5.

5. Villacís-Chiriboga, J.; Vera, E.; Van Camp, J.; Ruales, J.; Elst, K. Valorization of byproducts from tropical fruits: A review, Part 2: Applications, economic, and environmental aspects of biorefinery via supercritical fluid extraction. *Compr. Rev. Food Sci. Food Saf.* **2021**, *20*, 2305–2331, doi:10.1111/1541-4337.12744.

6. Santeramo, F.G.; Carlucci, D.; De Devitiis, B.; Seccia, A.; Stasi, A.; Viscecchia, R.; Nardone, G. Emerging trends in European food, diets and food industry. *Food Res. Int.* **2018**, *104*, 39–47, doi:10.1016/j.foodres.2017.10.039.

7. Abejón, R. A bibliometric study of scientific publications regarding hemicellulose valorization during the 2000–2016 period: Identification of alternatives and hot topics. *ChemEngineering* **2018**, *2*, 7, doi:10.3390/chemengineering2010007.

8. Wang, Z.W.; Zhu, M.Q.; Li, M.F.; Wang, J.Q.; Wei, Q.; Sun, R.C. Comprehensive evaluation of the liquid fraction during the hydrothermal treatment of rapeseed straw. *Biotechnol. Biofuels* **2016**, *9*, 142, doi:10.1186/s13068-016-0552-8.

9. Negahdar, L.; Delidovich, I.; Palkovits, R. Aqueous-phase hydrolysis of cellulose and hemicelluloses over molecular acidic catalysts: Insights into the kinetics and reaction mechanism. *Appl. Catal. B Environ.* **2016**, *184*, 285–298, doi:10.1016/j.apcatb.2015.11.039.

10. Luo, Y.; Li, Z.; Li, X.; Liu, X.; Fan, J.; Clark, J.H.; Hu, C. The production of furfural directly from hemicellulose in lignocellulosic biomass: A review. *Catal. Today* **2019**, *319*, 14–24, doi:10.1016/j.cattod.2018.06.042.

11. Terrett, O.M.; Dupree, P. Covalent interactions between lignin and hemicelluloses in plant secondary cell walls. *Curr. Opin. Biotechnol.* **2019**, *56*, 97–104, doi:10.1016/j.copbio.2018.10.010.

12. Kumari, D.; Singh, R. Pretreatment of lignocellulosic wastes for biofuel production: A critical review. *Renew. Sustain. Energy Rev.* **2018**, *90*, 877–891, doi:10.1016/j.rser.2018.03.111.

13. Aachary, A.A.; Prapulla, S.G. Xylooligosaccharides (XOS) as an Emerging Prebiotic: Microbial Synthesis, Utilization, Structural Characterization, Bioactive Properties, and Applications. *Compr. Rev. Food Sci. Food Saf.* **2011**, *10*, 2–16, doi:10.1111/j.1541-4337.2010.00135.x.

14. Rasmussen, H.; Sørensen, H.R.; Meyer, A.S. Formation of degradation compounds from lignocellulosic biomass in the biorefinery: Sugar reaction mechanisms. *Carbohydr. Res.* **2014**, *385*, 45–57, doi:10.1016/j.carres.2013.08.029.

15. Gullón, B.; Yáñez, R.; Alonso, J.L.; Parajó, J.C. Production of oligosaccharides and sugars from rye straw: A kinetic approach. *Bioresour. Technol.* **2010**, *101*, 6676–6684, doi:10.1016/j.biortech.2010.03.080.

16. Gullón, B.; Eibes, G.; Dávila, I.; Moreira, M.T.; Labidi, J.; Gullón, P. Hydrothermal treatment of chestnut shells (Castanea sativa) to produce oligosaccharides and antioxidant compounds. *Carbohydr. Polym.* **2018**, *192*, 75–83, doi:10.1016/j.carbpol.2018.03.051.

17. Gao, Y.; Wang, H.; Guo, J.; Peng, P.; Zhai, M.; She, D. Hydrothermal degradation of hemicelluloses from triploid poplar in hot compressed water at 180-340 °c. *Polym. Degrad. Stab.* **2016**, *126*, 179–187, doi:10.1016/j.polymdegradstab.2016.02.003.

18. AOAC Official Method of Analysis. 16th Edition. Association of official analytical, Washington DC. **2002**.

19. Xia, Y.G.; Wang, T.L.; Sun, H.M.; Liang, J.; Kuang, H.X. Gas chromatography–mass spectrometry-based trimethylsilyl-alditol derivatives for quantitation and fingerprint analysis of Anemarrhena asphodeloides Bunge polysaccharides. *Carbohydr. Polym.* **2018**, doi:10.1016/j.carbpol.2018.06.066.

20. Musio, B.; Ragone, R.; Todisco, S.; Rizzuti, A.; Latronico, M.; Mastrorilli, P.; Pontrelli, S.; Intini, N.; Scapicchio, P.; Triggiani, M.; et al. A community-built calibration system: The case study of quantification of metabolites in grape juice by qNMR spectroscopy. *Talanta* **2020**, *214*, 120855, doi:10.1016/j.talanta.2020.120855.

21. Pyo, S.H.; Glaser, S.J.; Rehnberg, N.; Hatti-Kaul, R. Clean Production of Levulinic Acid from Fructose and Glucose in Salt Water by Heterogeneous Catalytic Dehydration. *ACS Omega* **2020**, *5*, 14275–14282, doi:10.1021/acsomega.9b04406.

22. Fahy, E.; Subramaniam, S.; Murphy, R.C.; Nishijima, M.; Raetz, C.R.H.; Shimizu, T.; Spener, F.; Van Meer, G.; Wakelam, M.J.O.; Dennis, E.A. Update of the LIPID MAPS comprehensive classification system for lipids. *J. Lipid Res.* **2009**, *50*, 9–14, doi:10.1194/jlr.R800095-JLR200.

23. Wishart, D.S.; Jewison, T.; Guo, A.C.; Wilson, M.; Knox, C.; Liu, Y.; Djoumbou, Y.; Mandal, R.; Aziat, F.; Dong, E.; et al. HMDB 3.0-The Human Metabolome Database in 2013. *Nucleic Acids Res.* **2013**, *41*, 801–807, doi:10.1093/nar/gks1065.

24. Smith, C.A.; O'Maille, G.; Want, E.J.; Qin, C.; Trauger, S.A.; Brandon, T.R.; Custodio, D.E.; Abagyan, R.; Siuzdak, G. METLIN: A metabolite mass spectral database. *Ther. Drug Monit.* **2005**, *27*, 747–751, doi:10.1097/01.ftd.0000179845.53213.39.

25. Fuso, A.; Risso, D.; Rosso, G.; Rosso, F.; Manini, F.; Manera, I.; Caligiani, A. Potential valorization of hazelnut shells through extraction, purification and structural characterization of prebiotic compounds: A critical review. *Foods* **2021**, *10*, 1197, doi:10.3390/foods10061197.

26. Mudgil, D. The Interaction Between Insoluble and Soluble Fiber. In *Dietary Fiber for the Prevention of Cardiovascular Disease: Fiber's Interaction between Gut Micoflora, Sugar Metabolism, Weight Control and Cardiovascular Health*; 2017 ISBN 9780128052754.

27. Onda, A.; Ochi, T.; Kajiyoshi, K.; Yanagisawa, K. A new chemical process for catalytic conversion of d-glucose into lactic acid and gluconic acid. *Appl. Catal. A Gen.* **2008**, *343*, 49–54, doi:10.1016/J.APCATA.2008.03.017.

28. Sun, W.J.; Yun, Q.Q.; Zhou, Y.Z.; Cui, F.J.; Yu, S.L.; Zhou, Q.; Sun, L. Continuous 2-keto-gluconic acid (2KGA) production from corn starch hydrolysate by Pseudomonas fluorescens AR4. *Biochem. Eng. J.* **2013**, *77*, 97–102, doi:10.1016/j.bej.2013.05.010.

29. Shende, R. V.; Levee, J. Kinetics of wet oxidation of propionic and 3-hydroxypropionic acids. *Ind. Eng. Chem. Res.* **1999**, *38*, 2557–2563, doi:10.1021/ie9900061.

30. Asano, T.; Takagi, H.; Nakagawa, Y.; Tamura, M.; Tomishige, K. Selective hydrogenolysis of 2-furancarboxylic acid to 5-hydroxyvaleric acid derivatives over supported platinum catalysts. *Green Chem.* **2019**, *21*, 6133–6145, doi:10.1039/c9gc03315g.

31. Yan, H.; Yao, S.; Zhao, S.; Liu, M.; Zhang, W.; Zhou, X.; Zhang, G.; Jin, X.; Liu, Y.; Feng, X.; et al. Insight into the basic strength-dependent catalytic performance in aqueous phase oxidation of glycerol to glyceric acid. *Chem. Eng. Sci.* **2021**, *230*, 116191, doi:10.1016/j.ces.2020.116191.

32. Esteves, B.; Ayata, U.; Cruz-Lopes, L.; Brás, I.; Ferreira, J.; Domingos, I. Changes in the content and composition of the extractives in thermally modified tropical hardwoods. *Maderas. Cienc. y Tecnol.* **2022**, *24*, 1–14, doi:http://dx.doi.org/10.4067/s0718-221x2022000100422.

33. Almeida, J.R.M.; Modig, T.; Petersson, A.; Hähn-Hägerdal, B.; Lidén, G.; Gorwa-Grauslund, M.F. Increased tolerance and conversion of inhibitors in lignocellulosic hydrolysates by Saccharomyces cerevisiae. *J. Chem. Technol. Biotechnol.* **2007**, *82*, 340–349, doi:10.1002/jctb.1676.

34. Doherty, W.O.S.; Mousavioun, P.; Fellows, C.M. Value-adding to cellulosic ethanol: Lignin polymers. *Ind. Crops Prod.* **2011**, *33*, 259–276, doi:10.1016/j.indcrop.2010.10.022.

35. Ramachandran, V.; Ismail, F.S.; Noor, M.J.M.M.; Akhir, F.N.M.D.; Othman, N.; Zakaria, Z.; Hara, H. Extraction and intensive conversion of lignocellulose from oil palm solid waste into lignin monomer by the combination of hydrothermal pretreatment and biological treatment. *Bioresour. Technol. Reports* **2020**, *11*, 100456, doi:10.1016/j.biteb.2020.100456.

36. Dunn, J.B.; Burns, M.L.; Hunter, S.E.; Savage, P.E. Hydrothermal stability of aromatic carboxylic acids. *J. Supercrit. Fluids* **2003**, *27*, 263–274, doi:10.1016/S0896-8446(02)00241-3.

37. Mattonai, M.; Licursi, D.; Antonetti, C.; Raspolli Galletti, A.M.; Ribechini, E. Py-GC/MS and HPLC-DAD characterization of hazelnut shell and cuticle: Insights into possible re-evaluation of waste biomass. *J. Anal. Appl. Pyrolysis* **2017**, *127*, 321–328, doi:10.1016/j.jaap.2017.07.019.

38. Bohren, K.M.; Bullock, B.; Wermuth, B.; Gabbay, K.H. The Aldo-Keto Reductase Superfamily. *J. Biol. Chem.* **1989**, *264*, 9547–9551, doi:10.1016/s0021-9258(18)60566-6.

39. Heuel, H.; Shakeri-Garakani, A.; Turgut, S.; Lengeler, J.W. Genes for D-arabinitol and ribitol catabolism from Klebsiella pneumoniae. *Microbiology* **1998**, *144*, doi:10.1099/00221287-144-6-1631.

40. Verduyn, C.; van Kleef, R.; Frank, J.; Schreuder, H.; Van Dijken, J.P.; Scheffers, W.A. Properties of the NAD(P)H-dependent xylose reductase from the xylose-fermenting yeast Pichia stipitis. *Biochem. J.* **1985**, *226*, 669–677, doi:10.1042/bj2260669.

41. Kobayashi, H.; Fukuoka, A. Synthesis and utilisation of sugar compounds derived from lignocellulosic biomass. *Green Chem.* **2013**, *15*, 1740–1763, doi:10.1039/c3gc00060e.

42. Sheikh, M.A.; Saini, C.S. Combined effect of microwave and hydrothermal treatment on anti-nutritional factors, antioxidant potential and bioactive compounds of plum (Prunus domestica L.) kernels. *Food Biosci.* **2022**, *46*, 101467, doi:10.1016/j.fbio.2021.101467.

43. Reuhs, B.L.; Glenn, J.; Stephens, S.B.; Kim, J.S.; Christie, D.B.; Glushka, J.G.; Zablackis, E.; Albersheim, P.; Darvill, A.G.; O'Neill, M.A. L-galactose replaces L-fucose in the pectic polysaccharide rhamnogalacturonan II synthesized by the L-fucose-deficient mur1 Arabidopsis mutant. *Planta* **2004**, *219*, 147–157, doi:10.1007/s00425-004-1205-x.

44. Pellerin, P.; Doco, T.; Vidal, S.; Williams, P.; Brillouet, J.M.; O'Neill, M.A. Structural characterization of red wine rhamnogalacturonan II. *Carbohydr. Res.* **1996**, *290*, 183–197, doi:10.1016/0008-6215(96)00139-5.

45. Wang, R.; Neoh, T.L.; Kobayashi, T.; Miyake, Y.; Hosoda, A.; Taniguchi, H.; Adachi, S. Degradation kinetics of glucuronic acid in subcritical water. *Biosci. Biotechnol. Biochem.* **2010**, *74*, 601– 605, doi:10.1271/bbb.90818.

46. Yu-Chiang, O.; Chi-Tang, H.; Hartman, T.G. Volatile Compounds Generated from the Maillard Reaction of Pro-Gly, Gly-Pro, and a Mixture of Glycine and Proline with Glucose. *J. Agric. Food Chem.* **1992**, *40*, 1878–1880, doi:10.1021/jf00022a030.

47. Xiao, L.P.; Shi, Z.J.; Xu, F.; Sun, R.C. Hydrothermal carbonization of lignocellulosic biomass. *Bioresour. Technol.* **2012**, *118*, 619–623, doi:10.1016/j.biortech.2012.05.060.

48. Borrega, M.; Niemela, K.; Sixta, H. Effect of hydrothermal treatment intensity on the formation of degradation products from birchwood. *Holzforschung* **2013**, *67*, 871–879, doi:10.1515/hf-2013-0019.

49. Yan, Y.H.; Li, H.L.; Ren, J.L.; Lin, Q.X.; Peng, F.; Sun, R.C.; Chen, K.F. Xylo-sugars production by microwave-induced hydrothermal treatment of corncob: Trace sodium hydroxide addition for suppression of side effects. *Ind. Crops Prod.* **2017**, *101*, 36–45, doi:10.1016/j.indcrop.2017.02.024.

50. Zhu, Z.; Liu, Z.; Zhang, Y.; Li, B.; Lu, H.; Duan, N.; Si, B.; Shen, R.; Lu, J. Recovery of reducing sugars and volatile fatty acids from cornstalk at different hydrothermal treatment severity. *Bioresour. Technol.* **2016**, *199*, 220–227, doi:10.1016/j.biortech.2015.08.043.

51. Morales, A.; Labidi, J.; Gullón, P. Hydrothermal treatments of walnut shells: A potential pretreatment for subsequent product obtaining. *Sci. Total Environ.* **2021**, *764*, 142800, doi:10.1016/j.scitotenv.2020.142800.

52. Singh, J.; Suhag, M.; Dhaka, A. Augmented digestion of lignocellulose by steam explosion, acid and alkaline pretreatment methods: A review. *Carbohydr. Polym.* **2015**, *7*, 19–27, doi:10.1016/j.carbpol.2014.10.012.

53. Leng, E.; Costa, M.; Peng, Y.; Zhang, Y.; Gong, X.; Zheng, A.; Huang, Y.; Xu, M. Role of different chain end types in pyrolysis of glucose-based anhydro-sugars and oligosaccharides. *Fuel* **2018**, *234*, 738–745, doi:10.1016/j.fuel.2018.07.075.

54. Manley-Harris, M.; Richards, G.N. Anhydro sugars and oligosaccharides from the thermolysis of sucrose. *Carbohydr. Res.* **1994**, *254*, 195–202, doi:10.1016/0008-6215(94)84252-3.

55. Lodowska, J.; Wolny, D.; Weglarz, L. The sugar 3-deoxy-D-manno-oct-2-ulosonic acid (Kdo) as a characteristic component of bacterial endotoxin - A review of its biosynthesis, function, and placement in the lipopolysaccharide core. *Can. J. Microbiol.* **2013**, *59*, 645–655, doi:10.1139/cjm-2013-0490.

56. Temple, H.; Saez-Aguayo, S.; Reyes, F.C.; Orellana, A. The inside and outside: Topological issues in plant cell wall biosynthesis and the roles of nucleotide sugar transporters. *Glycobiology* **2016**, *26*, 913–925, doi:10.1093/glycob/cww054.

57. Dias, C.; Rauter, A.P. *Carbohydrates and glycomimetics in Alzheimer's disease therapeutics and diagnosis - Chapter 8*; 2015;

58. Qi, J.; Shao, C.L.; Li, Z.Y.; Gan, L.S.; Fu, X.M.; Bian, W.T.; Zhao, H.Y.; Wang, C.Y. Isocoumarin derivatives and benzofurans from a sponge-derived Penicillium sp. fungus. *J. Nat. Prod.* **2013**, *76*, 571–579, doi:10.1021/np3007556.

59. Yang, K.L.; Wei, M.Y.; Shao, C.L.; Fu, X.M.; Guo, Z.Y.; Xu, R.F.; Zheng, C.J.; She, Z.G.; Lin, Y.C.; Wang, C.Y. Antibacterial anthraquinone derivatives from a sea anemone-derived fungus Nigrospora sp. *J. Nat. Prod.* **2012**, *75*, 935–941, doi:10.1021/np300103w.

60. Zhang, F.; Li, L.; Niu, S.; Si, Y.; Guo, L.; Jiang, X.; Che, Y. A thiopyranchromenone and other chromone derivatives from an endolichenic fungus, Preussia africana. *J. Nat. Prod.* **2012**, *75*, 230–237, doi:10.1021/np2009362.

61. Corthout, J.; Pieters, L.; Claeys, M.; Berghe, D. Vanden; Vlietinck, A. Antiviral caffeoyl esters from Spondias mombin. *Phytochemistry* **1992**, *31*, 1979–1981, doi:10.1016/0031-9422(92)80344-E.

62. Szabó, R.; Pál, C.P.; Dulf, F.V. Bioavailability Improvement Strategies for Icariin and Its Derivates: A Review. *Int. J. Mol. Sci.* **2022**, *23*, 7519.

63. Bottone, A.; Cerulli, A.; Durso, G.; Masullo, M.; Montoro, P.; Napolitano, A.; Piacente, S. Plant Specialized Metabolites in Hazelnut (Corylus avellana) Kernel and Byproducts: An Update on Chemistry, Biological Activity, and Analytical Aspects.

Planta Med. **2019**, *85*, 840–855, doi:10.1055/a-0947-5725.

64. Lee, Y.R.; Lee, W.K.; Noh, S.K.; Lyoo, W.S. A concise route for the synthesis of biologically interesting pyranocoumarins - Seselin, (±)-cis-khellactone, (±)- quianhucoumarin D, and the (±)-5-deoxyprotobruceol-I regioisomer. *Synthesis (Stuttg).* **2006**, *5*, 853–859, doi:10.1055/s-2006-926329.

65. Kim, J.Y.; Hwang, H.; Oh, S.; Kim, Y.S.; Kim, U.J.; Choi, J.W. Investigation of structural modification and thermal characteristics of lignin after heat treatment. *Int. J. Biol. Macromol.* **2014**, *66*, 57–65, doi:10.1016/j.ijbiomac.2014.02.013.

66. An, J.; Sun, G.; Xia, H. Aerobic Oxidation of 5-Hydroxymethylfurfural to High-Yield 5-Hydroxymethyl-2-furancarboxylic Acid by Poly(vinylpyrrolidone)-Capped Ag Nanoparticle Catalysts. *ACS Sustain. Chem. Eng.* **2019**, *7*, 6696–6706, doi:10.1021/acssuschemeng.8b05916.

67. Chen, X.; Zheng, Y.; Shen, Y. Natural products with maleic anhydride structure: Nonadrides, tautomycin, chaetomellic anhydride, and other compounds. *Chem. Rev.* **2007**, *107*, 1777–1830, doi:10.1021/cr050029r.

68. Gandini, A.; M. Lacerda, T. Furan Polymers: State of the Art and Perspectives. *Macromol. Mater. Eng.* **2022**, *307*, 2100902, doi:10.1002/mame.202100902.

CHAPTER 5

Hydrothermal treatment of hazelnut shells: impact of temperature on degradation compounds and fibre's structure

The content of this chapter has also been submitted as:

Andrea Fuso, Pio Viscusi, Franco Rosso, Ginevra Rosso, Clara Pedrazzani, Augusta Caligiani. Hydrothermal treatment of hazelnut shells: impact of temperature on degradation compounds and fibre's structure.

ABSTRACT

Hemicellulose extraction from lignocellulosic biomasses has gained interest over the years. The aim of this study was to evaluate the effect of different hydrothermal treatment temperatures both on the type and structure of extracted fibres from hazelnut shells and on the formation of various products derived from matrix degradation. The extract composition was investigated by GC-MS, HPSEC-RID, 1H NMR, UPLC/ESI-MS and UHPLC-IM-QTOF-MS. The highest extraction yield of total fibres and xylan was obtained at 150 °C and 175 °C, respectively. The characterization step showed that high-Mw pectin fractions were achieved at 125 °C, at 150 °C a heterogeneous mixture of xylan, XOS and pectin was present and higher temperatures led to a prevalence of XOS. Finally, more than 500 compounds were putatively identified, they appeared to be present in different amounts depending on the temperature employed for the treatment and belonged to several different chemical classes.

1. Introduction

To face the phenomenon of waste in the food industry, increasing importance has been gradually attributed to convert it into a by-product which could be reused and transformed into a new product with increased added value. In this context, dietary fibre is one of the main protagonists, since scientific research on its proven health benefits has grown, and a trend of consumption of healthy products has spread among consumers [1]. Therefore, the reuse of fruit and vegetable by-products extracting and using their fibres in functional foods or nutraceuticals is a promising approach for the environment, the food industry and the health of consumers [2]. Among the potentially most interesting by-products for the reuse of fibre, one can certainly find lignocellulosic residues, which make up 90% of the total residual plant biomass [3]. They are mainly made of lignin, cellulose and hemicellulose in varying proportions, bound together in complex structures, and hence the extraction of hemicelluloses requires "strong" methods. One of the most used in this sense is the hydrothermal treatment, also called as liquid hot water (LHW), which consists of subjecting the matrix to an extraction at high temperatures (above 100 °C) in water, maintained in the liquid state thanks to high pressures, for a variable time [4]. Actually, the result of the extraction with this method has not to be taken for granted. Different processes with different parameters (temperature, time, pH) may indeed affect very strongly the composition of the final liquor, because of the chemical modification of hemicellulose, cellulose and lignin [5]. According to Cocero and colleagues, hemicellulose undergoes five different chemical modifications during the hydrothermal treatment, namely hydrolysis of glycosidic bonds which leads to the formation of oligosaccharides, hemicellulose deacetylation, hemicellulose dissolution and mass transfer between the solid and the liquid, production of sugars and sugars degradation, and porosity modification [6]. Hence, higher temperatures could lead to a greater hydrolysis of hemicellulose, with consequent reduction of the molecular weight, and to the production of sugar degradation products (such furfural, HMF, acetic, levulinic and formic acid) [7]. In addition to these latter modifications of sugars, if very pure products are desired, it is necessary to take into account the chemical modifications which occur to lignin as well, such as methoxyl groups cleavage, propane side chains cleavage, depolymerization and condensation reactions [8], with the consequent release of many complex compounds, the majority of whom are phenolics. At the same time, however, the use of lower temperatures is often not convenient in terms of yield, due to the scarce modification of lignin structure that consequently results in recovering lower quantities of hemicellulose [9]. Furthermore, the matrix from which hemicellulose is extracted has a significant impact on the results as well, in terms of resistance to temperature [10]. Finally, a certain matrix could contain different hemicelluloses or various polysaccharides, constituted by different monosaccharide residues, which could be more or less susceptible to a specific hydrothermal treatment, as emerged in a previous work of our group [11]. For all these reasons, and since it is widely recognized that the chemical structure of dietary fibres is related to their biological activity [12], it is fundamental to determine the best process depending on the specific goal. The

complete understanding of these correlations between the parameters of the hydrothermal treatment and the chemical structure of the compounds that are generated is necessary to develop an economically efficient process. Among the lignocellulose by-products, hazelnut shells are very abundant but still too much undervalued [13]. Corylus avellana L., the European hazelnut, whose production ranges from North Africa and Europe to the Asia Minor and Caucasus region, is the second most popular nut worldwide just after almonds. Its crop added up to over 528,000 metric tons (kernel basis) in 2019/20. One of the main drawbacks associated with hazelnut production is the large amount of by-products. In fact, hazelnuts are collected in the form of dried in-shell nuts that are further processed to be introduced into the industrial food chain. The residual biomass resulting from the cracking process, the hazelnut shell (HS), represents approximately 50–55% of the weight of the in-shell product and today is mainly used as a boiler fuel. HS main constituent is lignin, with quantities found around 40–51%, followed by hemicellulose (rich in xylans substituted with uronic acids/acetyl groups and small quantities of arabinans and galactans) with 13–32%, and cellulose (17–27%) [14–19]. In recent years, scientific research has focused heavily on studying different ways to exploit lignocellulose, but despite the large availability of HS residual biomass, only few studies have focused their attention on their hemicellulosic fraction and especially on the effect of different hydrothermal treatments on fibre yield and molecular composition [16,17].

To give a contribution in this field, we have evaluated how different temperatures employed in the hydrothermal treatment can affect the presence of potentially undesired compounds derived from the degradation of sugars and lignin, as well as the chemical structure of HS' dietary fibre (in terms of molecular weight, monosaccharide composition and degree of substitution). The former characterization was made for the first time on hazelnut shells HT liquors, utilizing a "reactomics" approach based on high resolution NMR and UHPLC-IM-QTOF-MS. Finally, the effect of ethanol precipitation for fibre purification from undesired compounds was also evaluated.

2. Materials and methods

2.1. Materials and chemicals

2.1.1. Materials

Milled and sieved hazelnut shells (HS) having a particle size < 500 µm were collected from Ferrero S.p.A. (Cuneo, Italy).

2.1.2. Chemicals

HPLC-grade acetonitrile, ammonium formiate, D-glucose, D-fructose, D-arabinose, D-galactose, D-mannose, D-rhamnose, D-ribose, D-xylose, D-fucose, D-galacturonic acid, D-glucuronic acid, phenyl β-D-glucopyranoside, dimethylformamide (DMF), trifluoroacetic acid (TFA), ammonium hydroxyde and N,O-Bis(trimethylsilyl)trifluoroacetamide (BSTFA) were purchased from Sigma-Aldrich (Taufkirchen, Germany); ethanol was purchased from Carlo Erba (Milan, Italy); bidistilled water was obtained using Milli-Q System (Millipore, Bedford, MA, USA); MS-grade formic acid from Fisher Chemical (San Jose, CA, USA), while methanol, deuterium oxide (D_2O) and trimethylsilylpropanoic acid (TSP) from VWR International (Milan, Italy).

2.2. Composition of hazelnut shells (HS)

The composition of the starting material, namely ground and sieved HS, was investigated in terms of dry matter, proteins, lipids, ash, soluble and insoluble fibres. These analyses were carried out using standard procedures [20]. Moisture/dry matter was determined drying the sample in an oven at 105 °C for 24 h, while ash was quantified through mineralization at 550 °C for 5 h. Proteins were determined with a Kjeldahl system (DKL heating digestor and UDK 139 semiautomatic distillation unit, VELP SCIENTIFICA) by using 6.25 as nitrogen-to-protein conversion factor. Total lipid content was calculated with an automatized Soxhlet extractor (SER 148/3 VELP SCIENTIFICA, Usmate Velate, Italy) using diethyl ether as solvent. Both soluble and insoluble fibres were determined with AOAC 991.43 method [21].

2.3. Hydrothermal treatment

Hydrothermal extractions were conducted using a Parr Mini Bench Reactor, type 4560 (Parr Instruments Co., Illinois, USA) equipped with a magnetic drive stirring system and a reaction vessel of 300 mL capacity. About 2.5 g of ground HS were used in each experiment, and 77.5 mL of bidistilled water were added in the reactor as extracting solvent. Four different temperatures were tested (i.e., 125 °C, 150 °C, 175 °C, and 200 °C), and the reaction time was set at 60 minutes. Although generally the reaction time is lower when hydrothermal treatments are applied, it was decided to elevate it since the main purpose was to evaluate the degradation compounds which can originate from HS, rather than the extraction of XOS.

Actually, the time necessary to reach the desired temperature ranged from 15 to 30 minutes, while to cool down the system between 5 and 10 minutes elapsed. Figure 5.1 shows the heating and cooling profiles for every experiment.

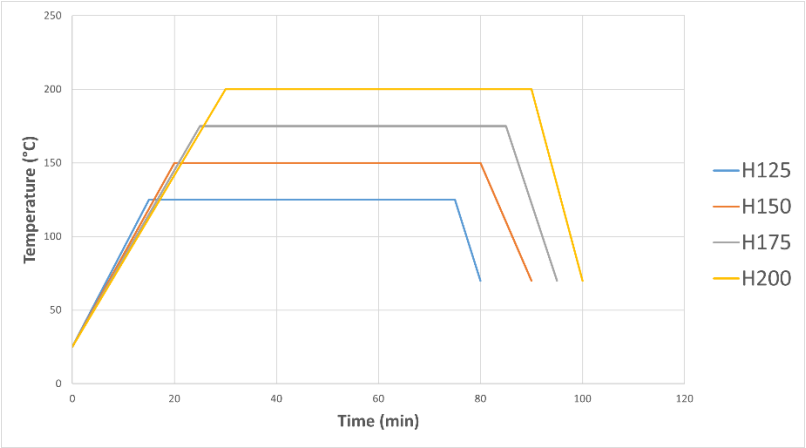

***Figure 5.1**: Heating and cooling profiles of the hydrothermal treatment in ever experiment.*

Once each reaction mixture was recovered from the reactor vessel, it was centrifuged at 3900 rpm, at 4 °C for 40 minutes to separate the extracted hemicellulose, solubilized in the aqueous supernatant, from the solid phase. The supernatant was collected and stored at -18 °C for further analyses.

2.4. Characterization of liquor obtained from hydrothermal treatment

2.4.1. Total monosaccharide composition

The total monosaccharide composition of the liquor obtained from hydrothermal treatment of HS was investigated qualitatively, in terms of type of sugars, by gaschromatography coupled with mass spectrometry (GC-MS) according to a protocol reported elsewhere with few modification [11]. Briefly, the supernatant collected after centrifugation (Section 2.3) was thawed out and 1000 µL were withdrawn and dried by rotavapor. Subsequently, 3 mL of 2N trifluoroacetic acid (TFA) were added and the acid hydrolysis was carried out for 2 hours at 110 °C. Then, 1000 µL were withdrawn and put in a round-bottomed flask, then dried by rotavapor. When the solvent was evaporated, the obtained dried hydrolysate was washed with 1 mL of methanol to remove the TFA residues and evaporated again. 1 mL of 0.5 M NH_4OH was subsequently added to delactonize the eventually present sugar acid lactones in the solution, and again evaporated by rotavapor. Finally, the dried hydrolysate was dissolved in 800 µL of DMF and 200 µL of BSTFA, used as derivatizing agent. The reaction was kept for 1 hour at 60 °C under stirring and then the derivatized sample was injected in gas chromatography. GC-MS analysis of monosaccharides was performed with a 6890 N gas chromatograph coupled to a 5973 N mass selective detector (Agilent technologies, Santa Clara, CA). A SLB-5ms, 30 m × 0.25 mm, 0.25 µm of thickness column (Supelco, Bellafonte, PA, USA) was used. The chromatogram was recorded in the scan mode (40–500 *m/z*) with a programmed temperature from 60 °C to 270 °C. The initial temperature was 60 °C, held for 2 minutes, then increased to 160 °C at a rate of 10 °C/min, held isothermal for 5 minutes,

increased to 220 °C at a rate of 10 °C/min, kept for 5 minutes, increased to 270 °C at a rate of 20 °C/min and maintained for 5 minutes. A response factor was also injected to normalize the signals, considering the area and concentration ratios between phenyl β-D-glucopyranoside and several monosaccharides likely to be present in the samples, namely D-glucose, D-fructose, D-Arabinose, D-galactose, D-mannose, D-rhamnose, D-ribose, D-xylose, D-fucose, D-galacturonic acid and D-glucuronic acid. In summary, response factor (RF) was calculated as follows:

$$\mathrm{RF} = \frac{Area\ analyte}{Area\ phenyl\ \beta - D - glucopyranoside} * \frac{Concentration\ phenyl\ \beta - D - glucopyranoside}{Concentration\ analyte}$$

Then, the areas of each monosaccharide in the samples were corrected dividing them by the response factor.

2.4.2. Evaluation of the molecular weight (Mw)

The molecular weight of poly- and/or oligosaccharides extracted from HS was evaluated through High-Performance Size-Exclusion Chromatography coupled with Refractive Index Detector (HPSEC-RID). 120 µL of the supernatant obtained from HT were mixed with 880 µL of ultrapure water, then injected in an Agilent 1260 Infinity II LC system equipped with a refractive index detector (RID) (Agilent, Santa Clara, CA, USA). Ultrapure water was used as eluent at a flow rate equal to 0.7 mL/min, and a PL aquagel-OH 20, 7.5 x 300 mm, 8 µm column (Agilent, Santa Clara, CA, USA) was employed for the separation. The injection sample volume was set at 50 µL, column temperature 30 °C and RID temperature 35 °C. Standard pullulans having known molecular weight, namely 180 Da, 667 Da, 6300 Da, 9800 Da and 22000 Da were used for the calibration curve.

2.4.3. Characterization of oligosaccharides through UPLC/ESI-MS

The analysis of oligosaccharides present in the supernatant obtained from HT was performed through hydrophilic interaction chromatography (HILIC) coupled with mass spectrometry. An aliquot of the supernatant collected after centrifugation was taken and filtered through 0.45 µm nylon membranes, then 1500 µL of the permeate were dried under nitrogen flow and subsequently re-dissolved in 50/50 acetonitrile/water. Then, samples were analysed by ultra-performance liquid chromatography with electrospray ionization in negative mode and single-quadrupole mass spectrometer detector (UPLC/ESI-MS, WATERS ACQUITY). UPLC/ESI-MS analysis was performed by using an ACQUITY UPLC® BEH Amide column (2.1 x 100 mm, 1.7 µm). The mobile phase was composed by 80 % CH_3CN + 20 % H_2O + 0.1 % NH_4OH (eluent A) and 30 % CH_3CN + 70 % H_2O + 0.1 % NH_4OH (eluent B). Gradient elution was performed as follows: from 100 % A to 40 % A and 60 % B by linear gradient in the first 10 minutes, from 40 % to 100 % A in 0.02 minutes, isocratic 100 % A from 10.02 to 30 minutes. Flow rate was set at 0.17 mL/min, injection volume 2 µL, strong needle wash 20 % CH_3CN + 80 % H_2O, weak needle wash 75 % CH_3CN + 25 % H_2O, seal wash 50 % CH_3CN + 50

% H_2O, column temperature 35 °C and sample temperature 18 °C. Detection was performed by using Waters SQ mass spectrometer: ESI source in negative ionization mode, capillary voltage 2.8 kV, cone voltage 25 V, source temperature 120 °C, desolvation temperature 350 °C, cone gas flow (N_2) 50 L/hr, desolvation gas flow (N_2) 500 L/hr, full scan acquisition (100-2000 *m/z*). Integration was performed by extracting the following mass ions (*m/z*) for deacetylated XOS: 149 for xylose, 281 for DP2, 413 for DP3, 545 for DP4, 677 for DP5, 809 for DP6, 941 for DP7, 1073 for DP8, 1205 for DP9, 1337 for DP10. For acetylated XOS, numerous mass ions can be theoretically present (see Chapter 7) and the presence of each of them was checked by extracting the corresponding fragment. The various XOS were semi-quantified, taking into account ratios between peak areas, because an exact quantification is not possible due to the lack of each standard compound.

2.4.4. Total sugar content, degree of acetylation and main lignocellulose degradation products through ^{1}H NMR

The total quantity of sugars and the degree of acetylation were calculated through ^{1}H NMR analysis, and at the same time HMF, formic acid, free acetic acid and methanol were investigated as well. Briefly, 400 µL of the supernatant obtained after HT were directly added in the NMR tube, together with 300 µL of deuterium oxide (D_2O) and 100 µL of 2000 ppm 3-(trimethylsilyl)propionate-*d4* (TSP) dissolved in D_2O. ^{1}H NMR spectra were registered on a Bruker Avance III 400 MHz NMR Spectrometer (Bruker BioSpin, Rheinstetten, Karlsruhe, Germany) operating at a magnetic field-strength of 9.4 T. Spectra were acquired at 298 K, with 32 K complex points, using a 90° pulse length and 5 s of relaxation delay (d1). 128 scans were acquired with a spectral width of 9595.8 Hz and an acquisition time of 1.707 s. The relaxation delay and acquisition time ensure the complete relaxation of the protons, allowing their integrals for quantitative purposes. The experiments were carried out with water suppression by low power selective water signal presaturation during 5 s of the relaxation delay. The NMR spectra were processed by MestreNova software. The spectra were Fourier transformed with FT size of 64 K and 0.2 Hz line-broadening factor, phased and baseline corrected, and referenced TSP peak.

Different spectral zones were manually integrated and used for a quantification of the total sugars and other main compounds found in the extracts, namely free acetic acid (1.99-2.05 ppm), acetyl groups bound to sugars (2.08-2.20 ppm), total sugars (zones 3.13-3.32 ppm, 3.37-4.65 ppm and 4.95-5.26 ppm), free methanol (3.34 - 3.36 ppm), formic acid (8.37-8.48 ppm) and hydroxymethylfurfural (HMF, 9.47-9.52 ppm) Integrals were normalized to the area of TSP, added to each sample in an exactly known amount, and the values were converted in mass/volume (mg/100 ml) as previously reported [22].

2.4.5. In depth characterization of the degradation compounds

The degradation compounds originated from hydrothermal treatments of HS were in depth characterized according to a ”reactomics” approach by Ultra-High-Performance Liquid Chromatography - Ion mobility – quadrupole time-of-flight – mass spectrometry (UHPLC-IM-Q-TOF-MS). Briefly, after HT, the solutions were centrifuged, and 500 µL of the supernatants were withdrawn and diluted in 1:1 ratio with 500 µL of ultrapure water, then injected (samples “125”, “150”, “175”, “200”). Later, an aliquot of each supernatant was also taken and added to four volumes of ethanol, in order to allow the extracted fibres to precipitate. After that, a centrifugation step was performed at 4 °C, 20 minutes and 3900 g. The hydroalcoholic liquid fraction was discarded, while the precipitate corresponding to fibres was collected, and 1 mg was weighed and dissolved in 1000 µL of ultrapure water, then injected (samples “125f”, “150f”, “175f”, “200f”, where “f” stands for fibres).

ACQUITY I-Class UHPLC separation system coupled to a VION IMS QTOF mass spectrometer (Waters, Wilmslow, UK) equipped with an electrospray ionization (ESI) interface was employed. Samples were injected (2 µL) and chromatographically separated using a reversed-phase ACQUITY Premier HSS T3 column 2.1 × 100 mm, 1.8 µm particle size (Waters, Milford, MA, USA). A gradient profile was applied using water 5mM ammonium formiate (eluent A) and acetonitrile (eluent B) both acidified with 0.1% formic acid as mobile phases. Initial conditions were set at 2% B, after 3 min of isocratic step, a linear change to 100% B was achieved in 12 min and holding for 5 min to allow for column washing before returning to initial conditions. Column recondition was achieved over 3 min, providing a total run time of 23 min. The column was maintained at 45 °C and a flow rate of 0.35 mL/min used.

Mass spectrometry data were collected in positive and negative electrospray mode over the mass range of *m/z* 50−1100. Source settings were maintained using a capillary voltage, 2.5 kV and 2 kV for positive and negative ESI modes, respectively; source temperature, 150 °C; desolvation temperature, 500 °C and desolvation gas flow, 950 L/h. The TOF analyzer was operated in sensitivity mode and data acquired using HDMSE, which is a data independent approach (DIA) coupled with ion mobility. The optimized ion mobility settings included: nitrogen flow rate, 90 mL/min (3.2 mbar); wave velocity 650 m/s and wave height, 40 V. Device within the Vion was calibrated using the Major Mix IMS calibration kit (Waters, Wilmslow, UK) to allow for CCS values to be determined in nitrogen. The calibration covered the CCS range from 130-306 Å2. The TOF was also calibrated prior to data acquisition and covered the mass range from 151 Da to 1013 Da. TOF and CCS calibrations were performed for both positive and negative ion mode. Data acquisition was conducted using UNIFI 1.8 (Waters, Wilmslow, UK). Data processing was performed according to reports in Chapter 4.

3. Results and discussion

3.1. Proximate composition of HS

Hazelnut shells (HS) were first subjected to different analyses to look into their proximate composition, in terms of lipid, protein, fibre, ash and moisture contents. The results are reported in Table 5.1.

***Table 5.1**: Proximate composition of hazelnut shells.*

	g/100g HS
Moisture	7.08 ± 0.01
Lipid	2.82 ± 0.85
Protein	2.2 ± 0.02
Ash	1.95 ± 0.17
Soluble fibre	3.27 ± 0.04
Insoluble fibre	86.26 ± 0.05
Total dietary fibre	89.53 ± 0.09

As evident in the table, HS were mainly constituted by fibre, which accounted for almost 90% of the fresh matter (% wt). Very small quantities of proteins, lipids and ashes were found too, close to 2-3%. A part of the total fibre content, equal to 3% of the biomass, was constituted by soluble fibre, while the rest was insoluble, easily identifiable as cellulose, hemicellulose and lignin, as reported in previous studies [13].

3.2. Composition of the hydrothermal liquors

3.2.1. Monosaccharide distribution

The presence of different monosaccharide was investigated through GC-MS in the four hydrothermal liquors obtained with different temperatures, and it is reported in Figure 5.2.

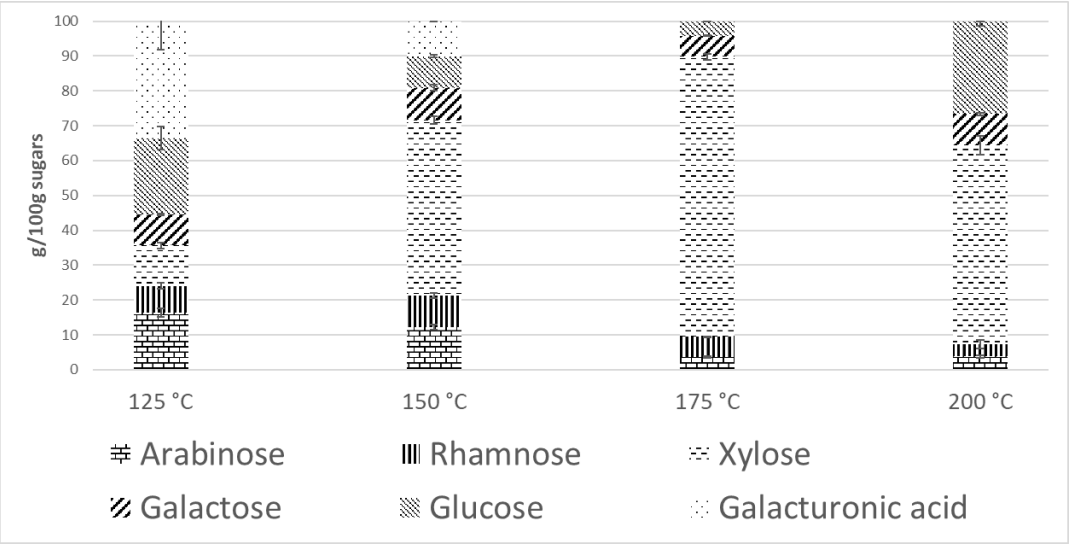

Figure 5.2: *Monosaccharide profile of HS' hydrothermal extracts at different temperatures.*

Figure 5.2 shows a quite diverse monosaccharide profile for each extract depending on the temperature employed for the hydrothermal treatment. At 125 °C a good amount of galacturonic acid was detected, equal to 32 ± 7 % of the total sugars. Although based on our knowledge pectin has never been reported to be present within hazelnut shells, the identification of this hexuronic acid is supposedly attributable to this polymer. Moreover, the presence of arabinose, rhamnose and galactose in relative percentages equal to 16%, 8% and 9%, respectively, nearly reminds to an average neutral monosaccharide distribution of pectin. In a previous work of ours, a similar monosaccharide distribution from another lignocellulosic material, namely grape stalks, was found after hydrothermal extraction in the same conditions [11], further confirming the feasibility of extracting pectic fractions in this way. Xylose, that is the main monosaccharide making up HS' hemicellulose, was instead found to be in a low amount (11%), suggesting how this treatment is not adequate to satisfactorily extract this fraction. Indeed, as shown in the figure, xylose content only increased when temperature increased as well, rising to 50% of the total sugars at 150 °C and to 80% at 175 °C. At 150 °C a good proportion of galacturonic acid (10%) was still detected, indicating the feasibility of pectin extraction even with higher temperatures. Compared to the extraction at 125 °C, this percentage dropped as well as rhamnose's, galactose's and glucose's ones, and it is likely that this is mainly due to the simultaneous great increase of xylose, rather than lower pectin extraction or galacturonic acid degradation. At the same time, however, galacturonic acid was not detected anymore in the chromatogram when the extracts at 175 °C and 200 °C were analyzed, meaning that its degradation at higher temperatures occurs. A previous study indeed reported how hexuronic acids are more susceptible to thermal degradation than pentoses [23]. Interestingly, at 200 °C the portion of xylose dropped again to 57%, likely indicating its high extraction rate but with simultaneous dehydration to furfural and other compounds. Moreover, in this sample a net increase in glucose percentage appeared, probably due to a partial hydrolysis of cellulose. This extract may therefore be defined as containing holocellulose rather than hemicellulose. In Rivas' work, the

percentage of xylose in the hazelnut liquor always increased together with the temperature in the range from 190 °C to 225 °C [17], differently from our results, but it is necessary to underline the difference in the reaction time, much higher in our experiments, thus resulting in a higher severity.

3.2.2. Total sugars, degree of acetylation and principal degradation products

^{1}H NMR technique was employed in order to quantify the total sugars released in the hydrothermal extracts of HS, using TSP as internal standard, as well as to determine the degree of acetylation and the formation of some degradation compounds, and the results are presented in Table 5.2. The total quantity of sugars varied a lot among the different samples: the highest amount was found at 150 °C, with a total of 253 mg of sugars obtained per 100 mL, corresponding to almost 8% of the total weight of HS used in the experiment. Then, 219 mg/100 mL were obtained at 175 °C (corresponding to 6.7% of HS). Since the average amount of xylan in HS has been reported to be around 20% [13], these percentages, considered together with the xylose relative amount reported in figure 5.2, should correspond to a recovery close to 20-30% of total xylan at 150 °C and 175 °C, respectively. These values are a bit lower than the ones found in previous studies conducted on HS [16,17]. The yield hugely diminished both at 125 °C and 200 °C, with a total sugar content in the liquor of 43 mg/100 mL and 45 mg/100 mL (corresponding to 1.6% and 1.4% of HS), respectively. Although these two latter low yields are similar to each other, the reasons are opposite: at 125 °C simply low quantities of sugars were extracted, due to an insufficient temperature to allow all the hemicellulose to be dissolved, and at 200 °C a high quantity of sugars was extracted but degraded at the same time, with consequent formation of undesired compounds. Through ^{1}H NMR, in fact, it was possible to quantify four different products that are known to be generated from sugars degradation, namely free acetic acid, methanol, formic acid and HMF/furfural, detectable in different zones of NMR spectra. The aforementioned hypothesis is confirmed from this investigation. Indeed, at 125 °C only 7.7 mg of total degradation compounds were obtained, against 130 mg obtained at 200 °C. In the four samples, acetic acid turned out to be always present in the highest amount, and this is not surprising since it is freed up from hydrolysis of acetyl groups covalently bound to polysaccharides, mainly xylan [24]. A very high quantity has been found in particular at 200 °C, suggesting a strong deacetylation of the hemicellulose when extracted. Then, in the extract at 175 °C more acetic acid was found compared to the one at 150 °C, despite a lower quantity of total sugars. The reason might be found in a different extraction proportion of different polysaccharides in the two experiments (i.e., xylan, known to be strongly acetylated, and other soluble polysaccharides such as pectin, with a much lower degree of acetylation). As regards methanol, it was detected in low amounts when HS underwent HT at 125 °C, a high quantity was found at 150 °C and then it decreased at 175 °C and 200 °C. Methanol may derive from pectin demethylation (and therefore these results might suggest the presence of pectin in hazelnut shells with different extraction yields and degradation rate), but also from methoxy groups cleavage from lignin [25].

Formic acid is known to be one of the reaction products of sugars degradation [26], as well as HMF and furfural, from hexoses and pentoses, respectively [27], thus it makes sense that they showed a positive correlation with the treatment temperature, reaching very high values at 200 °C. Note that at this latter temperature 35 mg of sugars and 61 mg of HMF/furfural + formic acid were obtained, demonstrating how degradation of sugars goes faster than their extraction. Finally, the acetylation degree of total sugars, in percentage, was very low at 125 °C (8%), confirming the non-xylan nature of the polysaccharides extracted, then increased to 35% at 150 °C and decreased to 28% at 175 °C, demonstrating how a stronger treatment favors xylan extraction and simultaneous deacetylation reactions with consequent expected autohydrolysis processes, theoretically leading also to higher XOS contents. Surprisingly, at 200 °C the acetylation degree went back to high values, equal to 57%. In our opinion, it is possible that unsubstituted monosaccharides are easier to be degraded to formic acid, HMF or furfural, respect to the acetylated ones.

Table 5.2: *Total sugar content, acetylation degree and degradation products content obtained with hydrothermal extraction at different temperatures, starting from 2.5 g hazelnut shells, quantified by ^{1}H NMR.*

	HT 125 °C	HT 150 °C	HT 175 °C	HT 200 °C
Total sugars (mg)	40.0	195.3	168.7	34.7
Total acetyl groups (mg)	1.1	25.4	18.1	6.9
Approximate acetylation degree (%)	8.1	35.0	27.9	56.8
Degradation compounds from sugars:				
Acetic acid (mg)	3.6	19.0	35.5	62.7
Methanol (mg)	1.6	10.7	8.7	6.6
Formic acid (mg)	2.2	8.6	7.8	13.2
HMF/furfural (mg)	0.3	0.9	7.8	47.7
Total degradation compounds (mg)	7.7	39.2	59.8	130.2

3.2.3. Evaluation of molecular weight

HPSEC-RID was performed for the same four samples in order to evaluate the molecular weight of the extracted fractions. Although the principle of this technique is based on the hydrodynamic volume of molecules rather than the molecular weight itself, it can provide important gross information about the latter. The results are reported in Figure 5.3.

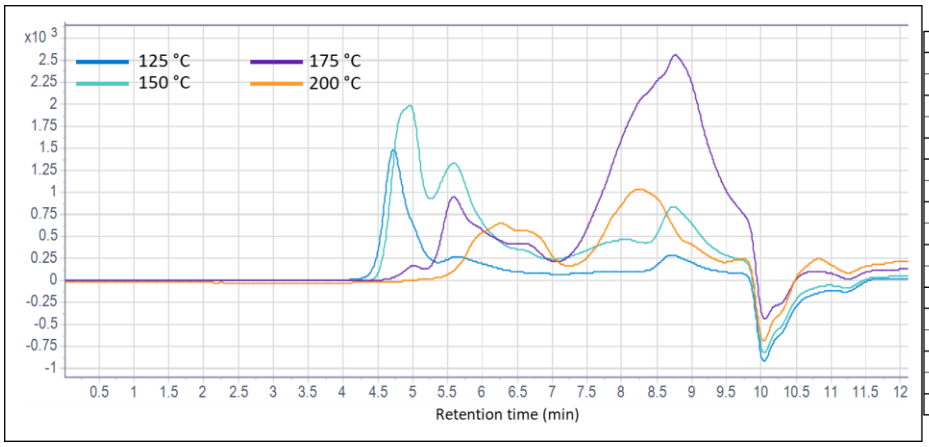

	Peak #	RT (min)	Mw (Da)	Area%
125 °C				
	1	4,722	>> 20,000	73,781
	2	5,642	> 20,000	16,137
	3	8,715	< 180	10,083
150 °C				
	1	4,96	>> 20,000	28,658
	2	5,589	> 20,000	33,727
	3	8,064	1350	16,661
	4	8,74	< 180	20,954
175 °C				
	1	5,587	> 20,000	14,118
	2	6,56	7773	4,504
	3	8,765	413	81,378
200 °C				
	1	6,267	17954	36,932
	2	8,254	510	59,03
	3	9,749	< 180	4,038

***Figure 5.3**: Molecular weight distribution of HS polysaccharides extracted at different temperatures.*

The results coming from HPSEC seem to confirm the hypotheses made in the previous sections. At 125 °C, three separated zones were detected: the first two had a Mw bigger than 20 kDa (that is the upper limit the chromatographic column was able to distinguish, and outside the calibration curve range) and putatively indicated as 217 kDa and 40 kDa, respectively, while the third was indicated as < 180 Da. The first one represented 73% of the total area and is attributable to pectin polymers, even though they are generally slightly smaller [28]. This result is in accordance with GC-MS analysis, which showed the sum of galacturonic acid, arabinose, rhamnose, glucose and galactose a little bit higher and close to 85%, but it is necessary to consider that arabinose residues are also present as substituents of xylans and therefore not only attributable to pectin. Given the quantity of soluble fibre (Section 3.1), the monosaccharide distribution of the extract (Section 3.2.1), the total quantity of sugars calculated with NMR (Section 3.2.2) and the results obtained by HPSEC, it is possible to calculate the yield of the pectin extraction in these conditions. Indeed, being the total sugars obtained in the extract equal to 1.6% of the total weight of HS and given that 70% seems to correspond to pectin because of the HPSEC area and monosaccharide distribution, it can be calculated that 1.12% of HS has been extracted as pectin. Since soluble fibres represent 3.27% of HS (Table 5.1), it can be concluded that if this portion would be entirely constituted by pectin, 34% of the latter was extracted by this method. The second fraction accounted for 16% of the total area and could correspond to hemicellulose. The molecular weight of hemicellulose can be various, and it has been reported to be in the range 26-36 kDa in different wood species [29], but even 70 kDa elsewhere [30]. The third small fraction, accounting for 10%, may be represented by low-Mw sugars and oligosaccharides.

In the liquor derived from hydrothermal treatment at 150 °C, on the other hand, four fractions were detected and again one of them presented very high Mw, likely traceable to pectin, in this case representing 29% of the total area, again quite in agreement with GC-MS results. Following the previous reasoning, it can be stated that about 67% of the pectin has been extracted in these conditions. A higher percentage, nearly twice the one found at 125 °C, was found for the hemicellulose fraction, with a putative Mw equal to 39 kDa, in

agreement with a higher quantity of xylose detected by GC-MS, and two small fractions appeared too, indicating the presence of low-Mw sugars. The area corresponding to high-Mw pectin disappeared in the sample extracted at 175 °C, confirming the absence of this polymer, as already discussed in GC-MS section, while the area attributable to hemicellulose was still present but in lower quantities, equal to 14%. The most area in the chromatogram (i.e., 81%) was found to correspond to low-Mw molecules, with average Mw putatively calculated equal to 400 Da, and being xylose the main monosaccharide in this sample, these are likely to be XOS. Finally, when HS underwent hydrothermal extraction at 200 °C low Mw fractions were mainly present, once again likely due to the formation of short xylose-based chains. In addition to this, a medium Mw fraction, equivalent to 17 kDa, was found accounting for 37% of the total area, probably attributable to partially degraded holocellulose.

3.2.4. Distribution profile of XOS

Since from the previous analyses XOS are likely present in the hydrolysates and since XOS production is usually one of the main objectives when xylan-rich hemicellulose is extracted through HT, their distribution in the liquors was investigated with a HILIC chromatographic method by UPLC-MS. The results are presented in Table 5.3.

Table 5.3: *Semiquantitative profile of different hydrothermal extracts, in terms of acetylated and deacetylated XOS with degree of polymerization 1-10, and total chromatographic area. "ac"=acetylated.*

	Area % (Area/Area total XOS*100)			
	HT125	**HT150**	**HT175**	**HT200**
DP1	22.93 ± 1.90	42.82 ± 2.15	14.30 ± 1.79	77.95 ± 3.15
DP1 ac	nd	nd	nd	nd
DP2	4.47 ± 0.48	5.95 ± 0.41	9.45 ± 0.18	4.91 ± 0.13
DP2 ac	49.59 ± 2.03	nd	5.46 ± 0.19	1.45 ± 0.11
DP3	2.21 ± 0.14	3.79 ± 0.09	4.96 ± 0.03	1.71 ± 0.08
DP3 ac	2.23 ± 0.14	4.16 ± 0.20	10.68 ± 0.17	2.45 ± 0.17
DP4	2.80 ± 0.75	2.14 ± 0.02	4.32 ± 0.01	1.48 ± 0.11
DP4 ac	6.30 ± 1.02	11.50 ± 0.84	19.69 ± 0.25	3.00 ± 0.41
DP5	1.29 ± 0.03	0.79 ± 0.07	1.50 ± 0.20	0.82 ± 0.03
DP5 ac	6.67 ± 0.49	9.33 ± 0.39	15.94 ± 0.34	3.28 ± 0.13
DP6	0.49 ± 0.12	0.56 ± 0.08	0.44 ± 0.18	0.18 ± 0.01
DP6 ac	1.03 ± 0.40	2.92 ± 0.55	6.54 ± 0.54	1.10 ± 0.02
DP7	nd	nd	0.25 ± 0.07	0.09 ± 0.02
DP7 ac	nd	7.06 ± 0.31	3.91 ± 0.61	1.30 ± 0.21
DP8	nd	nd	0.16 ± 0.03	nd
DP8 ac	nd	4.99 ± 0.54	1.58 ± 0.35	0.29 ± 0.06
DP9	nd	nd	nd	nd
DP9 ac	nd	3.98 ± 1.11	0.67 ± 0.01	nd
DP10	nd	nd	nd	nd

DP10 ac	nd	nd	0.15 ± 0.06	nd
Area TOT	11 mln	17 mln	102 mln	30 mln

Table 5.3 reports distribution of deacetylated and acetylated XOS, for DPs that range from 1 (i.e., xylose) to 10. First of all, what catches the eye is the total area, calculated as sum of the absolute areas for each XOS. In this sense, the liquor obtained after HT at 175 °C turned out to contain much more XOS in general, followed in descending order by the extracts at 200 °C, 150 °C and 125 °C, confirming the results arising from HPSEC, in which the peaks corresponding to molecular weights < 1500 Da followed the same trend among the samples. This parabolic total area trend is in accordance with the study performed by Surek and Buyukkileci, who tested different autohydrolysis extractions from HS and showed how XOS content increased up to a certain severity factor (190 °C for 30 minutes), then dropped [16]. As regards XOS distribution, the treatment at 125°C allowed to obtain xylose and XOS with DP 2-6 only, while at 150 °C, 175 °C and 200 °C XOS up to DP 9, to DP 10 and to DP 8 appeared in the reaction medium, respectively. These results do not totally agree with other works on HS hydrothermal extractions, which obtained the detection of XOS up to DP 16 [17] and the presence of DP 2-6 only when temperatures higher than 160 °C were employed, even though for shorter times [16]. Regarding high-DP XOS, however, it is possible that after a certain size that they are not able to ionize with electrospray anymore, thus not being detected. Although the total area at 175 °C was much bigger than in the other samples and showed the widest range of XOS, it turned out that the ones with higher DP, especially between 8 and 10, were in low amount. On the contrary, relevant percentages of DP 7, 8 and 9, equal to 16% of the total XOS, appeared when 150 °C was selected as operative temperature. This should be kept in mind when such treatments are applied, since it was shown in previous works how XOS with higher DPs seem to improve their antioxidant potential (see Chapter 7 of this dissertation), while smaller DPs seem to better stimulate the growth of many prebiotic bacteria [31]. Another interesting result concerns xylose: very big quantities emerged at 200 °C (78% of total XOS), indicating a rather strong degradation of xylan into its monomer. At 125 °C a fair proportion of xylose, equal to 23% of total XOS, was present and can be justified due to the simultaneous low amount of XOS with higher DPs. Surprisingly, higher xylose amounts were detected at 150 °C rather than at 175 °C: this may be explained by a faster xylose degradation at higher temperature.

3.2.5. In depth characterization of degradation compounds

The four hydrothermal extracts obtained with different temperatures were also analysed by UHPLC-IM-Q-TOF-MS aiming to evaluate differences in the metabolomic profile. This approach has been used also in Chapter 4 of this dissertation, but as far as we know, it has never been used in literature for the characterization of the wide range of compounds that may originate at such high temperatures from lignocellulosic biomasses. The reactions that are supposed to occur involve mainly sugars and phenols [32],

even though no clear and well explained mechanisms are reported in literature. The supernatant derived from hot liquid water process was firstly withdrawn, diluted and injected as it is. In parallel, an aliquot was taken and the high-Mw fibre extracted with HT was also precipitated from the supernatant by adding four volumes of ethanol, therefore isolated, re-dissolved in water and analysed. This procedure has long been applied to isolate high-Mw fibres [33], and therefore it is of interest to investigate whether such alcohol-addition step may have an impact in lowering the degradation compounds content. Each of the eight samples (four supernatants and four purified fibre fractions) were analysed in triplicate both in positive and negative ion mode. MS data were acquired and automatically processed by Progenesis QI software. In total, 7893 features were detected in ESI- mode and 7478 in ESI+ mode.

As a first approach, the samples distribution was inspected through principal component analysis (PCA) taking into account all the features detected, thus allowing us to describe the system variability in a simpler way, using only a few components, reducing the complexity and projecting the samples in a two-dimensional graph. Figure 5.4 reports the scatter plot of the PCA performed on the 7478 features detected in ESI+, and 30% of the total variation is explained by the first component (PC1) and another 22% by the second one (PC2).

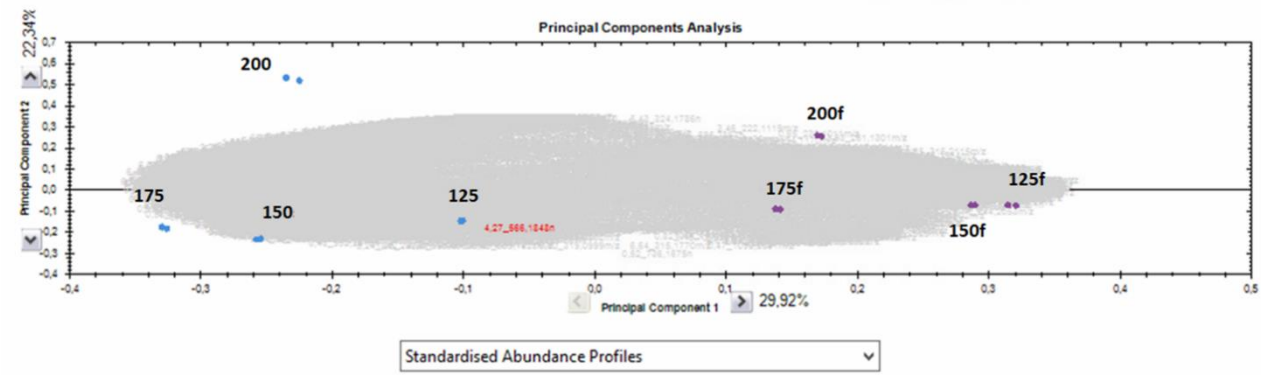

***Figure 5.4**: Distribution of hydrothermal supernatants and precipitated fibres (indicated as "f" following the temperature) on the first two principal components, built considering all the 7478 features detected in ESI+ through UHPLC-IM-Q-TOF-MS and automatically processed by Progenesis QI software.*

Figure 5.4 shows a clear separation between supernatants as such and precipitated fibres through ethanol addition (the latter indicated as "f"), which can be found in correspondence with negative and positive values of PC1, respectively. This may indicate that ethanol addition, when employed to isolate fibres, potentially has the capacity to change the metabolic profile of degradation compounds. Then, it can also be noticed that samples 200s and 200f are in the upper part of the graph, and although separated from each other along PC1, both of them are located at positive values of PC2, while all the other samples are at negative values.

Then, to further investigate the molecular characteristics of the compounds present in the liquor and retained in alcohol insoluble residues, these huge number of features was reduced at first by filtering them

on the base of fragmentation score and significativity among the samples (ANOVA, p-level 0.05). Here, only the compounds having fragmentation score ≥ 90 were considered, then only those compounds whose experimental fragmentation pattern matched with the theoretical and/or with the one present in the online databases were retained. Finally, duplicate metabolites (such as those ionizing in both polarities) were checked, and in the end a total of 531 molecules were putatively identified, then they were divided in chemical classes according to the main functional group. The whole list of compounds is reported in Table S2. Twenty-two chemical classes were found: figure 5.5 reports the number of compounds identified, together with the relative presence of every class for every HT supernatant, namely 125, 150, 175 and 200, and for alcohol insoluble residues obtained after ethanol treatment of the supernatant (these samples are indicated as "f" following the temperature).

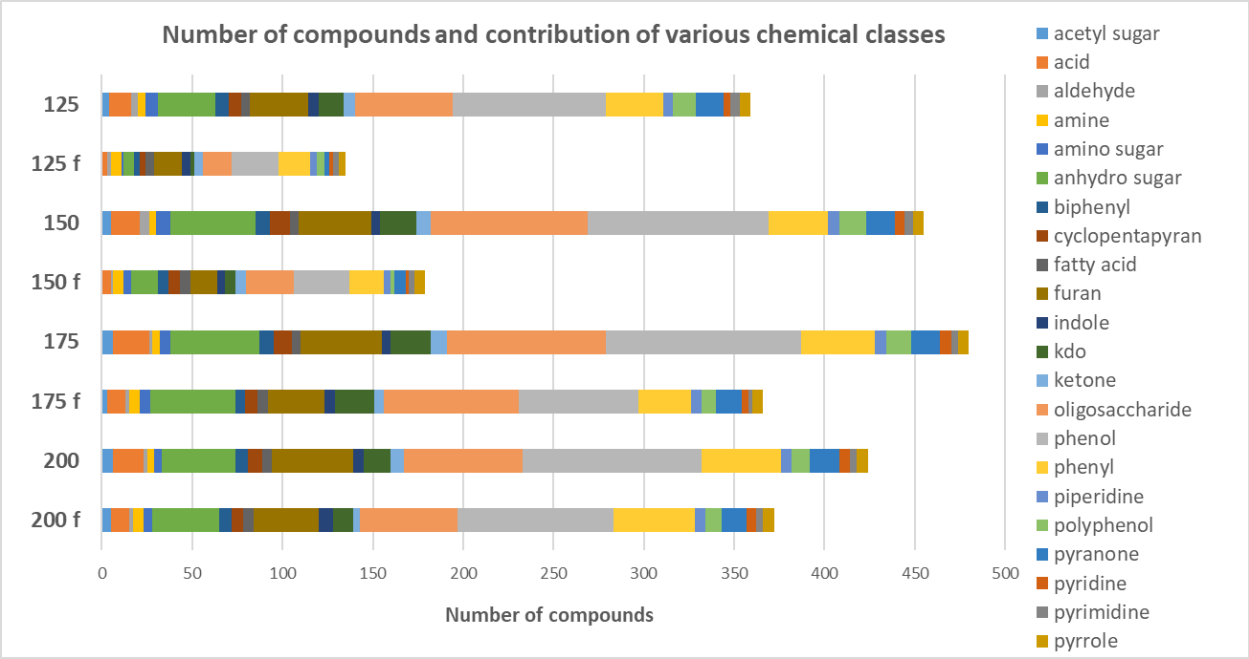

Figure 5.5: *Representation of the total number of compounds identified for each hydrothermal treatment and contribution of each chemical class. The numbers indicate the temperature employed in a specific experiment, "f" indicates the fibres precipitate in the supernatants after ethanol addition.*

It can be observed in Figure 5.5 that the total number of molecules in each supernatant collected after HT at diverse temperatures varied. At 125 °C, 359 compounds appeared, increasing to 455 at 150 °C, to 480 at 175 °C and then dropping to 424 at 200 °C. The increasing number of compounds from 125 °C to 175 °C is not surprising, since higher temperatures lead to greater sugars degradation [34], while the lower total number in the experiment carried out at 200 °C can be probably due to the formation and consequent loss of smaller molecules with lower boiling points. However, it can also be seen that the relative distribution of the chemical classes did not change a lot, in terms of number of compounds. The most abundant class was always constituted by phenols, which can be either present in hazelnut shells as such [35] (for instance in the form of quinones, anthraquinones, flavonoids or tannins), or derived from lignin degradation [36]. Regardless of

the experimental temperature, oligosaccharides were always the second most abundant class. Then, a lot of furans and molecules containing phenyl groups were also present, coming from sugars dehydration and lignin hydrolysis, respectively, followed by good quantities of anhydro sugars and acids, but also heterocyclic compounds such as pyranones and pyridines, and also Kdos (ketodeoxyoctonic acids) (Figure 5.5), as also reported in Chapter 4 of this dissertation.

The total number of compounds always decreased when ethanol was added to precipitate fibres, suggesting the effect of alcohol employment in diminishing the total content of compounds, both the desired, namely oligosaccharides, and undesired ones. Actually, not always this decrease occurred in the same proportion: indeed, if on the one hand at 125 °C and 150 °C the number of compounds diminished 2.6 and 2.5 times, respectively, at 175 °C and 200 °C this proportion changed a lot, with a decrease factor of 1.3 and 1.1 times, respectively. These data might be explained by the different nature of the molecules which originated from the process, not only in terms of chemical class but also of size. Higher temperatures could have led to intermolecular reactions, giving rise to more complex structures with lower solubility in alcohol, thus causing their precipitation together with fibres.

Data related to supernatants were also evaluated on the basis of the compounds relative abundance, a value automatically extrapolated by the Progenesis QI software for every compound, which compares the ion intensities of an individual compound to total ion abundance. The relative abundance per class, expressed in percentage, is reported in Figure 5.6 for the supernatants. If on the one hand the number of compounds belonging to a specific chemical class does not change a lot in proportion to the total number of compounds for every experiment (Figure 5.5), on the other hand the abundance profile is different.

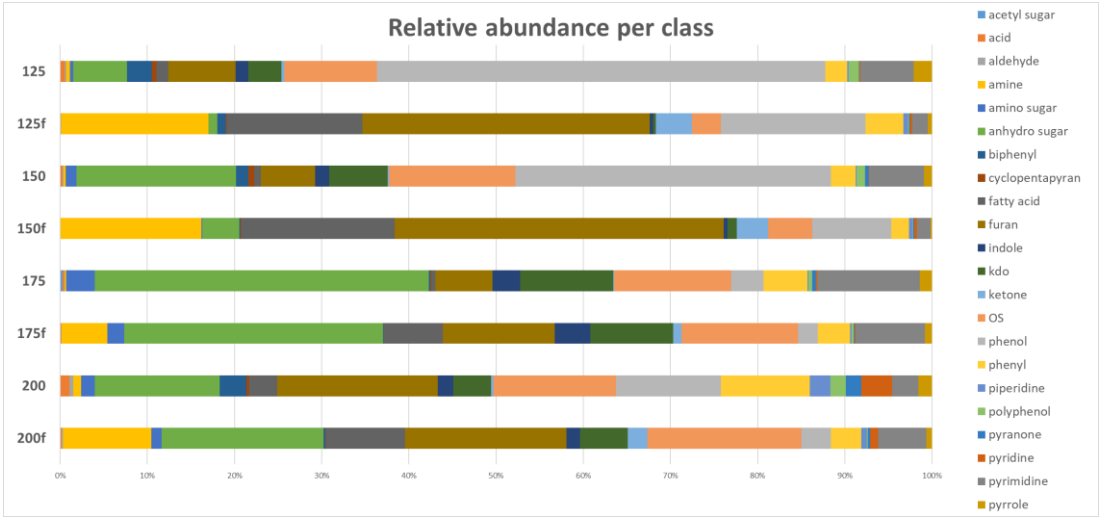

Figure 5.6: *Total ion abundance per chemical class compared to the total ion abundance for the whole liquor samples. The numbers indicate the temperature employed in a specific experiment, "f" indicates the fibres precipitate in the supernatants after ethanol addition.*

Figure 5.6 indeed shows a great variability in the abundance of compounds belonging to different chemical classes when hydrothermal treatment is carried out at different temperatures. Comparing supernatants ("125", "150", "175" and "200"), what catches the eye is phenols' behaviour: when extraction at 125 °C was employed, this class constituted in terms of abundance 51% of the total abundance, but then this value dropped to 36% at 150 °C and even to 4% at 175 °C, then going back up again to 11% when HS were treated at 200 °C. The relative abundance is a value that needs to be regarded overall, since the percentage drop in one class may be due to the actual drop of those compounds and/or to the increase of others. In this case, the reasons for the trend observed for phenols content can be multiple. First of all, it seems that the concentration in the reaction medium of phenols derived from lignin is not always directly correlated with increases in temperature, unlike sugars. In a recent study, indeed, it has been shown that lignin increased in the HT hydrolysate only until reaching a maximum value of severity factor, and then dropped. The reason likely needs to be found in the re-condensation of lignin, which leads to a lowering of its solubility, thus leading to precipitation as pellet after centrifugation [37]. According to our results, there is the possibility that the HT at 125°C led mainly to the extraction of "simple" phenols, namely not derived from lignin hydrolysis, since this temperature is not supposed to allow the degradation of lignin [13], and that this fraction resulted to be relatively high because of the lower formation of compounds belonging to other classes. In correspondence of the most pronounced decrease of phenols, namely at 175 °C, a great increase of anhydro sugars was also detected. Anhydro sugars have been reported to be formed from cellulose pyrolysis from 300 °C on [38], but their detection in our experiment carried out with longer reaction times might suggest their formation even with lower temperatures and through liquid hot water. At 200 °C, however, their relative abundance decreased again and this can be explained because of the simultaneous net increase in furans and phenyls, compounds that are widely accepted to be formed respectively from sugar and lignin degradation with high temperatures. In particular, furans are molecules commonly originated from sugars dehydration, both starting from hexoses to form 5-HMF as well as from pentoses to form furfural, then potentially further reacting to more complex structures [39]. Molecules containing phenyl group on the other hand, can come from lignin degradation, often in the form of complexes with carbohydrates [40]. Among the less abundant chemical classes, also some organic acids, aldehydes, ketones and heterocyclic compounds (such as pyranones, pyridines, pyrimidines, pyrroles, indoles) were present, most of them likely to be derived from sugars through different mechanisms [27]. Then amines, biphenyls, polyphenols, cyclopentapyranans, fatty acids, Kdos, amino sugars and indoles were also found in the reaction medium (Table S2), even if generally with very small abundances. Actually, although their abundances look very low if compared to other major classes, their presence should also be kept in mind together with the other more abundant compounds when such treatments are applied aiming to produce functional foods from lignocellulosic materials, in a risk assessment perspective.

When one looks into Figure 5.6 comparing "f" samples to the supernatants as such for every temperature, it comes out that some chemical classes tend to increase or to decrease their abundance depending on ethanol addition. For example, it is evident how amines always increase their relative abundance when fibres extracted from HS are induced to precipitate with alcohol, and the same behaviour clearly occurs for fatty acids, ketones and furans, even though for the latter this trend is not marked at 200 °C. For this reason, in a perspective of industrial scale-up, this purification step with alcohol could be considered as not very useful to remove these molecules, especially furans, that are one of the most undesired compounds when the production of functional ingredients is the main purpose of the hydrothermal treatment. On the other hand, anhydro sugars, phenols and pyrimidines were the compounds which relatively decreased the most in ethanol-purified fibres, suggesting their tendency to remain dissolved in the hydroalcoholic solution, thus being discarded and lost. Oligosaccharides, often the main target compounds for this kind of process, showed a variable behaviour, remaining quite constant at high temperatures, namely 175 °C and 200 °C, and relatively decreasing in the purified sample at 125 °C and 150 °C. In general, it is important to specify that this evaluation of the abundances gives an interesting indication on what happens but it is largely an approximate evaluation, being the relative ion intensities a semi-quantitative approach, and improvements in a more accurate quantification are necessary in the next future, especially in a risk assessment perspective.

4. Conclusions

Hydrothermal treatment (HT), or liquid hot water treatment, is increasingly being applied on lignocellulosic matrices with several purposes, including the extraction of hemicelluloses for the recovery of fibres and functional oligosaccharides. In this work, we tested hydrothermal treatments at different temperatures on hazelnut shells, an under-utilized valuable substrate for hemicellulose extraction, aiming to evaluate mainly how they impact on the pattern of degradation compounds, but also on the total sugars yield and on the chemical structure of fibres. Although generally HT is performed for a shorter time, in this work a longer operating time (i.e., 60 minutes) was chosen in order to better understand the effect of temperature on how hazelnut shells' components can be degraded.

Results globally highlight that it is possible to modulate the HT temperature to obtain hazelnut fibre extracts with very different composition and, as a consequence, different potential end uses. The highest yield of total fibres was obtained at 150 °C and the highest yield of xylan at 175 °C. A very interesting result indeed emerged from the monosaccharide composition of these fibres, showing that different polysaccharides were extracted in different proportions at different temperatures. In particular, pectin, reported in hazelnut for the first time, was present only when the experiment was performed at 125 °C and 150 °C, while xylans were predominant at higher temperatures. Molecular weight, a variable of outmost importance for the intended use of the extracted fibre, was also found to be highly variable. In this sense, the hydrothermal liquor at 125

°C almost exclusively resulted in the obtainment of high Mw pectin and those at 175 °C and 200 °C in a net prevalence of XOS; liquor obtained at 150 °C resulted to be the most heterogeneous, consisting in a mix of fractions with different molecular weights suitable for various purposes: XOS can be applied in new prebiotic-enriched feed and food, while pectin has potential to be applied to modify texturizing properties of food. As expected, the temperature of the process had an impact on the co-extraction or neo-formation of a huge number of compounds, depending on the heat treatment severity. A general high content of phenols and phenyl compounds derived from lignin was observed, together with oligosaccharides, anhydro-sugars and furans derived from sugars. However, the abundance of these compounds was variable as well, depending on the temperature and on purification steps eventually performed to further isolate polysaccharides.

As a whole, our results suggest the possibility to obtain from the same hazelnut shells biomass different types of fibres. The latter can be potentially extracted with a sequential fractionation approach, as a function of the severity of the extraction parameters, as also highlighted in chapter 3 and chapter 6 for other lignocellulosic matrices.

Fibres' composition should not be the only aspect to be taken into account when a specific extraction system is designed, because a huge number of secondary compounds are formed depending on the temperature, and most of them are unknown or poorly evaluated in terms of risk assessment for a safe introduction of the fibre extract in the food chain.

REFERENCES

1. Farias, D. de P.; de Araújo, F.F.; Neri-Numa, I.A.; Pastore, G.M. Prebiotics: Trends in food, health and technological applications. *Trends Food Sci. Technol.* **2019**, *93*, 23–35, doi:10.1016/j.tifs.2019.09.004.

2. Pop, C.; Suharoschi, R.; Pop, O.L. Dietary fiber and prebiotic compounds in fruits and vegetables food waste. *Sustain.* **2021**, *13*, 7219, doi:10.3390/su13137219.

3. Saini, J.K.; Saini, R.; Tewari, L. Lignocellulosic agriculture wastes as biomass feedstocks for second-generation bioethanol production: concepts and recent developments. *3 Biotech* **2015**, *5*, 337–353, doi:10.1007/s13205-014-0246-5.

4. Kumari, D.; Singh, R. Pretreatment of lignocellulosic wastes for biofuel production: A critical review. *Renew. Sustain. Energy Rev.* **2018**, *90*, 877–891, doi:10.1016/j.rser.2018.03.111.

5. Scapini, T.; dos Santos, M.S.N.; Bonatto, C.; Wancura, J.H.C.; Mulinari, J.; Camargo, A.F.; Klanovicz, N.; Zabot, G.L.; Tres, M. V.; Fongaro, G.; et al. Hydrothermal pretreatment of lignocellulosic biomass for hemicellulose recovery. *Bioresour. Technol.* **2021**, *342*, 126033, doi:10.1016/j.biortech.2021.126033.

6. Cocero, M.J.; Cabeza, Á.; Abad, N.; Adamovic, T.; Vaquerizo, L.; Martínez, C.M.; Pazo-Cepeda, M.V. Understanding biomass fractionation in subcritical & supercritical water. *J. Supercrit. Fluids* **2018**, *133*, 550–565, doi:10.1016/j.supflu.2017.08.012.

7. Ilanidis, D.; Wu, G.; Stagge, S.; Martín, C.; Jönsson, L.J. Effects of redox environment on hydrothermal pretreatment of lignocellulosic biomass under acidic conditions. *Bioresour. Technol.* **2021**, *319*, 124211, doi:10.1016/j.biortech.2020.124211.

8. Kim, J.Y.; Hwang, H.; Oh, S.; Kim, Y.S.; Kim, U.J.; Choi, J.W. Investigation of structural modification and thermal characteristics of lignin after heat treatment. *Int. J. Biol. Macromol.* **2014**, *66*, 57–65, doi:10.1016/j.ijbiomac.2014.02.013.

9. Batista, G.; Souza, R.B.A.; Pratto, B.; dos Santos-Rocha, M.S.R.; Cruz, A.J.G. Effect of severity factor on the hydrothermal pretreatment of sugarcane straw. *Bioresour. Technol.* **2019**, *275*, 321–327, doi:10.1016/j.biortech.2018.12.073.

10. Wells, J.M.; Drielak, E.; Surendra, K.C.; Kumar Khanal, S. Hot water pretreatment of lignocellulosic biomass: Modeling the effects of temperature, enzyme and biomass loadings on sugar yield. *Bioresour. Technol.* **2020**, *300*, 122593, doi:10.1016/j.biortech.2019.122593.

11. Fuso, A.; Rosso, F.; Rosso, G.; Risso, D.; Manera, I.; Caligiani, A. Production of xylo-oligosaccharides (XOS) of tailored degree of polymerization from acetylated xylans through modelling of enzymatic hydrolysis. *Food Res. Int.* **2022**, *162*, 112019.

12. de Freitas, C.; Carmona, E.; Brienzo, M. Xylooligosaccharides production process from lignocellulosic biomass and bioactive effects. *Bioact. Carbohydrates Diet. Fibre* **2019**, *18*, 100184, doi:10.1016/j.bcdf.2019.100184.

13. Fuso, A.; Risso, D.; Rosso, G.; Rosso, F.; Manini, F.; Manera, I.; Caligiani, A. Potential valorization of hazelnut shells through extraction, purification and structural characterization of prebiotic compounds: A critical review. *Foods* **2021**, *10*, 1197, doi:10.3390/foods10061197.

14. Demirbas, A. Furfural production from fruit shells by acid-catalyzed hydrolysis. *Energy Sources, Part A Recover. Util. Environ. Eff.* **2006**, *28*, 157–165, doi:10.1080/009083190889816.

15. Demirbaş, A. Estimating of structural composition of wood and non-wood biomass samples. *Energy Sources* **2005**, *27*, 761–767, doi:10.1080/00908310490450971.

16. Surek, E.; Buyukkileci, A.O. Production of xylooligosaccharides by autohydrolysis of hazelnut (Corylus avellana L.) shell. *Carbohydr. Polym.* **2017**, *174*, 565–571, doi:10.1016/j.carbpol.2017.06.109.

17. Rivas, S.; Moure, A.; Parajó, J.C. Pretreatment of hazelnut shells as a key strategy for the solubilization and valorization of hemicelluloses into bioactive compounds. *Agronomy* **2020**, *10*, 760, doi:10.3390/agronomy10060760.

18. Hoşgün, E.Z.; Bozan, B. Effect of Different Types of Thermochemical Pretreatment on the Enzymatic Hydrolysis and the Composition of Hazelnut Shells. *Waste and Biomass Valorization* **2019**, *11*, 3739–3748, doi:10.1007/s12649-019-00711-z.

19. Pérez-Armada, L.; Rivas, S.; González, B.; Moure, A. Extraction of phenolic compounds from hazelnut shells by green processes. *J. Food Eng.* **2019**, *255*, 1–8, doi:10.1016/j.jfoodeng.2019.03.008.

20. AOAC Official Method of Analysis. 16th Edition. Association of official analytical, Washington DC. **2002**.

21. AOAC AOAC Official Method 991.43 Total, Soluble, and Insoluble Dietary Fibre in Foods. *J. AOAC Int.* **2012**, doi:10.5740/jaoacint.CS2011_25.

22. Caligiani, A.; Acquotti, D.; Palla, G.; Bocchi, V. Identification and quantification of the main organic components of vinegars by high resolution 1H NMR spectroscopy. *Anal. Chim. Acta* **2007**, *585*, 110–119, doi:10.1016/j.aca.2006.12.016.

23. Usuki, C.; Kimura, Y.; Adachi, S. Degradation of pentoses and hexouronic acids in subcritical water. *Chem. Eng. Technol.* **2008**, *31*, 133–137, doi:10.1002/ceat.200700391.

24. Parajó, J.C.; Garrote, G.; Cruz, J.M.; Dominguez, H. Production of xylooligosaccharides by autohydrolysis of lignocellulosic materials. *Trends Food Sci. Technol.* **2004**, *15*, 115–120, doi:10.1016/j.tifs.2003.09.009.

25. Ramachandran, V.; Ismail, F.S.; Noor, M.J.M.M.; Akhir, F.N.M.D.; Othman, N.; Zakaria, Z.; Hara, H. Extraction and intensive conversion of lignocellulose from oil palm solid waste into lignin monomer by the combination of hydrothermal pretreatment and biological treatment. *Bioresour. Technol. Reports* **2020**, *11*, 100456, doi:10.1016/j.biteb.2020.100456.

26. Pyo, S.H.; Glaser, S.J.; Rehnberg, N.; Hatti-Kaul, R. Clean Production of Levulinic Acid from Fructose and Glucose in Salt Water by Heterogeneous Catalytic Dehydration. *ACS Omega* **2020**, *5*, 14275–14282, doi:10.1021/acsomega.9b04406.

27. Rasmussen, H.; Sørensen, H.R.; Meyer, A.S. Formation of degradation compounds from lignocellulosic biomass in the biorefinery: Sugar reaction mechanisms. *Carbohydr. Res.* **2014**, *385*, 45–57, doi:10.1016/j.carres.2013.08.029.

28. Nasrollahzadeh, M.; Sajjadi, M.; Sajadi, S.M.; Issaabadi, Z. Chapter 5 - Green Nanotechnology. *Interface Sci. Technol.* **2019**, *28*, 145–198, doi:10.1016/B978-0-12-813586-0.00005-5.

29. Evtuguin, D. V; Neto, C.P. Recent Advances in Eucalyptus Wood Chemistry: Structural Features Through the Prism of Technological Response. *Proc. 3rd Int. Colloq. Eucalyptus pulp* **2007**.

30. Sharma, K.; Khaire, K.C.; Thakur, A.; Moholkar, V.S.; Goyal, A.; Goyal, A. Acacia Xylan as a Substitute for Commercially Available Xylan and Its Application in the Production of Xylooligosaccharides. *ACS Omega* **2020**, *5*, 13729–13738, doi:10.1021/acsomega.0c00896.

31. Ho, A.L.; Kosik, O.; Lovegrove, A.; Charalampopoulos, D.; Rastall, R.A. In vitro fermentability of xylo-oligosaccharide and xylo-polysaccharide fractions with different molecular weights by human faecal bacteria. *Carbohydr. Polym.* **2018**, *179*, 50–58, doi:10.1016/j.carbpol.2017.08.077.

32. Poletto, P.; Pereira, G.N.; Monteiro, C.R.M.; Pereira, M.A.F.; Bordignon, S.E.; de Oliveira, D. Xylooligosaccharides: Transforming the lignocellulosic biomasses into valuable 5-carbon sugar prebiotics. *Process Biochem.* **2020**, *91*, doi:10.1016/j.procbio.2020.01.005.

33. Schweizer, T.F.; Würsch, P. Analysis of dietary fibre. *J. Sci. Food Agric.* **1979**, *30*, 613–619, doi:10.1002/jsfa.2740300610.

34. Yu, Q.; Zhuang, X.; Wang, Q.; Qi, W.; Tan, X.; Yuan, Z. Hydrolysis of sweet sorghum bagasse and eucalyptus wood chips with liquid hot water. *Bioresour. Technol.* **2012**, *116*, 220–225, doi:10.1016/j.biortech.2012.04.031.

35. Stévigny, C.; Rolle, L.; Valentini, N.; Zeppa, G. Optimization of extraction of phenolic content from hazelnut shell using response surface methodology. *J. Sci. Food Agric.* **2007**, *87*, 2817–2822, doi:10.1002/jsfa.2994.

36. Kang, S.; Li, X.; Fan, J.; Chang, J. Hydrothermal conversion of lignin: A review. *Renew. Sustain. Energy Rev.* **2013**, *27*, 546–558, doi:10.1016/j.rser.2013.07.013.

37. Serna-Loaiza, S.; Dias, M.; Daza-Serna, L.; de Carvalho, C.C.C.R.; Friedl, A. Integral analysis of liquid-hot-water pretreatment of wheat straw: Evaluation of the production of sugars, degradation products, and lignin. *Sustain.* **2022**, *14*, 362, doi:10.3390/su14010362.

38. Leng, E.; Costa, M.; Peng, Y.; Zhang, Y.; Gong, X.; Zheng, A.; Huang, Y.; Xu, M. Role of different chain end types in pyrolysis of glucose-based anhydro-sugars and oligosaccharides. *Fuel* **2018**, *234*, 738–745, doi:10.1016/j.fuel.2018.07.075.

39. Gandini, A.; M. Lacerda, T. Furan Polymers: State of the Art and Perspectives. *Macromol. Mater. Eng.* **2022**, *307*, 2100902, doi:10.1002/mame.202100902.

40. Jeong, S.Y.; Lee, E.J.; Ban, S.E.; Lee, J.W. Structural characterization of the lignin-carbohydrate complex in biomass pretreated with Fenton oxidation and hydrothermal treatment and consequences on enzymatic hydrolysis efficiency. Carbohydr. Polym. 2021, 270, 118375, doi:10.1016/j.carbpol.2021.118375.

CHAPTER 6

Production of xylo-oligosaccharides (XOS) of tailored degree of polymerization from acetylated xylans through modelling of enzymatic hydrolysis

The content of this chapter has also been published as:

Andrea Fuso, Franco Rosso, Ginevra Rosso, Davide Risso, Ileana Manera, Augusta Caligiani (**2022**). Production of xylo-oligosaccharides (XOS) of tailored degree of polymerization from acetylated xylans through modelling of enzymatic hydrolysis. *Food Research International*, 162(A), 112019.

ABSTRACT

Xylo-oligosaccharides (XOS) are emerging prebiotics that have recently been gained a great interest in the market of functional foods. Since their beneficial activity strictly depends on their chemical structure and on their degree of polymerization (DP), in this work an enzymatic method was developed to produce XOS with variable and modellable DPs, involving a combination of a commercial endo-β-1,4-xylanase M3 from *Trichoderma longibrachiatum* and a deacetylase, using a commercial acetylated standard xylan as substrate. A Design of Experiment (DoE) was developed and through the variation of some hydrolysis conditions, some experiments allowed to obtain significant amounts of XOS with DP 7-10, up to 11%, despite XOS with DP 2-4 were always the most abundant (60-96% of total XOS). The most impacting parameter on the XOS distribution was the order of addition of the xylanase and deacetylating enzyme, while pH showed to have a great influence on the total yield. The method was also tested on an acetylated xylan extracted from grape stalks, structurally similar to the commercial standard xylan. The model was found to work in a very similar way also on the non-purified xylan sample, allowing the manipulation of enzymatic hydrolysis on a low-cost by-product, with the potential to obtain on a large scale XOS with high added value and with a specific DP, depending on the final application.

1. Introduction

Nowadays, the global interest in healthy foods is continuously increasing and in this sense consumers' choices are changing [1]. This growing and marked interest is aimed at all functional foods and in particular at those containing probiotics and prebiotics, with the market for the latter that is growing rapidly [2]. Although the prebiotic efficacy of several molecules has been demonstrated, recently the researchers are strongly focusing on xylo-oligosaccharides (XOS), emerging prebiotics with an enormous potential [3,4]. XOS can be obtained by chemical, physical or enzymatic degradation of xylan, which is the most abundant plant polysaccharide after cellulose [5]. Xylans are present in many different sources, such bamboo shoots, fruits, vegetables, wheat bran and straw, sugarcane residues, corn cobs, rice straw, etc. [6,7] and for this reason the XOS production from agroforestry by-products should be strongly encouraged. However, achieving the specific desired prebiotic effect is not simple. In fact, it is widely recognized by the scientific literature that the health effects of prebiotic compounds are strictly related to their chemical structure [8] and in this sense the degree of polymerization (DP) is considered one of the most impacting parameters on the functional properties of the molecule [9]. XOS' degrees of polymerization are usually 2–7 but a lot of research has pointed out that a low DP (2-5 xylose units) favours a high growth of *Bifidobacterium* and lactic bacteria [10,11]. At the same time, very little is known about the properties of XOS having a DP comprised between 7 and 10: in fact, if on the one hand the availability of analytical XOS standards in the market is limited to DP 2-6, on the other hand it is quite complex to hydrolyse the xylan polymer obtaining oligosaccharides with specific and precise DPs to be able to study their properties. Furthermore, data related to XOS' mechanism of action and fermentation products are very limited [9]. In addition to this, it is necessary to consider that different microorganisms may have different preferences to oligosaccharides [12,13]. In a 2010 study, Mäkeläinen and colleagues tested four different XOS mixtures having different DPs, showing how every mixture favoured in a different way the growth of different *Bifidobacterium* and *Lactobacillus* strains and hence demonstrating their variable prebiotic effectiveness [14]. Numerous authors have obtained medium-DP XOS from a multitude of agricultural by-products, but mostly through the use of chemical or autohydrolysis methods, [15–17]. However, when such treatments are applied, it is highly likely that several other undesirable compounds will appear in the reaction medium, such as monosaccharides, sugar dehydration products or acid-soluble fractions of lignin [12]. For this reason, the production of XOS by enzymatic hydrolysis has been gaining interest over the time and it is also considered more environmentally friendly due to the lower amount of waste generated [18]. The downside is mainly related to the high costs, even if some techniques, like the immobilization of enzymes or in-situ production by fermentation, are emerging tools to stem this problem. When enzymatic hydrolyses were applied, however, they often resulted in the formation of XOS with a low DP, generally less than 6 [19–22]. Enzymes responsible for the hydrolysis of xylans are xylanases, that are ubiquitous in nature and present above all in bacteria and fungi [23]. Xylanases can have different amino acid

sequences and structures, and consequently variable biochemical properties, and for this reason they have been grouped into different families of glycosyl hydrolases (GH). Among all of them, according to the CAZy (Carbohydrate Active Enzymes) database, most endo-1,4-β-xylanases belong to the GH10 and GH11 family. The difference lies in their physicochemical properties, such isoelectric point, molecular weight, three-dimensional structures, and catalytic mechanisms. Xylanases from GH11 family have a lower molecular weight than members of GH10, and a β-jelly-roll catalytic domain that makes them more susceptible to influence by side chains, and for this reason they are recommended for the production of XOS, since they do not produce xylose [24,25]. Therefore, all the products originated by a xylanase from a given substrate depend on the substrate specificity, which in turn depends on the structure of the xylanase [4]. In addition to this, other factors may affect the yield and the structure of the hydrolysis products, such as temperature, pH, reaction time and synergy between xylanase and other enzymes able to hydrolyse the substituent groups present in the polymer chain (including, in particular, acetylxylan esterase, glucuronidase or arabinofuranosidase). As a consequence, the production of XOS with a well-defined DP is not a foregone conclusion.

In this work we focused on xylans substituted with acetyl groups, since they are present in many agri-food by-products, like hazelnut shells [26], apricot pit shells [27], mango seed shells [28], Hawthorn kernels [29] or grape stalks [30]. Firstly, we monitored the DP of XOS that were originated from the hydrolysis of a commercial acetylated xylan through the employment of a GH11 family endo-β-1,4 xylanase from *T. longibrachiatum* (EC number 3.2.1.8). This xylanase is a commercially available 20 KDa molecular weight enzyme, responsible for endo-hydrolysis of (1,4)-β-D-xylosidic linkages in xylans. We tried to understand how to maximize different DPs in the range DP 2-10 by varying some hydrolysis conditions through an experimental design approach: in particular, XOS with DP 7-10 were the main target, because they are more difficult to be obtained, being the DP 2-6 the preferred outcome of the xylanase activity. Then, we also tested the feasibility to apply these different hydrolysis conditions on an acetylated xylan previously extracted from grape stalks. These latter are potentially one of the most abundant natural sources of acetylated xylans, constituting up to 5-7% of the total grapes' crop, which amounts to about 77.8 million tons/year [31].

2. Materials and methods

2.1. Materials

D-xylose was purchased from Fluka Chemicals (Buchs, Switzerland); 1,4-β-D-xylobiose, 1,4-β-D-xylotriose, 1,4-β-D-xylotetraose, 1,4-β-D-xylopentaose, 1,4-β-D-xylohexaose, xylan (from birchwood, partially acetylated), acetylxylan esterase from *Orpinomyces sp.*, endo-1,4-β-Xylanase M3 from *T. longibrachiatum*,

endo-1,4-β-Xylanase M6 from rumen microorganism were purchased from Megazyme (Bray, County Wicklow, Ireland). D-glucose, D-fructose, D-Arabinose, D-galactose, D-mannose, D-rhamnose, D-ribose, D-xylose, D-fucose, D-galacturonic acid, D-glucuronic acid, phenyl β-D-glucopyranoside, Amberlite® 200 Na+ form and Amberlite® IRA-96 free base were purchased from Sigma-Aldrich (St. Louis, MO, USA).

2.2. Enzymatic hydrolysis of commercial xylan through Design of Experiments (DoE)

2.2.1. Set up of the DoE experiment

The activity of a commercially available endo-1,4-β-xylanase (M3, from *T. longibrachiatum*) was investigated on standard, partially acetylated xylan from birchwood (24% acetyl groups). In addition to the xylanase, acetylxylan esterase was always added to fully hydrolyse the acetyl groups and obtain unsubstituted XOS. In particular, 2 acetylxylan esterase Units/10 mg of xylan was added in each experiment at constant conditions of optimal pH 7 and 40 °C temperature, followed by 16 minutes of incubation.

With regard to endo-β-1,4-xylanase, different hydrolysis parameters were selected as potentially influential on the products outcome: pH, temperature, enzyme/substrate ratio and order of addition (i.e. before or after the acetylxylan esterase employment). Aiming to reduce the number of experiments and to obtain models able to predict correlations and interactions among the selected parameters, a Design of Experiments (DoE) was employed (Table 6.1) using the software MODDE® Pro 13 (Sartorius). Being the optimal temperature for xylanase equal to 50 °C, the selected temperatures for the experiments were 35, 42.5 and 50 °C. Being the optimal pH equal to 6, the selected pHs were 4.5, 6 and 7.5. The xylan/buffer ratio was constant and equal to 10 mg/mL, as reported in Megazyme specifications. Initially, the reaction time had been arbitrarily set at 20 minutes: to completely hydrolyse 10 mg xylan in 20 minutes, according to Megazyme specifications, 3.3 enzyme units would have been necessary. Because of this, the selected enzyme/substrate ratios were 1, 3 and 5 enzyme Units/10 mg of substrate (low, medium, and high, respectively, Table 6.1). Each hydrolysis step, both with xylanase and acetylxylan esterase, was always followed by enzyme inactivation, by maintaining the solution at 90 °C for 10 minutes.

***Table 6.1**: Experimental plan generated for the hydrolysis of a commercial acetylated xylan.*

Exp Name	Run Order	pH xylanase	Temperature xylanase	xylanase/substrate ratio	Order of enzymes
N1	8	4.5	35	low	First acetylase, then xylanase
N2	10	7.5	35	low	First acetylase, then xylanase
N3	11	4.5	50	low	First acetylase, then xylanase
N4	7	7.5	50	low	First acetylase, then xylanase
N5	3	4.5	35	high	First acetylase, then xylanase

N6	17	7.5	35	high	First acetylase, then xylanase
N7	18	4.5	50	high	First acetylase, then xylanase
N8	2	7.5	50	high	First acetylase, then xylanase
N9	13	4.5	35	low	First xylanase, then acetylase
N10	6	7.5	35	low	First xylanase, then acetylase
N11	16	4.5	50	low	First xylanase, then acetylase
N12	9	7.5	50	low	First xylanase, then acetylase
N13	19	4.5	35	high	First xylanase, then acetylase
N14	4	7.5	35	high	First xylanase, then acetylase
N15	12	4.5	50	high	First xylanase, then acetylase
N16	15	7.5	50	high	First xylanase, then acetylase
N17	1	6	42.5	medium	First acetylase, then xylanase
N18	5	6	42.5	medium	First acetylase, then xylanase
N19	14	6	42.5	medium	First acetylase, then xylanase

2.2.2. Determination of the reaction time

In order to understand which reaction time was adequate to produce detectable amounts of XOS with DP 7-10, a preliminary test was conducted in conditions that were far from the optimal ones for xylanase activity. These conditions were low enzyme/substrate ratio, pH 4.5, low temperature (35°C), and this corresponded to N1 or N9 experiments (Table 6.1). In particular, N1 experiment was chosen for practical reasons, considering the more convenient order of addition of enzymes (first deacetylase, then xylanase). Indeed, here, an aliquot of the already deacetylated and partially hydrolysed xylan was withdrawn at different reaction times and the enzyme was immediately inactivated. The selected times were 2, 5, 8, 11 and 15 minutes. After this experiment, a new pre-test with another xylanase, namely endo-1,4-β-Xylanase M6 from rumen microorganism, was also performed in order to assess the repeatability of the experiment with a similar but different enzyme. The same conditions as for xylanase M3 were employed here, with a reaction time of 5 minutes.

2.2.3. Removal of buffer salts by ion-exchange resins

Since in the various experiments the enzymatic hydrolyses were carried out in different buffer solutions, containing 0.1 M sodium acetate and 0.1 M sodium phosphate in variable quantities depending on the desired pH, the hydrolysates underwent a sequential double passage through cationic and anionic resins. At first, 1 mL of Amberlite® 200 Na+ form (cationic resin) was regenerated with 1.5 mL of 2N HCl and subsequently washed with water until reaching a pH value of the eluate equal to 4. In parallel, 1 mL of Amberlite® IRA-96 free base (anionic resin) was regenerated with 2 mL of 4N NaOH and then washed with

water until pH of the eluate equal to 10. Later, 3 mL of hydrolysate were passed through 0.4 mL of cationic resin and the collected eluate was subsequently passed through 0.6 mL of anionic resin.

2.3. HILIC analysis of xylo-oligosaccharides

The separation of XOS mixtures was performed following a protocol proposed by Waters Corporation (Milford, MA, USA) to which minor modifications were applied (Waters Application note). An example of chromatogram is reported in Figure 6.1. The enzymatic reaction products were dried under nitrogen flow and then dissolved in 50/50 acetonitrile/water, together with phenyl β-D-glucopyranoside used as internal standard. Then, the sample was analysed by ultra-performance liquid chromatography with electrospray ionization in negative mode and single-quadrupole mass spectrometer detector (UPLC/ESI-MS, WATERS ACQUITY). UPLC/ESI-MS analysis was performed by using an ACQUITY UPLC® BEH Amide column (2.1 x 100 mm, 1.7 µm). The mobile phase was composed by 80 % CH_3CN + 20 % H_2O + 0.1 % NH_4OH (eluent A) and 30 % CH_3CN + 70 % H_2O + 0.1 % NH_4OH (eluent B). Gradient elution was performed: from 100 % A to 40 % A and 60 % B by linear gradient in the first 10 minutes, from 40 % to 100 % A in 0.02 minutes, isocratic 100 % A from 10.02 to 30 minutes. Flow rate was set at 0.17 mL/min, injection volume 2 µL, strong needle wash 20 % CH_3CN, weak needle wash 75 % CH_3CN, seal wash 50 % CH_3CN, column temperature 35 °C and sampler temperature 18 °C. Detection was performed by using Waters SQ mass spectrometer: ESI source in negative ionization mode, capillary voltage 2.8 kV, cone voltage 25 V, source temperature 120 °C, desolvation temperature 350 °C, cone gas flow (N_2) 50 L/hr, desolvation gas flow (N_2) 500 L/hr, full scan acquisition (100-2000 m/z). Integration was performed by extracting the following mass ions (m/z): 149 for xylose, 379 for DP2 (an adduct with phosphate was formed), 413 for DP3, 545 for DP4, 677 for DP5, 809 for DP6, 941 for DP7, 1073 for DP8, 1205 for DP9, 1337 for DP10. In Figure 6.1, mass spectra of DP 7-10 XOS are reported.

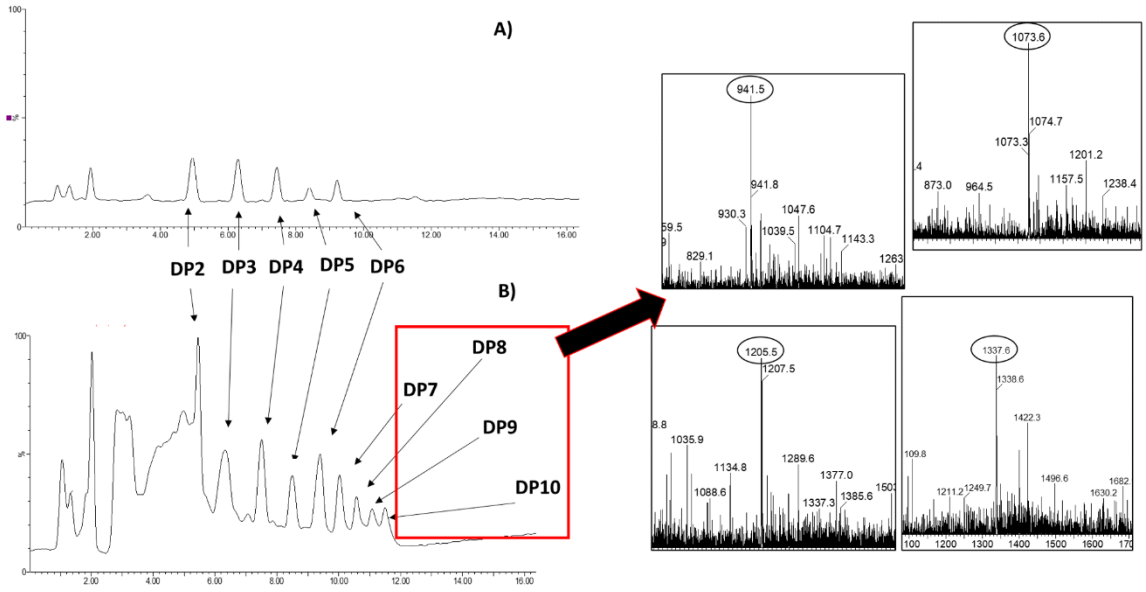

***Figure 6.1**: Example of chromatograms obtained by UPLC/ESI-MS, relative to A) standard XOS (DP 2-6), and B) XOS mixture originated from enzymatic hydrolysis of commercial, acetylated xylan. In the boxes the mass fragments found for DP 7-10 are reported.*

A six-point calibration curve was determined for D-xylose and for XOS having a DP between 2 and 6, because they are the only analytical standards available in the market. For this reason, the calculation of the concentrations of XOS having a DP higher than 6 was performed with DP6's calibration curve, providing a semi-quantification. Method of standard additions was employed: concentrations of standard xylose and XOS, added together with the samples, were 0, 10, 25, 50, 100 and 250 ppm. Sample was present in a concentration, relative to the initial xylan, varying from 950 to 1300 ppm. Phenyl β-D-glucopyranoside was selected as internal standard and added to both calibration curve and samples at a constant concentration, equal to 155 ppm.

2.4. Valorisation of grape stalks' fibres through enzymatic XOS production

2.4.1. Extraction of acetylated xylan from grape stalks

Grape stalks were collected in September 2021 in the province of Parma, Emilia-Romagna, Italy, and the hemicellulose fraction containing the xylan polymers was extracted (Figure 6.2) through a double-step hydrothermal treatment. The grape stalks were initially washed, dried and ground. Then, a first mild hydrothermal pretreatment was carried out using a pressure cooker, at a temperature of 120 °C for 1 h under stirring, aiming to extract the most soluble fibre fraction. The liquor obtained was then centrifuged at 3900 rpm, at 4 °C for 40 minutes. After that, the solid residue was kept aside, while an aliquot of 500 mL of the

supernatant was transferred to a flask, in which 2 L of ethanol were added. This solution was centrifuged again under the same aforementioned conditions, and the solid residue was collected and washed twice with ethanol in order to eliminate some eventually present contaminants, such proteins or tannins. The insoluble residue (extracted fibre 1, "EF1", Figure 6.2) was dried in an oven for 24 h at 40 °C and stored for the proximate composition analyses. The lignohemicellulosic solid residue obtained after the first hydrothermal treatment was then subjected to a second one, with an increased severity, in order to break down the lignin component and allow the total hemicellulose extraction. Therefore, this pellet was added to distilled water in a 1:25 ratio inside a stainless-steel model 4566 Parr reactor (Parr Instrument Company, Moline, Il, USA) and allowed to react for 45 minutes at 170 °C. Once it cooled, the liquor was centrifuged at 3900 rpm, at 4 °C for 40 minutes and the supernatant was collected. Ethanol was added in a 1:4 ratio and this new solution was centrifuged again. The precipitated pellet, containing the extracted fibre, was collected, washed again with ethanol, and dried in oven for 24 h at 40 °C (extracted fibre 2, "EF2", Figure 6.2).

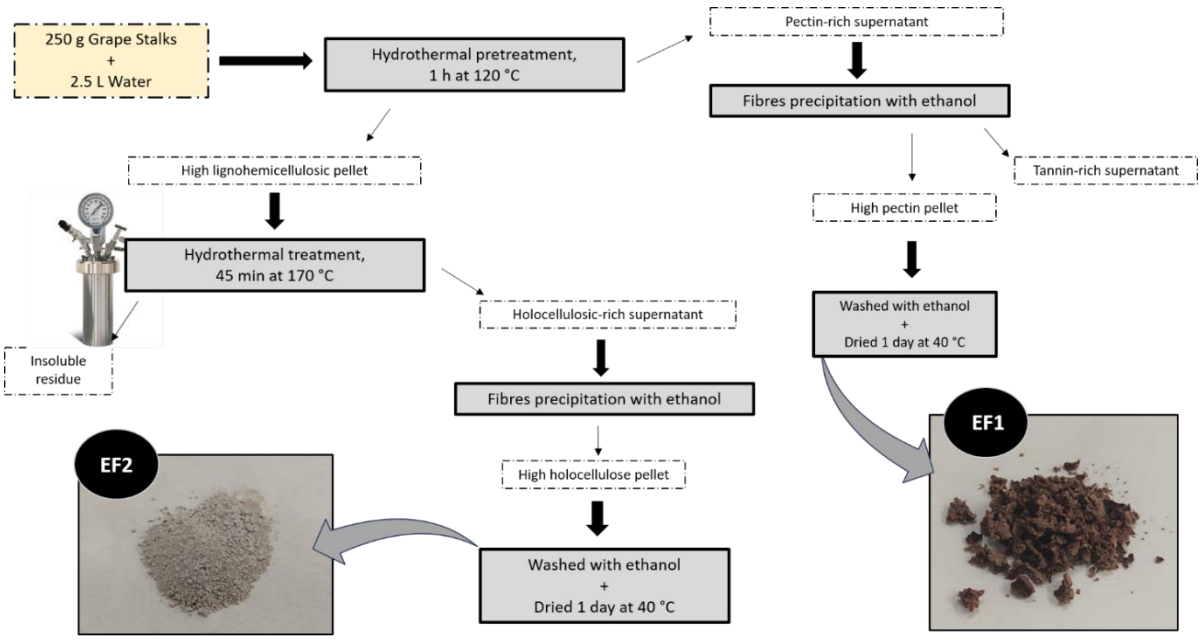

***Figure 6.2**: Schematic representation of the extraction process of grape stalks' fibres. EF: extracted fibre.*

2.4.2. Characterization of the hemicellulose extracted

2.4.2.1. Proximate composition

The proximate composition of the obtained hemicellulose was first investigated, in order to understand the degree of purity and the eventually present residues. These analyses were performed using standard procedures [32]. Moisture was determined in an oven at 105 °C for 24 h. Total ash was determined through mineralization at 550 °C for 5 h. Proteins were determined with a Kjeldahl system (DKL heating digestor and

UDK 139 semiautomatic distillation unit, VELP SCIENTIFICA) by using 6.25 as nitrogen-to-protein conversion factor.

2.4.2.2. Monosaccharide analysis through Gas chromatography–mass spectrometry (GC-MS)

The monosaccharide composition was investigated on both EF1 and EF2 samples following the method proposed by Xia et al. with some modifications [33]. 10 mg of sample were dissolved in 3 mL of 2N trifluoroacetic acid (TFA) and hydrolysed at 110 °C for 2 hours. Then, 850 µL of the solution was withdrawn and added together with 150 µL of 1000 ppm phenyl β-D-glucopyranoside, used as internal standard, then evaporated by rotavapor, and the obtained dried hydrolysate was washed with 1 mL of methanol to remove the residue of TFA and evaporated again. 1 mL of 0.5 M NH_4OH was subsequently added to delactonize the eventually present sugar acid lactones in the solution, and again evaporated by rotavapor. Finally, the dried hydrolysate was dissolved in 800 µL of dimethylformamide (DMF) and 200 µL of N,O-Bis(trimethylsilyl)trifluoroacetamide (BSTFA), used as derivatizing agent. The reaction was held for 1 hour at 60 °C and then the derivatized sample was injected in gas chromatography.

GC-MS analysis of monosaccharides was performed with a 6890 N gas chromatograph coupled to a 5973 N mass selective detector (Agilent technologies, Santa Clara, CA). A SLB-5ms, 30 m × 0.25 mm, 0.25 µm of thickness column (Supelco, Bellafonte, PA, USA) was used. The chromatogram was recorded in the scan mode (40–500 m/z) with a programmed temperature from 60 °C to 270 °C. The initial temperature was 60 °C, held for 2 minutes, then increased to 160 °C at a rate of 10 °C/min, held isothermal for 5 minutes, increased to 220 °C at a rate of 10 °C/min, kept for 5 minutes, increased to 270 °C at a rate of 20 °C/min and maintained for 5 minutes. Quantification was performed with response factors, considering the area and concentration ratios between the internal standard, phenyl β-D-glucopyranoside, and each monosaccharide present in the standard solutions (D-glucose, D-fructose, D-Arabinose, D-galactose, D-mannose, D-rhamnose, D-ribose, D-xylose, D-fucose, D-galacturonic acid, D-glucuronic acid).

2.4.2.3. Evaluation of the degree of acetylation through ^{1}H NMR

^{1}H NMR analysis was performed on the EF2 sample to investigate the degree of esterification, and in particular of acetylation, of the xylans extracted from grape stalks (paragraph 2.4.1). 20 mg of dried EF2 were dissolved in 800 µL of 0.4 N NaOH in deuterium oxide (D_2O) and 100 µL of 2000 ppm 3-(trimethylsilyl)propionate-*d4* (TSP) were added as internal standard. The reaction was held at room temperature for 2 h and then the sample was centrifuged at 1000 rpm for 10 minutes. The obtained supernatant was finally filtered through a 0.45 µm membrane into the NMR tube. ^{1}H NMR spectra spectra were registered on a Bruker Avance III 400 MHz NMR Spectrometer (Bruker BioSpin, Rheinstetten, Karlsruhe, Germany) operating at a magnetic field-strength of 9.4 T. Spectra were acquired at 298 K, with 32 K complex

points, using a 90° pulse length and 5 s of relaxation delay (d1). 128 scans were acquired with a spectral width of 9595.8 Hz and an acquisition time of 1.707 s. The relaxation delay and acquisition time ensure the complete relaxation of the protons, allowing their integrals for quantitative purposes. The experiments were carried out with water suppression by low power selective water signal presaturation during 5 s of the relaxation delay. The NMR spectra were processed by MestreC software. The spectra were Fourier transformed with FT size of 64 K and 0.2 Hz line-broadening factor, phased and baseline corrected, and referenced to 3-(trimethylsilyl)-propionate-d4 (TSP) peak (0 ppm). The quantitative determination of acetate was obtained by manual integration of the corresponding signals (1.92 ppm) and the comparison with TSP area. The values obtained by the integration were converted in mass value (mg) according to the formula reported in Müller-Maatsch et al. [34].

2.4.2.4. Determination of the molecular weight through Size-exclusion Chromatography (HPSEC)

The molecular weight (Mw) of the fibre obtained from grape stalks was investigated through high-performance size-exclusion chromatography (HPSEC), with an Agilent 1260 Infinity II LC system equipped with a refractive index detector (RID) (Agilent, Santa Clara, CA, USA). The extracted powder was dissolved in ultrapure water at a concentration of 2 mg/mL and subsequently filtered through a 0.45 µm membrane. Ultrapure water was used as mobile phase at a flow rate of 0.7 mL/min and a PL aquagel-OH MIXED-M column, 7.5 x 300 mm, 8 µm (Agilent, Santa Clara, CA, USA) was employed to separate the different molecular weight fractions. The injection sample volume was set at 5 µL, the column temperature at 50 °C and RID temperature at 55 °C. Standard pullulans having known molecular weight were injected in the same conditions and used for the calibration curve.

2.5. Statistical analysis

The relative distribution of XOS with different DPs produced from grape stalks' hydrolysis was subjected to one-way analysis of variance (ANOVA) followed by a Tukey post hoc test, by employing IBM SPSS software version 21.0 (SPSS Inc., Chicago, IL, USA). Moreover, the quantities of specific XOS originated from the hydrolysis of grape stalks' xylan were compared to the ones obtained from commercial xylan, using t-test. In both cases, significant differences were compared at a level of $p < 0.05$.

The DoE and data analysis were performed using the MODDE 13 software. 19 runs were generated of which three of these were replicated to estimate the pure error for the study. The randomization of the order of the experiments was carried out. Relationships between factors and responses were analysed by fitting them in multiple linear regression (MLR) and partial least squares (PLS) regression models. The statistical parameters used to evaluate the quality of the model (R2, Q2, Model validity and

reproducibility) were calculated. Parameter R2 was considered significant when higher than 0.5; Q2 > 0.1 and > 0.5 indicated respectively a significant and a good model. Model validity should be higher than 0.25 and reproducibility should be above 0.5. Main effects and interactions were evaluated for each response and contour plots were created.

3. Results and discussion

3.1. Enzymatic hydrolysis of commercial xylan through Design of Experiments (DoE)

3.1.1. Preliminary trials for hydrolysis time set up

In order to have a preliminary idea about the kinetic of formation of the different DPs and establish the reaction time to employ in all the experiments, a preliminary enzymatic hydrolysis was conducted under the conditions reported in "N1" experiment (Table 6.1), and aliquots were withdrawn at different hydrolysis times, as described in paragraph 2.2. This trial was necessary because time was not considered among the parameters to be optimized by Design of experiment approach for two different reasons. From one side, one of the main targets of this work was to find the best conditions for production of XOS with DP 7-10, however, being the DP 2-6 the preferred outcome of the xylanase activity, they are more difficult to be obtained, because they are further hydrolysed by xylanase in short time. Therefore, it was necessary to determinate the time threshold allowing to produce DP 7-10. On the other hand, in a perspective of future scale-up of the enzymatic hydrolysis, the possibility of using continuous systems with molecular weight cut-off makes the optimization of time less important respect to the other variables. In this optic, the time of hydrolysis was kept dissociated from the DoE. Results of the preliminary trial are reported in Table 6.2 of the supplementary material. The sum of the different XOS detected constituted a percentage ranging from 37 to 43% (yield%) respect to the starting amount of polysaccharide, indicating that other high molecular weight fractions can still be present in the hydrolysate. Moreover, the amount of acetic acid removed by acetylxylan esterase (representing 24% of the initial xylan) was not taken into account. As expected, differences emerged in terms of oligosaccharides detected. After 11 minutes of hydrolysis, only XOS with DP ranging from 2 to 6 were detected, whilst after 8 minutes also DP7 and 8 were found, and after 2 and 5 minutes also DP9 was present. The relative distribution of the oligosaccharides varied too, although XOS having DP3 and DP4 were almost always the most abundant. In particular, in Table 6.2 it can be observed how DP2 suddenly increased its relative percentage after 11 minutes, going from 18% to 32% in a short time. Anyway, the amount of DP7-10 XOS remained quite low in every trial, but one of the higher was found after a hydrolysis time of 5 minutes. For this reason, being one of the main objectives of our work to obtain XOS with different DPs , it was decided to keep this reaction time as preferred.

In order to briefly assess the potential repeatability of the experiment with a diverse xylanase, a pre-test was also carried out in the same aforementioned conditions and at the optimized reaction time, that is 5 minutes, with endo-1,4-β-Xylanase M6 from rumen microorganism. The XOS distribution obtained in this experiment is reported in Table 6.2 of the supplementary material as well. The results showed a very similar distribution profile of XOS, in terms of relative percentage, even though a slight smaller amount of higher DPs was found. For this reason, it was decided to carry on the following experiments employing M3 xylanase, but this pre-test suggested the potential use of different xylanases having the same activity obtaining similar results.

Table 6.2: *Comparison of different XOS fractions originated from xylan hydrolysis with M3 xylanase from Trichoderma longibrachiatum, at different reaction times.*

2 MIN	**Rt**	**concentration (ppm)**	**relative %**	**Yield%**
DP1		n.d.	n.d.	
DP2	5.51	312 ± 52	18 ± 3	
DP3	6.88	379 ± 11	22 ± 3	
DP4	8.06	471 ± 42	27 ± 2	
DP5	8.99	209 ± 26	12 ± 3	
DP6	9.53	118 ± 12	7 ± 1	
DP7	10.35	86 ± 16	5 ± 1	
DP8	10.9	75 ± 15	4 ± 2	
DP9	11.4	71 ± 35	4 ± 3	
sum		1721	100	37 ± 10
5 MIN	**Rt**	**concentration (ppm)**	**relative %**	**Yield%**
DP1		n.d.	n.d.	
DP2	5.49	257 ± 39	16 ± 2	
DP3	6.91	317 ± 18	20 ± 2	
DP4	8.03	365 ± 42	23 ± 2	
DP5	8.97	235 ± 34	15 ± 2	
DP6	9.76	166 ± 19	10 ± 1	
DP7	10.42	111 ± 21	7 ± 1	
DP 8	10.9	84 ± 16	5 ± 3	
DP 9	11.26	72 ± 36	4 ± 3	
sum		1607	100	35 ± 9
8 MIN	**Rt**	**concentration (ppm)**	**relative %**	**Yield%**
DP1		n.d.	n.d.	
DP2	5.49	344 ± 78	18 ± 3	
DP3	6.90	467 ± 14	25 ± 3	
DP4	8.11	553 ± 60	30 ± 3	
DP5	9.02	201 ± 19	11 ± 3	
DP6	9.79	136 ± 9	7 ± 1	
DP7	10.46	87 ± 16	5 ± 1	
DP8	11.06	76 ± 15	4 ± 3	
sum		1864	100	40 ± 11
11 MIN	**Rt**	**concentration (ppm)**	**relative %**	**Yield%**

DP1		n.d.	n.d.	
DP2	5.48	549 ± 68	32 ± 4	
DP3	6.90	561 ± 28	32 ± 4	
DP4	8.06	464 ± 49	27 ± 2	
DP5	8.97	85 ± 10	5 ± 1	
DP6	9.76	82 ± 4	4 ± 1	
sum		1741	100	38 ± 10
15 MIN	**Rt**	**concentration (ppm)**	**relative %**	**Yield%**
DP1		n.d.	n.d.	
DP2	5.45	465 ± 70	41 ± 6	
DP3	6.88	245 ± 25	21 ± 3	
DP4	8.06	234 ± 11	20 ± 2	
DP5	8.94	99 ± 12	9 ± 2	
DP6	9.75	102 ± 10	9 ± 2	
sum		1145	100	25 ± 7

Pre-test with endo-1,4-β-Xylanase M6 from rumen microorganism				
5 MIN	**Rt**	**concentration (ppm)**	**relative %**	**Yield%**
DP1		n.d.	n.d.	
DP2	5.46	214 ± 29	15 ± 2	
DP3	6.88	325 ± 12	23 ± 2	
DP4	8.00	329 ± 19	23 ± 3	
DP5	8.95	270 ± 24	19 ± 3	
DP6	9.76	115 ± 11	8 ± 2	
DP7	10.40	88 ± 15	6 ± 2	
DP8	10.89	56 ± 8	4 ± 2	
DP9	11.23	30 ± 4	2 ± 2	
sum		1427	100	30 ± 2

3.1.2. DoE experiments

Once the reaction time was chosen, all the 19 experiments foreseen by DoE (Table 6.1) were carried out, and their results are reported in Table 6.3, in terms of relative percentage of each DP obtained, total yield (expressed as g XOS/g starting xylan) and total amount of low (1-6) and medium (7-10) DPs. Each enzymatic hydrolysis test brought to obtain all the XOS having DP between 1 (xylose) and 6. At the same time, DP7 and DP8 were detected in most of the tests, reaching a maximum content of 6% and 3% of the total XOS, respectively. Finally, DP9 appeared in several tests, with a maximum percentage equal to 1.2%, while DP10 was found in only one experiment (N2), with a quantity of 0.4% (Table 6.3). Low-DP XOS, considered as a sum, were always found to be the much larger portion of the hydrolysate, with a relative percentage variable between 89% and 100%. Actually, this result is not surprising, since the employed enzyme, obtained from *T. longibrachiatum* and belonging to the GH11 family, is known to have a preference for the production of low-

DP XOS (2-6) [35]. The total yield of XOS had strong variations, oscillating between 15% and 59%. These values are quite in line with the recent literature dealing with enzymatic hydrolysis of xylans deriving from agricultural or agroforestry by-products [36,37].

***Table 6.3**: Results of the 19 experiments in terms of DP's relative distribution, total yield and sum of low- and medium-DP XOS.*

Exp Name	Relative % (g/100g hydrolysate)										Yield % (g/100g initial xylan)	DP 1-6 (sum)	DP 7-10 (sum)
	DP1	**DP2**	**DP3**	**DP4**	**DP5**	**DP6**	**DP7**	**DP8**	**DP9**	**DP10**			
N1	0.3 ± 0.1	20.7 ± 2.2	32.1 ± 2.5	25.4 ± 2.5	12.6 ± 0.9	6.0 ± 0.4	2.0 ± 0.2	0.8 ± 0.1	0.2 ± 0.0	0.0 ± 0.0	29 ± 1	97	3
N2	0.6 ± 0.1	9.2 ± 1.0	32.5 ± 3.1	23.5 ± 2.1	14.2 ± 1.0	9.5 ± 0.6	6.0 ± 0.6	3.1 ± 0.4	1.0 ± 0.2	0.4 ± 0.0	43 ± 2	89	11
N3	0.3 ± 0.0	22.9 ± 2.9	42.2 ± 4.0	21.7 ± 1.9	9.6 ± 0.7	2.7 ± 0.2	0.6 ± 0.1	0.0 ± 0.0	0.0 ± 0.0	0.0 ± 0.0	25 ± 1	99	1
N4	0.9 ± 0.1	15.1 ± 1.3	34.4 ± 3.3	22.3 ± 2.0	13.4 ± 0.9	7.1 ± 0.5	4.3 ± 0.4	1.7 ± 0.2	0.8 ± 0.2	0.0 ± 0.0	39 ± 2	93	7
N5	0.7 ± 0.1	36.3 ± 10.2	48.2 ± 4.6	11.9 ± 1.1	2.7 ± 0.2	0.4 ± 0.0	0.0 ± 0.0	0.0 ± 0.0	0.0 ± 0.0	0.0 ± 0.0	35 ± 2	100	0
N6	1.2 ± 0.2	24.1 ± 2.9	35.9 ± 3.4	20.1 ± 1.8	10.7 ± 0.7	5.2 ± 0.3	1.9 ± 0.2	0.6 ± 0.1	0.2 ± 0.0	0.0 ± 0.0	41 ± 2	97	3
N7	0.8 ± 0.1	35.4 ± 3.3	47.3 ± 4.5	13.8 ± 1.2	2.4 ± 0.2	0.2 ± 0.0	0.0 ± 0.0	0.0 ± 0.0	0.0 ± 0.0	0.0 ± 0.0	39 ± 2	100	0
N8	1.5 ± 0.2	19.2 ± 2.0	42.8 ± 4.1	20.9 ± 1.9	10.9 ± 0.7	3.2 ± 0.2	1.2 ± 0.1	0.3 ± 0.0	0.1 ± 0.0	0.0 ± 0.0	54 ± 3	98	2
N9	2.7 ± 0.4	8.5 ± 1.0	32.0 ± 3.1	23.8 ± 2.1	18.3 ± 1.3	8.2 ± 0.5	4.6 ± 0.5	1.5 ± 0.2	0.5 ± 0.1	0.0 ± 0.0	51 ± 3	93	7
N10	2.9 ± 0.4	35.1 ± 4.2	31.9 ± 3.0	16.2 ± 1.4	9.0 ± 0.6	3.0 ± 0.2	1.6 ± 0.2	0.5 ± 0.1	0.0 ± 0.0	0.0 ± 0.0	15 ± 1	98	2
N11	2.7 ± 0.5	20.8 ± 1.9	35.5 ± 3.6	20.4 ± 1.8	10.3 ± 0.7	3.2 ± 0.2	3.4 ± 0.2	2.5 ± 0.1	1.2 ± 0.1	0.0 ± 0.0	42 ± 2	93	7
N12	1.4 ± 0.2	14.1 ± 1.5	31.4 ± 3.0	23.4 ± 2.1	13.7 ± 0.9	8.2 ± 0.5	4.8 ± 0.5	2.0 ± 0.3	1.0 ± 0.2	0.0 ± 0.0	55 ± 3	92	8
N13	3.2 ± 0.5	14.4 ± 1.9	27.5 ± 2.0	17.9 ± 1.7	19.0 ± 1.4	9.6 ± 0.7	5.6 ± 0.6	2.1 ± 0.3	0.8 ± 0.2	0.0 ± 0.0	34 ± 2	92	8
N14	1.4 ± 0.3	20.4 ± 1.6	29.7 ± 1.8	20.5 ± 1.9	13.3 ± 1.1	8.2 ± 0.7	4.2 ± 0.5	1.8 ± 0.3	0.6 ± 0.1	0.0 ± 0.0	59 ± 3	93	7
N15	4.3 ± 0.7	22.1 ± 2.4	38.8 ± 3.7	21.9 ± 2.0	8.4 ± 0.6	3.0 ± 0.2	0.9 ± 0.1	0.6 ± 0.1	0.0 ± 0.0	0.0 ± 0.0	18 ± 1	98	2
N16	1.2 ± 0.2	18 ± 2.2	29.7 ± 2.8	22.8 ± 2.0	14.8 ± 1.0	7.3 ± 0.5	4.1 ± 0.4	1.4 ± 0.2	0.6 ± 0.1	0.0 ± 0.0	54 ± 3	94	6
N17	0.8 ± 0.1	33.1 ± 6.0	41.0 ± 3.8	16.9 ± 1.8	6.1 ± 0.5	1.7 ± 0.1	0.5 ± 0.0	0.0 ± 0.0	0.0 ± 0.0	0.0 ± 0.0	40 ± 2	100	0
N18	0.9 ± 0.1	29.1 ± 3.5	41.4 ± 3.9	20.1 ± 1.8	6.7 ± 0.5	1.6 ± 0.1	0.3 ± 0.0	0.0 ± 0.0	0.0 ± 0.0	0.0 ± 0.0	36 ± 2	100	0
N19	0.7 ± 0.4	29.1 ± 3.0	40.1 ± 5.0	20.3 ± 1.3	7.4 ± 0.2	1.9 ± 0.0	0.6 ± 0.0	0.0 ± 0.0	0.0 ± 0.0	0.0 ± 0.0	41 ± 2	99	1

A statistical analysis was applied to assess which parameters, among those considered in the DoE, were more or less impacting on the xylanolytic action of the enzyme and more specifically on the formation of each DP of the XOS mixture, as well as on the yield. Actually, only the response for DP 1-5 was reliably modelled, while for the other ones the model was not found to be reliable, probably due to the detectable presence of most of these components only in a few experiments. In particular, two of the experiments performed (N2 and N7, Table 6.1) turned out to be the farthest respect to the models, and for this reason they were excluded from the statistical analysis. After exclusion, the results were modelled using Multiple Linear Regression (MLR). Figure 6.3 shows how the individual process factors, or the combination of two of them, had a positive or negative impact on the formation of XOS with low or medium DP.

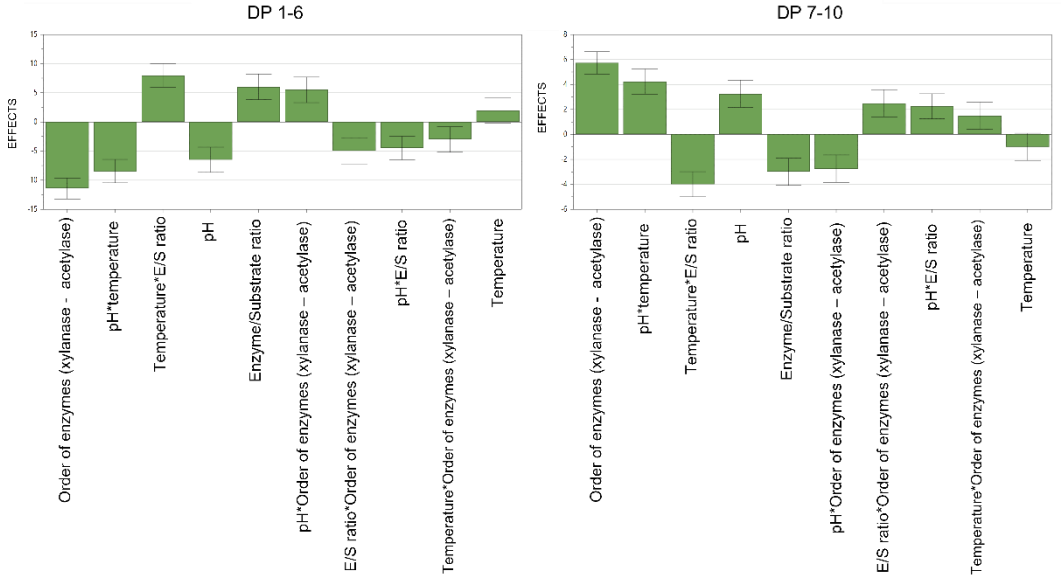

***Figure 6.3**: Impact of process factors on leading the formation of XOS with different DPs.*

The most impacting parameter was the order of addition of the endoxylanase and acetylxylan esterase: in fact, the removal of the acetyl groups before the hydrolysis of the xylan backbone leads to an increased tendency of the xylanase to produce shorter XOS, while vice versa, when xylanase acts on the substituted xylan, it produces a greater quantity of higher DPs. This behaviour agrees with the literature, where it is reported that the use of auxiliary enzymes is generally strongly recommended if the aim is to produce low-DP XOS. The substituent groups in the xylan backbone may be various, but they all have the ability of interfering with the enzymatic hydrolysis of endoxylanase, due to a matter of steric hindrance, inhibiting its action [25]. In a recent work, Pereira and colleagues showed how the yield of XOS obtained by enzymatic hydrolysis starting from arabinoxylans was changed by as much as 75% after the employment of arabinofuranosidase as an auxiliary enzyme, compared to the use of endoxylanase alone [38], while the steric hindrance of acetyl groups has been studied and highlighted in the work of Zhang's group [39]. In our work, the maximum amount of XOS having DP 7-10 was found to be just equal to 11% of the hydrolysate. The

results obtained suggest that further trials might be made considering a much more substituted xylan, namely with a higher degree of acetylation or with more than one substitutent, for instance a xylan substituted with acetyl groups and glucuronic acid. In this way, increasing the steric hyndrance it is quite likely that a bigger quantity of high-DP XOS can be obtained.

The total yield of XOS obtained was found to be inadequately described by the model: however, the latter turned out to be reliable by eliminating a single experiment (N10). The main results are reported in the response surface plot in Figure 6.4: as can be observed, it emerged that pH was in this case the most positively impacting parameter on the yield, possibly due to the ionization or deionization of functional groups within the active centre of the enzyme at lowest pH, and in accordance with the optimum pH reported for xylanase, close to neutrality. At the same time also the enzyme/substrate ratio turned out to be positively correlated with the total yield. As highlighted in the plot, when the acetylase is employed as first enzyme, yields up to 55 % can be achieved at the highest temperature tested (i.e. 50 °C) by setting the pH at 7.5 and adding a high quantity of enzyme (Figure 6.4a). Otherwise, maintaining the same order of enzymes but keeping the temperature lower, the XOS yield tends to be lower too, up to 42 %. In this case, however, good results can be achieved also lowering the amount of enzyme (Figure 6.4b), in a perspective of future scale-up.

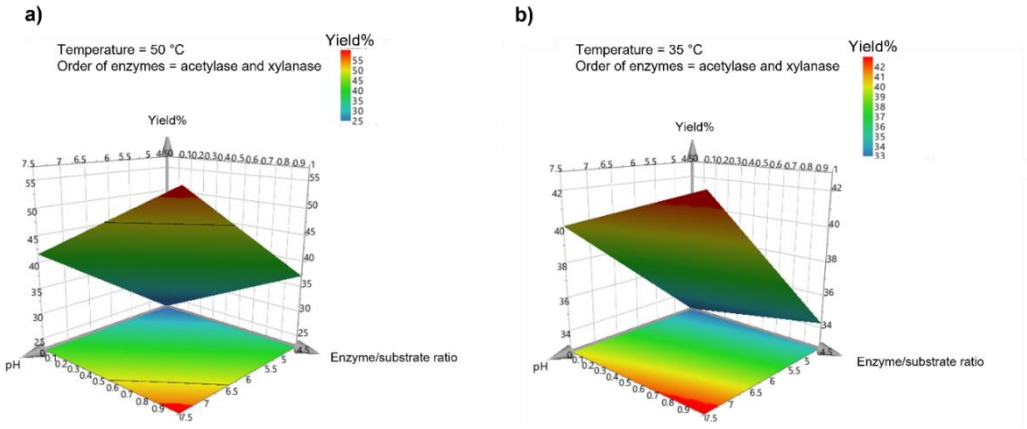

***Figure 6.4**: Response surface plot for optimizing the yield% of XOS (calculated on the amount of initial xylan) with high (a) and low (b) temperature.*

3.2. Application of optimized enzymatic hydrolyses on grape stalks' xylan

The aim of this part of the work was to understand whether the combination of acetylxylan esterase and endoxylanase, in the hydrolysis conditions previously optimized according to the final desired-DP XOS, was also applicable to a "real" un-purified xylan, namely xylan extracted from grape stalks, in a perspective of circular economy and by-products valorisation. Preliminarily, the fibre fractions extracted from grape stalks were evaluated in terms of chemical structure, to verify their similarity to the standard xylan used in the optimization experiments.

3.2.1. Structural characterization of grape stalks' xylan

Fibre fractions extracted from grape stalks according to Paragraph 2.4.1 were characterized in terms of proximate composition, molecular weight, degree of acetylation and monosaccharide composition (Paragraph 2.4.2). Table 6.4 reports the results about proximate and monosaccharide composition of fibres extracted with the mild hydrothermal pretreatment (EF1) and the following harsh treatment (EF2).

***Table 6.4**: Proximate composition and monosaccharide composition of the fibres extracted with two different consecutive hydrothermal treatments (HT).*

	PROXIMATE COMPOSITION	
	% (g/100g extract)	
	EF1 (HT: 1h at 120 °C)	**EF2** (HT: 45 min at 170 °C)
Moisture	7.7 ± 0.1	4.1 ± 0.9
Ash	27.3 ± 6.4	14.3 ± 0.5
Proteins	1.6 ± 0.4	12.3 ± 0.3
Total monosaccharides	19.7 ± 1.2	75.5 ± 0.8
	MONOSACCHARIDE DISTRIBUTION	
	% (g/100g monosaccharides)	
Arabinose	10.2 ± 2.3	1.7 ± 0.1
Rhamnose	4.4 ± 1.0	2.0 ± 0.3
Xylose	1.8 ± 0.4	28.4 ± 1.0
Galactose	13.4 ± 1.3	13.2 ± 0.2
Glucose	12.2 ± 0.1	52.2 ± 0.2
Mannose	2.4 ± 0.2	1.2 ± 0.0
Galacturonic acid	54.5 ± 15.3	1.2 ± 0.2
Glucuronic acid	1.0 ± 0.2	0.0 ± 0.0

The mild pretreatment led to obtain an extract (EF1) very poor of fibre (about 20 %), probably due to a co-extraction of tannic materials [40,41] and, more importantly, gas chromatographic analysis showed that the main monosaccharide was represented by galacturonic acid, suggesting the pectin nature of this fraction. This agrees with the literature, where many authors showed how temperatures above 170 °C are needed to extract hemicellulose from lignocellulosic biomasses, when hydrothermal treatment is applied alone [18]. Alternatively, lower temperatures have been also used to achieve this goal in some cases, but when the simultaneous use of other reagents occurred, like formic acid [42], or hydrogen peroxide [43]. On the other hand, the second extract (EF2) proved to be of greater interest for the aim of this work: in fact, from GC-MS analysis carried out after acid hydrolysis, it came out that this extract was made up of 75.5% total sugars, and

within this class about 28% was xylose. The high amount of glucose (52.2%), however, suggested that this sample was actually holocellulose and not pure hemicellulose. These percentages are in line with some findings in literature: two different recent works by Prozil's group reported a very similar monosaccharide composition for the holocellulose obtained by grape stalks through delignification with peracetic acid and subsequent DMSO extraction [30,44].

EF2 was further analysed by HPSEC-RID and ^{1}H NMR in order to evaluate the molecular weight and the degree of acetylation, respectively (Figure 6.5).

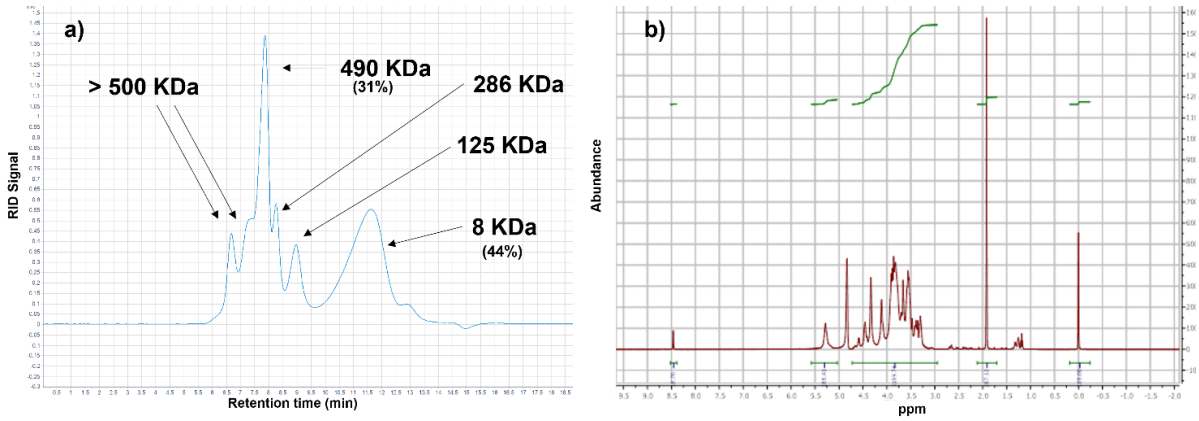

***Figure 6.5**: Molecular weight distribution by HPSEC-RID (a) and acetylation degree determination by ^{1}H NMR (b) of grape stalks' holocellulose.*

The HPSEC-RID showed the presence of different fractions, having different molecular weights, varying between 8 KDa and >500 KDa. Concerning the abundance, the two main fractions were those at 490 KDa, present for 31 %, and the one at 8 KDa, which made up about 44 % of the total polysaccharide. According to the literature, it is likely that the high Mw fraction and the low Mw fraction correspond, respectively, to the cellulose and xylan polymers of the holocellulose extracted. The Mw of purified xylan from grape stalks has been reported to be about 19 KDa [44] and the lower Mw found in this study (8 KDa) could be due to differences in the extraction conditions. It is actually difficult to compare this chemical feature among different studies because polysaccharide's molecular weight is strictly related to the extraction method [45]. This is also confirmed by Josefsson' work, who studied the Mw of aspen wood's cellulose, showing how it changed when different extraction temperatures were tested. In a study employing steam explosion [46], the calculated Mw was about 500 KDa, which is comparable to our results. Anyway, the absence of very low molecular weight fractions indicates a low extent of autohydrolysis during extraction, making the xylan obtained (theoretical DP=60) suitable as substrate for xylanase.

^{1}H NMR results showed that acetyl groups were effectively present along the xylan backbone, and that they constituted about 32% of the total xylan: this value is comparable to the degree of acetylation of the commercial xylan used for the optimization of enzymatic hydrolysis, equal to 24%.

3.2.2. Production of XOS with different DP from grape stalks

As highlighted above, the chemical characteristics of xylan obtained from grape stalks make it a perfect substrate to test on a real sample the applicability of the different hydrolysis conditions, previously optimized on standard xylan. In order to test the effectiveness of the different hydrolysis conditions set up through the DoE approach, 3 out of 19 experiments conducted on the standard xylan were selected and repeated in triplicate under the same conditions on grape stalks' xylan. The general idea was to select experiments able to maximize different XOS DPs in the range DP 2-9. Firstly, we selected the conditions which had allowed to maximize XOS having DP2 + DP3, corresponding to N5 experiment (Table 6.3). This consisted in employing the xylanase at 35 °C, pH 4.5, with high enzyme/substrate ratio and after the deacetylation step (Table 6.1). Then, we selected a second experiment which had previously maximized the amount of XOS having DP5 + DP6, corresponding to N13 experiment (Table 6.3): the xylanase was here added before the acetylxylan esterase employment, at 35 °C, pH 4.5 and with high enzyme/substrate ratio (Table 6.1). Finally, the experiment which had maximized the sum of DP8 + DP9 was selected (experiment N11, Table 6.3). Here, the hydrolysis conditions for xylanase were the following: temperature 50 °C, pH 4.5, low enzyme/substrate ratio and addition before the deacetylation step (Table 6.1).

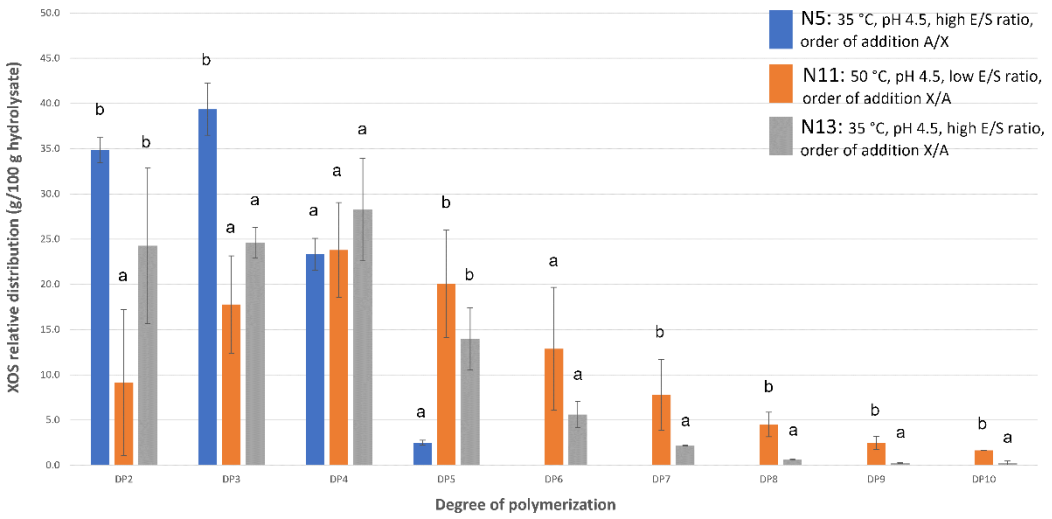

***Figure 6.6**: Relative distribution of XOS after enzymatic hydrolysis on grape stalks' xylan. Each datum is the mean of three replicates. One-way ANOVA was employed in order to compare the global mean of each group (p-level 0.05). Different letters above the bars indicate significantly different values.*

The results obtained are reported in the histogram in Figure 6.6: many differences in terms of DP distribution emerged, highlighting the overall effect of the different hydrolysis conditions even on a non-pure xylan sample. In detail, it can be seen that the N5 experiment resulted in detecting only XOS with a DP up to 5 in the hydrolysate, in accordance with the same experiment on standard xylan: actually, in that case, DP6 had also detected, but in very low concentrations (Table 6.3). XOS distribution is also comparable. Indeed, the

percentages of DP2 + DP3 obtained by commercial (84%) and grape stalks' xylan (75%) were compared by t-test ($p < 0.05$), and the difference was found to be not significant.

N11 experiment, chosen with the aim to maximize XOS with DP8 + DP9, also confirmed the results obtained in the experiment with commercial xylan and led to the formation of all DPs up to 10. Although DP10 did not appear when commercial xylan was used for hydrolysis, the relative distribution of XOS was found to be in line between the two different trials. In particular, DP8 + DP9 amount was found to be not significantly different from that obtained on the standard xylan under the same conditions (t-test, $p < 0.05$).

Finally, in the N13 experiment, aimed at maximizing DP5 + DP6, DP4 was instead the most abundant in the hydrolysate and all the XOS with DP up to 10 were present, but those with DP>5 were generally in lower amount respect to the experiment N11. As a consequence, in this case, the enzymatic hydrolysis on non-pure xylan has demonstrated a different behaviour respect to the commercial xylan. In fact, the sum of DP5 + DP6 was not actually significantly different from that obtained when N11 experiment was performed (t -test, $p < 0.05$), even if significantly higher than in N5.

Globally, the strictest similarity among experiments on commercial xylan and on non-pure xylan was found in N5: this may be explained by the fact that this was the only experiment, among the three selected, in which acetylxylan esterase was used as first enzyme. It is likely that by removing all the substituent groups before using xylanase, a less complex and more "standardized" xylan can be obtained, and the action of xylanase is more repeatable here. On the other hand, when xylanase is employed to hydrolyse an acetylated xylan, more variable results are obtained, likely due to the different position and distribution of acetyl groups on the xylans from different sources. However, also in this case, it is still possible to model the distribution of DP by acting on enzymatic hydrolysis conditions.

As regards the total quantity of XOS obtained (calculated as yield, g XOS / g xylan) it was found to be 41.4 ± 8.5%, 41.5 ± 9.6% and 68.8 ± 3.3% for the N5, N11 and N13 experiments, respectively. These values are equivalent or significantly higher (in the case of N13) respect to the ones obtained in the trials with standard xylan and reported in Table 6.3 (35 ± 2%, 42 ± 2% and 34 ± 2%, respectively).

It is important to highlight that these results have been obtained despite the presence of high amount of cellulose in the xylan extracted from grape stalks, demonstrating that xylanase works in a similar way on pure xylans and in holocellulose, both in terms of XOS obtained and global yield. This result is of particular relevance from the perspective of the valorization of lignohemicellulose materials because it opens up the possibility of obtaining high-value prebiotic XOS from unpurified fibre-rich materials, with the related obvious economic advantages. XOS obtained from in-situ enzymatic hydrolysis of holocellulose can then be easily separated and purified due to the enormous molecular weight differences.

4. Conclusions

This work proposes the reuse of hemicellulose extracted from agricultural by-products (namely grape stalks) as a starting material to produce prebiotic oligosaccharides (XOS) by the aid of xylanase and deacetylase enzymes. The model was tested on a common natural form of xylans, that is acetylated xylan, but it could be easily extended to xylans 'decorated' with other functional groups, such as arabinose or uronic acids, introducing the correct auxiliary enzyme in the model. One of the main points fixed was demonstrating the possibility to obtain XOS with a varied and modeled range of DP, between 2 and 10, by changing some enzymatic hydrolysis parameters as temperature, pH, E/S ratio and order of addition of enzymes. It emerged that XOS with DP 2-6 were always present and DP 2-4 the most abundant, but in many experiments XOS with DP 7-9 were detected too, and also DP10 in one case. In general, it came out that the order of addition of xylanase and acetylase was the most impacting parameter on the products outcome, and together with pH it had a great influence on the total yield of XOS obtained. The possibility to tailor the composition of the XOS mixture is of outmost importance in a global research context more and more interested in evaluating the punctual activity of different prebiotics in the modulation of the human microbiome. A second important point of this work was to demonstrate the possibility of extending the model to a non-pure xylan, similar to the commercial one in terms of chemical structure, extracted from grape stalks. The three enzymatic hydrolyses carried out under different conditions showed in any case that the XOS mixtures obtained resemble those obtained on pure xylans both in terms of DP distribution and yield, confirming the feasibility of application of this method on non-pure holocellulose samples. Therefore, this work makes an important contribution to the enhancement of agricultural by-products containing acetylated xylans, proposing a method for obtaining, with a more environmentally friendly technique, high value-added products with different chemical structures, tailored on the specific application envisioned.

REFERENCES

1. Dixit, Y.; Wagle, A.; Vakil, B. Patents in the Field of Probiotics, Prebiotics, Synbiotics: A Review. *J. Food Microbiol. Saf. Hyg.* **2016**, *1*, 1–13, doi:10.4172/2476-2059.1000111.

2. Farias, D. de P.; de Araújo, F.F.; Neri-Numa, I.A.; Pastore, G.M. Prebiotics: Trends in food, health and technological applications. *Trends Food Sci. Technol.* **2019**, *93*, 23–35, doi:10.1016/j.tifs.2019.09.004.

3. Amorim, C.; Silvério, S.C.; Prather, K.L.J.; Rodrigues, L.R. From lignocellulosic residues to market: Production and commercial potential of xylooligosaccharides. *Biotechnol. Adv.* **2019**, *37*, 107397, doi:10.1016/j.biotechadv.2019.05.003.

4. Linares-Pasten, J.A.; Aronsson, A.; Karlsson, E.N. Structural Considerations on the Use of Endo-Xylanases for the Production of prebiotic Xylooligosaccharides from Biomass. *Curr. Protein Pept. Sci.* **2018**, *19*, 48–67, doi:10.2174/1389203717666160923155209.

5. Dodd, D.; Moon, Y.H.; Swaminathan, K.; Mackie, R.I.; Cann, I.K.O. Transcriptomic analyses of xylan degradation by Prevotella bryantii and insights into energy acquisition by xylanolytic bacteroidetes. *J. Biol. Chem.* **2010**, *285*, 30261–30273, doi:10.1074/jbc.M110.141788.

6. Joshi, D.; Roy, S.; Banerjee, S. Prebiotics: A Functional Food in Health and Disease. *Nat. Prod. Drug Discov. An Integr. Approach* **2018**, 507–523, doi:10.1016/B978-0-08-102081-4.00019-8.

7. Jain, I.; Kumar, V.; Satyanarayana, T. Xylooligosaccharides: An economical prebiotic from agroresidues and their health benefits. *Indian J. Exp. Biol.* **2015**, *53*, 131–42.

8. de Freitas, C.; Carmona, E.; Brienzo, M. Xylooligosaccharides production process from lignocellulosic biomass and bioactive effects. *Bioact. Carbohydrates Diet. Fibre* **2019**, *18*, 100184, doi:10.1016/j.bcdf.2019.100184.

9. Singh, R.D.; Banerjee, J.; Arora, A. Prebiotic potential of oligosaccharides: A focus on xylan derived oligosaccharides. *Bioact. Carbohydrates Diet. Fibre* **2015**, *5*, 19–30, doi:10.1016/j.bcdf.2014.11.003.

10. Ho, A.L.; Kosik, O.; Lovegrove, A.; Charalampopoulos, D.; Rastall, R.A. In vitro fermentability of xylo-oligosaccharide and xylo-polysaccharide fractions with different molecular weights by human faecal bacteria. *Carbohydr. Polym.* **2018**, *179*, 50–58, doi:10.1016/j.carbpol.2017.08.077.

11. Reddy, S.S.; Krishnan, C. Production of high-pure xylooligosaccharides from sugarcane bagasse using crude β-xylosidase-free xylanase of Bacillus subtilis KCX006 and their bifidogenic function. *LWT - Food Sci. Technol.* **2016**, *65*, 237–245, doi:10.1016/j.lwt.2015.08.013.

12. Aachary, A.A.; Prapulla, S.G. Xylooligosaccharides (XOS) as an Emerging Prebiotic: Microbial Synthesis, Utilization, Structural Characterization, Bioactive Properties, and Applications. *Compr. Rev. Food Sci. Food Saf.* **2011**, *10*, 2–16, doi:10.1111/j.1541-4337.2010.00135.x.

13. Poletto, P.; Pereira, G.N.; Monteiro, C.R.M.; Pereira, M.A.F.; Bordignon, S.E.; de Oliveira, D. Xylooligosaccharides: Transforming the lignocellulosic biomasses into valuable 5-carbon sugar prebiotics. *Process Biochem.* **2020**, *91*, doi:10.1016/j.procbio.2020.01.005.

14. Mäkeläinen, H.; Forssten, S.; Saarinen, M.; Stowell, J.; Rautonen, N.; Ouwehand, A.C. Xylo-oligosaccharides enhance the growth of bifidobacteria and Bifidobacterium lactis in a simulated colon model. *Benef. Microbes* **2010**, *1*, 81–91, doi:10.3920/BM2009.0025.

15. Han, J.; Cao, R.; Zhou, X.; Xu, Y. An integrated biorefinery process for adding values to corncob in co-production of xylooligosaccharides and glucose starting from pretreatment with gluconic acid. *Bioresour. Technol.* **2020**, *307*, 123200, doi:10.1016/j.biortech.2020.123200.

16. Otieno, D.O.; Ahring, B.K. A thermochemical pretreatment process to produce xylooligosaccharides (XOS), arabinooligosaccharides (AOS) and mannooligosaccharides (MOS) from lignocellulosic biomasses. *Bioresour. Technol.* **2012**, *112*, 285–292, doi:10.1016/j.biortech.2012.01.162.

17. Zhou, X.; Xu, Y. Eco-friendly consolidated process for co-production of xylooligosaccharides and fermentable sugars using self-providing xylonic acid as key pretreatment catalyst. *Biotechnol. Biofuels* **2019**, *12*, 272, doi:10.1186/s13068-019-1614-5.

18. Fuso, A.; Risso, D.; Rosso, G.; Rosso, F.; Manini, F.; Manera, I.; Caligiani, A. Potential valorization of hazelnut shells through extraction, purification and structural characterization of prebiotic compounds: A critical review. *Foods* **2021**, *10*, 1197, doi:10.3390/foods10061197.

19. Chapla, D.; Pandit, P.; Shah, A. Production of xylooligosaccharides from corncob xylan by fungal xylanase and their utilization

by probiotics. *Bioresour. Technol.* **2012**, *115*, 215–221, doi:10.1016/j.biortech.2011.10.083.

20. Immerzeel, P.; Falck, P.; Galbe, M.; Adlercreutz, P.; Nordberg Karlsson, E.; Stålbrand, H. Extraction of water-soluble xylan from wheat bran and utilization of enzymatically produced xylooligosaccharides by Lactobacillus, Bifidobacterium and Weissella spp. *LWT - Food Sci. Technol.* **2014**, *56*, 321–327, doi:10.1016/j.lwt.2013.12.013.

21. Sabiha-Hanim, S.; Noor, M.A.M.; Rosma, A. Effect of autohydrolysis and enzymatic treatment on oil palm (Elaeis guineensis Jacq.) frond fibres for xylose and xylooligosaccharides production. *Bioresour. Technol.* **2011**, *102*, 1234–1239, doi:10.1016/j.biortech.2010.08.017.

22. Singh, R.D.; Nadar, C.G.; Muir, J.; Arora, A. Green and clean process to obtain low degree of polymerisation xylooligosaccharides from almond shell. *J. Clean. Prod.* **2019**, *241*, 118237, doi:10.1016/j.jclepro.2019.118237.

23. Bhardwaj, N.; Kumar, B.; Verma, P. A detailed overview of xylanases: an emerging biomolecule for current and future prospective. *Bioresour. Bioprocess.* **2019**, *6*, 40, doi:10.1186/s40643-019-0276-2.

24. Rahmani, N.; Kahar, P.; Lisdiyanti, P.; Lee, J.; Yopi; Prasetya, B.; Ogino, C.; Kondo, A. GH-10 and GH-11 Endo-1,4-β-xylanase enzymes from Kitasatospora sp. produce xylose and xylooligosaccharides from sugarcane bagasse with no xylose inhibition. *Bioresour. Technol.* **2019**, *272*, 315–325, doi:10.1016/J.BIORTECH.2018.10.007.

25. Santibáñez, L.; Henríquez, C.; Corro-Tejeda, R.; Bernal, S.; Armijo, B.; Salazar, O. Xylooligosaccharides from lignocellulosic biomass: A comprehensive review. *Carbohydr. Polym.* **2021**, *251*, 117118, doi:10.1016/j.carbpol.2020.117118.

26. Surek, E.; Buyukkileci, A.O. Production of xylooligosaccharides by autohydrolysis of hazelnut (Corylus avellana L.) shell. *Carbohydr. Polym.* **2017**, *174*, 565–571, doi:10.1016/j.carbpol.2017.06.109.

27. Corbett, D.B.; Kohan, N.; Machado, G.; Jing, C.; Nagardeolekar, A.; Bujanovic, B.M. Chemical composition of apricot pit shells and effect of hot-water extraction. *Energies* **2015**, *8*, 9640–9654, doi:10.3390/en8099640.

28. Monteiro, C.R.M.; Ávila, P.F.; Pereira, M.A.F.; Pereira, G.N.; Bordignon, S.E.; Zanella, E.; Stambuk, B.U.; de Oliveira, D.; Goldbeck, R.; Poletto, P. Hydrothermal treatment on depolymerization of hemicellulose of mango seed shell for the production of xylooligosaccharides. *Carbohydr. Polym.* **2021**, *253*, 117274, doi:10.1016/j.carbpol.2020.117274.

29. Liu, X.; Yang, S.; Ma, J.; Yu, J.; Yan, Q.; Jiang, Z. Efficient production of acetylated xylooligosaccharides from Hawthorn kernels by a xylanase from Paecilomyces aerugineus. *Ind. Crops Prod.* **2020**, *158*, 112962, doi:10.1016/j.indcrop.2020.112962.

30. Prozil, S.O.; Evtuguin, D. V.; Lopes, L.P.C. Chemical composition of grape stalks of Vitis vinifera L. from red grape pomaces. *Ind. Crops Prod.* **2012**, *35*, 178–184, doi:10.1016/j.indcrop.2011.06.035.

31. Atatoprak, T.; Amorim, M.M.; Ribeiro, T.; Pintado, M.; Madureira, A.R. Grape Stalks Valorization for Fermentation Purposes. *Food Chem. Mol. Sci.* **2021**, *4*, 100067, doi:https://doi.org/10.1016/j.fochms.2021.100067.

32. AOAC Official Method of Analysis. 16th Edition. Association of official analytical, Washington DC. **2002**.

33. Xia, Y.G.; Wang, T.L.; Sun, H.M.; Liang, J.; Kuang, H.X. Gas chromatography–mass spectrometry-based trimethylsilyl-alditol derivatives for quantitation and fingerprint analysis of Anemarrhena asphodeloides Bunge polysaccharides. *Carbohydr. Polym.* **2018**, doi:10.1016/j.carbpol.2018.06.066.

34. Müller-Maatsch, J.; Caligiani, A.; Tedeschi, T.; Elst, K.; Sforza, S. Simple and validated quantitative 1H NMR method for the determination of methylation, acetylation, and feruloylation degree of pectin. *J. Agric. Food Chem.* **2014**, *62*, 9081–9087, doi:10.1021/jf502679s.

35. Chen, L.L.; Zhang, M.; Zhang, D.H.; Chen, X.L.; Sun, C.Y.; Zhou, B.C.; Zhang, Y.Z. Purification and enzymatic characterization of two β-endoxylanases from Trichoderma sp. K9301 and their actions in xylooligosaccharide production. *Bioresour. Technol.* **2009**, doi:10.1016/j.biortech.2009.05.038.

36. Ataei, D.; Hamidi-Esfahani, Z.; Ahmadi-Gavlighi, H. Enzymatic production of xylooligosaccharide from date (Phoenix dactylifera L.) seed. *Food Sci. Nutr.* **2020**, *8*, 6699–6707, doi:10.1002/fsn3.1964.

37. Sharma, K.; Khaire, K.C.; Thakur, A.; Moholkar, V.S.; Goyal, A.; Goyal, A. Acacia Xylan as a Substitute for Commercially Available Xylan and Its Application in the Production of Xylooligosaccharides. *ACS Omega* **2020**, *5*, 13729–13738, doi:10.1021/acsomega.0c00896.

38. Pereira, G.F.; de Bastiani, D.; Gabardo, S.; Squina, F.; Ayub, M.A.Z. Solid-state cultivation of recombinant Aspergillus nidulans to co-produce xylanase, arabinofuranosidase, and xylooligosaccharides from soybean fibre. *Biocatal. Agric. Biotechnol.* **2018**, doi:10.1016/j.bcab.2018.05.012.

39. Zhang, J.; Siika-Aho, M.; Tenkanen, M.; Viikari, L. The role of acetyl xylan esterase in the solubilization of xylan and enzymatic hydrolysis of wheat straw and giant reed. *Biotechnol. Biofuels* **2011**, doi:10.1186/1754-6834-4-60.

40. Giroletti, C.L.; Menezes, J.C.S. dos S.; Dalri-Cecato, L.; Dalari, B.L.S.K.; Hassemer, M.E.N. TANNIN EXTRACTION FROM GRAPE STEMS THROUGH A SOLID-LIQUID PROCESS: OPTIMIZING EFFICIENCY BY APPLYING THE RESPONSE SURFACE METHODOLOGY. *Brazilian J. Dev.* **2021**, *7*, 28894–28914, doi:10.34117/bjdv7n3-554.

41. Spinei, M.; Oroian, M. The potential of grape pomace varieties as a dietary source of pectic substances. *Foods* **2021**, *10*, 867, doi:10.3390/foods10040867.

42. Xu, J.; Fu, Y.; Tian, G.; Li, Q.; Liu, N.; Qin, M.; Wang, Z. Mild and efficient extraction of hardwood hemicellulose using recyclable formic acid/water binary solvent. *Bioresour. Technol.* **2018**, *254*, 353–356, doi:10.1016/j.biortech.2018.01.094.

43. Brienzo, M.; Siqueira, A.F.; Milagres, A.M.F. Search for optimum conditions of sugarcane bagasse hemicellulose extraction. *Biochem. Eng. J.* **2009**, *46*, 199–204, doi:10.1016/j.bej.2009.05.012.

44. Prozil, S.O.; Costa, E. V.; Evtuguin, D. V.; Cruz Lopes, L.P.; Domingues, M.R.M. Structural characterization of polysaccharides isolated from grape stalks of Vitis vinifera L. In Proceedings of the Carbohydrate Research; 2012; pp. 252–259.

45. Canalejo, D.; Guadalupe, Z.; Martínez-Lapuente, L.; Ayestarán, B.; Pérez-Magariño, S. Optimization of a method to extract polysaccharides from white grape pomace by-products. *Food Chem.* **2021**, *365*, 130445, doi:10.1016/j.foodchem.2021.130445.

46. Josefsson, T.; Lennholm, H.; Gellerstedt, G. Changes in cellulose supramolecular structure and molecular weight distribution during steam explosion of aspen wood. *Cellulose* **2001**, *8*, 289–296, doi:10.1023/A:1015168327450.

CHAPTER 7

Antioxidant and prebiotic activities of xylo-oligosaccharides mixtures of controlled composition: a step forward in understanding structure-activity relationship

The content of this chapter has also been published as:

Andrea Fuso, Winnie Dejonghe, Lieve Cauwenberghs, Ginevra Rosso, Franco Rosso, Ileana Manera, Augusta Caligiani (**2023)**. DPPH radical scavenging activity of xylo-oligosaccharides mixtures of controlled composition: a step forward in understanding structure-activity relationship. *Journal of Functional Foods* (no Volume/Issue/doi numbers are available yet).

ABSTRACT

Xylo-oligosaccharides (XOS) are taking hold in scientific research as one of the most promising functional ingredients for their potential prebiotic and antioxidant activities. Despite a large literature is present about the XOS prebiotic activity for bifidobacteria, scarce information is reported for LAB. Moreover, among all the XOS bioactive properties, antioxidant activity is one of the most discussed, and scientists struggle to explain the relationship between chemical structure and functionality. In this work, different mixtures of XOS of controlled composition, namely different degrees of polymerization (DP), of acetylation and of purity, were produced starting from commercial xylans by enzymatic hydrolysis coupled with tangential ultrafiltration. A purified mixture containing DP 6-9 XOS was also produced. A detailed molecular characterization of all the XOS mixtures was performed by LC-MS, HPSEC-RID and ^{1}H NMR. *In vitro* antioxidant activity was then tested against the stable DPPH (2,2-diphenyl-1-picryl-hydrazyl-hydrate) free-radical. It was found that standard pure xylose and DP 2-6 XOS had very low scavenging capacity (ranging from 11% to 38%) at concentrations up to 2 mg/mL, while high-Mw xylans showed higher percentages, around 50%, already at 1 mg/mL. Mixtures of XOS with different structures and containing different quantities of impurities had quite different antioxidant activities, indicating the influence of both these features on this property. In general, a mixture of XOS with DP 2-10 showed higher scavenging capacity (IC50 = 0.08 mg/mL) than one with DP 2-6 (IC50 = 0.25 mg/mL) and acetyl groups showed a negative effect under a similar DP distribution (IC50 raised to 0.52 mg/mL). Finally, the pure mixture containing DP 6-9 XOS showed the best IC50 among the mixtures tested, equal to 0.06 mg/mL. *In vitro* fermentation of the XOS mixtures and xylans with two different gut bacteria, namely *Lactobacillus brevis* DSM 20054 and the pathogenic *Escherichia coli* K88 was also performed, and results confirmed the prebiotic potential of XOS. *E. coli* was not able to grow with any of the XOS mixtures, while *L. brevis* exhibited preferences for unsubstituted XOS, especially with higher DP (DP2-10).

1. Introduction

The functional food market size was valued at $177,770.0 million in 2019, and is estimated to reach $267,924.4 million by 2027, registering a CAGR of 6.7% from 2021 to 2027 [1]. A functional food is made of biologically and physiologically active compounds and provides health benefits beyond its basic nutritional capacities [2]. Among these compounds, xylo-oligosaccharides (XOS) are gaining a lot of interest in the last years [3]. XOS are oligosaccharides made of a linear β-(1→4)-D-xylopyranan main chain which may present different substituent groups along it, such as acetyl groups, phenolic and uronic acids or other monosaccharides [4], and they can be obtained in many different ways starting from xylan, that is the most abundant hemicellulose in the cell wall of plants [5]. A lot of bioactive properties have been attributed to the consumption of XOS, such as prebiotic activity, reduction of blood cholesterol, immunostimulatory, antioxidant- and anticancer activity, and all these effects have been largely reviewed over the years [6–9]. What is clear to the scientific community is that there is a strict correlation between functional properties and chemical structure of oligosaccharides but, despite this awareness, a lot of uncertainty still exists on this structure-function relationship. It is commonly accepted that the most impacting parameters for XOS functional properties are their degree of polymerization (DP) and degree of substitution (DS) [10]. Regarding prebiotic activity, some studies have shown that small XOS, with a DP between 2 and 5, have really high prebiotic activity [11,12] and that often the smaller is the DP and the higher is the proliferation of prebiotic bacteria [13]. Then, when the degree of substitution (DS) is taken into account, it seems that unsubstituted XOS are generally preferred by bacteria [10,14] and that therefore these are more suitable to be used as prebiotic ingredients. However, it is important to underline that different microorganisms may have different preferences to oligosaccharides [15] and most of the studies are made on bifidobacteria [16]. For this reason, we decided to test in this study the *in vitro* prebiotic activity of a LAB strain, namely L. brevis DSM 20054. Among other XOS bioactive effects, *in vitro* antioxidant activity has been studied for a long time, but we are actually very far from the comprehension of its mechanism, despite the growing interest evidenced by the number of papers published in this field in the last 20 years, passing from 7 papers published in 2001 to 201 in 2021 with a mean annual growth rate of 130% (Data mining from Scopus database, access April 2022, query string: TITLE-ABS-KEY “XOS*antioxidant”). To quantify the antioxidant activity *in vitro*, many assays have been proposed, and the most common ones are DPPH (2-diphenyl-1-picrylhydrazyl radical scavenging activity) assay, ABTS (2,2’-azinobis(3-ethylbenzothiazoline-6-sulfonic acid) assay, hydroxyl radical scavenging activity, ferric reducing antioxidant power (FRAP), superoxide anion radical scavenging, reducing power, and ferrous ion chelating activity [17]. Every method has its principle, advantages and disadvantages. DPPH assay is the most used one for testing antioxidant activity of food and beverages components, and it is valid, easy, accurate, sensitive, and economic, giving highly reproducible results [18]. Concerning antioxidant activity,

XOS with higher DP have been presented elsewhere as better antioxidants compared to the low-DP ones [19], while for DS it depends on the quantity and the type of substituent groups. For example, it is widely recognized that the presence of uronic acids in the chain, like glucuronic or galacturonic acid, strongly improves oligosaccharide's capacity of free radical scavenging [19–22], while acetyl groups have been controversially associated sometimes to an improvement [23] or to a decrease [24,25] in the antioxidant activity of oligosaccharides in general. Although scientific literature is greatly trying to contribute to shed light on oligosaccharide's structure-antioxidant activity relationship, to our knowledge there have been no clear reports on the mechanisms underlying this cause-effect connection and for this reason further studies are necessary. Moreover, in some studies authors reported that the antioxidant activity of oligo- and polysaccharides extracted from different by-products may be due to the presence of other compounds, mainly phenols, that are simultaneously extracted [22]. However, the exact composition of oligosaccharide mixtures is generally not thoroughly investigated in the literature, often generating partial and speculative interpretation of the results. This work aims to provide further knowledge on prebiotic and antioxidant properties of XOS, through the production of XOS mixtures having controlled composition and obtained starting from commercially available pure xylans. Specifically, XOS with different DPs and with or without acetyl group substituents were tested, since the literature is almost unanimous about the effect that uronic acids have on the antioxidant activity. Each XOS mix composition was studied in detail by LC-MS and ^{1}H NMR techniques, especially with the aim to find a better link between structure and antioxidant activity. To further strengthen this latter point, purified fractions were produced and tested as well, together with commercially available pure standards of xylose and DP2-6 XOS.

2. Materials and methods

2.1. Materials and chemicals

D-xylose was purchased from Fluka Chemicals (Buchs, Switzerland); 1,4-β-D-xylobiose, 1,4-β-D-xylotriose, 1,4-β-D-xylotetraose, 1,4-β-D-xylopentaose, 1,4-β-D-xylohexaose, xylan (partially acetylated), acetylxylan esterase from *Orpinomyces sp.*, α-glucuronidase from *Geobacillus stearothermophilus*, endo-1,4-β-Xylanase M3 from *Trichoderma longibrachiatum* were purchased from Megazyme (Bray, County Wicklow, Ireland). Xylan from beechwood with acetyl and glucuronic acid groups was purchased from Iris Biotech GmbH (Marktredwitz, Germany).

2.2. Production of XOS mixtures by xylan enzymatic hydrolysis with simultaneous tangential ultrafiltration

Preliminary tests of enzymatic hydrolyses by xylanase were performed to compare the static hydrolysis (i.e., hydrolysis carried out in a flask) to hydrolyses with simultaneous tangential ultrafiltration (TUF) in different conditions. The static one was carried out dissolving 10 mg of standard xylan in 1 mL of 0.1 M sodium phosphate buffer, then adding 2.32 U of endo-β-1,4-xylanase M3 from *T. longibrachiatum* and let it react for 5 minutes at 50 °C and pH 7.5, then inactivating for 10 minutes at 100 °C. TUF hydrolyses consisted in filtrating the same solution containing xylan and enzyme (in the same ratio as in the static hydrolysis), immediately after the addition of the xylanase, through a tangential ultrafiltration system consisting of a 230 V peristaltic pump and a VIVAFLOW 50 R HYDROSART cassette, both purchased from Sartorius (Goettingen, Germany). In particular, two different membranes (cut-off 10 or 30 kDa) and cross-flows (200 or 400 mL/min) were assessed, and every 5 minutes the permeate was heated for 10 minutes at 100 °C to inactivate the enzyme collected in the permeate. The reaction was always interrupted when the total volume of 200 mL was permeated (about 15-20 minutes, depending on the experiment). Once the solutions cooled down, a deacetylation step was performed in order to obtain deacetylated XOS, by adding 2 µL acetylxylan esterase/10 mg xylan and maintaining for 20 minutes at 40 °C and pH 7. After that, the enzyme was inactivated again at 100 °C for 10 minutes and the solutions were centrifuged at 4 °C and 3900 g for 10 minutes. The obtained XOS were semi-quantified through UPLC/ESI-MS in conditions reported in Section 2.5.1. After these preliminary trials, the final TUF protocol was selected on the basis of XOS distribution and total yield (calculated as g XOS/100 g xylan), and it corresponded to the use of 30 kDa cut-off membrane and flow equal to 200 mL/min. Then, these reaction conditions were employed for the production of different XOS mixtures from standard xylan.

2.3. Production of different XOS mixtures

Standard xylan substituted with acetyl groups and glucuronic acid (XYL), purchased from Iris Biotech, was subjected to four different enzymatic hydrolyses, in order to obtain different mixtures of XOS. These mixtures were called Deglucuronidated Xylan (DEGXYL), High-DP Acetylated XOS (HAXOS), High-DP Deacetylated XOS (HDXOS) and Low-DP Deacetylated XOS (LDXOS) (Figure 7.1). The four samples had in common a first step with α-glucuronidase in order to remove glucuronic acid residues linked to the polymeric chain. This enzymatic reaction was performed by dissolving 5 g of xylan in 90 mL of demi water at 70 °C, adjusting the pH to 7 with sodium hydroxide and subsequently adding 100 µL of enzyme. The reaction was run for 8 hours with gradual addition of 0.1 N NaOH to keep the pH constant, thanks to the automatic titrator pH-stat 902

Titrando combined with *tiamo* software (Metrohm AG, Herisau, CH). Then, the enzyme in DEGXYL sample was inactivated at 100 °C for 10 minutes and the solution underwent centrifugation for 20 minutes at 4°C and 3900 g, before being dried by rotavapor and stored at -20 °C.

The samples with different DP and substitution pattern were obtained from DEGXYL according to the conditions set in a previous work [26]. LDXOS sample was produced by performing a deacetylation step starting from 5 g of deglucuronidated xylan in 90 mL water with 50 µL of acetylxylan esterase and keeping for 8 hours at 40 °C and pH 7 (maintained at this value through the automatic titrator). Later, acetylxylan esterase was inactivated at 100 °C for 10 minutes, the solution was diluted to 200 mL with demi water and transferred into the TUF reservoir and endo-1,4-β-Xylanase M3 from *T. longibrachiatum* was added in 5U/10 mg xylan ratio, at pH 4.5 and 35 °C. The solution was flushed through a 30 kDa membrane at a flow equal to 200 mL/min inactivating the permeate every 5 minutes, for 10 minutes at 100 °C, until the whole permeate was collected. The solution was finally centrifuged at 3900 g and 4 °C for 20 minutes and the supernatant was dried by rotavapor and stored at -20 °C.

HAXOS and HDXOS were both produced starting from 5 g of deglucuronidated xylan in 200 mL water, under the optimal conditions for the maximization of XOS with higher DPs, i.e., employing endo-1,4-β-Xylanase M3 from *T. longibrachiatum* in 2.32U/10 mg xylan ratio, at 50 ° C and pH 7.5 [26]. The enzymatic reaction with xylanase was performed through TUF, as described above for LDXOS. Then, HAXOS sample was simply centrifuged and dried by rotavapor. On the other hand, HDXOS was subjected to a deacetylation step in the same conditions as for LDXOS, followed by centrifugation and drying.

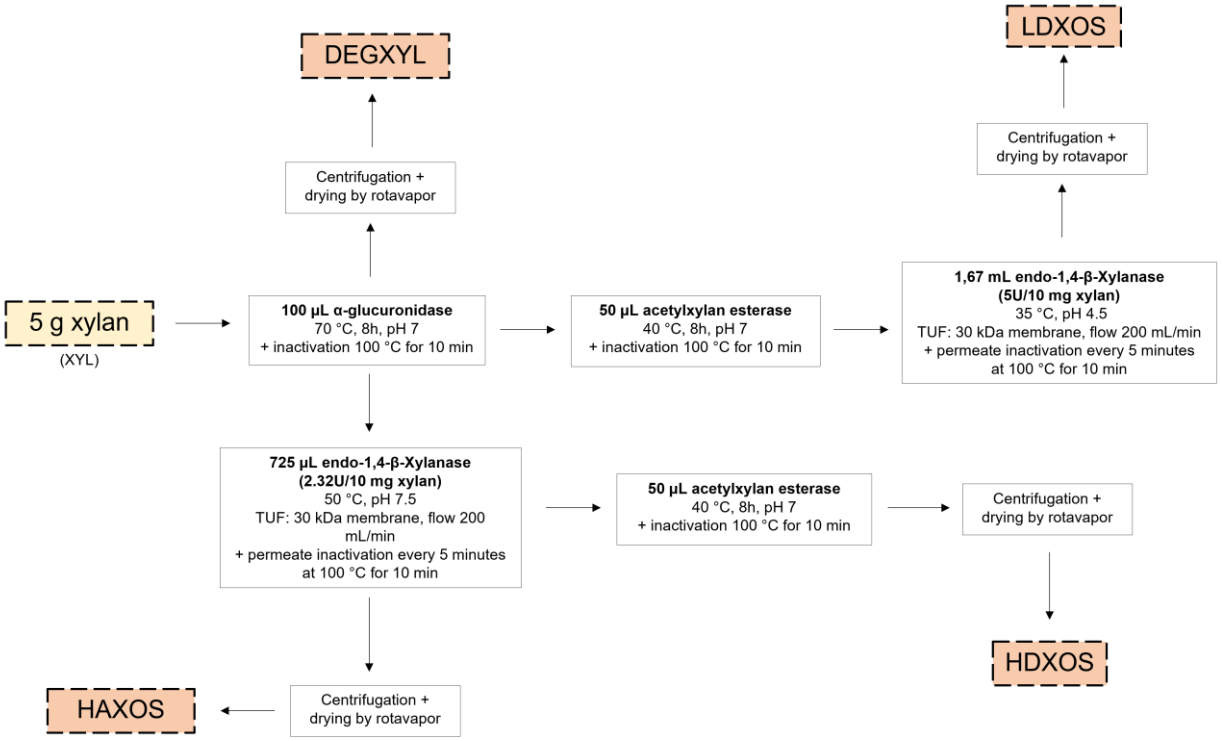

Figure 7.1: *Representation of the process for the production of different XOS mixtures.*

2.4. Production and purification of high-DP XOS

2.4.1. Enzymatic hydrolysis of pure xylan standard

Due to the lack of commercial XOS standards with DP higher than 6, they were produced in this work by enzymatic hydrolysis coupled with TUF from pure xylan according to conditions optimized in a previous work [26]. In this case, 1 g of a pure xylan standard, namely acetylated but not glucuronidated xylan purchased from Megazyme (Bray, County Wicklow, Ireland) was dissolved in 400 mL of distilled water into the TUF reservoir, then the same identical conditions of the enzymatic hydrolysis used for HDXOS were applied (Section 2.3), namely hydrolysis by xylanase followed by deacetylation by acetylxylan esterase. Finally, the supernatant was dried by rotavapor and frozen at -20 °C until the next use.

2.4.2. High-DP XOS separation through preparative Size-Exclusion Chromatography (SEC)

XOS originating from the enzymatic hydrolysis of pure xylan (Section 2.4.1) were separated by preparative SEC through the size exclusion Bio-Gel P-2 Gel, composed of extra fine polyacrylamide beads purchased from BioRad (Hercules, CA, USA). Thirty-three grams of Bio-Gel P-2 Gel powder were weighed and prepared as reported in the BioRad manual. Briefly, they were added to 200 mL of water and the gel was allowed to settle for 1 h. After removing about half of the supernatant, the solution was poured into a vacuum flask and degassed for 10 minutes. Another 200 mL of previously degassed water was added to the flask and after a

slight swirl, the gel was allowed to settle, then the suspended particles were removed aspirating the supernatant with a pipette. Then, 40 mL of water was added to a 45 x 2.5 column (cm height x cm width), and the gel solution was subsequently added. The gel was left to pack in the column and was then conditioned with 100 mL of water. Once eluted all the volume, the dry hydrolysate containing XOS (Section 2.4.1) was re-dissolved in 5 mL of water and subsequently added to the gel, then left to percolate up to the level of the gel. Finally, 100 mL of eluent were added and volumes equal to 1 mL were collected into glass measuring tubes, then analysed by flow injection-electrospray ionization mass spectrometry (Section 2.4.3). Since one separation was insufficient to separate high-DP XOS, the process was repeated four times with slightly different conditions, such as column size, eluent, and mL used to dissolve the sample, as summarized in Table 7.1. After every separation, depending on the results obtained from flow injection-ESI-MS, the glass measuring tubes containing DP from 6 to 10 were mixed together again, dried by rotavapor, re-dissolved and separated again.

Table 7.1: *Conditions of in series separations of XOS through preparative SEC using Bio-Gel P-2 Gel (BioRad).*

# Separation	Column size (cm height x cm width)	Eluent	mL sample	initial mg sample	Notes
1	45 x 2.5	H_2O	5	900	First 25 mL were discarded. Then, 32 tubes collected (1 mL each)
2	45 x 2.5	0.1 M acetic acid in H_2O	5	140	First 25 mL were discarded. Then, 35 tubes collected (1 mL each)
3	55 x 2	0.1 M acetic acid in H_2O	2	73	First 15 mL were discarded. Then, 37 tubes collected (1 mL each)
4	55 x 2	0.1 M acetic acid in H_2O	1	28	First 30 mL were discarded. Then, 37 tubes collected (1 mL each)

After the last separation, tubes containing DP 6-10 were mixed together again, dried under nitrogen flow and stored at -20 °C for further analyses (PURXOS sample).

2.4.3. Characterization of fractions by Flow injection-electrospray ionization mass spectrometry (flow-ESI-MS) analysis

The aliquots eluted from the column (Section 2.4.2) were analysed by flow injection-ESI-MS, using ultrapure water as mobile phase. In particular, the analysis of XOS was performed through the autosampler and injection system of an ultra-performance liquid chromatography system coupled with electrospray ionization

and mass spectrometry detector (UPLC/ESI-MS, WATERS ACQUITY) without column separation. Flow rate was set at 0.17 mL/min, injection volume 10 µL, strong needle wash 80 % CH_3CN + 20 % H_2O, weak needle wash 5 % CH_3CN + 95 % H_2O, seal wash 10 % CH_3CN + 90 % H_2O, column temperature 35 °C and sample temperature 18 °C. Detection was performed by using Waters SQ mass spectrometer: ESI source in negative ionization mode, capillary voltage 2.8 kV, cone voltage 25 V, source temperature 120 °C, desolvation temperature 350 °C, cone gas flow (N_2) 50 L/h, desolvation gas flow (N_2) 500 L/h, full scan acquisition (100-2000 m/z). Mass spectral search was performed based on [M-H]- mass of XOS: 149 for xylose, 281 for DP2, 413 for DP3, 545 for DP4, 677 for DP5, 809 for DP6, 941 for DP7, 1073 for DP8, 1205 for DP9, 1337 for DP10.

2.5. Structural characterization of XOS mixtures

2.5.1. UPLC/ESI-MS analysis of XOS mixes

The separation of XOS in the mixtures was performed following a protocol proposed by Waters Corporation [27] with minor modifications. Analytes and reaction products were dried under nitrogen flow and then dissolved in 50/50 acetonitrile/water in a final concentration of 5000 ppm. Then, samples were analysed by ultra-performance liquid chromatography with electrospray ionization in negative mode and single-quadrupole mass spectrometer detector (UPLC/ESI-MS, WATERS ACQUITY). UPLC/ESI-MS analysis was performed by using an ACQUITY UPLC® BEH Amide column (2.1 x 100 mm, 1.7 µm). The mobile phase was composed by 80 % CH_3CN + 20 % H_2O + 0.1 % NH_4OH (eluent A) and 30 % CH_3CN + 70 % H_2O + 0.1 % NH_4OH (eluent B). Gradient elution was performed: from 100 % A to 40 % A and 60 % B by linear gradient in the first 10 minutes, from 40 % to 100 % A in 0.02 minutes, isocratic 100 % A from 10.02 to 30 minutes. Flow rate was set at 0.17 mL/min, injection volume 2 µL, strong needle wash 20 % CH_3CN + 80 % H_2O, weak needle wash 75 % CH_3CN + 25 % H_2O, seal wash 50 % CH_3CN + 50 % H_2O, column temperature 35 °C and sample temperature 18 °C. Detection was performed by using Waters SQ mass spectrometer: ESI source in negative ionization mode, capillary voltage 2.8 kV, cone voltage 25 V, source temperature 120 °C, desolvation temperature 350 °C, cone gas flow (N_2) 50 L/h, desolvation gas flow (N_2) 500 L/h, full scan acquisition (100-2000 m/z). Integration was performed by extracting the following mass ions (m/z) for deacetylated XOS: 149 for xylose, 281 for DP2, 413 for DP3, 545 for DP4, 677 for DP5, 809 for DP6, 941 for DP7, 1073 for DP8, 1205 for DP9, 1337 for DP10. For acetylated XOS, numerous mass ions can be theoretically present (Figure 7.2), and the presence of each of them was checked by extracting the corresponding fragment. The various XOS were semi-quantified, taking into account ratios between peak areas, because an exact quantification is not possible due to the lack of each standard compound.

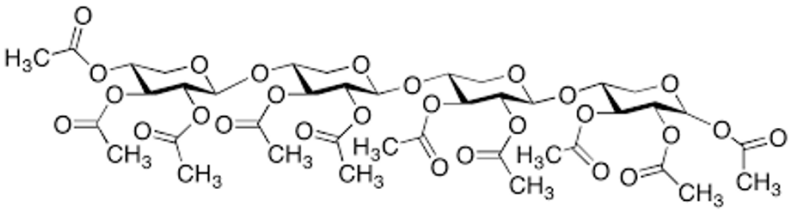

number of acetyl groups	DP1	DP2	DP3	DP4	DP5	DP6	DP7	DP8	DP9	DP10
1	191	323	455	587	719	851	983	1115	1247	1379
2	233	365	497	629	761	893	1025	1157	1289	1421
3	275	407	539	671	803	935	1067	1199	1331	1463
4	-	449	581	713	845	977	1109	1241	1373	1505
5	-	491	623	755	887	1019	1151	1283	1415	1547
6	-	533	665	797	929	1061	1193	1325	1457	1589
7	-	-	707	839	971	1103	1235	1367	1499	1631
8	-	-	749	881	1013	1145	1277	1409	1541	1673
9	-	-	-	923	1055	1187	1319	1451	1583	1715
10	-	-	-	965	1097	1229	1361	1493	1625	1757
11	-	-	-	-	1139	1271	1403	1535	1667	1799
12	-	-	-	-	1181	1313	1445	1577	1709	1841
13	-	-	-	-	-	1355	1487	1619	1751	1883
14	-	-	-	-	-	1397	1529	1661	1793	1925
15	-	-	-	-	-	-	1571	1703	1835	1967
16	-	-	-	-	-	-	1613	1745	1877	2009
17	-	-	-	-	-	-	-	1787	1919	2051
18	-	-	-	-	-	-	-	1829	1961	2093
19	-	-	-	-	-	-	-	-	2003	2135
20	-	-	-	-	-	-	-	-	2045	2177
21	-	-	-	-	-	-	-	-	-	2219
22	-	-	-	-	-	-	-	-	-	2261

***Figure 7.2**: Chemical structure of decaacetyl xylotetraose and mass fragments expressed as [M-H]- of every possible combination of acetylated XOS (DP 1-10).*

2.5.2. Evaluation of the degree of purity through 1H NMR metabolomics

^{1}H NMR analysis was performed on every sample to qualitatively investigate whether they contained impurities. Twenty mg of dried sample were dissolved in 600 µL of deuterium oxide (D_2O) and 100 µL of 2000 ppm 3-(trimethylsilyl)propionate-*d4* (TSP) were added as internal standard and the temperature was increased to 50 °C to facilitate the solubilisation of high Mw polymers. Then, the solutions were transferred directly into the NMR tube. ^{1}H NMR spectra were registered on a Bruker Avance III 400 MHz NMR Spectrometer (Bruker BioSpin, Rheinstetten, Karlsruhe, Germany) operating at a magnetic field-strength of 9.4 T. Spectra were acquired at 298 K, with 32 K complex points, using a 90° pulse length and 5 s of relaxation delay (d1). 128 scans were acquired with a spectral width of 9595.8 Hz and an acquisition time of 1.707 s. The relaxation delay and acquisition time ensure the complete relaxation of the protons, allowing their integrals for quantitative purposes. The experiments were carried out with water suppression by low power selective water signal presaturation during 5 s of the relaxation delay. The NMR spectra were processed by MestreNova software. The spectra were Fourier transformed with FT size of 64 K and 0.2 Hz line-broadening factor, phased and baseline corrected, and referenced to 3-(trimethylsilyl)-propionate-d4 (TSP) peak (0 ppm).

Different spectral zones were integrated and used for a preliminary crude quantification of the different impurities found in the XOS samples. The zone ranging from 1.00 to 1.52 ppm and from 2.32 to 3.08 ppm

were used as determinant indicative of organic acids and other polar compounds as amino acids and alcohols. Acetyl groups deriving from free acetate and substituted sugars (mainly acetylated xylans) were quantified integrating the spectral zone 1.87-2.28 ppm. The zone 6.68-7.31 ppm was indicative of aromatic/phenolic compounds, while the zone 8.28-9.06 contained the signal of formic acid and aldehydes, representative of sugar degradation. The integrals were referred to the whole sugar zone integrals (3.2-5.5 ppm), allowing a comparison among different samples.

2.5.3. Evaluation of xylan-into-XOS conversion through High-Performance Size-Exclusion Chromatography (HPSEC-RID)

High-Performance Size-Exclusion Chromatography was performed to further investigate whether XOS mixtures actually contained just XOS or high-Mw non-hydrolysed xylan. Dried XOS (Section 2.4) were dissolved in ultrapure water at a concentration of 1 mg/mL, then injected in an Agilent 1260 Infinity II LC system equipped with a refractive index detector (RID) (Agilent, Santa Clara, CA, USA). A 100 mM $NaNO_3$ aqueous solution was used as eluent at a flow rate equal to 0.5 mL/min, and a PL aquagel-OH 20, 7.5 x 300 mm, 8 µm (Agilent, Santa Clara, CA, USA) was employed for the separation. The injection sample volume was set at 50 µL, column temperature 30 °C and RID temperature 35 °C. Standard pullulans having known molecular weight were used for the calibration curve.

2.6. Determination of antioxidant activity

The antioxidant activity was determined on different XOS mixtures (LDXOS, HDXOS, HAXOS, PURXOS), on xylans (XYL, DEGXYL) and on xylose and commercial standard XOS (DP 2-6) by a procedure consisting in the quantification of the 2,2-Diphenyl-1-picrylhydrazyl radical (DPPH) decoloration. DPPH was purchased from Sigma-Aldrich (St. Louis, MO, USA). Xylose and XOS standard were tested at 2 mg/mL, just allowing to calculate the percentage of scavenging in this concentration, while XOS mixtures and xylans were tested in 7 different final concentrations, namely 1, 0.75, 0.5, 0.375, 0.25, 0.125 and 0.0625 mg/mL, aiming to calculate IC50 value, defined as the concentration of the compound providing 50% reduction of DPPH radicals. IC50 was calculated using an online tool [28]. Every sample was analysed as shown in Figure 7.3. Briefly, seven different solutions of each sample, dissolved in distilled water and having twice the aforementioned concentrations, were prepared in duplicate, and 1000 µL were made to react with 1000 µL of 100 µM DPPH in methanol, or with 1000 µL of methanol (color control, CC) in a centrifuge tube. The reaction was kept for 30 minutes in the dark under shaking to avoid precipitation of xylans, then the solutions were centrifuged at room temperature for 5 minutes at 1000 g and the supernatant was subsequently quickly transferred in a 96-wells plate with a multi-channel pipette. Every sample and color control were analysed in quadruplicate (Figure 7.3). The absorbance was measured with Tecan Infinite 200 PRO (Tecan Group Ltd., Mannedorf,

Switzerland) at 517 nm. Ascorbic acid was used as positive control. The % of scavenging was calculated as follows:

$$\%\ \text{DPPH scavenging} = \frac{\text{Abs Blank} - \text{Corrected Abs Sample}}{\text{Abs Blank}} \times 100$$

Where Abs Blank is the average absorbance of the blanks (i.e., distilled water + DPPH) measured 8 times, and Corrected Abs Sample is the average absorbance of the sample (i.e., sample in distilled water + DPPH) from which the absorbance value of the color control (CC, i.e., sample in distilled water + methanol) has been subtracted.

96-well	1	2	3	4	5	6	7	8	9
A	1	0,75	0,5	0,375	0,25	0,125	0,0625	C-	C+
B	1	0,75	0,5	0,375	0,25	0,125	0,0625	C-	C+
C	1	0,75	0,5	0,375	0,25	0,125	0,0625	C-	C+
D	1	0,75	0,5	0,375	0,25	0,125	0,0625	C-	C+
E	CC_1	$CC_{0,75}$	$CC_{0,5}$	$CC_{0,375}$	$CC_{0,25}$	$CC_{0,125}$	$CC_{0,0625}$	C-	C+
F	CC_1	$CC_{0,75}$	$CC_{0,5}$	$CC_{0,375}$	$CC_{0,25}$	$CC_{0,125}$	$CC_{0,0625}$	C-	C+
G	CC_1	$CC_{0,75}$	$CC_{0,5}$	$CC_{0,375}$	$CC_{0,25}$	$CC_{0,125}$	$CC_{0,0625}$	C-	C+
H	CC_1	$CC_{0,75}$	$CC_{0,5}$	$CC_{0,375}$	$CC_{0,25}$	$CC_{0,125}$	$CC_{0,0625}$	C-	C+

CC	1000 µL sample + 1000 µL MeOH
C-	1000 µL water + 1000 µL DPPH
C+	1000 µL ascorbic acid + 1000 µL DPPH

***Figure 7.3**: Representation of a 96-well plate for IC50 test, performed on different XOS/xylan samples. The numbers indicate the final concentration of XOS solutions in mg/mL, "CC" indicates the color control, "C-" indicates the negative control and "C+" indicates the positive control (ascorbic acid).*

2.7. Evaluation of prebiotic properties

2.7.1. Culture media and XOS fermentation

The determination of prebiotic properties of *Lactobacillus brevis* DSM 20054 and *Escherichia coli* K88 were investigated following a protocol in literature with slight modifications [29]. The reaction media for *L. brevis* was prepared as follows: 10 g tryptone, 10 g meat extract, 5 g yeast extract, 1 mL Tween80, 2 g dipotassium phosphate, 8.3 g sodium acetate trihydrate, 2.15 g ammonium citrate dibasic, 0.2 g magnesium sulfate and 0.05 g manganese sulfate were dissolved in 1 L of water and pH was adjusted to 6.5. The reaction media for *E. coli* was prepared dissolving 17 g tryptone, 3 g soytone, 5 g NaCl, and 2.5 g K_2HPO_4 in 1 L water, then pH was adjusted to 7.3. Then, these two media were autoclaved for 20 minutes at 121 °C. Both *L. brevis* DSM 20054 and *E. coli* K88 were purchased from the Leibniz Institute DSMZ – German Collection of

Microorganisms and Cell Cultures (Braunschweig, Germany) and grown in microaerophilic conditions and aerobic conditions, respectively. Before starting to test XOS fermentation, bacteria were pre-cultured for 72 h at 37 °C in 10 mL of the aforementioned basal media enriched with 1% (w/v) glucose, then 0.2 mL of this solution was inoculated in 10 mL of new fresh media with glucose as the only carbon source and cultured again for 24 h. After that, 0.2 mL of this solution were transferred in 10 mL basal medium enriched with different XOS fractions, previously sterilized by filtration through 0.22 µm membrane, and cultivated again for 48 h at 37 °C. A negative control (i.e., only basal culture broths, without carbon sources) and a positive control (i.e., culture broths containing glucose as the only carbon source) were also considered for each experiment with the two strains. All the experiments were performed in duplicates and bacterial growth was monitored by measuring optical density, using a spectrophotometer Infinite 200Pro with Tecan i-control (2.0.10.0) software at 600 nm, and pH with a pHmeter (Metrohm 719 S Titrino, Switzerland). At the end of the growth, 2 mL of culture samples were centrifuged at 10000 rpm for 10 min and the supernatant was kept for further analyses.

2.7.2. Analysis of short chain fatty acids (SCFAs) and lactic acid

The organic acids (formic, acetic, propionic, butyric and lactic acid) together with ethanol that were present in the media before and after fermentation were quantified following a protocol in literature [30]. Briefly, an HPLC analysis (Agilent 1200 series, Germany) was performed using an Agilent Hi-Plex H (300 × 7.7 mm and 8 µm particle size) column and an Agilent 1260 RID and MWD SL detector. The column temperature was set at 60 °C using an Agilent TCC SL column oven. A 0.01 mM H_2SO_4 solution was employed as mobile phase at a flow rate of 0.8 mL.min^{-1}. A calibration curve containing formic-, acetic, propionic-, butyric- and lactic acid and ethanol (Merck) was used in concentrations from 0.05 to 25 g/L.

3. Results and discussion

3.1. Production of XOS mix from standard xylans by tangential ultrafiltration

3.1.1. Optimization of TUF conditions for xylan hydrolysis

Some preliminary experiments were carried out under the same conditions (temperature, pH, E/S ratio, order of addition of enzymes as optimized in [26]) comparing a static hydrolysis and one with simultaneous of Tangential ultrafiltration (TUF). TUF was specifically used to remove XOS with a specific molecular weight from the hydrolysis mixture as soon as they were permeable, which could protect them (especially the highest DPs, 7-10) from further hydrolysis to unwanted smaller fragments. This may also allow the recovery of larger amounts of targeted XOS mixtures.

Optimization of TUF was made in terms of yield and composition of XOS. To this aim, a standard xylan was hydrolyzed by xylanase in the conditions allowing to obtain also higher DP XOS (Section 2.2). Two different flows (200 and 400 mL/min) and two membranes with different cut-offs (10 and 30 kDa) were tested to investigate how the modification of these parameters could influence the product outcome. Subsequently, the permeates were analyzed and quantified by UPLC/ESI-MS, and the results are reported in Table 7.2.

Table 7.2: *Relative distribution and yield of XOS with various DPs in preliminary tests with static or TUF hydrolysis.*

EXP. Name	STATIC	TUF1	TUF2	TUF3
flow (mL/min)	NO	200	400	200
membrane (kDa)	NO	30	30	10
	RELATIVE % (g/100 g hydrolysate XOS DP1 to DP10)			
Xylose	0,9	1,3	0,6	0,7
DP2	23,0	25,9	23,7	23,8
DP3	30,2	33,7	30,6	32,3
DP4	16,2	13,4	18,8	19,5
DP5	13,2	12,4	14,2	13,7
DP6	8,8	7,5	8,5	7,7
DP7	4,1	3,2	2,4	1,4
DP8	2,7	2,0	1,0	0,9
DP9	0,8	0,4	0,2	0,0
DP10	0,1	0,1	0,0	0,0
	YIELD % (g XOS/100g initial xylan)			
	34,1	73,5	67,1	69,1

As can be observed in the table, the four tests led to distribution profiles of DPs that are very similar to each other. What is most evident, is a difference in the total quantity of XOS DP1 to DP10 in the permeate, calculated on the initial quantity of xylan and expressed as yield %. Indeed, it appears clearly that the hydrolysis using TUF has led to a net increase in the amount of XOS, on average about two times higher than that obtained after the static hydrolysis. To our knowledge, no study has been reported in literature regarding the difference in hydrolysis yield when TUF was used in place of a 'traditional' static hydrolysis. The increase in yield of XOS DP1 to DP10 in the TUF might be due to two reasons: first, it is likely that the cross-flows used favored an increase in the contact between enzyme and substrate, compared to the static test. Furthermore, another reason could be that the static reaction was maintained in total for 5 minutes before inactivating the enzyme, while the one with TUF lasted in total between 15 and 20 minutes, inactivating the enzyme which passed in the permeate every 5 minutes: this could lead to an increase in yield due to the longer total hydrolysis time in TUF. At the same time, since the enzyme was inactivated every 5 min in the permeate, the same XOS profile as in the static reactor (where also a hydrolysis time of 5 min was used) was obtained. Once it was established that TUF hydrolysis led to obtaining a greater conversion of xylan into XOS, the conditions allowing the highest yield of XOS were chosen (namely flow 200 mL/min, membrane 30 kDa cut-off, Table 7.2) and applied for the production of the different XOS mixtures, as reported in Section 2.3 and Figure 7.1.

The mixture obtained from pure xylan standard was further purified to isolate XOS with DP7-10 to be used in analytics.

3.1.2. Production and purification of DP7-10 XOS

A specific hydrolysis was carried out starting from 1 g of pure acetylated xylan, in order to obtain significant quantities of unsubstituted high-DP XOS (DP 7-10) to then carry out the separation by preparative SEC. Four serial separations were conducted by slightly modifying the conditions from time to time (Table 7.1). Figure 7.4 shows the results of these separations, obtained by flow injection-ESI-MS:

1st separation

Tube number	XOS detected
1-7	No XOS
8-9	DP7, DP8, DP9, DP10
10-17	DP5, DP6, DP7, DP8, DP9, DP10
18-19	DP4, DP5, DP6, DP7, DP8, DP9, DP10
20	DP3, DP4, DP5, DP6, DP7, DP8, DP9
21-23	DP2, DP3, DP4, DP5, DP6, DP7, DP8, DP9
24-25	DP2, DP3, DP4, DP5, DP6, DP7, DP8
26-31	DP2, DP3, DP4, DP5, DP6, DP7
32	DP2, DP3, DP4, DP5

2nd separation

Tube number	XOS detected
1-18	No XOS
19-20	DP8, DP9, DP10
21	DP7, DP8, DP9, DP10
22	DP7, DP8, DP9
23-25	DP6, DP7, DP8, DP9
26	DP5, DP6, DP7, DP8, DP9
27	DP5, DP6, DP7, DP8
28-29	DP4, DP5, DP6, DP7, DP8
30	DP3, DP4, DP5, DP6, DP7, DP8
31	DP3, DP4, DP5, DP6, DP7
32-35	DP2, DP3, DP4, DP5, DP6, DP7

3rd separation

Tube number	XOS detected
1 - 22	No XOS
23-24	DP9, DP10
25	DP8, DP9, DP10
26-27	DP7, DP8, DP9, DP10
28	DP6, DP7, DP8, DP9, DP10
29	DP6, DP7, DP8, DP9
30-31	DP5, DP6, DP7, DP8, DP9
32-33	DP5, DP6, DP7, DP8
34	DP4, DP5, DP6, DP7, DP8
35-36	DP4, DP5, DP6, DP7
37	DP3, DP4, DP5, DP6, DP7

4th separation

Tube number	XOS detected
1-10	No XOS
11	DP9, DP10
12-13	DP8, DP9, DP10
14-15	DP7, DP8, DP9, DP10
16-17	DP6, DP7, DP8, DP9, DP10
18-20	DP6, DP7, DP8, DP9
21-32	DP5, DP6, DP7, DP8

***Figure 7.4**: Results of four different serial separations of XOS originated from enzymatic hydrolysis of commercial xylan.*

As shown in Figure 7.4, the separation by Bio-Gel P-2 Gel did not lead to the separation and the obtainment of pure fractions of XOS with fixed DP, but nevertheless allowed to isolate fractions with higher DP (DP 7-10) from those with lower DP (DP 2-6). This result can be considered quite satisfactory when compared with results obtained from previous similar attempts [31]. In general, in literature no studies were found in which the separation of XOS in a mixture led to obtaining pure fractions having a single DP that is higher than 6, and the challenge of this separation is also demonstrated by the lack of these analytical standards in the market. However, obtaining purified fractions of XOS having DP varying between 7 and 10 is a very important first step, in order to be able to draw an initial evaluation of their functional properties. The final purified

sample containing high-DP XOS (7-10), and named as PURXOS, was derived from mixing tubes from 11 to 20 of the 4th separation (Figure 7.4).

3.2. Molecular characterization of different XOS mixtures produced from standard xylans

3.2.1. Evaluation of xylan-into-XOS conversion through HPSEC-RID

High-Performance Size-Exclusion Chromatography coupled with Refractive Index Detector (HPSEC-RID) was performed aiming to evaluate the conversion of xylan into XOS in every mixture, and the chromatogram obtained is reported in Figure 7.5. As expected, XYL and DEGXYL showed the presence of a single peak, corresponding to a Mw higher than 20 kDa, that is the maximum Mw the column employed was able to separate. All the other samples showed low Mw fractions, indicating an extensive hydrolysis by the enzyme. LDXOS and HAXOS showed the presence of two different, separated peaks: the second one, corresponding to an average Mw of 350 Da, accounted for 40% of the total area in LDXOS and for 55% of the total area in HAXOS, while the first peak indicates a bigger residue deriving from the initial xylan, with an estimated Mw of 1.8-2 kDa. As concerns HDXOS, the profile was a bit different, with a fraction of average Mw of 450 Da equal to 20% of the total area, another 50% of about 2 kDa and a 30% of higher-Mw xylan. These results confirm the high conversion rates of xylan in XOS with the optimized TUF hydrolysis: the yield in XOS for HDXOS resembles the one reported in Table 7.2 (equivalent hydrolysis conditions), while for the other samples the conversion in XOS is even better.

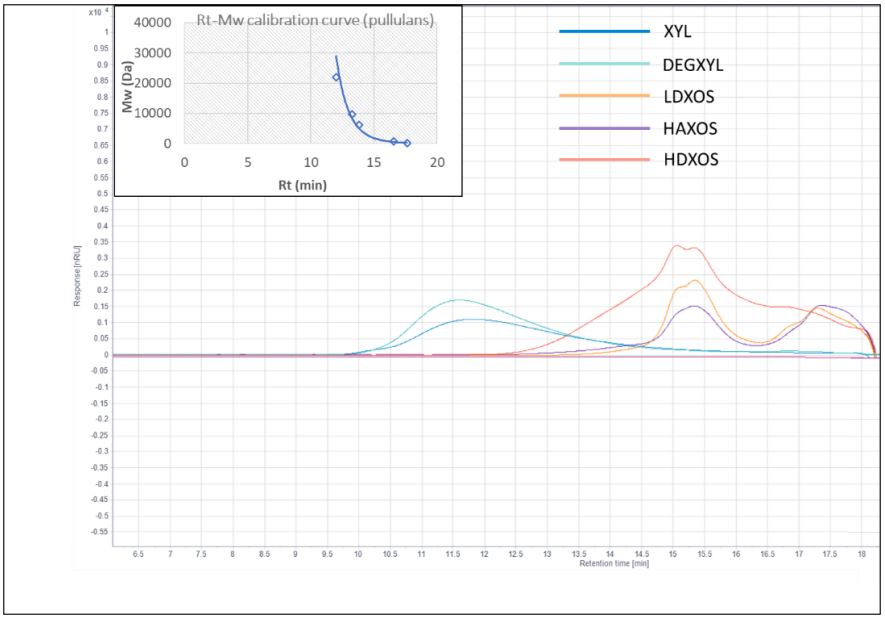

Figure 7.5: *HPSEC-RID chromatogram relative to Mw distribution of different XOS mixtures.*

3.2.2. Evaluation of degree of polymerization (DP) and degree of substitution (DS) through UPLC/ESI-MS

The reaction products of the enzymatic hydrolyses reported in Section 2.3 and Section 2.4 were analyzed for LDXOS, HDXOS, HAXOS and PURXOS samples by UPLC/ESI-MS (Section 2.5.1) to verify the actual expected obtainment of XOS mixes with different DP profiles. Results are reported in Table 7.3.

Table 7.3: *Relative distribution of DPs in the various hydrolysates and number of acetyl groups bound on acetylated XOS.*

	HDXOS	**LDXOS**	**HAXOS**		**PURXOS**
	gXOS/100g total XOS	gXOS/100g total XOS	gXOS/100g total XOS	number of acetyl groups	gXOS/100g total XOS
DP1 deac	1.4 ± 1.2	2.2 ± 0.1	1.6 ± 0.5	-	0 ± 0
DP1 ac	0 ± 0	0 ± 0	0 ± 0	0	0 ± 0
DP2 deac	14.4 ± 2.3	43.7 ± 0	16.1 ± 6.5	-	0 ± 0
DP2 ac	0 ± 0	0 ± 0	1.5 ± 0	1	0 ± 0
DP3 deac	21.8 ± 0.1	31.9 ± 0.5	9.6 ± 0.3	-	0 ± 0
DP3 ac	0 ± 0	0 ± 0	8.6 ± 1.3	1,2	0 ± 0
DP4 deac	20.8 ± 0.7	15.3 ± 0.1	1.6 ± 0.3	-	0 ± 0
DP4 ac	0 ± 0	0 ± 0	31.4 ± 2.9	1,2	0 ± 0
DP5 deac	20.8 ± 1.2	5.4 ± 0.1	0.3 ± 0.1	-	0 ± 0
DP5 ac	0 ± 0	0 ± 0	15.0 ± 2.1	1,2,3	0 ± 0
DP6 deac	9.1 ± 0.5	1.3 ± 0.1	0 ± 0	-	9.7 ± 0.1
DP6 ac	0 ± 0	0 ± 0	7.4 ± 0.8	1,2,3,4	0 ± 0
DP7 deac	6.4 ± 0.7	0 ± 0	0 ± 0	-	50.8 ± 1.1
DP7 ac	0 ± 0	0 ± 0	3.6 ± 0.7	1,2,3,4	0 ± 0
DP8 deac	2.8 ± 0.3	0 ± 0	0 ± 0	-	29.1 ± 1.4
DP8 ac	0 ± 0	0 ± 0	1.8 ± 0.5	2,3,4	0 ± 0
DP9 deac	1.4 ± 0.1	0 ± 0	0 ± 0	-	10.4 ± 0.1
DP9 ac	0 ± 0	0 ± 0	0.7 ± 0.1	3,4,5,6	0 ± 0
DP10 deac	1.1 ± 0.1	0 ± 0	0 ± 0	-	0.0 ± 0.0
DP10 ac	0 ± 0	0 ± 0	0.7 ± 0.2	4,5,6,7	0 ± 0

Since it was not possible to perform an accurate quantification with a calibration curve, due to the lack of DP7-10 standards in the market, a semi-quantification based on ratio of peak areas was performed. Moreover, the simultaneous presence of many different XOS with different patterns of acetylation made the resolution of analytes unfeasible in HAXOS sample, especially in the first part of the chromatogram (Figure 7.6c). Recently, a HILIC-based method for the separation of unsubstituted XOS with DP 2-8 and monoacetyl-substituted XOS with DP 3-8 was proposed [32]. However, as can be observed in Table 7.3, HAXOS hydrolysate contained acetylated XOS with DP up to 10 and all of them, except for xylose and xylobiose, were also found to be present with more than one acetyl group bound to the chain. Among them, the most

abundant turned out to be DP4, which accounted for 31% of the total XOS, followed by the DP5, representing 15%. HDXOS sample contained only deacetylated XOS, again having DPs up to 10, confirming the results of a previous work of our group [26]. In this case, the various XOS showed a percentage of DP ≥ 5 accounting for more than 40%. In general, the percentage distribution of the various deacetylated XOS in HDXOS and the one of the acetylated + deacetylated XOS in HAXOS was found to be similar, except for a slight difference in DP4 content (20.8% and 33% in HDXOS and HAXOS, respectively), indicating a good repeatability of the enzymatic hydrolysis. The hydrolysis conditions used for the LDXOS sample led, as expected, to obtain a mix of deacetylated XOS containing mainly low DPs. In detail, in this sample, over 75% of the XOS were made up of DP 2-3 and about 91% of DP 2-4. Finally, when the purified solution (PURXOS) was analyzed, it came out that it contained only four DPs, from 6 to 9. In particular, DP6 and DP9 accounted for about 10% of total XOS each, while DP7 turned out to be the most abundant, with more than 50% (Table 7.3). DP10 was also expected to be present in PURXOS, because it was detected in flow-ESI-MS in some tubes, but it was likely in trace amount.

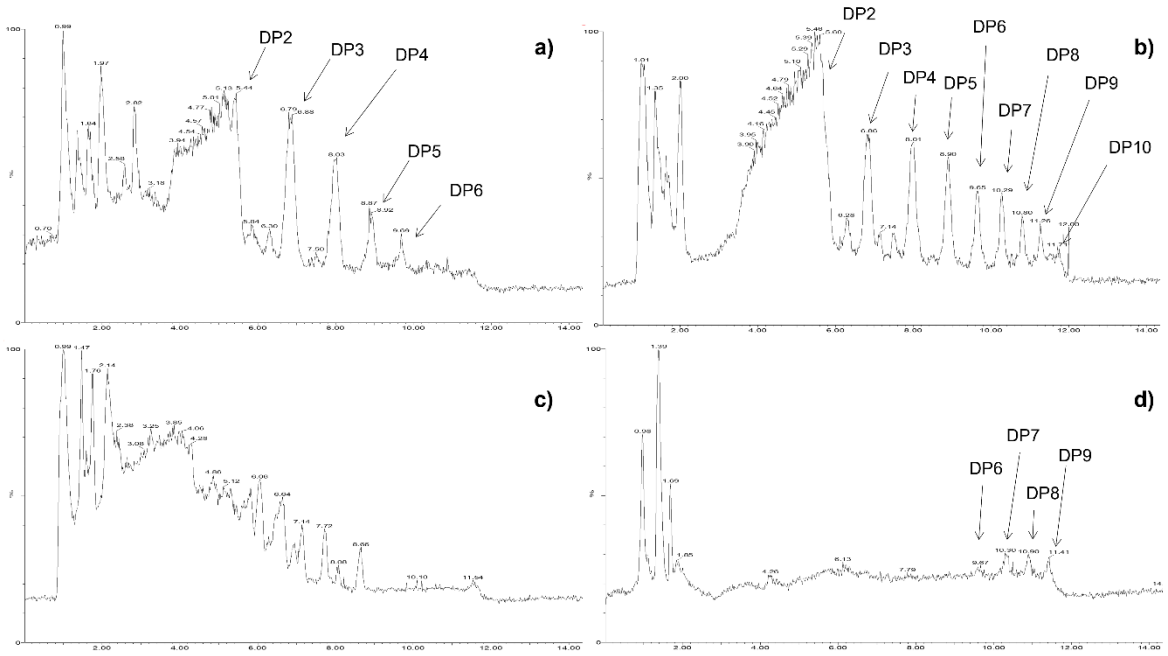

Figure 7.6: *Chromatograms obtained from UPLC/ESI-MS analysis carried out on LDXOS (a), HDXOS (b), HAXOS (c) and PURXOS (d).*

3.2.3. Metabolomic characterization through ^{1}HNMR

^{1}H NMR was performed as a metabolomic approach on every XOS and xylan sample, in order to investigate whether they actually consisted in pure fractions, or they contained other compounds that potentially influenced their functional properties, namely antioxidant activity. NMR spectra are reported in Figure 7.7.

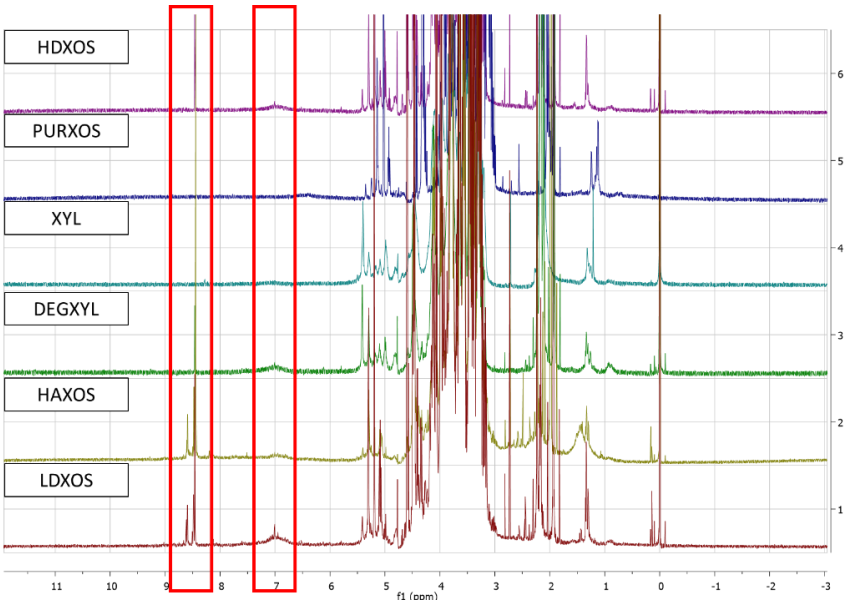

***Figure 7.7**: [1]H NMR spectra of different XOS mixtures. Zones of aromatics (6.5-7.5 ppm) and formic acid/aldehydes (8-9 ppm) are highlighted in red.*

Different compounds or classes of compounds were identified as formic acid/aldehydes, acetic acid, organic acids/amino acids, aromatic/phenolics, and semi-quantified as area ratios in respect to total sugars area. The sum of all these compounds was quite different among the samples, suggesting that the degree of purity was different. XYL, DEGXYL, HAXOS and PURXOS showed a total ^{1}H NMR area of impurities ranging from 2.8% to 3.6% of total sugar residues area, while LDXOS and HDXOS contained much higher values equal to 22% and 42%, respectively. In particular, in these two samples the most abundant compound was acetic acid, and this is totally in line with what was expected, being them the only samples where acetylxylan esterase was employed. At the same time, LDXOS and HDXOS were also the samples showing the highest quantity of organic acids/amino acids, with a spectral area that was around 2% and 5%, respectively, versus traces amount in the other samples. Finally, aromatics/phenolics and formic acid/aldehydes were present in the same samples in small amounts, with a spectral area between 0.4 and 1.5% in respect to sugar area and absent in the other samples. Since these samples came from the same standard commercial xylan (except for PURXOS, that was produced from a different one), the reasons for these various compositions may be found in thermal treatments carried out to inactivate the enzymes. Indeed, LDXOS and HDXOS, richer in secondary compounds, are the ones which underwent more times the inactivation step, at 100 °C for 10 minutes, being hydrolysed with three different times (Figure 7.1), and this could have led to the formation of more degradation compounds from xylose, as previously reported [33].

3.3. Antioxidant activity of XOS mixtures

The DPPH radical scavenging activity is one of the most used and accepted tools for estimating the anti-radical activity of different compounds. With the aim to better elucidate the carbohydrate structure-function relationship, the various xylans and XOS mixtures with different structures were analyzed to test their antioxidant activity. The results are reported in Figure 7.8.

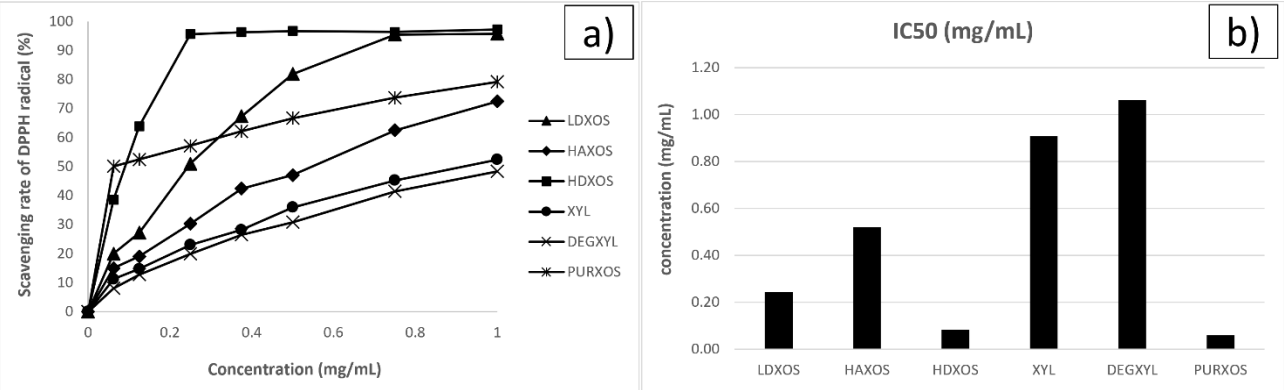

***Figure 7.8**: Radical scavenging activity, given as percentage inhibition, of different XOS/xylan mixtures in different concentrations (a), and calculated IC50 values (b).*

As expected, XOS exhibited a concentration-dependent antioxidant activity, meaning that the percentage of inhibition gradually increases when the concentration increases. Interestingly, many differences among samples were found: the high-molecular weight polysaccharides, that are XYL and DEGXYL, exhibited a relatively low antioxidant activity, with calculated IC50 values equal to 0.91 mg/mL and 1.06 mg/mL, respectively (Figure 7.8b). This better scavenging capacity found in XYL compared to DEGXYL, even if slight, is likely due to the presence of glucuronic acid present along the chain, which was instead removed in DEGXYL sample. Indeed, it has been previously reported how uronic acids increase antioxidant activity of cell wall polysaccharides, probably because of the presence of carboxyl groups [34]. Comparing DEGXYL with the three samples obtained after enzymatic hydrolysis of the same polysaccharide, namely LDXOS, HAXOS and HDXOS, the difference in IC50 was much bigger. Specifically, the calculated IC50 turned out to be 0.25 mg/mL for LDXOS, 0.52 mg/mL for HAXOS and 0.08 mg/mL for HDXOS. Hence, it can be stated that oligosaccharides in general showed a better antioxidant activity than polysaccharides: this may be explained by the higher solution mobility of low-Mw xylose-based chains [35] and by the weaker activity of high-Mw xylan's hydroxyl groups, being these compounds more susceptible to intra- and intermolecular forces [36]. Among oligosaccharides, the presence or absence of acetyl groups on XOS emerged to be of concern: IC50 of HDXOS turned out to be about 6 times lower compared to the one of HAXOS, which have a very similar distribution in DP (Table 7.2), but with much higher degree of substitution (DS). About that, in literature contrasting results have been obtained and proposed over the years. For instance, Rao & Muralikrishna stated that the

presence of sugars with higher amounts of C=O groups imparts strong antioxidant activity to cereal polysaccharides [23], while for chito-oligosaccharides a clear positive correlation between deacetylation degree and antioxidant activity was reported, although in this case this is likely attributed to the formation of more amino groups at the C-2 positions, absent in XOS [24,25,37]. According to recent studies, it is likely that acetyl groups are useful to enhance the scavenging capacity of XOS, but up to a certain DS. In fact, it has been reported how xylans could enhance their antioxidant activity when substituted with carboxymethyl groups, because of the intensification of the electron cloud density of the active hydroxyl groups, but at the same time a high DS of carboxymethyl groups could reduce this activity due to the small number of hydroxyl groups available as hydrogen donors [38]. Then, among the unsubstituted oligosaccharides obtained from the same commercial xylan (LDXOS and HDXOS), the ones having a higher DP showed a much better antioxidant activity. This positive correlation between antioxidant activity and DP was already proposed for XOS with DP up to 10 [19], although other studies on chitosans with different Mw, even though always > 10 kDa, showed the opposite trend [39,40]. Actually, the results obtained by testing these XOS and xylans mixtures (obtained from the same starting molecule) could be related not only to their chemical structure, but also to a variety of impurities, present in more or less high quantities and only partially quantified by ^{1}H NMR. In fact, LDXOS and HDXOS, which showed the highest scavenging capacity, were also the least pure ones (Section 3.2.2). Different molecules may have formed following the various heat treatments in the samples, affecting the results. In particular, aromatic/phenolic compounds were almost exclusively present in these two samples, albeit in low concentrations, and their antioxidant properties have been known for a long time [41]. Furthermore, the presence of formic acid in NMR spectra of LDXOS and HDXOS suggests that xylose has undergone thermal degradation [42], with the potential formation of a myriad of other compounds deriving from the metabolism of sugars with potential antioxidant capacity. Indeed, it has been previously reported how Maillard reaction was helpful to improve antioxidant activity of xylans [43] and how the rate of Maillard modification is increased when small molecules reactants are present because of reasons of steric hindrance (i.e., xylo-oligosaccharides rather than high-Mw xylans) [44]. At the same time, sugars dehydration could lead to double bonds and enolic compounds formation, which are notorious reducing agents. This agrees with results in our work, where HDXOS was the sample which underwent the enzyme inactivation (100 °C for 10 minutes) the greatest number of times together with LDXOS, but the first was hydrolysed in XOS as second step, whilst LDXOS as third (Figure 7.1). To shed more light on this aspect, the antioxidant test was also carried out on PURXOS, containing only XOS with DP 6-9 (Figure 7.8), on pure standard xylose and on pure XOS having a fixed degree of polymerization, that is DP2, DP3, DP4, DP5 and DP6, in order to understand and further confirm whether the length of the chain affected the antioxidant activity. The results were surprising: all the commercial compounds, purchased from Megazyme (Bray, County Wicklow, Ireland) or Fluka Chemicals (Buchs, Switzerland) and having a degree of purity greater than 90-95% showed little or almost no ability to reduce the DPPH radical. In detail, at the concentration of 2

mg/mL, xylose showed a percentage of scavenging equal to 11%, while DP2, DP3, DP4, DP5 and DP6 resulted in 38%, 16%, 15%, 15% and 12% of DPPH reduction capacity, respectively. These values were so low that it was not possible to calculate an IC50 value. Anyway, the activity of these standard XOS is far lower than the one obtained with all the samples previously tested, including xylans with high Mw, and the values themselves are quite in line with the ones calculated for malto-oligosaccharides in a previous work [45]. On the contrary, PURXOS turned out to be extremely antioxidant, even the best one among all samples tested, with an IC50 value equal to 0.06 mg/mL. This is in contradiction with the matter of impurities: indeed, this sample resulted to be the purest one, although in line with HAXOS, XYL and DEGXYL (Section 3.2.2). As concerns the absolute IC50 values that have been found in this work, it is important to underline that over time a lot of different ways for quantifying DPPH radical scavenging activity have been used, with different sample/DPPH ratios, incubation time and calculations [46], and this led to the obtainment of many different IC50 values in different works. Anyway, comparing the findings in this work with others in recent papers, it can be found that they are quite in line. For example, in XOS mixtures similar to LDXOS, containing XOS with DP 2-6, IC50 values of 0.6 or 0.7 mg/ml were calculated elsewhere [47,48], while other authors observed higher values, at nearly 1 mg/ml [49,50] or even incredibly higher, such as 14 or 35 mg/ml [51]. In the work of Huang and colleagues, a XOS mix similar to HDXOS and HAXOS in terms of DP but with a diverse pattern of substitution was tested, showing an IC50 of 1.1 mg/mL, that is two times the value calculated here [50].

From all these results it is clear once again that the antioxidant activity of oligo- and polysaccharides is anything but clearly understood. Even in recent literature, many contradictory results have been reported and abundantly summarized in the review by Wang and colleagues [22] and in general the mechanism of action is unclear. Furthermore, the authors rightly pointed out in their conclusions that most of the studies were performed on different matrices, and with different extraction and processing methods. Therefore, one can say that the antioxidant activity of oligo- and polysaccharides is determined by a combination of several factors related to each other [22]. In this sense, our study was carried out on compounds obtained starting from high-purity commercial standards. Our results seem to indicate that thermal treatments have an influence on the intensification of antioxidant capacity, probably due to sugars modification by Maillard reaction. At the same time, however, a clear indication of the existence of a correlation between chemical structure and antioxidant effect was found in samples containing the same amount of degradation compounds. In fact, it seems that XOS with higher Mw are somehow able to reduce DPPH radical much more easily than those with lower Mw: xylose and XOS with DP between 2 and 6 do not have a great effect, while those with DP between 6 and 9 do. At the same time, when the polysaccharide chain becomes much bigger, with the same purity and DS, the antioxidant capacity goes back down (HAXOS compared with DEGXYL), probably due to the coming into play of other factors, such as solubility and charge density.

3.4. Evaluation of prebiotic properties

XOS metabolism of Bifidobacteriaceae has been deeply investigated over the years, while information regarding lactic acid bacteria (LAB) is nowadays more unexplored [16,52]. For this reason, we decided to test in this study the *in vitro* prebiotic activity of a LAB strain, namely *L. brevis* DSM 20054, with different XOS mixtures as the only carbon source, namely LDXOS, HDXOS, HAXOS. Xylan samples, XYL and DEGXYL were also tested. In fact, a previous work showed how this strain gets some glycoside hydrolases adapt to metabolize XOS [16,53]. Together with it, the pathogenic bacteria *E. coli* K88 was also tested, in order to check if its growth was promoted as well, since it can cause intestinal infections [54]. In particular, change in turbidity (OD600 nm), pH, SCFA and lactic acid production were investigated and analysed. The results are reported in Figure 7.9.

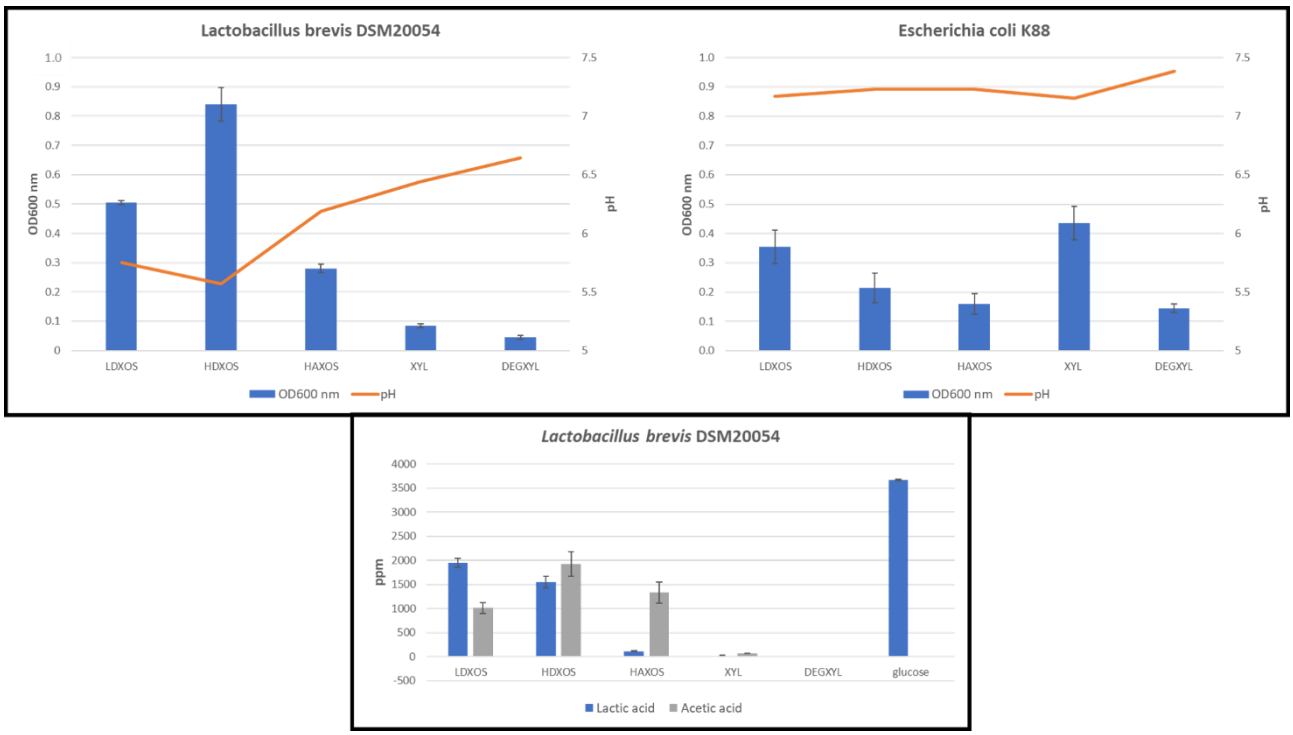

***Figure 7.9**: Changes in turbidity and in pH and organic acids production due to in vitro fermentation of different XOS mixtures by L. brevis DSM 20054 and E. coli K88. The results of turbidity and acids concentration are reported as a difference from the negative control.*

Figure 7.9 shows the changes in turbidity (OD600 nm) and in the pH of the culture broth, together with the production of organic acids after 48 h of *in vitro* fermentation of different XOS mixtures by the two strains tested. Both the strains showed a marked growth in terms of OD and pH changes when fed with glucose (positive control, data not shown). *L. brevis* also showed a good capability to metabolise XOS. Indeed, pH values close to 5.5 were reached in HDXOS and LDXOS, and the production of organic acids turned out to be quantitatively similar to the positive control. Interestingly, *L. brevis* produced lactic acid as the only organic acid, in an amount equal to 3.67 g/L when grown with glucose as the only carbon source, while also acetic

acid was abundantly present when it was fed with the three mixtures of XOS. No production of formic acid, propionic acid, butyric acid and ethanol was detected. HDXOS was the XOS sample which allowed to obtain the highest total organic acid production, equal to 3.47 g/L, followed by LDXOS (2.96 g/L) and HAXOS (1.45 g/L). Both the samples which did not undergo the hydrolysis with xylanase, namely XYL and DEGXYL, did not permit any growth for *L. brevis*: very small concentration of organic acids was found for XYL (0.08 g/L), and very small changes in OD and pH were spotted, in accordance with previous studies [55,56]. Lactic/acetic acid ratio came out to change a lot with the different carbon sources: if on one hand only lactic acid was detected employing glucose, on the other hand the quantity of acetic acid suddenly increased in LDXOS sample and increased again in HDXOS and HAXOS, suggesting a correlation between chain length of XOS and quantity of acetate, as already noticed by Iliev and colleagues [57]. However, a general preference of this strain for unsubstituted XOS was observed, and among the two unsubstituted XOS mixtures HDXOS was preferred, indicating a potential better effect for XOS with a higher DP in stimulating the growth of *L. brevis*.

E.coli K88 gave very easy to interpret results, showing no ability to grow on any of the carbon sources but glucose. Indeed, if on the one hand some small changes in turbidity were observed in XOS-enriched broths (OD600 nm= 0.18 – 0.35), no drops in pH were detected and no production of organic acids was observed, except for the positive control. In this latter case, a reduction in pH and a marked increase in turbidity demonstrated the ability of *E. coli* to grow with glucose, and HPLC analysis detected the presence of lactic acid among the metabolites produced, with lower amounts of ethanol (data not shown). These results are in accordance with previous works [29,55].

In general, these results show once again the great potential of XOS to be used as prebiotic compounds, thanks to their ability to stimulate the growth of positive bacteria, simultaneously inhibiting pathogenic ones.

4. Conclusions

XOS have been emerging for several years as compounds with a myriad of potential activities, but the relationship between their chemical structure and beneficial effects is still unclear. The prebiotic features have been largely studied, but there is still uncertainty about the structure-function relationship and the preferences of different strains for XOS with specific characteristics. On the other hand, the antioxidant activity is a property that has been experimentally attributed to XOS and oligosaccharides in general, without fully explaining the *in vitro* mechanism. Several authors have also reported how this property could be due not to oligosaccharides themselves, but to other compounds that are simultaneously extracted from agro-forestry by-products, such as phenolics. In this work, several XOS mixtures were produced starting from high-purity commercially available xylans by means of enzymatic hydrolysis coupled with tangential ultrafiltration. Several parameters of enzymatic hydrolysis were modified in order to obtain mixtures of XOS having different DP and degrees of acetylation and also a mixture of XOS with high DP (6-9) was produced by enzymatic

hydrolysis followed by purification through size-exclusion chromatography. Every mixture was characterized in terms of chemical structure and degree of purity, and the scavenging capacity against the DPPH radical together with the prebiotic potential were tested. Commercially available xylose and XOS showed almost no antioxidant activity, while the XOS obtained by enzymatic hydrolysis from xylan showed good values of IC50, between 0.06 and 0.5 mg/mL. Although this difference may be explained by the different degrees of purity, the sample containing XOS with DP 6-9 obtained by hydrolysis and purification nevertheless showed a very high scavenging capacity. Finally, at the same or similar degree of purity, acetylated XOS were found to be less effective than unsubstituted ones, and XOS with higher DP more effective than those with lower DP. Then, the prebiotic functionality of XOS was demonstrated once again since every mixture of XOS allowed the growth of *L. brevis* and inhibited *E. coli*. The former one exhibited a preference to deacetylated XOS, and among these a higher DP caused and even better proliferation. Non-hydrolysed xylans did not lead to any bacterial growth.

This work especially makes a further important contribution to understand the relationship between the chemical structure and the antioxidant activity of oligosaccharides, suggesting that the latter is on the one hand influenced by the impurities present in oligosaccharides extracts, but at the same time that XOS themselves have an evident activity, which is strongly correlated to the chemical structure.

REFERENCES

1. Kamble, A.; Deshmukh, R. Functional Food Market by Ingredient (Probiotics, Minerals, Proteins & Amino Acids, Prebiotics, & Dietary Fibers, Vitamins and Others), Product (Bakery & Cereals, Dairy Products, Meat, Fish & Eggs, Soy Products, Fats & Oils and Others), Application (Sport Available online: https://www.alliedmarketresearch.com/functional-food-market#:~:text=The functional food market size,that claims to improve health.

2. Daliri, E.B.-M.; Lee, B.H. Current Trends and Future Perspectives on Functional Foods and Nutraceuticals. **2015**, *27*, 221–244, doi:10.1007/978-3-319-23177-8_10.

3. Amorim, C.; Silvério, S.C.; Prather, K.L.J.; Rodrigues, L.R. From lignocellulosic residues to market: Production and commercial potential of xylooligosaccharides. *Biotechnol. Adv.* 2019.

4. Singh, R.D.; Banerjee, J.; Arora, A. Prebiotic potential of oligosaccharides: A focus on xylan derived oligosaccharides. *Bioact. Carbohydrates Diet. Fibre* **2015**, *5*, 19–30, doi:10.1016/j.bcdf.2014.11.003.

5. Xiang, L.; Wang, M.; Wu, L.; Lu, Z.; Tang, J.; Zhou, J.; Huang, W.; Zhang, G. Structural insights into xylanase mutant 254RL1 for improved activity and lower pH optimum. *Enzyme Microb. Technol.* **2021**, *147*, 109786, doi:10.1016/j.enzmictec.2021.109786.

6. Palaniappan, A.; Antony, U.; Emmambux, M.N. Current status of xylooligosaccharides: Production, characterization, health benefits and food application. *Trends Food Sci. Technol.* **2021**, *111*, 506–519, doi:10.1016/j.tifs.2021.02.047.

7. Broekaert, W.F.; Courtin, C.M.; Verbeke, K.; van de Wiele, T.; Verstraete, W.; Delcour, J.A. Prebiotic and other health-related effects of cereal-derived arabinoxylans, arabinoxylan-oligosaccharides, and xylooligosaccharides. *Crit. Rev. Food Sci. Nutr.* **2011**, *51*, 178–194, doi:10.1080/10408390903044768.

8. Aachary, A.A.; Prapulla, S.G. Xylooligosaccharides (XOS) as an Emerging Prebiotic: Microbial Synthesis, Utilization, Structural Characterization, Bioactive Properties, and Applications. *Compr. Rev. Food Sci. Food Saf.* **2011**, *10*, 2–16, doi:10.1111/j.1541-4337.2010.00135.x.

9. Fuso, A.; Risso, D.; Rosso, G.; Rosso, F.; Manini, F.; Manera, I.; Caligiani, A. Potential valorization of hazelnut shells through extraction, purification and structural characterization of prebiotic compounds: A critical review. *Foods* **2021**, *10*, 1197, doi:10.3390/foods10061197.

10. Wu, Y.; Chen, Y.; Lu, Y.; Hao, H.; Liu, J.; Huang, R. Structural features, interaction with the gut microbiota and anti-tumor activity of oligosaccharides. *RSC Adv.* **2020**, *10*, 16339–16348, doi:10.1039/d0ra00344a.

11. Ho, A.L.; Kosik, O.; Lovegrove, A.; Charalampopoulos, D.; Rastall, R.A. In vitro fermentability of xylo-oligosaccharide and xylo-polysaccharide fractions with different molecular weights by human faecal bacteria. *Carbohydr. Polym.* **2018**, *179*, 50–58, doi:10.1016/j.carbpol.2017.08.077.

12. Gullón, P.; Moura, P.; Esteves, M.P.; Girio, F.M.; Domínguez, H.; Parajó, J.C. Assessment on the fermentability of xylooligosaccharides from rice husks by probiotic bacteria. *J. Agric. Food Chem.* **2008**, *56*, 7482–7487, doi:10.1021/jf800715b.

13. Mendis, M.; Martens, E.C.; Simsek, S. How Fine Structural Differences of Xylooligosaccharides and Arabinoxylooligosaccharides Regulate Differential Growth of Bacteroides Species. *J. Agric. Food Chem.* **2018**, *66*, 8398–8405, doi:10.1021/acs.jafc.8b01263.

14. Kabel, M.A.; Kortenoeven, L.; Schols, H.A.; Voragen, A.G.J. In vitro fermentability of differently substituted xylo-oligosaccharides. *J. Agric. Food Chem.* **2002**, *50*, 6205–10, doi:10.1021/jf020220r.

15. Poletto, P.; Pereira, G.N.; Monteiro, C.R.M.; Pereira, M.A.F.; Bordignon, S.E.; de Oliveira, D. Xylooligosaccharides: Transforming the lignocellulosic biomasses into valuable 5-carbon sugar prebiotics. *Process Biochem.* **2020**, *91*, doi:10.1016/j.procbio.2020.01.005.

16. Michlmayr, H.; Hell, J.; Lorenz, C.; Böhmdorfer, S.; Rosenau, T.; Kneifel, W. Arabinoxylan oligosaccharide hydrolysis by family 43 and 51 glycosidases from Lactobacillus brevis DSM 20054. *Appl. Environ. Microbiol.* **2013**, *79*, 6747–6754, doi:10.1128/AEM.02130-13.

17. Vieira, T.F.; Corrêa, R.C.G.; Peralta, R.A.; Peralta-Muniz-Moreira, R.F.; Bracht, A.; Peralta, R.M. An Overview of Structural Aspects and Health Beneficial Effects of Antioxidant Oligosaccharides. *Curr. Pharm. Des.* **2018**, *26*, 1759–1777, doi:10.2174/1381612824666180517120642.

18. Singh, S.; Singh, R.P. In vitro methods of assay of antioxidants: An overview. *Food Rev. Int.* **2008**, *24*, 392–415, doi:10.1080/87559120802304269.

19. Valls, C.; Pastor, F.I.J.; Vidal, T.; Roncero, M.B.; Díaz, P.; Martínez, J.; Valenzuela, S. V. Antioxidant activity of

xylooligosaccharides produced from glucuronoxylan by Xyn10A and Xyn30D xylanases and eucalyptus autohydrolysates. *Carbohydr. Polym.* **2018**, *194*, 43–50, doi:10.1016/j.carbpol.2018.04.028.

20. Bouiche, C.; Boucherba, N.; Benallaoua, S.; Martinez, J.; Diaz, P.; Pastor, F.I.J.; Valenzuela, S. V. Differential antioxidant activity of glucuronoxylooligosaccharides (UXOS) and arabinoxylooligosaccharides (AXOS) produced by two novel xylanases. *Int. J. Biol. Macromol.* **2020**, *155*, 1075–1083, doi:10.1016/J.IJBIOMAC.2019.11.073.

21. Hung, Y.H.R.; Chen, G.W.; Pan, C.L.; Lin, H.T.V. Production of ulvan oligosaccharides with antioxidant and angiotensin-converting enzyme-inhibitory activities by microbial enzymatic hydrolysis. *Fermentation* **2021**, *7*, 160, doi:10.3390/fermentation7030160.

22. Wang, J.; Hu, S.; Nie, S.; Yu, Q.; Xie, M. Reviews on Mechanisms of in Vitro Antioxidant Activity of Polysaccharides. *Oxid. Med. Cell. Longev.* 2016, 1–13.

23. Rao, R.S.P.; Muralikrishna, G. Water soluble feruloyl arabinoxylans from rice and ragi: Changes upon malting and their consequence on antioxidant activity. *Phytochemistry* **2006**, *67*, 91–99, doi:10.1016/j.phytochem.2005.09.036.

24. Mengíbar, M.; Mateos-Aparicio, I.; Miralles, B.; Heras, Á. Influence of the physico-chemical characteristics of chito-oligosaccharides (COS) on antioxidant activity. *Carbohydr. Polym.* **2013**, *97*, 776–782, doi:10.1016/j.carbpol.2013.05.035.

25. Anraku, M.; Gebicki, J.M.; Iohara, D.; Tomida, H.; Uekama, K.; Maruyama, T.; Hirayama, F.; Otagiri, M. Antioxidant activities of chitosans and its derivatives in in vitro and in vivo studies. *Carbohydr. Polym.* **2018**, *199*, 141–149, doi:10.1016/j.carbpol.2018.07.016.

26. Fuso, A.; Rosso, F.; Rosso, G.; Risso, D.; Manera, I.; Caligiani, A. Production of xylo-oligosaccharides (XOS) of tailored degree of polymerization from acetylated xylans through modelling of enzymatic hydrolysis. *Food Res. Int.* **2022**, *UNDER PUBL*.

27. Waters UPLC/MS analysis of mono-, di- and oligosaccharides using Acquity UPLC BEH Amide columns. *Waters*.

28. AAT BIOQUEST Available online: https://www.aatbio.com/tools/ic50-calculator (accessed on Jun 26, 2022).

29. Ríos-Ríos, K.L.; Remond, C.; Dejonghe, W.; Van Roy, S.; Vangeel, S.; Van Hecke, W. Production of tailored xylo-oligosaccharides from beechwood xylan by different enzyme membrane reactors and evaluation of their prebiotic activity. *Biochem. Eng. J.* **2022**, *185*, 108494.

30. Ríos-Ríos, K.L.; Dejonghe, W.; Vanbroekhoven, K.; Rakotoarivonina, H.; Rémond, C. Enzymatic Production of Xylo-oligosaccharides from Destarched Wheat Bran and the Impact of Their Degree of Polymerization and Substituents on Their Utilization as a Carbon Source by Probiotic Bacteria. *J. Agric. Food Chem.* **2021**, *69*, 13217–13226, doi:10.1021/acs.jafc.1c02888.

31. Kabel, M.A. Characterisation of Complex Xylo-Oligosaccharides from Xylan Rich By-Products, 2002.

32. Pu, J.; Zhao, X.; Xiao, L.; Zhao, H. Development and validation of a HILIC-ELSD method for simultaneous analysis of non-substituted and acetylated xylo-oligosaccharides. *J. Pharm. Biomed. Anal.* **2017**, *139*, 232–237, doi:10.1016/j.jpba.2017.03.007.

33. Lindgren, G.; Pernemalm, P.A. A High Performance Preparative Procedure For The Isolation Of Degradation Products From D-Xylose. *J. Liq. Chromatogr.* **1980**, *3*, 1737–1742, doi:10.1080/01483918008064764.

34. Pristov, J.B.; Mitrović, A.; Spasojević, I. A comparative study of antioxidative activities of cell-wall polysaccharides. *Carbohydr. Res.* **2011**, *346*, 2255–2259, doi:10.1016/j.carres.2011.07.015.

35. Chen, H.; Liu, Y.; Yang, T.; Chen, D.; Xiao, Y.; Qin, W.; Wu, D.; Zhang, Q.; Lin, D.; Liu, Y.; et al. Interactive effects of molecular weight and degree of substitution on biological activities of arabinoxylan and its hydrolysates from triticale bran. *Int. J. Biol. Macromol.* **2021**, *166*, 1409–1418, doi:10.1016/j.ijbiomac.2020.11.020.

36. Mendez-Encinas, M.A.; Carvajal-Millan, E.; Ortega-García, J.; Santiago-Gómez, L.B.; De Anda-Flores, Y.; Martínez-Robinson, K.G.; Valencia-Rivera, D.E. Effect of ultrasound-treated arabinoxylans on the oxidative stability of soybean oil. *Antioxidants* **2020**, *9*, 147, doi:10.3390/antiox9020147.

37. Yen, M.T.; Yang, J.H.; Mau, J.L. Antioxidant properties of chitosan from crab shells. *Carbohydr. Polym.* **2008**, *74*, 840–844, doi:10.1016/j.carbpol.2008.05.003.

38. Marquez-Escalante, J.A.; Rascón-Chu, A.; Campa-Mada, A.; Martínez-Robinson, K.G.; Carvajal-Millan, E. Influence of carboxymethylation on the gelling capacity, rheological properties, and antioxidant activity of feruloylated arabinoxylans from different sources. *J. Appl. Polym. Sci.* **2020**, *137*, 48325, doi:10.1002/app.48325.

39. Sun, T.; Zhou, D.; Xie, J.; Mao, F. Preparation of chitosan oligomers and their antioxidant activity. *Eur. Food Res. Technol.* **2007**, *225*, 451–456, doi:10.1007/s00217-006-0439-1.

40. Tomida, H.; Fujii, T.; Furutani, N.; Michihara, A.; Yasufuku, T.; Akasaki, K.; Maruyama, T.; Otagiri, M.; Gebicki, J.M.; Anraku, M. Antioxidant properties of some different molecular weight chitosans. *Carbohydr. Res.* **2009**, *344*, 1690–1696, doi:10.1016/j.carres.2009.05.006.

41. Hromádková, Z.; Košťálová, Z.; Ebringerová, A. Comparison of conventional and ultrasound-assisted extraction of phenolics-rich heteroxylans from wheat bran. *Ultrason. Sonochem.* **2008**, *15*, 1062–1068, doi:10.1016/j.ultsonch.2008.04.008.

42. JING, Q.; LÜ, X. Kinetics of Non-catalyzed Decomposition of D-xylose in High Temperature Liquid Water* * Supported by the National Natural Science Foundation of China (No.20476089) and the Project of the Ministry of Science and Technology of China (No.2004CCA05500). *Chinese J. Chem. Eng.* **2007**, *15*, 666–669, doi:10.1016/S1004-9541(07)60143-8.

43. Deng, W.; Luo, J.; Yan, X. Maillard reaction between chitosan and xylan in ionic liquids. *Ferroelectrics* **2020**, *562*, 39–45, doi:10.1080/00150193.2020.1760582.

44. Zhang, M.; Zhan, A.; Ye, Y.; Liu, C.; Hang, F.; Li, K.; Li, J. Molecular modification, structural characterization, and biological activity of xylans. *Carbohydr. Polym.* **2021**, *269*, 118248, doi:10.1016/j.carbpol.2021.118248.

45. Hu, S.; Yin, J.; Nie, S.; Wang, J.; Phillips, G.O.; Xie, M.; Cui, S.W. In vitro evaluation of the antioxidant activities of carbohydrates. *Bioact. Carbohydrates Diet. Fibre* **2016**, doi:10.1016/j.bcdf.2016.04.001.

46. Marinova, G.; Batchvarov, V. Evaluation of the methods for determination of the free radical scavenging activity by DPPH. *Bulg. J. Agric. Sci.* **2011**, *17*, 11–24.

47. Bian, J.; Peng, F.; Peng, X.P.; Peng, P.; Xu, F.; Sun, R.C. Structural features and antioxidant activity of xylooligosaccharides enzymatically produced from sugarcane bagasse. *Bioresour. Technol.* **2013**, *127*, 236–241, doi:10.1016/j.biortech.2012.09.112.

48. Abdella, A.; Ramadan, S.; Hamouda, R.A.; Saddiq, A.A.; Alhazmi, N.M.; Al-Saman, M.A. Paecilomyces variotii xylanase production, purification and characterization with antioxidant xylo-oligosaccharides production. *Sci. Rep.* **2021**, *11*, 16468, doi:10.1038/s41598-021-95965-w.

49. Zhang, L.; Zeng, X.; Qiu, J.; Du, J.; Cao, X.; Tang, X.; Sun, Y.; Li, S.; Lei, T.; Liu, S.; et al. Spray-dried xylooligosaccharides carried by gum Arabic. *Ind. Crops Prod.* **2019**, *135*, 330–343, doi:10.1016/j.indcrop.2019.04.045.

50. Huang, C.; Wang, X.; Liang, C.; Jiang, X.; Yang, G.; Xu, J.; Yong, Q. A sustainable process for procuring biologically active fractions of high-purity xylooligosaccharides and water-soluble lignin from Moso bamboo prehydrolyzate. *Biotechnol. Biofuels* **2019**, *12*, 189, doi:10.1186/s13068-019-1527-3.

51. Victoria Gautério, G.; Amorim, C.; Silvério, S.C.; Cardoso, B.B.; Ballesteros, L.F.; Alves, J.I.; Alcina Pereira, M.; Silva, S.P.; Coelho, E.; Coimbra, M.A.; et al. Hydrolysates containing xylooligosaccharides produced by different strategies: Structural characterization, antioxidant and prebiotic activities. *Food Chem.* **2022**, *391*, 133231, doi:10.1016/J.FOODCHEM.2022.133231.

52. Mäkeläinen, H.; Forssten, S.; Saarinen, M.; Stowell, J.; Rautonen, N.; Ouwehand, A.C. Xylo-oligosaccharides enhance the growth of bifidobacteria and Bifidobacterium lactis in a simulated colon model. *Benef. Microbes* **2010**, *1*, 81–91, doi:10.3920/BM2009.0025.

53. Moura, P.; Barata, R.; Carvalheiro, F.; Gírio, F.; Loureiro-Dias, M.C.; Esteves, M.P. In vitro fermentation of xylo-oligosaccharides from corn cobs autohydrolysis by Bifidobacterium and Lactobacillus strains. *LWT - Food Sci. Technol.* **2007**, *40*, 963–972, doi:10.1016/j.lwt.2006.07.013.

54. Deneke, C.F.; McGowan, K.; Larson, A.D.; Gorbach, S.L. Attachment of human and pig (K88) enterotoxigenic Escherichia coli strains to either human or porcine small intestinal cells. *Infect. Immun.* **1984**, *45*, 522–524, doi:10.1128/iai.45.2.522-524.1984.

55. Falck, P.; Precha-Atsawanan, S.; Grey, C.; Immerzeel, P.; Staìšlbrand, H.; Adlercreutz, P.; Nordberg Karlsson, E. Xylooligosaccharides from hardwood and cereal xylans produced by a thermostable xylanase as carbon sources for lactobacillus brevis and bifidobacterium adolescentis. *J. Agric. Food Chem.* **2013**, *61*, 7333–7340, doi:10.1021/jf401249g.

56. Mäkeläinen, H.; Saarinen, M.; Stowell, J.; Rautonen, N.; Ouwehand, A.C. Xylo-oligosaccharides and lactitol promote the growth of Bifidobacterium lactis and Lactobacillus species in pure cultures. *Benef. Microbes* **2010**, *1*, 139–148, doi:10.3920/BM2009.0029.

57. Iliev, I.; Vasileva, T.; Bivolarski, V.; Momchilova, A.; Ivanova, I. Metabolic profiling of xylooligosaccharides by lactobacilli. *Polymers (Basel).* **2020**, *12*, 2387, doi:10.3390/polym12102387.

CHAPTER 8

Conclusions and future perspectives

8.1. Background scenario

Scientific research on dietary fibre has greatly increased in recent years, mainly due to the need for consumers to move toward healthier diets. In parallel, therefore, attention has been gradually gained more and more from new potential sources of dietary fibre to meet the growing market demand. These new sources often match with wastes and by-products (mainly vegetable ones, but not only) coming from agro-forestry, food and feed industries in a re-valorisation perspective, due to the need for a linear-to -circular economy transition, dictated by economic, environmental and ethical reasons. However, reusing dietary fibre in a smart way achieving products with a high added value is far from obvious and indeed very challenging. Different fibres are in fact contained in different matrices, which are therefore more or less suitable for extraction by different methods, and the latter can strongly impact the chemical structure of the extracts as well. In addition, when the goal is the production of functional foods, the dietary fibre extract is often and willingly subjected to further transformations, such as enzymatic hydrolysis to obtain oligosaccharides, which as well as extraction methods are still far from being optimized, standardized, and fully understood. All of this is very important, since it is universally recognized in science that the chemical structure of dietary fibres (in terms of monosaccharide composition, type of glycosidic bonds, molecular weight and degree of polymerization, amount and type of substituents along the main chain, etc.) is strictly related to their techno/bio-functional properties. Thus, it is easy to deduce that the need to refine analytical techniques is another necessary step, in order to be able to understand quickly and easily all the structural features of the obtained dietary fibre, and more in general all the secondary compounds that can be formed, so that we can be able to delineate a sort of process-structure-functionality relationship.

8.2. Principal findings of this PhD thesis and future prospects

This dissertation dealt with the potential reuse of dietary fibre from sources that to date are highly unexplored. Different studies were carried out within the various chapters, concerning extractions by innovative methods, enzymatic modification, and characterization of fibre and other compounds simultaneously originating from certain processes.

First, for the extraction of some soluble fibres, enzymatic-assisted extraction (EAE) methods were tested. They are currently of great interest and have the peculiarity of exploiting the hydrolytic action of one or more enzymes on compounds that are not of interest, in order to facilitate the passage into solution of other compounds, in this case indigestible polysaccharides. Specifically, AOAC method 991.43, which is generally used for the quantification of dietary fibre in complex matrices, was tested for the first time to isolate and purify bacterial-derived exopolysaccharides (EPS) produced by strains of the genus *Lactobacillus*, previously isolated from food matrices. Subsequent addition of an alcohol solution to induce precipitation of

unhydrolyzed polysaccharides (i.e., EPS) was performed to promote recovery to a high degree of purity of these molecules. The results showed good extraction yields from a quantitative point of view, although these extracts had a rather high residual nitrogen content. Amino acids analysis showed that a good portion of the latter was indeed attributable to unhydrolyzed proteins, suggesting the need to further optimize the proteolytic activity to obtain totally pure EPS fractions. An EAE method was also tested in this thesis for the purpose of obtaining soluble fibre from fruit by-products, namely seeds, peels and kernels, in a fractionation approach that is supposed to involve the simultaneous passage of peptides into solution by means of a protease. Again, isolation and purification of the extracted soluble fibre was achieved by addition of alcohol. It was evident from the results that this method was more or less advantageous depending on the by-product considered, probably due to different complex inter- and intramolecular interactions and bonds. As well as allowing the extraction of proteins, in fact, the same process allowed in some cases to obtain yields of soluble fibre close to 71% of the initial content, showing the applicability of the method for the simultaneous recovery of different compounds with a consequent interesting economic interest for companies. Despite the swinging results, it is worth considering how the enzymatic assisted extraction will likely be at the forefront in the near future as one of the most promising extraction methods for micro- and macromolecules (including dietary fibre) due to its peculiarity of being non-invasive, in terms of pH and temperature conditions and in terms of use of acids, bases, and solvents, thus allowing for low-degraded dietary fibre recovery. In particular, future studies could focus further on understanding how to raise this degree of purity, for example through the use of other enzyme mixtures with different and various activities. In addition, it should be kept in mind that, for example, EPS could potentially be produced by fermentation of a wide range of food products, containing different compositions. For this reason, the EAE should be adapted and refined on a case-by-case basis, and further studies are therefore encouraged.

As repeatedly mentioned in this thesis, dietary fibre and the matrices they are contained in are enormously variable. For this reason, although in some cases a "mild" extraction such as EAE is applicable to obtain soluble fibre fractions, in others it is not because of the great structural complexity of biomasses. This is the case with hemicellulose extraction from lignocellulosic matrices, which have recently gained great interest in the scientific literature because of the high availability of by-products. Hydrothermal treatment (HT) is one of the most widely used methods in recent years to solubilize hemicellulose. It has been applied in the present thesis on hazelnut shells, and it has been investigated in particular in the form of two aspects, namely the impact it has on the formation of degradation compounds (originated especially from lignin and sugars, but not only) and the impact that the process temperature has on the same compounds and on the chemical structure of polysaccharides. This is the first time that an untargeted metabolomics approach has been applied on such an extract to investigate in this degree of detail which compounds are present. In fact, several

techniques were combined, and among them for the first time UHPLC-ESI-Q-TOF-MS, thanks to which more than 200 compounds were putatively identified in a single extract. In most cases, in fact, scientific articles have focused only on the detection of small and volatile molecules by GC-MS, but in this work it was shown how the latter method actually allows the characterization of a very small portion compared to the totality of products actually present. Phenols, phenyls, furans, modified sugars (such as anhydrous sugars, deoxy sugars), but also aldehydes, ketones, fatty and organic acids were detected, often organized in complex structures containing more than one functional group. When the goal of using this type of treatment on lignocellulosic biomass is to produce functional ingredients, as repeatedly proposed in the literature, our approach would become of utmost importance from a risk assessment point of view. The work about HT lays the foundation for the future construction of "reactomics" databases, which could be exploited in the future to create predictive models, based on the matrix employed and on the time/temperature coupling. Indeed, it is known that different treatments can lead to different reaction mechanisms. The effect caused by a change in temperature was studied by testing the HT process from 125 °C to 200 °C and, in fact, a change was detected in the number of compounds and in the relative abundance of the main chemical classes, although furans and phenols were almost always among the most abundant ones, due to the predominant degradation of sugars and lignin. At the same time, the change in the operative temperature also highlighted the possibility of obtaining different dietary fibre extracts with varying compositions. Pectin can be extracted at lower temperatures without excessively impacting their molecular weights, while xylans or their xylo-oligosaccharide oligomers (XOS) were only extractable with more severe heat treatments. These results give advice for a hypothetical hydrothermal treatment-based fractionation of the various hazelnut shell fibres, in order to derive the highest possible value.

Xylans, the most abundant hemicellulose in nature, have frequently been reported as an ideal substrate for further post-extraction enzymatic modification by xylanase to produce XOS, which have shown strong bioactivity. However, the relationship between chemical structure of XOS and their functional properties has never been fully elucidated in the literature, and most studies have focused on getting a low degree of polymerization (DP), which are easier to be obtained and have better prebiotic properties according to many authors. In this thesis, enzymatic modelling was proposed for the purpose of understanding how the products outcome could vary, using always the same commercial enzymes and substrates but varying some hydrolysis conditions, and XOS with varying DP profiles were obtained, up to a maximum of 10. The method was also found to work on a non-standard xylan previously extracted from grape stalks, demonstrating its potential applicability to a wide range of acetylated xylans from different sources. These results were then exploited to produce in higher quantities mixtures of XOS with varying chemical structures, i.e., DP and degree of acetylation, and their antioxidant and prebiotic properties were studied. It was found that both functional

properties were highly dependent on the mixture tested, with a general improvement when unsubstituted XOS with a slightly higher DP were considered. These results are strongly impactful because they suggest that gut-level fermentability, while reported to be generally enhanced by XOS with low DPs, probably actually depends on the strain considered. In addition, further light has been shed in this thesis on the mechanism of *in-vitro* antioxidant activity of oligosaccharides, which has been debated at length over time, showing first and foremost that small variations in DP can have a very high influence, and that oligosaccharides can be considered antioxidants *per se* and not only because they are extracted together with phenolic components, as often claimed in the literature. Despite these advances, we are still quite far from a total understanding of the structure-function relationship of oligosaccharides, and therefore many more studies in this field are required. However, a correct approach is to characterize these structures in as much detail as possible, so that more plausible hypotheses can be made as to why a particular bioactive effect then occurs.

What is certain is that dietary fibre still needs a tremendous amount of research, which must be pursued simultaneously on different fronts. Extractions need to be refined and if possible conducted as much as possible toward environmentally friendly methods. Characterization needs to be conducted in detail, also by improving analytical techniques for carbohydrates (which to date are rather far from giving a complete and high throughput overview about every structural aspect) but also for all the compounds that can originate from their extraction. Enzymatic hydrolysis still needs to be optimized and programmed upstream, depending on the products that one wants to obtain. Only when all these aspects will be clarified, it will be possible to fully take advantage of dietary fibre, with potentially great benefits for everyone, from companies to consumers.

SUPPLEMENTARY MATERIAL

Table S1: *Whole list of compounds identified by UHPLC-ESI-Q-TOF-MS (Chapter 4).*

Compound	m/z	Retention time (min)	CCS (angstrom ^2)	Identifications	Abundance	Accepted Compound ID	Adducts	Formula	Fragmentation Score	Mass Error (ppm)	Chemical class	2nd functional group
1	221,0446	3,51	145,2017	95	0,36457746	CSID3826452	M-H2O-H	C11H12O6	80,2	-3,76569	acid	
2	131,0343	2,03	227,61243	90	0,09433611	CSID11391544	M-H2O-H	C5H10O5	93,7	-4,7894	acid	
3	169,0135	1,65	124,76945	28	60,0835449	CSID30791782	M-H2O-H	C7H8O6	91,1	-4,19057	acid	aconitate
4	271,0961	5,51	217,73666	179	221,129877	CSID34243986	M-H2O-H	C16H18O5	83,2	-4,97281	acid	indeno
5	239,055	4,44	149,63265	43	10,4093715	CSID76759102	M-H	C11H12O6	88,8	-4,73636	acid	pyranone
6	175,0593	3,34	258,93797	173	21,6999601	CSID2282560	M+H	C7H10O5	80	-4,68369	acid	oxopimelic
7	175,0593	2,23	221,7438	172	2,22295424	CSID10246715	M+H-H2O	C7H12O6	93,2	-3,99817	acid	quinic
8	371,1451	5,97	189,81578	997	349,412828	CSID24625183	M+Na	C19H24O6	81,29	-4,13594	acid	
9	217,0698	5,20	263,88963	178	2,42360915	CSID28639106	M+H	C9H12O6	82,2	-3,82135	acid	aconitic acid
10	365,1926	8,08	204,1858	247	229,37975	CSID30776552	M+Na	C18H30O6	96,1	-2,57747	acid	oxopentanoic
11	137,0237	3,19	124,72099	54	1,35358312	CSID26333149	M-H2O-H	C7H8O4	87,8	-4,57538	aldehyde	
12	203,0906	4,28	237,13133	215	345,761268	CSID26629356	M+H	C9H14O5	87,8	-3,74217	aldehyde	
13	773,2333	5,81	270,24699	13	1,61858656	CSID59053982	M-H2O-H	C30H48O24	89,9	-3,08854	anhydro sugar	
14	323,0971	1,23	215,43754	808	4,41896935	CSID59054002	M-H	C12H20O10	94,5	-3,84003	anhydro sugar	
15	611,1804	5,23	269,8688	97	1,85562805	CSID59054021	M-H2O-H	C24H38O19	92,4	-3,89666	anhydro sugar	
16	485,1509	0,64	228,05636	132	90,8316262	CSID59054022	M-H2O-H, M-H	C18H30O15	81,8	-0,58343	anhydro sugar	
17	981,2943	3,95	298,03268	6	36,6228923	CSID59054032	M+FA-H	C36H56O28	94,8	0,293428	anhydro sugar	
18	307,1014	3,03	227,1024	522	2,28771499	CSID35035383	M+H-H2O	C12H20O10	82,3	-2,94679	anhydro sugar	
19	325,1116	0,59	244,32032	1252	0,72245101	CSID58837516	M+H	C12H20O10	88,8	-4,22266	anhydro sugar	
20	335,097	1,36	206,38489	484	0,52719615	CSID11602677	M+FA-H	C12H18O8	85	-4,84896	conjugated sugar	methyl
21	341,1075	1,36	209,02995	901	0,85595769	CSID14950152	M+FA-H	C15H20O4S	87,1	3,694706	conjugated sugar	thio, phenyl
22	641,4247	8,58	263,30579	11	28,2300188	CSID23282469	M-H	C35H62O10	80	-3,63764	conjugated sugar	fatty acids
23	337,1129	0,77	170,14007	550	11,6260369	CSID24707775	M+FA-H	C12H20O8	81,1	-3,95299	conjugated sugar	cyclohexene
24	419,1185	4,72	229,71191	649	4,59791384	CSID24783244	M+FA-H	C16H22O10	92	-2,63177	conjugated sugar	pyran
25	467,1395	3,27	228,47543	495	0,97286408	CSID28510575	M+FA-H	C17H26O12	85,2	-2,70463	conjugated sugar	cyclopentapyran
26	343,1165	6,55	183,64687	171	0,63611187	CSID28520124	M-H2O-H	C15H18N6O5	88,6	1,355806	conjugated sugar	pyrrol pyrimidine
27	593,1854	7,02	240,45105	130	41,9824928	CSID31121633	M-H2O-H	C28H36O15	80	-3,65353	conjugated sugar	cyclopentapyran
28	341,1081	0,60	172,73558	701	9,9963752	CSID58827461	M-H	C12H22O11	84,3	-2,47194	conjugated sugar	polyol
29	1031,309	4,66	322,33562	5	5,35624228	CSID76963261	M-H	C38H64O30S	87,7	-3,84008	conjugated sugar	methyl-thio
30	419,1184	3,27	218,12611	646	3,99182287	CSID29420015	M-H	C17H24O12	93,2	-2,59929	conjugated sugar	ketone
31	741,2743	6,01	264,70473	41	186,922875	CSID78439066	M-H2O-H	C38H48O16	82,4	-2,76807	conjugated sugar	anthraquinone
32	405,1366	2,20	188,73603	201	114,725527	CSID18500537	M+Na, M+K	C15H26O11	87,5	-0,26445	conjugated sugar	allyl
33	217,0692	5,55	270,25137	272	4,52164751	CSID19101799	M+Na	C7H14O6	86,3	4,624374	conjugated sugar	methyl
34	389,1055	3,11	183,673	252	2237,01109	CSID23228223	M+H-H2O, M+Na	C15H18N4O7	89,41	-3,43512	conjugated sugar	purine
35	732,2564	5,61	257,12494	64	33,0138475	CSID23243407	M+H-H2O	C28H47NO22	81,7	0,981081	conjugated sugar	tri-hydroxypropyl, amino sugar
36	387,1049	5,20	192,09294	928	903,002236	CSID24647090	M+K	C15H24O9	80,2	-0,75885	conjugated sugar	cyclopentapyran
37	439,1439	3,38	270,59609	1056	16,6379188	CSID24695921	M+Na	C15H28O13	84,6	4,020173	conjugated sugar	propyl,
38	439,1443	2,01	245,93005	981	1,04828546	CSID28506451	M+H	C17H26O13	81	-0,60623	conjugated sugar	cyclopentapyran
39	403,1358	5,20	188,7963	757	65,9170211	CSID28667993	M+K	C16H28O9	87	-2,00097	conjugated sugar	cyclopentapyran
40	488,1914	3,73	211,94887	670	125,0899	CSID29395950	M+H	C25H29NO9	83,4	-0,2548	conjugated sugar	quinoline
41	704,2597	4,18	254,60648	71	0,89212087	CSID58921850	M+NH4	C27H42O20	85,8	-1,54527	conjugated sugar	cyclopentapyran
42	558,2021	4,40	221,85919	414	13,7277946	CSID59001605	M+NH4	C22H28N4O12	83,3	-3,78363	conjugated sugar	pyridin uridin
43	523,1654	5,11	277,38657	633	0,37052302	CSID76963227	M+Na	C19H32O15	83,9	3,996077	conjugated sugar	propyl acetate
44	439,144	3,74	239,8853	1056	6,70633563	CSID88294435	M+Na	C15H28O13	88	4,232707	conjugated sugar	propyl
45	627,1761	3,61	234,02254	59	14,7208207	CSID5257038	M-H2O-H	C24H38O20	91,3	-2,56653	deoxy sugar	
46	645,1883	1,50	239,55678	46	257,714766	CSID64808493	M-H	C24H38O20	95,9	-0,11388	deoxy sugar	uronic
47	717,2092	4,49	262,07315	24	79,3013328	CSID4450778	M-H	C27H42O22	80	-0,44765	kdo	
48	479,14	3,75	242,82477	452	25,0191106	CSID4450780	M-H2O-H	C19H30O15	93,4	-1,33636	kdo	
49	471,135	1,33	199,83145	433	9,40710427	CSID26331896	M-H	C17H28O15	94,6	-1,15863	kdo	
50	423,1132	3,22	192,54505	641	0,17657748	CSID26332278	M-H	C16H24O13	81,9	-2,84898	kdo	
51	573,1658	2,88	229,1631	115	0,35146841	CSID28533587	M-H2O-H	C21H36O19	82,7	-2,43861	kdn	
52	481,1552	4,01	250,71759	955	44,8358484	CSID28533759	M+H	C19H28O14	92,4	0,045539	kdo	
53	481,155	3,26	250,7176	905	23,1150179	CSID30786392	M+H	C19H28O14	87,4	-0,37084	kdo	
54	269,2111	7,97	175,32489	57	7,47303912	CSID4446129	M-H	C16H30O3	80,8	-4,20976	fatty acid	oxo
55	183,0291	0,99	144,75555	27	22,2616688	CSID9358110	M-H2O-H, M-H	C8H8O5	90,6	-4,51374	furan	acid
56	339,1992	7,80	203,39555	86	3939,0448	CSID15342562	M-H	C19H32O3S	80,6	-2,03415	furan	acid-S-hydrocarbon
57	255,05	0,72	148,93861	90	0,24652954	CSID21378038	M+FA-H	C10H10O5	80,7	-4,89934	furan	benzo
58	239,0551	4,17	149,63264	44	2,8895317	CSID23234785	M-H2O-H	C11H14O7	81,5	-3,7463	furan	hydro, acetyl
59	325,1068	5,19	201,05562	635	52,9751612	CSID23331761	M-H	C19H18O5	84,1	-4,15904	furan	phenol
60	697,4882	9,10	274,41064	17	60,4074094	CSID24685809	M+FA-H	C38H68O8	96,2	-2,197	furan	fatty acids
61	241,05	3,77	160,24483	235	0,50870927	CSID24709261	M-H2O-H	C14H12O5	98,6	-2,60991	furan	phenyl
62	751,2962	6,25	270,56371	37	431,043754	CSID26343912	M+FA-H	C39H46O12	94	-1,35842	furan	
63	293,0679	0,56	155,45474	163	89,9933477	CSID26355255	M-H	C14H14O7	92,8	4,063733	furan	phenol
64	209,0446	3,90	140,55776	75	8,86641038	CSID34250432	M-H	C10H10O5	83,1	-4,55437	furan	
65	209,0444	5,97	140,55777	26	0,12499321	CSID34485443	M-H2O-H	C10H12O6	94	-4,89576	furan	acid
66	373,0913	6,32	188,29471	416	1,28631323	CSID76771869	M-H2O-H	C19H20O9	82,4	-4,13006	furan	
67	587,1763	4,61	226,02082	144	112,402664	CSID76790927	M+FA-H	C24H26N6O9	81,4	3,557125	furan	adenosine
68	217,0699	3,81	223,77383	179	20,0743942	CSID23234438	M+H	C9H12O6	97,3	-3,35558	furan	
69	359,1099	4,43	184,65245	780	4,35084981	CSID24642312	M+Na	C17H20O7	90	-0,62293	furan	benzofuran
70	367,2082	6,29	189,94916	269	11,4316168	CSID113369383	M+Na	C18H32O6	81,9	-2,72665	furan	fatty acid
71	177,0548	6,21	137,22443	142	30,4707096	CSID20037401	M-H2O-H	C10H12O4	95,6	-4,64806	ketone	
72	297,0607	1,26	160,65732	138	14,42138	CSID23138575	M+FA-H	C12H12O6	97,3	-3,59371	ketone	
73	137,0592	4,68	122,9472	285	127,105679	CSID121746	M+H-H2O	C8H10O3	96,2	-3,3226	ketone	
74	363,107	4,35	183,04554	346	52,0593665	CSID10404377	M+FA-H	C17H18O6	84,5	-4,92076	phenol	polyphenol
75	327,0862	6,60	181,40234	643	63,5711792	CSID10481709	M+FA-H	C17H14O4	90,6	-4,20228	phenol	anthraquinone
76	293,1749	7,14	185,40672	183	79,9919729	CSID15492673	M-H	C17H26O4	86	-3,17547	phenol	
77	255,05	3,39	151,58775	91	117,072661	CSID17250122	M+FA-H	C10H10O5	86,6	-4,69142	phenol	naphtalenone
78	467,1706	5,40	211,22095	633	1239,04594	CSID17613806	M+FA-H	C25H26O6	94,6	-1,39337	phenol	

81	361,1281	3,86	188,64214	412	108,186223	CSID23237598	M+FA-H	C18H20O5	95,7	-3,8228	phenol	benzoic
82	385,0917	6,89	193,52939	431	0,25379392	CSID23237714	M+FA-H	C19H16O6	96,5	-3,4849	phenol	
83	403,138	6,15	198,64545	306	157,721259	CSID23275381	M-H	C21H24O8	87,8	-4,689	phenol	cycloheandienone
84	675,2426	6,14	256,76673	73	76,3054956	CSID23339930	M-H	C37H40O12	89,2	-3,11238	phenol	bi-flavan
85	343,1177	6,17	175,40148	567	552,560357	CSID24677850	M-H2O-H	C19H22O7	81,2	-2,86197	phenol	cyclic
86	355,1171	6,51	200,03688	523	33,0266109	CSID24691019	M-H	C20H20O6	81,9	-4,46064	phenol	polyphenol
87	343,117	5,26	186,41709	426	214,991662	CSID24704446	M-H	C19H20O6	89,6	-4,92118	phenol	benzoate
88	257,0651	0,89	148,85596	66	0,26385534	CSID24710929	M-H	C15H14O2S	90,1	3,74306	phenol	thio
89	421,1129	5,65	189,81421	375	140,722781	CSID24843088	M+FA-H	C19H20O8	88,3	-2,96921	phenol	benzoquinone
90	355,117	6,32	194,40892	527	24,6861647	CSID26621665	M-H2O-H	C20H22O7	94,3	-4,66298	phenol	
91	311,091	6,43	179,19438	548	29,8001838	CSID26628360	M-H2O-H	C18H18O6	81,7	-4,57554	phenol	
92	343,1179	5,78	189,19806	551	68,1572484	CSID28289687	M+FA-H	C18H18O4	85,1	-2,82685	phenol	cyclic
93	445,1123	5,57	197,60921	487	36,6086241	CSID28497556	M-H	C22H22O10	90,5	-3,8324	phenol	dimer
94	373,1278	6,13	191,07562	535	1688,15832	CSID28502964	M+FA-H	C19H20O5	86,2	-4,64854	phenol	cyclic
95	301,0707	6,50	168,61052	503	119,881124	CSID28524789	M-H2O-H	C16H16O7	97,7	-3,1847	phenol	
96	319,1173	5,39	212,70889	208	125,112553	CSID28528888	M-H2O-H	C17H22O7	98,5	-4,21822	phenol	anthracene
97	237,0394	5,73	147,0774	53	19,1853159	CSID29417418	M-H	C11H10O6	86,4	-4,50416	phenol	
98	195,0291	3,31	133,49666	68	11,0430151	CSID30778482	M-H	C9H8O5	80,2	-4,1122	phenol	acid
99	305,0808	6,86	182,17382	345	40,2002999	CSID30791352	M-H2O-H	C19H16O5	82,8	-3,42822	phenol	benzoanthracene
100	363,1071	5,21	177,55086	324	50,4789431	CSID34448447	M-H	C18H20O8	92,2	-4,05125	phenol	vanillic
101	513,1759	5,99	210,2438	284	666,789428	CSID58131499	M+FA-H	C26H28O8	84,6	-1,57533	phenol	cyclic
102	337,1066	6,54	189,39328	586	45,7057132	CSID58837470	M-H2O-H	C20H20O6	87,3	-4,42534	phenol	tetraphene
103	509,1805	6,18	218,88248	299	42,2313792	CSID58967839	M-H2O-H	C28H32O10	85,5	-2,16534	phenol	dimer
104	225,0758	5,22	150,30183	104	213,382174	CSID65727490	M-H	C11H14O5	98,1	-4,42014	phenol	
105	315,0861	5,21	179,05405	543	68,9440383	CSID74851586	M-H2O-H	C17H18O7	84,9	-4,01283	phenol	stilbene
106	225,0393	2,98	142,37278	46	1,55124131	CSID74851747	M-H	C10H10O6	87,2	-4,96179	phenol	oxirane
107	363,1077	4,97	188,58351	314	352,751255	CSID74852044	M+FA-H	C17H18O6	86,6	-2,80908	phenol	polyphenol
108	361,1282	3,79	185,86714	392	38,7876545	CSID76742486	M+FA-H	C18H20O5	87,7	-3,46587	phenol	
109	551,1896	6,36	232,48063	184	141,084629	CSID76765780	M-H	C30H32O10	82,2	-4,76294	phenol	trimer
110	507,2003	6,28	224,679	244	46,2592134	CSID90633377	M+FA-H	C28H30O6	94,6	-4,62936	phenol	
111	729,2085	4,62	255,93586	13	8,13238679	CSID90636923	M-H	C41H34N2O11	89	-0,67533	phenol	
112	167,0698	2,37	127,91336	462	6,78200145	CSID11594935	M+H	C9H10O3	89,1	-2,5098	phenol	
113	315,1216	4,62	175,24628	1042	28,4860013	CSID11704719	M+H	C18H18O5	91,2	-3,43574	phenol	
114	455,1667	6,98	195,72161	129	62,6042721	CSID17241798	M+NH4, M+Na	C23H28O8	92,9	-2,03718	phenol	
115	433,1466	5,80	204,84599	803	24,1094884	CSID20151407	M+Na	C20H26O9	84,6	-0,81042	phenol	chlorogenic
116	253,0852	4,60	167,12756	949	98,6116322	CSID21782013	M+H-H2O	C16H14O4	87,9	-2,5998	phenol	
117	627,2052	5,14	235,08781	36	4578,69933	CSID23173031	M+Na, M+K	C31H32N4O9	83,2	-1,59951	phenol	
118	579,1511	3,22	218,47906	338	27,7831951	CSID24647781	M+H-H2O	C30H28O13	81,9	2,277168	phenol	polyphenol
119	421,164	6,06	225,55538	1251	233,921857	CSID24842497	M+H	C25H24O6	98,6	-1,25449	phenol	
120	433,1477	3,85	204,84596	182	9507,82773	CSID25065916	M+Na, M+K	C21H22N4O5	91,5	-1,33341	phenol	benzoic acid-phenol-pirimidine
121	339,1212	6,10	182,59188	1526	55,0042929	CSID26369952	M+Na	C18H20O5	93,4	2,997969	phenol	
122	637,2246	6,53	268,28947	164	226,190462	CSID26607197	M+Na	C32H38O12	85,5	-1,57951	phenol	lignan-furofuran
123	373,1259	5,22	189,74937	982	3266,86409	CSID28502846	M+Na	C18H22O7	96,2	0,213665	phenol	
124	274,1067	4,27	166,10958	821	112,469673	CSID28505583	M+H	C15H15NO4	85,4	-2,29953	phenol	
125	179,0696	6,20	137,23168	318	244,4667	CSID31107037	M+H-H2O, M+H	C10H10O3	91,6	-3,52567	phenol	
126	373,1259	5,09	192,55338	348	3366,13784	CSID31107281	M+Na, M+K	C18H22O7	80	0,368531	phenol	stilbene
127	357,131	6,36	187,50331	1213	0,875224	CSID31128872	M+Na	C18H22O6	86,1	0,56928	phenol	
128	209,0802	2,37	140,42785	627	4,10924261	CSID35015217	M+H-H2O	C11H14O5	93,5	-2,58918	phenol	
129	375,1428	6,10	186,89241	1003	2,02973054	CSID35516836	M+H	C20H22O7	94,5	-2,68633	phenol	
130	607,2152	6,56	265,87079	279	230,804166	CSID58919814	M+Na	C31H36O11	87,7	0,389137	phenol	lignan-furofuran
131	321,1114	6,53	191,66956	1032	68,067087	CSID64869948	M+H-H2O	C20H18O5	89,7	-2,25514	phenol	piranone
132	295,0447	3,57	163,4165	164	0,1987849	CSID2341148	M-H2O-H	C13H14O9	86,6	-3,98322	phenol sugar	
133	453,1392	3,53	194,6333	404	22,4616783	CSID23250328	M+FA-H	C20H24O9	84,5	-2,55035	phenol sugar	furan
134	671,2036	4,52	259,81217	48	187,05216	CSID24611611	M+FA-H	C25H38O18	85,9	-0,72049	phenol sugar	
135	641,1925	4,71	233,79227	58	5,62627833	CSID24620764	M+FA-H	C24H36O17	85,5	-1,65588	phenol sugar	
136	709,2186	3,24	253,26787	33	24,7302915	CSID24643621	M+FA-H	C28H40O18	81,3	-1,55039	phenol sugar	
137	363,107	5,46	194,1642	244	49,0640548	CSID24694781	M-H2O-H	C18H22O9	86,9	-4,12259	phenol sugar	
138	483,1644	5,01	216,5727	361	29,4653433	CSID24846348	M-H2O-H	C26H30O10	86,4	-3,23508	phenol sugar	polyphenol
139	901,2793	5,76	289,78617	5	4,82257964	CSID26380758	M+FA-H	C42H48O19	93	2,490563	phenol sugar	polyphenol
140	389,123	5,61	201,84501	454	232,060385	CSID28517153	M-H2O-H	C20H24O9	86,4	-2,92175	phenol sugar	condensed
141	377,108	3,82	219,34053	607	45,7720261	CSID31115248	M+FA-H	C14H20O9	91,1	-2,76926	phenol sugar	
142	373,1278	5,07	199,4847	535	205,563363	CSID34448433	M-H2O-H	C20H24O8	94,8	-3,88428	phenol sugar	
143	495,1648	6,24	219,17811	314	211,175295	CSID58115060	M-H	C27H28O9	86,5	-2,57613	phenol sugar	
144	569,201	6,16	237,9681	136	1025,51143	CSID58133901	M-H2O-H	C30H36O12	80,8	-3,24578	phenol sugar	cyclo
145	653,192	5,62	269,11178	69	1,04498321	CSID58837450	M+FA-H	C25H36O17	80,6	-2,37869	phenol sugar	
146	941,2765	5,67	304,68462	3	1,41001776	CSID58859723	M-H2O-H	C45H52O23	90	4,621777	phenol sugar	
147	363,0378	2,95	180,29473	169	4,39038281	CSID76787382	M-H	C13H16O10S	84,6	-3,81829	phenol sugar	sulphate
148	411,1285	3,95	192,84148	372	20,0204608	CSID76962639	M+FA-H	C16H20N3O7-	87,9	-1,05628	phenol sugar	pyrimidoquinoline
149	529,1693	5,87	215,61974	216	31,3560589	CSID90654801	M-H2O-H	C27H32O12	86,4	-4,08413	phenol sugar	
150	521,165	5,35	212,92676	291	26,5895637	CSID90659472	M-H2O-H	C25H32O13	86,3	-2,55465	phenol sugar	
151	487,1573	5,29	197,71441	637	590,504385	CSID390804	M+Na	C23H28O10	96,9	-0,30709	phenol sugar	diffutine
152	363,1409	6,54	178,99507	477	550,544698	CSID21379031	M+Na	C17H24O7	98,4	-1,421	phenol sugar	
153	667,2054	4,21	237,25431	113	6,84230735	CSID23228441	M+H-H2O	C35H32N4O11	99,4	2,730447	phenol sugar	purine
154	499,1565	6,16	205,93049	776	156,671161	CSID23250372	M+Na	C24H28O10	81,9	-2,12287	phenol sugar	benzodioxine
155	345,1319	5,18	185,14662	1086	45,7624465	CSID23320289	M+Na	C17H22O6	86,7	3,10916	phenol sugar	propylidene
156	431,1171	4,70	187,98598	974	325,734967	CSID23326458	M+H-H2O	C18H24O13	86,9	-2,98558	phenol sugar	
157	505,1685	5,04	220,21817	620	0,52075371	CSID24677040	M+H-H2O	C25H30O12	85,7	-3,65214	phenol sugar	furan
158	537,1731	5,99	225,28217	78	2735,05227	CSID24708206	M+Na, M+K	C27H30O10	94,2	-0,07636	phenol sugar	polyphenol
159	565,1665	6,10	233,48141	378	115,415063	CSID24844468	M+Na	C28H30O11	80,3	-2,84164	phenol sugar	polyphenol
160	888,2933	7,31	276,03754	7	220,428398	CSID25050706	M+NH4, M+Na	C42H46O20	88,6	1,432992	phenol sugar	
161	431,1312	4,57	193,57222	178	3512,7847	CSID26347909	M+H-H2O, M+Na, M+I	C20H24O9	97,4	-0,13073	phenol sugar	stilbene
162	605,2203	7,31	232,58574	67	536,59372	CSID26632985	M+H, M+Na, M+K	C28H38O13	81,9	-0,23021	phenol sugar	lignan
163	764,2106	1,77	262,66608	23	85,5724417	CSID35031951	M+Na	C33H41O19+	82,6	-3,01635	phenol sugar	pelargonidina
164	581,1973	5,58	236,08787	309	91,4943012	CSID58859132	M+2Na-H	C27H36O11	88,7	0,60126	phenol sugar	gallic acid

165	1067,329	1,44	321,2419	4	25,4890585	CSID59696251	M+H	C48H58O27	98,9	4,941246	phenol sugar	
166	765,2727	6,00	271,92163	54	1417,06134	CSID78439059	M+Na	C38H46O15	85,4	-0,2371	phenol sugar	antracene
167	449,1062	0,59	197,51766	316	12,8305607	CSID58164029	M-H	C16H22N2O13	88,8	2,815814	peptide	citric
168	763,2569	6,07	268,85528	9	982,539294	CSID76793986	M+Na, M+K	C34H40N6O13	89,1	3,215095	peptide	
169	271,0967	4,68	175,24382	472	742,646453	CSID20051020	M-H2O-H	C16H18O5	83,9	-2,89589	phenyl	condensed
170	373,0911	5,25	191,07667	216	42,4250551	CSID30777034	M-H2O-H, M-H	C19H18O8	85,1	-4,63644	phenyl	naphtalene
171	175,1111	7,15	137,52436	640	51,2206305	CSID71995	M+H-H2O	C12H16O2	90	-3,3113	phenyl	fatty acid
172	147,0435	6,20	137,33723	196	95,9983121	CSID109958	M+H	C9H6O2	91,5	-3,6675	phenyl	
173	147,0437	1,75	132,16222	195	8,89955281	CSID133480	M+H-H2O	C9H8O3	97,4	-2,05039	phenyl	
174	223,0961	4,09	150,04013	376	125,562398	CSID11552701	M+H, M+Na	C12H14O4	86,2	-1,67946	phenyl	
175	297,1111	5,09	170,52223	1220	40,4485565	CSID23226256	M+H-H2O	C18H18O5	80,6	-3,33641	phenyl	
176	313,1055	6,42	180,82975	1365	32,8280742	CSID26629012	M+H-H2O	C18H18O6	81,1	-4,70737	phenyl	naphtyl
177	189,0901	6,04	144,30656	680	17,4750152	CSID58876663	M+H	C12H12O2	92,3	-4,89866	phenyl	
178	399,1416	6,24	200,18088	1143	1266,37274	CSID58917271	M+Na	C20H24O7	87,9	0,52993	phenyl	pyranone
179	405,1174	5,07	201,40806	516	56,5959379	CSID25033535	M+FA-H	C19H20O7	98,4	-4,69441	phenyl sugar	
180	281,0862	2,01	237,83124	375	1,0257227	CSID26392259	M-H2O-H	C14H20O5S	83,6	2,946321	phenyl sugar	tio
181	409,1498	4,06	187,33714	457	167,306771	CSID58112527	M-H2O-H	C20H28O10	83,9	-1,50104	phenyl sugar	
182	517,1671	5,91	205,49349	653	56,0730113	CSID22914151	M+Na	C24H30O11	86,6	-1,86373	phenyl sugar	
183	341,1374	5,83	190,88339	1392	181,823596	CSID24620226	M+H-H2O	C20H22O6	84,1	-2,65294	phenyl sugar	naphtyl
184	333,0939	6,68	166,44014	515	73,774295	CSID24785656	M+Na	C15H18O7	94,5	-1,88291	phenyl sugar	
185	555,1832	4,90	221,92841	405	682,433813	CSID29408698	M+Na	C27H32O11	83,9	-0,81657	phenyl sugar	anthracene
186	611,2098	6,05	247,42194	207	34,7792885	CSID34249053	M+K	C27H40O13	98,7	-0,3437	phenyl sugar	
187	329,1585	8,08	202,70844	310	274,452979	CSID90660067	M+H	C16H24O7	92,5	-3,0732	phenyl sugar	
188	585,1965	5,91	231,84402	137	685,140472	CSID90661213	M-H2O-H	C30H36O13	99,1	-2,08407	biphenyl sugar	
189	789,2727	6,07	274,59873	61	314,80626	CSID24712489	M+H	C37H44N2O17	84,6	1,841963	biphenyl-phenyl sugar	
190	371,1089	5,55	187,02582	116	7,78810579	CSID25033188	M+H, M+Na	C18H20O7	83,1	-3,63615	biphenyl sugar	
191	397,1258	6,13	177,93011	1267	3999,35336	CSID28643083	M+Na	C20H22O7	96,4	-0,00706	biphenyl sugar	furan
192	285,1118	4,60	165,62036	1033	340,408992	CSID28647748	M+H-H2O	C17H18O5	82,7	-1,07999	biphenyl sugar	
193	471,1628	5,61	215,29408	156	1237,46869	CSID29409377	M+Na, M+K	C23H28O9	82,2	0,64376	biphenyl sugar	
194	339,1214	5,24	185,36746	1495	8,8460683	CSID90635894	M+Na	C18H20O5	82	3,540957	biphenyl sugar	
195	179,0341	5,06	131,86548	106	14,79946	CSID208606	M-H2O-H	C9H10O5	94,9	-4,5503	quinone	
196	469,1496	6,11	211,17629	372	904,898126	CSID11016034	M-H2O-H	C26H24N4O6	80,4	-4,48715	pyrimidine	
197	225,0396	1,17	142,37276	31	19,3643967	CSID24691928	M-H2O-H, M-H	C10H10O6	84,3	-3,69943	pyranone	
198	255,05	0,80	148,93861	90	0,37637194	CSID24701096	M+FA-H	C10H10O5	96,7	-4,70038	pyranone	acrylate
199	319,1174	5,52	215,59264	317	254,654166	CSID74852763	M-H	C17H20O6	86,1	-4,1829	pyranone	phenol
200	175,0593	2,87	255,76681	174	0,62112682	CSID19969519	M+H	C7H10O5	80,5	-4,40895	ester	glycerol
201	217,07	4,70	235,88551	178	13,634339	CSID28489224	M+H	C9H12O6	98,3	-3,06823	ester	acetyl
202	217,0698	4,94	257,57785	179	7,13369955	CSID76785395	M+H	C9H12O6	83,1	-4,01421	ester	
203	384,1493	3,54	183,82792	992	0,5816586	CSID4450542	M+H	C14H25NO11	90,1	-2,01648	amino sugar	N-acetyl
204	676,2633	3,25	258,21484	108	24,2005792	CSID26331596	M+H	C26H45NO19	87,1	-3,88461	amino sugar	N-acetyl
205	738,2671	2,72	263,14397	41	18,3567716	CSID26331731	M+H	C27H47NO22	90,1	1,093776	amino sugar	N-acetyl
206	870,3096	2,82	285,7443	51	16,7778847	CSID26332408	M+H	C32H55NO26	89,1	1,27862	amino sugar	N-acetyl
207	706,2402	3,37	251,52859	63	13,6121357	CSID64808523	M+H-H2O	C26H45NO22	83,9	0,134609	amino sugar	aminoethyl
208	606,224	1,44	250,5628	243	4,73326079	CSID10293387	M+Na	C21H37N5O14	86,4	1,78403	sugar pyrimidinone	
209	265,0909	1,63	256,96959	274	1,31122076	CSID10662488	M+Na	C9H14N4O4	86,1	0,805374	sugar pyrimidinone	
210	399,1412	5,81	197,34511	1141	378,963673	CSID23271221	M+H	C17H22N2O9	90	3,462545	sugar pyrimidinone	
211	1012,336	4,33	302,60518	12	560,907557	CSID26332395	M+Na	C36H63NO30	97,7	3,43546	polyol	
212	365,1046	0,59	173,46705	1190	136,938241	CSID30777338	M+Na	C12H22O11	92,4	-2,33597	polyol	methyl

Table S2: Whole list of compounds identified by UHPLC-ESI-Q-TOF-MS (Chapter 5).

					Abundance														
Compound	m/z	Retention time (min)	CCS (angstrom^2)	Identifications	125 f	125	150 f	150	175 f	175	200 f	200	Accepted Compound ID	Adducts	Formula	Fragmentation Score	Mass Error (ppm)	Chemical class	2nd functional group	3rd functional group
1	245,0451	0,69	149,3645	116	0	0	0	0	0	0	10	3	CSID20149500	M-H2O-H	C13H12O6	90,4	-1,7283	acetyl sugar		
2	223,0239	1,79	139,8504	23	0	1	0	60	0	1	0	1	CSID20167396	M-H	C10H8O6	96,8	-4,1677	acetyl sugar		
3	323,0972	3,86	224,1442	805	0	1	0	11	97	114	37	3	CSID58827392	M+FA-H	C11H18O8	90	-4,0078	acetyl sugar		
4	349,1116	3,55	225,2137	872	0	0	0	9	15	151	4	3	CSID9188670	M+H	C14H20O10	95	-3,7324	acetyl sugar		
5	349,1119	4,12	243,2236	920	0	1	0	25	31	211	12	3	CSID9188670	M+H	C14H20O10	93,5	-2,9071	acetyl sugar		
6	774,2685	5,89	268,6547	22	0	0	0	1	0	22	0	0	CSID58145361	M+H	C30H47NO22	96,4	2,9235	acetyl sugar		
7	101,0242	2,02	234,1443	86	0	0	0	0	0	0	0	0	CSID290	M-H	C4H6O3	93,6	-2,4467	acid		
8	193,0496	3,43	281,1825	50	0	0	0	0	0	5	0	0	CSID160745	M-H2O-H	C10H12O5	94,1	-4,6521	acid	cyclic	
9	169,0499	2,90	271,4618	48	0	0	0	1	1	15	0	4	CSID389947	M-H2O-H, M-H	C8H10O4	91,6	-4,5673	acid	cyclic	
10	295,0447	3,57	163,4165	164	0	5	0	11	0	6	0	4	CSID2341148	M-H2O-H	C13H14O9	96,4	-3,9832	acid	salicylic	
11	167,0341	4,54	127,4833	100	0	0	0	0	0	2	0	19	CSID4955602	M-H	C8H8O4	96	-4,9903	acid	cyclic	
12	173,0446	3,81	227,9171	28	0	0	0	0	0	1	0	0	CSID10246715	M-H2O-H	C7H12O6	93,2	-4,6874	acid	quinic	
13	131,0343	2,03	227,6124	90	0	0	0	0	2	3	0	0	CSID11391544	M-H2O-H	C5H10O5	93,7	-4,7894	acid		
14	169,0135	1,65	124,7694	28	3	137	4	79	0	30	0	14	CSID15925247	M-H	C7H6O5	95,7	-4,6679	acid		
15	151,0394	5,12	126,0960	138	0	3	0	62	23	81	258	267	CSID21474558	M-H	C8H8O3	94	-4,2370	acid	cyclic	
16	151,0393	3,17	128,6963	51	0	0	0	13	0	20	3	29	CSID30778474	M-H2O-H	C8H10O4	93,5	-4,7590	acid		
17	153,0187	4,06	120,7841	46	0	0	0	11	0	6	0	10	CSID32809790	M-H2O-H	C7H8O5	91,7	-3,9371	acid		
18	228,0504	1,65	271,6443	27	0	0	0	0	0	0	0	0	CSID59696635	M-H	C9H11NO6	92,3	-4,4164	acid	amino	
19	217,0495	6,58	142,7682	75	0	0	0	0	0	4	0	19	CSID68015722	M-H2O-H	C12H12O5	94,6	-4,9191	acid		
20	175,0595	1,28	183,6465	174	0	0	0	6	2	5	0	0	CSID1063	M+H	C7H10O5	90	-3,4624	acid		
21	175,0593	2,23	221,7438	172	0	1	0	6	6	67	3	6	CSID10246715	M+H-H2O	C7H12O6	93,2	-3,9982	acid	quinic	
22	254,1601	2,69	164,3677	236	0	4	0	16	5	9	2	1	CSID10697657	M+NH4	C10H20O6	97,4	1,0249	acid		
23	175,0593	3,34	258,9380	173	0	3	0	57	31	209	20	17	CSID13500927	M+H	C7H10O5	96,1	-4,6837	acid		
24	151,0383	4,76	139,5601	218	0	26	0	21	0	2	0	1	CSID18519128	M+H-H2O	C8H8O4	96,1	-4,1229	acid	cyclic	
25	387,1411	5,87	192,0918	1070	8	732	0	188	0	18	4	148	CSID24625388	M+Na	C19H24O7	93,4	-0,7791	acid		
26	217,0698	5,20	263,8896	178	0	0	1	8	2	13	1	0	CSID28639106	M+H	C9H12O6	92,2	-3,8214	acid	aconitic	
27	299,0762	1,97	163,2739	196	0	0	0	0	0	5	1	0	CSID24679429	M+FA-H	C12H14O6	90	-4,1699	aldehyde		
28	137,0239	3,92	122,1269	87	15	297	22	195	164	128	511	200	CSID26333149	M-H2O-H	C7H8O4	90,6	-3,2717	aldehyde	acid	
29	409,0436	2,87	187,3398	218	0	63	0	2	0	0	0	0	CSID76787382	M+FA-H	C13H16O10S	95,2	-2,8151	aldehyde	phenyl	
30	363,0378	2,95	180,2947	169	0	52	0	12	0	0	0	0	CSID76787382	M-H	C13H16O10S	94,2	-3,8183	aldehyde	phenyl	
31	197,0801	5,26	195,9844	548	0	12	0	15	0	0	0	0	CSID24636192	M+H	C10H12O4	95,5	-4,0180	aldehyde	phenyl	
32	609,3406	7,14	291,2481	43	52	42	130	27	585	12	532	35	CSID76767679	M+FA-H	C31H44N6O4	97,5	-0,0604	amide		
33	677,4973	6,10	271,7159	8	523	0	1449	0	2688	0	2303	0	CSID10471886	M+FA-H	C34H68N2O8	95,1	2,3608	amine	sugar	
34	298,3457	7,63	204,0694	39	24	30	30	22	30	11	41	31	CSID74630	M+H	C20H43N	98,6	-3,8615	amine		
35	362,3262	7,00	207,1643	48	4499	172	5390	120	6037	53	9828	112	CSID3744847	M+H	C20H43NO4	98,6	-0,8499	amine		
36	286,3100	7,29	190,3865	41	95	0	97	0	104	0	145	0	CSID8101521	M+H	C18H39NO	95,4	-1,5585	amine		
37	326,3409	8,94	208,5891	32	406	529	410	381	418	180	715	414	CSID23237743	M+H-H2O	C21H45NO2	97,5	-2,5370	amine		
38	384,1493	3,54	183,8279	992	0	1	0	2	2	21	2	3	CSID4450542	M+H	C14H25NO11	91	-2,0165	amino sugar		
39	676,2633	3,25	258,2148	108	0	0	0	12	36	43	11	0	CSID26331596	M+H	C26H45NO19	97,6	-3,8846	amino sugar		
40	1012,3361	4,33	302,6052	12	0	27	3	925	142	825	33	7	CSID26332395	M+Na	C36H63NO30	97,7	3,4355	amino sugar		
41	870,3096	2,82	285,7443	51	0	21	0	56	155	766	31	57	CSID26332408	M+H	C32H55NO26	91,8	1,2786	amino sugar		
42	1069,3461	4,76	222,3164	14	0	0	0	29	0	0	0	0	CSID26332519	M+2Na-H	C38H64N4O28	91,4	4,1553	amino sugar		
43	826,2838	0,60	270,8413	25	0	6	24	162	0	0	0	0	CSID30786303	M+H	C30H51NO25	91,4	1,8499	amino sugar	hepp, kdo	
44	611,1800	1,89	238,4072	210	12	584	25	1165	2548	4685	1297	987	CSID107441460	M+2Na-H	C26H34N2O12	97,7	-4,1507	amino sugar		chroman
45	885,2486	3,84	279,2119	12	0	0	0	139	0	3	0	0	CSID107442513	M+K	C43H46N2O16	95,2	0,8432	amino sugar		phenyl
46	773,2346	3,82	273,2607	13	0	0	0	1	3	17	0	0	CSID59053982	M-H2O-H	C30H48O24	96	-1,4103	anhydro sugar		
47	773,2362	2,82	267,2419	3	0	3	0	38	293	367	24	7	CSID59053982	M-H2O-H, M-H	C30H48O24	95,1	0,6471	anhydro sugar		
48	773,2362	2,94	270,2469	12	0	0	0	27	240	424	6	6	CSID59053982	M-H2O-H	C30H48O24	92,9	0,6150	anhydro sugar		
49	773,2350	3,37	270,2470	13	0	0	0	10	62	91	0	0	CSID59053982	M-H2O-H	C30H48O24	97,5	-0,8556	anhydro sugar		
50	791,2462	2,52	276,0276	17	0	0	0	0	0	11	0	0	CSID59053982	M-H	C30H48O24	92,7	-0,0385	anhydro sugar		

51	773,2351	3,66	267,2419	13	0	0	0	12	85	144	1	0	CSID59053982	M-H2O-H	C30H48O24	94	-0,7435	anhydro sugar		
52	773,2352	2,01	264,2457	13	0	0	0	0	0	3	0	0	CSID59053982	M-H2O-H	C30H48O24	95,5	-0,6488	anhydro sugar		
53	323,0971	1,23	215,4375	808	0	0	0	3	27	31	7	1	CSID59054002	M-H	C12H20O10	94,5	-3,8400	anhydro sugar		
54	305,0863	3,03	219,0640	360	0	0	0	0	1	3	0	0	CSID59054002	M-H2O-H	C12H20O10	92	-4,6961	anhydro sugar		
55	305,0862	3,68	221,9738	350	0	0	0	0	8	9	0	0	CSID59054002	M-H2O-H	C12H20O10	93,1	-4,9108	anhydro sugar		
56	323,0973	3,20	221,2320	165	0	0	0	2	35	33	9	0	CSID59054002	M-H2O-H, M-H	C12H20O10	94,4	-3,3745	anhydro sugar		
57	629,1913	2,74	248,6411	108	0	0	0	0	0	10	0	0	CSID59054021	M-H	C24H38O19	92,5	-3,4334	anhydro sugar		
58	629,1926	2,37	254,5662	98	0	0	0	0	2	10	0	0	CSID59054021	M-H	C24H38O19	95,2	-1,3946	anhydro sugar		
59	675,1972	0,95	244,9394	41	0	0	0	2	0	2	5	3	CSID59054021	M+FA-H	C24H38O19	95	-2,7788	anhydro sugar		
60	629,1931	3,75	248,6411	92	0	55	4	258	1347	1656	533	78	CSID59054021	M-H	C24H38O19	94,3	-0,6145	anhydro sugar		
61	629,1929	4,03	251,5991	96	0	2	0	45	199	281	68	12	CSID59054021	M-H	C24H38O19	95,4	-0,9295	anhydro sugar		
62	675,1963	1,63	239,0802	56	0	0	0	0	0	1	0	0	CSID59054021	M+FA-H	C24H38O19	96,3	-4,2557	anhydro sugar		
63	675,1984	0,76	242,0051	41	0	0	0	8	3	71	1	6	CSID59054021	M+FA-H	C24H38O19	90,9	-0,8824	anhydro sugar		
64	629,1916	2,92	245,6922	97	0	0	0	0	1	7	0	0	CSID59054021	M-H	C24H38O19	96,6	-2,9001	anhydro sugar		
65	675,1986	3,35	247,8827	40	0	7	1	143	431	520	177	23	CSID59054021	M+FA-H	C24H38O19	91,2	-0,5608	anhydro sugar		
66	629,1930	3,27	245,6922	96	0	48	4	332	1512	1518	590	67	CSID59054021	M-H	C24H38O19	91,6	-0,6815	anhydro sugar		
67	675,1983	3,75	250,8352	42	0	3	0	27	139	173	59	7	CSID59054021	M+FA-H	C24H38O19	94,3	-0,9837	anhydro sugar		
68	611,1804	5,23	269,8688	97	0	0	0	0	1	10	0	0	CSID59054021	M-H2O-H	C24H38O19	92,4	-3,8967	anhydro sugar		
69	467,1398	2,96	228,4754	499	0	0	0	2	69	108	3	0	CSID59054022	M-H2O-H	C18H30O15	92	-1,7099	anhydro sugar		
70	467,1400	2,44	231,3851	502	0	0	0	2	7	49	1	0	CSID59054022	M-H2O-H	C18H30O15	95,8	-1,3025	anhydro sugar		
71	917,2777	5,21	304,9821	3	0	0	0	0	1	34	0	0	CSID59054032	M-H2O-H	C36H56O28	95	-0,3578	anhydro sugar		
72	935,2891	4,46	301,6641	7	0	25	3	287	952	1553	381	40	CSID59054032	M-H	C36H56O28	95,6	0,5549	anhydro sugar		
73	981,2939	4,45	304,2064	6	0	0	0	5	55	149	5	0	CSID59054032	M+FA-H	C36H56O28	96,1	-0,1435	anhydro sugar		
74	935,2889	3,86	298,5783	2	0	8	7	219	304	346	119	11	CSID59054032	M-H, M+FA-H	C36H56O28	94,4	0,3868	anhydro sugar		
75	935,2894	4,21	298,5783	2	0	27	6	409	787	1185	317	38	CSID59054032	M-H, M+FA-H	C36H56O28	90,2	0,8637	anhydro sugar		
76	981,2943	3,95	298,0327	6	0	0	0	41	41	82	9	1	CSID59054032	M+FA-H	C36H56O28	94,8	0,2934	anhydro sugar		
77	935,2893	3,95	298,5783	7	0	21	11	403	727	969	258	34	CSID59054032	M-H	C36H56O28	95,1	0,7614	anhydro sugar		
78	307,1013	3,84	242,1711	545	0	1	0	59	26	207	9	7	CSID389299	M+H-H2O	C12H20O10	92,6	-3,2400	anhydro sugar		
79	307,1016	3,60	266,9311	579	0	4	0	93	66	473	26	28	CSID389299	M+H-H2O	C12H20O10	94,4	-2,4372	anhydro sugar		
80	307,1018	3,74	242,1711	915	0	5	0	57	63	300	43	23	CSID389299	M+H-H2O	C12H20O10	94,9	-1,8446	anhydro sugar		
81	127,0383	3,46	121,4760	109	0	8	0	7	0	0	0	5	CSID26995246	M+H-H2O	C6H8O4	90	-4,6110	anhydro sugar		
82	325,1116	0,59	244,3203	1252	0	4	0	17	2	24	3	8	CSID58837516	M+H	C12H20O10	98,2	-4,2227	anhydro sugar		
83	307,1016	2,03	248,2868	580	0	0	0	8	22	161	5	11	CSID59054002	M+H-H2O	C12H20O10	91,2	-2,4606	anhydro sugar		
84	347,0950	2,72	246,3580	861	0	0	0	1	0	4	0	0	CSID59054002	M+Na	C12H20O10	97,4	0,4139	anhydro sugar		
85	613,1964	3,40	265,7326	216	0	2	0	21	38	300	9	5	CSID59054021	M+H-H2O	C24H38O19	90,4	-1,6122	anhydro sugar		
86	653,1883	3,81	312,4787	163	0	0	0	1	14	58	2	1	CSID59054021	M+Na	C24H38O19	94,1	-2,7072	anhydro sugar		
87	613,1972	4,46	294,0588	242	0	0	0	0	0	7	0	0	CSID59054021	M+H-H2O	C24H38O19	92,9	-0,3931	anhydro sugar		
88	653,1900	3,75	325,6103	162	0	0	0	17	20	69	2	0	CSID59054021	M+Na	C24H38O19	95,2	0,0890	anhydro sugar		
89	509,1472	1,23	208,5464	644	0	7	0	10	0	0	0	6	CSID59054022	M+Na	C18H30O15	96,6	-1,0583	anhydro sugar		
90	959,2867	4,45	290,6467	2	5	347	125	3725	4534	12202	1699	483	CSID59054032	M+NH4, M+Na	C36H56O28	97,9	1,7780	anhydro sugar		
91	959,2869	4,20	293,8225	2	11	868	378	8780	9508	19615	3550	955	CSID59054032	M+H-H2O,	C36H56O28	97,8	1,9843	anhydro sugar		
92	653,1907	3,88	231,5963	28	31	786	238	3872	5311	7333	2352	836	CSID107451054	M+Na, M+K	C24H38O19	97,8	1,1446	anhydro sugar		
93	653,1908	3,74	228,6468	28	121	3878	555	9464	13604	14677	5782	1696	CSID107451054	M+Na, M+K	C24H38O19	97,9	1,3503	anhydro sugar		
94	347,0953	1,24	168,6483	242	162	4436	489	8192	8310	10072	7377	5138	CSID107451074	M+Na, M+K	C12H20O10	95,9	1,2626	anhydro sugar		
95	347,0938	1,36	246,3580	757	0	0	0	0	0	0	0	0	CSID107451074	M+Na	C12H20O10	95,9	-3,4285	anhydro sugar		
96	861,2577	3,43	281,1497	15	0	0	0	0	1	3	0	0	CSID24695551	M+FA-H	C38H44N2O18	90,9	0,6973	biphenyl	sugar	
97	585,1965	5,91	231,8440	137	0	319	0	165	0	19	2	37	CSID90661213	M-H2O-H	C30H36O13	90,6	-2,0841	biphenyl		
98	555,1628	5,39	224,8570	443	304	3348	48	1601	23	67	2	3	CSID23122358	M+H-H2O	C36H28O5S	90,4	0,5501	biphenyl	thio	
99	789,2727	6,07	274,5987	61	0	201	0	176	0	182	184	1499	CSID24712489	M+H	C37H44N2O17	91,7	1,8420	biphenyl	amide	
100	371,1089	5,55	187,0258	116	0	2	0	12	0	17	13	177	CSID25033188	M+H, M+Na	C18H20O7	93,2	-3,6361	biphenyl		
101	331,1166	5,87	182,8912	933	0	164	1	295	0	37	13	313	CSID25048889	M+H-H2O	C18H20O7	95,5	-2,9464	biphenyl		
102	471,1628	5,61	215,2941	156	22	855	9	550	5	18	1	29	CSID29409377	M+Na, M+K	C23H28O9	92,2	0,6438	biphenyl	sugar	
103	339,1214	5,24	185,3675	1495	0	3	0	16	1	5	3	9	CSID90635894	M+Na	C18H20O5	90,1	3,5410	biphenyl	sugar	
104	593,1854	7,02	240,4510	130	21	53	45	29	69	14	101	23	CSID31121633	M-H2O-H	C28H36O15	90,8	-3,6535	cyclopentapyran	sugar	
105	701,2081	1,95	259,3341	38	0	0	0	0	0	4	0	0	CSID90636006	M-H2O-H	C34H40O17	95,6	-0,8157	cyclopentapyran		
106	521,1650	5,35	212,9268	291	0	68	0	35	0	6	0	1	CSID90659472	M-H2O-H	C25H32O13	98,3	-2,5546	cyclopentapyran		
107	399,1261	2,52	188,9183	838	2	115	0	65	0	1	0	0	CSID10264396	M+Na	C16H24O10	94,2	-0,2275	cyclopentapyran	sugar	
108	517,1671	5,91	205,4935	653	0	63	1	173	0	24	12	14	CSID22914151	M+Na	C24H30O11	96,6	-1,8637	cyclopentapyran	sugar	
109	599,1790	0,78	226,8131	202	0	75	8	82	0	0	0	0	CSID23339850	M+H-H2O	C30H32O14	95,5	4,9742	cyclopentapyran		

110	457,1333	3,63	204,1686	833	0	0	0	0	2	2	0	1	CSID23340010	M+H	C20H24O12	93,8	-1,5388	cyclopentapyran		
111	387,1049	5,20	192,0929	928	9	522	16	921	9	55	3	60	CSID24647090	M+K	C15H24O9	91	-0,7589	cyclopentapyran		
112	439,1443	2,01	245,9301	981	0	0	0	5	13	105	3	4	CSID28506451	M+H	C17H26O13	91,1	-0,6062	cyclopentapyran		
113	653,2197	6,13	246,5280	186	0	42	0	95	0	31	0	89	CSID28506506	M+K	C29H42O14	96,1	-1,4194	cyclopentapyran		
114	704,2597	4,18	254,6065	71	0	0	0	1	0	16	0	0	CSID58921850	M+NH4	C27H42O20	95,8	-1,5453	cyclopentapyran		
115	269,2111	7,97	175,3249	57	3	8	7	4	11	2	13	3	CSID4446129	M-H	C16H30O3	90,5	-4,2098	fatty acid	oxo	
116	641,4247	8,58	263,3058	11	17	35	32	23	44	9	58	13	CSID23282469	M-H	C35H62O10	90,9	-3,6376	fatty acid	sugar	
117	696,6138	9,02	298,9049	6	0	0	0	0	2154	0	0	281	CSID113381208	M+FA-H	C41H81NO4	94,5	-1,4878	fatty acid	amide	
118	402,3578	7,74	220,2896	109	1705	2224	1909	1493	1741	825	2786	1737	CSID7822619	M+NH4	C23H44O4	98,8	-0,0410	fatty acid	dicarboxylic	
119	416,3735	7,89	225,7110	112	22	21	25	25	17	6	34	20	CSID14810733	M+NH4	C24H46O4	98,8	0,1492	fatty acid	dicarboxylic	
120	334,2949	6,98	202,4989	55	3513	1	5574	0	7536	1	7884	0	CSID15392633	M+NH4	C18H36O4	94,7	-0,7822	fatty acid	hydroxy	
121	151,0394	4,53	123,5096	139	0	24	0	44	16	40	110	81	CSID11668	M-H	C8H8O3	95,9	-4,2313	furan		
122	257,0653	3,13	154,1641	66	0	0	0	0	0	1	0	0	CSID390250	M-H2O-H	C11H16O8	96,5	-4,8534	furan	sugar	
123	463,1091	1,66	211,3134	354	0	0	0	12	10	41	0	1	CSID1083691	M-H	C23H20N4O5S	98,9	1,9720	furan	complex	
124	153,0188	3,98	123,3536	49	0	1	0	2	0	3	0	7	CSID4946728	M-H	C7H6O4	93,4	-3,7179	furan	acid	
125	239,0552	3,21	146,9861	173	0	0	0	1	0	2	1	3	CSID8505706	M+FA-H	C10H10O4	91,6	-4,5579	furan	acid	
126	183,0291	0,99	144,7555	27	0	1	2	64	16	25	2	3	CSID9358110	M-H2O-H, M-H	C8H8O5	90,6	-4,5137	furan	acid	
127	469,1496	6,11	211,1763	372	0	1562	0	541	0	107	93	744	CSID11016034	M-H2O-H	C26H24N4O6	90,1	-4,4872	furan	complex	
128	339,1992	7,80	203,3956	86	1909	4361	3860	2523	5871	1302	8826	1580	CSID15342562	M-H	C19H32O3S	90,3	-2,0341	furan	sulpho-C14	
129	297,0607	1,26	160,6573	138	0	0	0	47	7	29	2	3	CSID23138575	M+FA-H	C12H12O6	97,3	-3,5937	furan	acid	
130	245,0655	1,87	216,2494	27	0	0	0	0	0	2	0	0	CSID23141837	M-H	C10H14O7	97,2	-4,6663	furan	acid	
131	269,0653	1,23	153,6788	100	0	0	0	1	0	3	0	2	CSID23141904	M-H2O-H	C12H16O8	93,7	-4,8118	furan	acid	
132	412,1898	8,94	209,7230	537	67	136	129	93	194	38	301	53	CSID23188006	M-H	C22H27N3O5	92,4	4,7515	furan	complex	
133	197,0445	1,25	146,5230	24	0	0	0	0	1	4	0	1	CSID23234438	M-H2O-H	C9H12O6	91,4	-4,9198	furan		
134	239,0551	4,17	149,6326	44	0	0	0	25	2	6	2	2	CSID23234785	M-H2O-H	C11H14O7	90,7	-3,7463	furan		
135	453,1392	3,53	194,6333	404	0	34	0	3	0	0	0	0	CSID23250328	M+FA-H	C20H24O9	94,1	-2,5503	furan	phenol	sugar
136	151,0394	3,71	131,3103	134	0	11	0	7	0	2	0	1	CSID24190085	M-H	C8H8O3	95,9	-4,4573	furan	aldehyde	
137	321,0606	1,52	167,9338	220	0	0	0	24	0	20	0	3	CSID24539701	M+FA-H	C14H12O6	95,1	-3,5990	furan	phenyl	
138	257,0469	7,34	162,2168	64	1	4	3	3	5	1	6	1	CSID24539701	M-H2O-H	C14H12O6	93,4	4,9295	furan	phenyl	
139	697,4882	9,10	274,4106	17	41	108	67	78	118	69	127	40	CSID24685809	M+FA-H	C38H68O8	96,2	-2,1970	furan		
140	241,0346	0,66	141,6441	65	0	33	19	512	5	33	18	20	CSID24697176	M+FA-H	C9H8O5	96,5	-4,0488	furan	acid	
141	751,2962	6,25	270,5637	37	0	383	0	139	0	14	0	10	CSID26343912	M+FA-H	C39H46O12	94,3	-1,3584	furan	phenyl	
142	245,0448	4,94	149,3645	117	0	20	1	115	40	221	31	42	CSID31109477	M-H	C13H10O5	92,8	-2,9336	furan	phenyl	
143	209,0446	1,87	137,9399	75	0	14	1	101	22	41	22	27	CSID34250432	M-H	C10H10O5	96,8	-4,3027	furan		
144	209,0446	3,90	140,5578	75	0	3	0	30	8	37	21	51	CSID34250432	M-H	C10H10O5	93,1	-4,5544	furan		
145	209,0444	5,97	140,5578	26	0	1	0	4	0	7	4	3	CSID34485443	M-H2O-H	C10H12O6	94	-4,8958	furan	acid	
146	587,1763	4,61	226,0208	144	0	34	0	44	0	1	0	0	CSID76790927	M+FA-H	C24H26N6O9	94,8	3,5571	furan	adenosine	
147	377,1596	5,21	228,0485	298	0	0	0	0	0	0	0	0	CSID90659048	M-H	C20H26O7	91,5	-2,5606	furan		
148	175,0383	5,71	132,3971	223	0	0	0	0	0	0	14	71	CSID137621	M+H-H2O	C10H8O4	93,1	-3,5102	furan		
149	206,0805	3,29	140,6067	840	0	0	0	0	0	3	57	194	CSID962910	M+H-H2O	C11H13NO4	90,2	-2,9424	furan	piperidine	
150	305,0617	3,89	224,2270	530	0	0	0	0	0	0	0	0	CSID10187221	M+2Na-H	C11H16O7	90,9	3,6296	furan	sugar	
151	193,0493	5,44	133,7183	427	0	8	0	80	17	371	229	2422	CSID10677991	M+H	C10H8O4	90,4	-1,4419	furan	phenyl	
152	187,0381	4,64	147,0751	294	0	0	0	0	0	0	0	21	CSID21117354	M+H-H2O	C11H8O4	93,5	-4,2353	furan	phenyl	
153	563,1585	4,41	213,0423	366	6	789	136	4485	5160	9432	3386	1063	CSID23228361	M+2Na-H	C21H26N8O8	97,4	-0,1117	furan	purine	pirimidine
154	217,0700	3,58	223,7738	177	0	0	0	2	4	45	5	3	CSID23234438	M+H	C9H12O6	97	-2,8941	furan		
155	430,3890	8,03	228,2182	98	1691	2140	1690	1508	1647	785	2624	1713	CSID23272503	M+NH4	C25H48O4	93,2	-0,1661	furan		
156	433,1476	3,95	193,5153	182	298	5646	175	2616	32	15	9	16	CSID23314537	M+Na, M+K	C20H26O9	94,8	1,6209	furan		
157	399,1402	6,70	203,0299	909	0	0	0	0	0	0	0	22	CSID23339312	M+Na	C20H24O7	92,8	-3,2874	furan	phenyl	
158	359,1099	4,43	184,6524	780	0	24	0	1	0	0	1	20	CSID24642312	M+Na	C17H20O7	91	-0,6229	furan	phenol	
159	505,1685	5,04	220,2182	620	0	0	0	0	0	0	0	1	CSID24677040	M+H-H2O	C25H30O12	90,3	-3,6521	furan	phenol	
160	152,0702	0,86	129,1429	496	0	3	0	5	15	61	256	375	CSID24690824	M+H-H2O	C8H11NO3	92,7	-2,5244	furan	amine	
161	152,0702	1,27	131,6983	494	0	4	0	5	18	48	185	273	CSID24690824	M+H-H2O	C8H11NO3	94,9	-2,6980	furan	amine	
162	166,1219	4,60	138,2294	849	0	0	0	0	2	16	179	370	CSID25992014	M+H-H2O	C10H17NO2	97,1	-3,9975	furan	amine	
163	579,1482	3,27	209,8216	367	0	0	0	9	0	4	0	0	CSID28430364	M+Na	C28H28O12	90,8	1,7008	furan	phenyl	
164	209,1279	1,70	143,0130	1134	0	0	0	0	0	0	13	40	CSID29372862	M+NH4	C11H13NO2	94,3	-2,8604	furan		
165	349,1133	3,44	216,3804	1069	0	0	0	2	1	21	0	0	CSID31133357	M+H	C15H16N4O6	91,1	-2,6807	furan	pyrrole	
166	679,5118	8,00	258,1490	10	6729	0	11601	1	9741	2	10118	2	CSID32033878	M+H	C40H70O8	91,8	-3,7437	furan	dimer	
167	309,1806	5,41	178,2299	701	0	1	0	1	30	122	381	1230	CSID58752941	M+H	C16H24N2O4	96,8	-1,0845	furan	amide	
168	320,1963	4,31	177,7905	194	0	0	0	0	0	0	192	590	CSID58771768	M+H, M+Na	C17H25N3O3	96,9	-1,7727	furan	amide	

169	256,0960	4,19	153,6018	830	0	0	0	0	0	0	0	40	CSID70371181	M+H-H2O	C15H15NO4	94,2	-2,9059	furan		
170	313,1034	5,70	175,3261	727	0	0	0	0	0	2	18	81	CSID113368397	M+2Na-H	C14H20O5	91,4	4,1681	furan		
171	367,2082	6,29	189,9492	269	3	37	0	39	1	13	0	5	CSID113369383	M+Na	C18H32O6	98,4	-2,7267	furan		
172	729,2085	4,62	255,9359	13	0	0	0	14	2	21	0	0	CSID90636923	M-H	C41H34N2O11	99	-0,6753	indole		
173	146,0597	2,87	124,6123	389	0	0	0	0	0	0	1	33	CSID10529891	M+H-H2O	C9H9NO2	96,3	-2,2839	indole	acid	
174	527,1580	0,84	210,9854	750	0	18	4	21	144	85	113	77	CSID13151012	M+K	C28H28N2O6	91,7	0,2538	indole	amide	
175	833,2544	1,15	267,6272	29	14	629	47	869	395	368	85	116	CSID21280067	M+H-H2O	C58H34N4O4	96,1	-0,3674	indole	complex	
176	743,2230	2,72	253,8749	49	36	1771	92	2313	5438	5594	1430	708	CSID26401604	M+2Na-H	C31H42N2O16	98,2	-2,2839	indole		
177	260,0913	3,20	153,4146	663	0	0	0	0	0	0	42	121	CSID31112385	M+H-H2O	C14H15NO5	96,7	-1,7164	indole		
178	249,1566	3,76	215,5172	328	65	0	62	0	106	0	152	0	CSID53616210	M+Na	C12H22N2O2	93,4	-3,4736	indole		
179	267,1336	3,91	163,7373	790	0	0	0	0	3	6	30	117	CSID76749680	M+NH4	C13H15NO4	94,1	-1,2761	indole		
180	497,1497	1,89	227,7888	371	0	0	0	0	0	1	0	0	CSID4450779	M-H	C19H30O15	92,6	-3,0268	kdo		
181	497,1503	2,72	227,7888	340	0	0	0	0	1	3	0	0	CSID4450779	M-H	C19H30O15	90,3	-1,8365	kdo		
182	497,1499	2,44	227,7888	362	0	0	0	0	1	8	0	0	CSID4450779	M-H	C19H30O15	96	-2,5365	kdo		
183	479,1400	3,75	242,8248	452	0	1	0	20	123	145	48	5	CSID4450780	M-H2O-H	C19H30O15	93,4	-1,3364	kdo		
184	479,1390	4,95	248,7429	474	0	0	0	1	4	28	1	1	CSID4450780	M-H2O-H	C19H30O15	93,6	-3,2487	kdo		
185	479,1390	4,53	242,8248	473	0	0	0	1	36	72	5	0	CSID4450780	M-H2O-H	C19H30O15	94,1	-3,3628	kdo		
186	479,1396	3,88	242,8248	450	0	0	0	6	35	64	8	1	CSID4450780	M-H2O-H	C19H30O15	91,2	-2,1597	kdo		
187	479,1399	3,27	239,8797	106	0	0	0	33	155	187	38	2	CSID4450780	M-H2O-H, M-H	C19H30O15	90,2	-1,4771	kdo		
188	795,2405	1,12	257,9802	13	0	2	0	18	0	0	0	0	CSID26331652	M-H2O-H	C29H50O26	97,5	-0,7890	kdo	hepp	
189	471,1350	1,33	199,8314	433	0	2	0	29	26	53	2	0	CSID26331896	M-H	C17H28O15	94,6	-1,1586	kdo		
190	453,1237	1,49	205,8675	500	0	0	0	4	1	9	0	0	CSID26331896	M-H2O-H	C17H28O15	93,3	-2,7337	kdo		
191	405,1023	3,05	190,2116	598	0	1	0	1	2	15	0	0	CSID26332278	M-H2O-H	C16H24O13	92	-3,6020	kdo		
192	461,1286	4,35	228,6203	513	0	0	0	1	4	10	2	0	CSID28533759	M-H2O-H	C19H28O14	98,4	-3,0331	kdo		
193	525,1455	1,62	212,8486	256	0	0	0	0	1	8	0	0	CSID28533759	M+FA-H	C19H28O14	90,1	-1,3263	kdo		
194	603,1776	0,64	225,7430	23	0	19	1	150	57	75	3	7	CSID31150583	M-H2O-H, M-H	C22H38O20	96,7	-0,2495	kdo	hepp	
195	603,1767	2,29	222,8657	85	0	0	0	5	8	15	0	0	CSID31150583	M-H2O-H	C22H38O20	94,7	-1,6661	kdo	hepp	
196	603,1770	2,03	222,8657	83	0	0	0	15	10	34	0	0	CSID31150583	M-H2O-H	C22H38O20	96,5	-1,1861	kdo	hepp	
197	603,1768	1,51	225,7430	83	0	2	0	4	3	8	0	0	CSID31150583	M-H2O-H	C22H38O20	95,2	-1,5273	kdo	hepp	
198	499,1659	3,26	250,2009	778	0	0	0	1	1	9	0	0	CSID4450779	M+H	C19H30O15	95	0,2871	kdo		
199	521,1481	3,52	219,8184	564	98	5831	447	12790	13938	19416	6398	2917	CSID4450780	M+Na	C19H30O15	97,3	0,8129	kdo		
200	481,1552	4,01	250,7176	955	0	1	0	72	89	638	42	23	CSID28533759	M+H	C19H28O14	92,4	0,0455	kdo		
201	503,1374	2,65	205,8323	132	12	689	2	115	0	0	0	0	CSID28533759	M+Na, M+K	C19H28O14	90,6	0,5359	kdo		
202	498,1815	3,81	220,3978	679	0	0	0	0	1	31	1	2	CSID30786392	M+NH4	C19H28O14	94,7	-0,6013	kdo		lactone
203	331,0660	1,23	173,0458	324	1	199	0	26	0	0	0	0	CSID19980678	M-H	C13H16O10	97,9	-3,0599	ketone	cyclic	
204	163,0392	4,98	132,9771	138	0	0	0	1	0	4	7	10	CSID21865628	M-H2O-H	C9H10O4	94,9	-4,9609	ketone	cyclic	
205	173,0448	2,10	129,6622	54	0	0	0	0	0	0	0	4	CSID58163466	M-H2O-H	C7H12O6	93,2	-3,8901	ketone		
206	181,0497	1,14	136,9589	152	0	0	0	0	0	0	0	1	CSID58837565	M-H	C9H10O4	94	-4,8665	ketone		
207	137,0592	4,68	122,9472	285	1	89	2	92	0	4	0	1	CSID121746	M+H-H2O	C8H10O3	96,2	-3,3226	ketone		
208	175,0594	1,29	255,7668	172	0	0	0	0	0	0	0	0	CSID10128103	M+H-H2O	C7H12O6	91,2	-3,4805	ketone	cyclic	
209	137,0592	4,60	122,9472	285	1	96	3	95	0	7	0	0	CSID23352799	M+H-H2O	C8H10O3	96,2	-3,3461	ketone		
210	217,0700	4,70	235,8855	178	0	1	1	19	15	104	17	5	CSID28489224	M+H	C9H12O6	98,3	-3,0682	ketone		
211	235,1686	7,75	162,6778	672	144	178	174	116	158	68	210	142	CSID35015002	M+H-H2O	C15H24O3	98	-2,4855	ketone	cyclic	
212	256,2631	6,96	183,4876	97	1259	19	1354	14	1331	8	2426	8	CSID57517343	M+NH4	C16H30O	90,7	-1,7883	ketone	hydrocarbon	
213	439,1439	3,90	264,3573	1053	0	0	0	4	6	53	2	1	CSID88294606	M+Na	C15H28O13	94,5	3,9519	OS		propyl
214	339,0925	1,64	172,7968	493	0	0	0	14	19	60	3	1	CSID167985	M-H2O-H	C12H22O12	90,1	-2,1570	OS		
215	501,1458	1,56	210,4877	335	0	7	0	22	99	179	46	10	CSID391765	M-H	C18H30O16	96,5	-0,5947	OS		
216	339,0928	0,59	172,7968	499	0	30	45	283	77	95	30	9	CSID4955243	M-H2O-H	C12H22O12	91	-1,2335	OS		
217	627,1761	3,61	234,0225	59	0	0	0	22	12	42	0	0	CSID5257038	M-H2O-H	C24H38O20	91,3	-2,5665	OS		
218	627,1770	3,88	242,7867	50	0	0	0	7	2	8	0	0	CSID5257038	M-H2O-H	C24H38O20	96,1	-1,1413	OS		
219	541,1767	2,28	221,1131	243	0	0	0	41	0	12	0	0	CSID9061499	M-H2O-H	C21H36O17	96	-1,3176	OS		
220	559,1876	1,46	223,6470	181	0	0	0	2	50	42	250	8	CSID9061499	M-H	C21H36O17	94,3	-0,7579	OS		methyl
221	629,1917	1,58	236,9009	98	0	0	0	0	21	5	17	0	CSID9860791	M-H2O-H	C24H40O20	95,9	-2,6643	OS		cyclic
222	499,1650	1,23	204,8691	410	0	51	0	6	0	0	0	0	CSID25779784	M-H2O-H	C19H34O16	95,7	-3,4919	OS	methyl	
223	737,2340	1,20	261,7736	24	0	16	0	4	0	0	0	0	CSID26331636	M-H2O-H	C27H48O24	93,7	-2,2981	OS	hepp	
224	527,1592	3,86	235,8794	278	0	0	0	0	3	8	0	0	CSID26332003	M-H2O-H	C20H34O17	95,1	-4,8196	OS		
225	665,2134	0,82	242,1620	123	0	1	0	6	6	37	120	138	CSID26332297	M-H	C24H42O21	91,7	-1,7735	OS		
226	455,1398	2,72	246,3828	520	0	0	0	0	5	13	0	0	CSID26332367	M-H2O-H	C17H30O15	95,7	-1,7292	OS		
227	809,2563	0,70	248,9218	44	0	0	0	0	0	13	0	0	CSID26332546	M-H2O-H	C30H52O26	93	-0,6617	OS		

228	873,2714	1,11	251,0748	40	0	0	0	0	0	0	4	20	CSID26332546	M+FA-H	C30H52O26	96,7	-1,7449	OS		
229	455,1398	2,03	217,2151	521	0	0	0	4	30	63	4	1	CSID26332660	M-H2O-H	C17H30O15	96,5	-1,7077	OS		
230	455,1396	2,91	246,3828	520	0	0	0	0	19	52	0	0	CSID26332660	M-H2O-H	C17H30O15	90,9	-2,2502	OS		
231	455,1392	3,64	258,3131	556	0	0	0	1	8	14	0	0	CSID26332660	M-H2O-H	C17H30O15	95,4	-3,0584	OS		
232	455,1398	1,23	214,3516	520	0	1	0	9	20	26	7	1	CSID26332660	M-H2O-H	C17H30O15	96,1	-1,7350	OS		
233	395,1184	2,91	224,5832	282	0	0	0	8	136	216	8	3	CSID26332868	M-H2O-H, M-H	C15H26O13	90,8	-2,7039	OS		
234	395,1185	2,01	215,9188	681	0	0	0	6	52	127	8	3	CSID26332868	M-H2O-H	C15H26O13	91,1	-2,4283	OS		
235	413,1293	1,64	235,7343	703	0	0	0	1	11	14	1	0	CSID26332878	M-H	C15H26O13	91,5	-1,7312	OS		
236	413,1289	1,99	238,6757	783	0	0	0	0	2	13	0	0	CSID26332878	M-H	C15H26O13	93	-2,8418	OS		
237	395,1186	1,63	218,7970	661	0	6	0	31	198	302	76	13	CSID26332878	M-H2O-H	C15H26O13	94,6	-2,0346	OS		
238	527,1608	0,90	227,1558	273	0	0	0	15	15	52	1	0	CSID26332939	M-H2O-H	C20H34O17	97	-1,8041	OS		
239	527,1603	3,41	232,9620	292	0	0	0	8	54	77	1	0	CSID26332939	M-H2O-H	C20H34O17	91,1	-2,7534	OS		
240	527,1603	3,62	232,9620	292	0	0	0	6	36	67	2	0	CSID26332939	M-H2O-H	C20H34O17	94,3	-2,7547	OS		
241	263,0759	3,04	221,0753	162	0	0	0	0	1	3	0	0	CSID30777300	M-H2O-H	C10H18O9	91	-4,9471	OS		
242	585,1681	1,48	228,9457	102	0	0	0	9	1	11	12	0	CSID30790754	M-H2O-H	C22H36O19	92,6	1,4684	OS		
243	585,1656	1,24	223,1767	82	0	0	0	4	0	4	0	0	CSID30790754	M-H2O-H	C22H36O19	98,4	-2,6625	OS		
244	585,1665	2,34	226,0564	89	0	0	0	5	0	3	0	0	CSID30790754	M-H2O-H	C22H36O19	97,5	-1,1110	OS		
245	603,1765	2,79	225,7430	81	0	0	0	4	3	9	0	0	CSID30790754	M-H	C22H36O19	96,5	-2,1774	OS		
246	989,3221	0,80	288,7434	28	0	0	0	0	0	63	0	0	CSID30984563	M-H	C36H62O31	98,2	1,8740	OS		
247	791,2465	2,94	276,0276	13	0	0	0	10	101	203	3	3	CSID31150612	M-H2O-H	C30H50O25	96,8	0,3165	OS		
248	809,2575	0,83	266,7470	4	0	11	0	31	217	326	21	21	CSID31150612	M-H, M+FA-H	C30H50O25	90,6	0,8778	OS		
249	1029,3147	3,06	294,4199	6	0	0	0	0	2	39	0	0	CSID34448969	M-H2O-H	C38H64O33	95,5	-0,4809	OS	kdo	
250	341,1081	0,60	172,7356	701	40	528	7	52	44	38	43	36	CSID58827461	M-H	C12H22O11	94	-2,4719	OS		
251	587,1825	2,91	240,5606	131	0	19	0	102	809	994	168	38	CSID58837749	M-H2O-H	C22H38O19	95,6	-0,6239	OS		
252	587,1825	2,44	237,6338	131	0	4	0	35	158	365	36	12	CSID58837749	M-H2O-H	C22H38O19	96,9	-0,6033	OS		
253	587,1824	2,72	246,4421	128	0	3	0	35	300	407	46	13	CSID58837749	M-H2O-H	C22H38O19	91,2	-0,7894	OS		
254	587,1823	1,03	237,6338	129	0	12	1	104	5	145	33	14	CSID58837749	M-H2O-H	C22H38O19	97,4	-1,0689	OS		
255	455,1397	3,03	246,3828	519	0	0	0	0	5	12	0	0	CSID58837790	M-H2O-H	C17H30O15	96,3	-2,0060	OS		
256	731,2234	1,60	252,9416	20	0	0	0	0	0	2	0	0	CSID58921850	M+FA-H	C27H42O20	92,2	-2,4935	OS	cyclopentapyra	
257	569,1707	2,49	243,8369	151	0	0	0	0	2	12	0	0	CSID58922033	M+FA-H	C21H32O15	94,1	-3,2063	OS	cyclopentapyra	
258	923,2927	3,17	295,6471	9	0	0	0	0	1	5	0	0	CSID76963250	M-H2O-H	C35H58O29	97,9	4,4188	OS		
259	923,2863	3,53	295,6471	4	0	0	0	0	0	0	0	0	CSID76963250	M-H2O-H	C35H58O29	93,1	-2,3811	OS		
260	753,2300	0,61	252,6266	15	0	0	0	10	1	38	0	1	CSID76963252	M+FA-H	C26H44O22	91,5	-0,9221	OS		
261	851,2682	2,82	278,2461	4	0	66	1	264	1754	2152	249	97	CSID76963257	M-H2O-H	C32H54O27	94,9	0,9209	OS		
262	851,2679	2,52	278,2461	4	0	0	0	2	14	65	0	0	CSID76963257	M-H2O-H	C32H54O27	92,1	0,5959	OS		
263	915,2827	0,62	271,4182	11	0	0	0	5	0	14	0	1	CSID76963257	M+FA-H	C32H54O27	96,6	-0,7993	OS		
264	851,2678	2,68	281,2792	10	0	1	0	17	107	153	9	4	CSID76963257	M-H2O-H	C32H54O27	95,4	0,4718	OS		
265	851,2675	3,44	278,2461	10	0	0	0	0	0	5	0	0	CSID76963257	M-H2O-H	C32H54O27	96	0,1518	OS		
266	1031,3091	4,66	322,3356	5	0	0	0	4	30	104	1	0	CSID76963261	M-H	C38H64O30S	97,7	-3,8401	OS		
267	1073,3424	1,62	300,0951	4	0	0	0	0	0	2	0	0	CSID76963268	M-H	C40H66O33	98	0,9760	OS		
268	1073,3414	2,79	303,1807	4	0	39	0	179	0	1	0	0	CSID76963268	M-H	C40H66O33	96,4	0,0848	OS		
269	1055,3269	3,07	297,2092	4	0	0	0	0	0	3	0	0	CSID76963269	M-H2O-H	C40H66O33	93,9	-3,5956	OS		
270	455,1400	3,18	200,1844	490	0	0	0	2	1	5	0	0	CSID88294297	M-H2O-H	C17H30O15	97,2	-1,4068	OS		
271	325,0773	0,53	165,1062	403	0	28	40	160	23	12	11	1	CSID88294686	M-H	C11H18O11	95,8	-1,0714	OS		
272	335,0946	0,59	166,3698	932	36	261	136	248	248	113	90	46	CSID167842	M+Na	C11H20O10	95,2	-0,8225	OS		
273	583,1820	1,14	236,0429	284	0	0	0	1	2	0	0	0	CSID9061499	M+Na	C21H36O17	92,3	-4,4081	OS	methyl	
274	439,1441	1,64	252,0239	992	0	0	0	3	11	79	1	2	CSID25034989	M+Na	C15H28O13	95,2	4,6593	OS		
275	738,2671	2,72	263,1440	41	0	15	0	59	136	836	32	56	CSID26331731	M+H	C27H47NO22	90,1	1,0938	OS	hepp	
276	713,2082	3,12	198,8001	79	0	0	1	1	25	1	0	0	CSID26332364	M+2Na-H	C24H44O21	96,3	-0,6235	OS		
277	1008,3619	0,53	289,9104	36	0	0	0	0	2	10	0	0	CSID26332387	M+NH4	C36H62O31	98,6	0,5629	OS		
278	659,2015	1,32	234,4390	107	0	0	0	1	0	0	2	34	CSID26332662	M+Na	C23H40O20	96,2	1,4906	OS		
279	659,1998	0,68	219,7579	122	1	27	7	52	15	17	6	2	CSID26332662	M+Na	C23H40O20	96,1	-1,0910	OS		
280	397,1338	0,81	244,3444	1114	0	2	0	8	16	76	1	6	CSID26332868	M+H-H2O	C15H26O13	92,8	-0,6409	OS		
281	867,2387	0,52	263,9871	40	1	10	5	41	67	139	9	9	CSID26332993	M+Na, M+K	C30H52O26	90,8	1,0298	OS		
282	885,3115	5,87	288,6560	33	0	0	0	1	0	0	0	0	CSID28499807	M+H	C33H56O27	92,8	3,7588	OS		oxirane
283	841,2587	4,03	273,6950	25	0	2	2	195	218	234	27	0	CSID28533191	M+2Na-H	C30H52O24	98,4	3,4205	OS		
284	790,2768	1,63	287,1447	18	0	0	0	0	0	0	0	27	CSID29368404	M+K	C29H53NO21	96,2	3,5022	OS		amine
285	379,1205	1,14	186,7627	1240	0	6	0	1	0	0	0	1	CSID30777082	M+Na	C13H24O11	93,4	-1,7337	OS		
286	703,2278	2,81	279,3730	62	0	0	0	0	1	24	0	0	CSID30777159	M+Na	C25H44O21	93,1	1,6643	OS		

287	365,1046	0,59	173,4671	1190	635	2129	304	152	292	93	698	432	CSID30777338	M+Na	C12H22O11	92,4	-2,3360	OS		
288	451,1425	0,79	201,4858	1113	10	92	4	38	223	114	31	7	CSID30845659	M+Na	C16H28O13	92	0,6327	OS		
289	701,2123	1,18	239,5842	17	88	3492	409	8359	13	11	26	183	CSID30984577	M+Na, M+K	C25H42O21	97,5	1,8351	OS		
290	595,2097	6,16	235,7741	260	0	2002	0	662	0	147	0	284	CSID31150582	M+H	C21H38O19	94,6	2,7889	OS	hepp	
291	307,1017	1,63	251,3634	914	0	2	0	16	35	189	12	12	CSID35035383	M+H-H2O	C12H20O10	97,1	-2,0084	OS		
292	347,0954	0,98	174,0684	716	265	6791	905	12134	16409	16699	19369	7702	CSID57621546	M+Na	C12H20O10	95,9	1,5983	OS		
293	349,1116	3,48	252,3974	872	0	0	0	3	2	25	0	0	CSID58145306	M+Na	C12H22O10	97,5	3,1496	OS		
294	629,1895	1,12	223,2589	158	1	89	2	109	9	10	1	9	CSID58837749	M+Na	C22H38O19	93	-0,7199	OS		
295	706,2402	3,37	251,5286	63	0	0	0	37	1	26	0	0	CSID64808523	M+H-H2O	C26H45NO22	93,1	0,1346	OS		amine
296	886,3051	0,60	307,8353	15	0	0	0	0	0	0	0	0	CSID64808579	M+H	C32H55NO27	95,3	1,8434	OS		amine
297	960,3397	1,43	303,4008	16	0	0	0	0	0	11	0	0	CSID76963250	M+NH4	C35H58O29	97,6	-0,5027	OS		
298	1055,3267	0,95	177,6899	10	9	0	198	0	3	0	0	0	CSID76963259	M+Na	C38H64O32	98,4	-0,5044	OS		
299	1015,3127	4,91	302,5608	6	0	0	0	308	265	941	40	1	CSID76963261	M+H-H2O	C38H64O30S	99,3	-4,1685	OS		thio
300	1015,3157	4,80	309,0039	12	0	0	0	37	34	80	0	0	CSID76963261	M+H-H2O	C38H64O30S	96,9	-1,3032	OS		thio
301	1097,3386	1,32	330,6674	3	0	10	0	4	33	28	3	5	CSID76963268	M+NH4, M+Na	C40H66O33	98,6	0,6960	OS		
302	1097,3385	1,88	330,6674	8	0	18	0	29	50	3	2	4	CSID76963268	M+Na	C40H66O33	94	0,6272	OS		
303	365,1071	4,51	230,5170	1292	2	355	2	177	0	0	0	0	CSID88294106	M+Na	C12H22O11	95,6	4,8895	OS		
304	497,1473	0,66	203,1303	160	8	295	59	293	51	40	37	42	CSID103885474	M+Na, M+K	C17H30O15	97,4	-0,7991	OS		
305	965,2972	2,30	281,0971	20	17	1895	76	4493	0	8	0	7	CSID107447694	M+Na	C35H58O29	97,6	1,7184	OS		
306	649,2191	0,61	264,9314	207	0	0	0	1	0	6	0	0	CSID26332545	M+H-H2O	C24H42O21	95,9	0,7239	OS		
307	109,0290	3,09	122,6212	83	0	40	1	25	10	10	6	3	289	M-H	C6H6O2	93,3	-4,4647	phenol	simple	
308	179,0339	3,03	131,8655	5	0	1	0	11	2	13	3	5	1549111	M-H	C9H8O4	99	-6,2526	phenol	acid	
309	181,0134	3,20	126,5706	39	0	8	0	13	0	8	2	8	CSID11319	M-H	C8H6O5	96	-4,7167	phenol	acid	
310	207,0653	3,96	143,2963	206	0	0	0	1	1	7	11	19	CSID13505	M-H2O-H	C11H14O5	93,8	-4,4939	phenol	gallate	
311	137,0237	3,32	129,9514	83	0	1	0	4	0	9	4	19	CSID64111	M-H	C7H6O3	95,2	-4,8727	phenol	aldehyde	
312	177,0548	5,58	131,9940	143	0	0	0	0	0	5	53	127	CSID136756	M-H2O-H	C10H12O4	94,5	-4,8170	phenol	hydroxy-tyrosol	
313	177,0549	5,39	134,6026	256	0	22	0	11	0	13	123	234	CSID136756	M-H2O-H	C10H12O4	94	-4,3687	phenol	hydroxy-tyrosol	
314	179,0341	5,61	131,8655	105	0	71	0	103	3	88	42	77	CSID4946686	M-H	C9H8O4	96,3	-4,7821	phenol	acid	
315	359,1119	5,57	183,1618	312	0	100	0	74	0	17	13	44	CSID10242997	M-H2O-H	C19H22O8	90,5	-4,5793	phenol	cyclic	
316	595,1659	1,03	237,4895	139	0	0	0	0	0	6	1	1	CSID10259084	M-H2O-H	C27H34O16	95,8	-1,6006	phenol	sugar	
317	167,0342	3,33	187,4799	98	0	10	0	3	0	0	0	0	CSID14032650	M-H	C8H8O4	96	-4,8823	phenol	gallate	
318	161,0235	4,66	130,5160	79	0	0	0	0	2	6	13	10	CSID15588232	M-H2O-H	C9H8O4	91	-4,9720	phenol		
319	255,0501	1,28	154,2490	87	0	0	0	12	0	3	0	0	CSID17250122	M+FA-H	C10H10O5	96,8	-4,5028	phenol	naphtyl	
320	239,0552	1,59	146,9861	175	0	2	0	67	13	62	25	40	CSID18845111	M+FA-H	C10H10O4	96,7	-4,4940	phenol	gallic glucoside	
321	365,1078	0,70	177,4946	679	0	88	1	120	0	10	0	2	CSID20165268	M-H2O-H	C14H24O12	96,6	-2,8227	phenol	acid	
322	205,0133	4,09	132,9511	35	0	0	0	5	0	0	0	0	CSID20167396	M-H2O-H	C10H8O6	93,8	-4,0330	phenol	acid	
323	299,0913	6,81	171,4022	573	0	0	0	1	0	12	3	229	CSID23207241	M-H	C17H16O5	93,8	-3,9064	phenol	calcone	
324	219,0289	3,42	140,0452	65	0	0	0	0	0	0	0	5	CSID23258021	M-H2O-H	C11H10O6	90,5	-4,1498	phenol	acid	
325	403,1380	6,15	198,6455	306	0	112	0	133	0	37	61	192	CSID23275381	M-H	C21H24O8	97,8	-4,6890	phenol	complex	
326	787,2501	2,44	261,0651	13	0	0	0	0	0	28	0	0	CSID24619262	M-H	C31H48O23	92,1	-1,6528	phenol	sugar	
327	641,1925	4,71	233,7923	58	0	1	0	1	0	3	0	0	CSID24620764	M+FA-H	C24H36O17	95,5	-1,6559	phenol	sugar	
328	709,2186	3,24	253,2679	33	0	0	0	3	5	17	0	0	CSID24643621	M+FA-H	C28H40O18	93,1	-1,5504	phenol	sugar	
329	315,0861	6,91	176,3061	545	0	0	0	1	0	11	3	128	CSID24647406	M-H	C17H16O6	95,4	-4,1070	phenol	tricyclic	
330	311,0761	1,81	165,5591	229	0	0	0	3	5	36	0	3	CSID24648290	M+FA-H	C13H14O6	95,2	-4,2474	phenol	chromenone	
331	235,0601	3,48	147,1683	96	0	0	0	1	1	6	26	30	CSID24694984	M-H	C12H12O5	94,9	-4,7371	phenol		
332	283,0814	3,13	163,8576	148	0	0	0	7	3	19	2	4	CSID24698381	M-H	C13H16O7	97,7	-3,3427	phenol	sugar	
333	377,1224	5,15	188,1812	263	0	16	0	29	2	18	8	13	CSID24705645	M-H	C19H22O8	93,7	-4,8687	phenol	stilbene	
334	257,0651	0,89	148,8560	66	0	0	0	2	1	7	1	4	CSID24710929	M-H	C15H14O2S	90	3,7431	phenol	thio	
335	299,0762	2,05	163,2739	196	0	0	0	0	0	9	2	0	CSID24717198	M-H	C13H16O8	90,8	-3,5626	phenol	sugar	
336	495,1671	1,80	219,1781	412	0	0	0	0	0	0	0	0	CSID24842827	M+FA-H	C26H26O7	96,8	2,2950	phenol		
337	421,1129	5,65	189,8142	375	0	35	0	52	0	2	0	4	CSID24843088	M+FA-H	C19H20O8	98,3	-2,9692	phenol	quinone	
338	253,0704	2,94	154,3335	49	0	0	0	1	1	8	9	19	CSID26378315	M-H2O-H	C12H16O7	97,6	-4,8568	phenol	sugar	
339	315,0710	2,39	170,8442	280	0	19	0	12	0	2	0	0	CSID28491505	M-H	C13H16O9	90,9	-3,5979	phenol	gallic sugar	
340	445,1123	5,57	197,6092	487	0	4	0	21	0	2	1	4	CSID28497556	M-H	C22H22O10	90	-3,8324	phenol	dimer	
341	237,0394	5,73	147,0774	53	0	16	0	34	0	31	2	23	CSID29417418	M-H	C11H10O6	96,6	-4,5042	phenol	chromenone	
342	195,0291	3,31	133,4967	68	0	15	0	44	2	26	12	17	CSID30778482	M-H	C9H8O5	92,6	-4,1122	phenol	acid	
343	301,0556	2,38	165,9023	171	0	0	0	3	2	21	0	0	CSID30778511	M-H	C12H14O9	93,7	-2,8636	phenol	sugar	
344	857,2773	0,60	275,1446	7	0	0	0	0	0	0	0	0	CSID30786096	M+FA-H	C30H52O25	91,1	-0,7885	phenol	sugar	
345	929,2974	0,63	277,2826	7	0	0	0	1	0	1	0	0	CSID30791599	M-H2O-H	C41H56O25	92,5	4,3351	phenol	sugar	
346	377,1080	3,82	219,3405	607	0	12	1	43	310	373	171	25	CSID31115248	M+FA-H	C14H20O9	99,1	-2,7693	phenol	sugar	

347	347,0763	3,05	175,2825	402	0	0	0	7	0	4	1	7	CSID31125638	M+FA-H	C16H14O6	94,3	-3,1568	phenol	chalcone	
348	281,0658	2,89	158,5566	139	0	1	0	19	17	58	101	129	CSID31128884	M+FA-H	C12H12O5	92,8	-3,7771	phenol	chromenone	
349	363,0910	1,51	194,1647	560	0	0	0	1	0	8	0	0	CSID34251929	M+FA-H	C17H18O4S	98,5	0,6588	phenol	thio	
350	363,1071	5,21	177,5509	324	0	17	0	33	0	9	2	14	CSID34448447	M-H	C18H20O8	92,3	-4,0512	phenol	vanillic	
351	495,1648	6,24	219,1781	314	0	338	0	141	0	20	19	96	CSID58115060	M-H	C27H28O9	96,6	-2,5761	phenol		
352	337,1066	6,54	189,3933	586	0	60	0	53	0	27	11	116	CSID58837470	M-H2O-H	C20H20O6	97	-4,4253	phenol	tetraphene	
353	941,2765	5,67	304,6846	3	0	0	0	1	1	63	1	0	CSID58859723	M-H2O-H	C45H52O23	92	4,6218	phenol	trimer	sugar
354	509,1805	6,18	218,8825	299	0	15	0	35	0	28	39	65	CSID58967839	M-H2O-H	C28H32O10	95,1	-2,1653	phenol	dimer	
355	625,1612	1,33	231,1532	67	0	0	0	0	0	1	0	0	CSID58979027	M-H	C37H26N2O8	91,5	-0,7117	phenol	amide	
356	225,0758	5,22	150,3018	104	0	53	0	74	2	6	0	0	CSID65727490	M-H	C11H14O5	98,9	-4,4201	phenol		
357	315,0861	5,21	179,0540	543	0	23	0	39	1	10	13	43	CSID74851586	M-H2O-H	C17H18O7	95,4	-4,0128	phenol	stilbene	
358	335,0399	0,93	164,8011	195	0	0	0	15	0	0	0	0	CSID74851669	M-H	C15H12O9	97,9	-2,7230	phenol	chalcone	
359	551,1896	6,36	232,4806	184	0	162	0	89	0	45	59	238	CSID76765780	M-H	C30H32O10	92,8	-4,7629	phenol	trimer	
360	411,1285	3,95	192,8415	372	0	1	0	3	0	1	0	0	CSID76962639	M+FA-H	C16H20N3O7-	97,4	-1,0563	phenol	quinoline	
361	741,2743	6,01	264,7047	41	0	125	0	77	0	0	0	0	CSID78439066	M-H2O-H	C38H48O16	92,4	-2,7681	phenol	anthraquinone	sugar
362	899,2859	0,77	213,2530	30	0	0	0	2	0	1	0	0	CSID88294154	M+FA-H	C39H50O21	98,8	3,7876	phenol	dimer	sugar
363	295,0822	1,27	166,1151	307	0	0	0	0	0	1	0	2	CSID90628977	M+FA-H	C13H14O5	97,5	-0,4364	phenol	chromenone	
364	507,2003	6,28	224,6790	244	0	42	0	22	0	7	0	31	CSID90633377	M+FA-H	C28H30O6	94,7	-4,6294	phenol		
365	223,0601	3,00	147,7463	30	0	0	0	1	0	6	6	7	CSID90670598	M-H2O-H	C11H14O6	97,3	-4,7294	phenol		
366	221,0802	4,98	147,5306	596	0	0	0	0	0	0	15	66	CSID65135	M+H-H2O	C12H14O5	93,7	-2,4558	phenol	acid	
367	625,1945	3,19	235,1298	198	0	27	0	28	63	108	4	3	CSID145391	M+H-H2O	C32H34O14	98	4,4539	phenol	sugar	
368	189,0652	3,36	136,5356	659	0	0	0	0	0	0	6	90	CSID212694	M+H-H2O	C10H10N2O3	96,9	-3,1647	phenol	imidazole	
369	210,0754	0,74	142,9566	567	0	3	0	3	2	11	11	13	CSID441917	M+H	C10H11NO4	97,3	-3,1483	phenol	amide	
370	210,0756	1,65	145,5592	565	0	9	0	19	6	54	26	92	CSID526422	M+H	C10H11NO4	93	-2,4478	phenol	amide	
371	180,1013	3,01	134,5883	1163	0	2	0	6	1	6	21	67	CSID2033322	M+H	C10H13NO2	94,9	-3,1936	phenol	quinoline	
372	217,0853	6,57	139,9690	603	0	0	0	0	0	1	4	54	CSID8418590	M+H-H2O	C13H14O4	91,4	-2,5351	phenol		
373	339,1043	2,34	177,0827	452	0	33	0	9	0	0	0	2	CSID10254186	M+Na	C14H20O8	98	-2,2791	phenol	vanillic	sugar
374	315,1216	4,62	175,2463	1042	0	16	0	64	0	3	4	16	CSID11704719	M+H	C18H18O5	99,4	-3,4357	phenol	chalcone	
375	208,0960	1,43	143,0750	881	0	0	0	0	0	0	6	56	CSID14576786	M+H	C11H13NO3	95,9	-3,9480	phenol	acrylamide	
376	259,0784	1,28	153,4617	196	0	10	0	31	11	13	1	1	CSID14908572	M+H-H2O	C15H16O3S	98,2	-0,9633	phenol	thio	
377	361,1117	0,64	245,7553	785	0	0	0	0	3	25	0	1	CSID17215958	M+H	C15H20O10	95	-3,5100	phenol	sugar	
378	455,1667	6,98	195,7216	129	0	96	0	63	0	39	0	54	CSID17241798	M+NH4, M+Na	C23H28O8	90,1	-2,0372	phenol	naphtalene	
379	417,1517	4,95	193,9762	865	5	235	0	87	1	3	2	19	CSID17769424	M+H	C18H20N6O6	98,6	0,0106	phenol	purine	
380	433,1466	5,80	204,8460	803	0	70	0	2	0	1	0	13	CSID20151407	M+Na	C20H26O9	90,1	-0,8104	phenol	chlorogenic	
381	363,1409	6,54	178,9951	477	406	591	528	372	459	160	619	181	CSID21379031	M+Na	C17H24O7	90,2	-1,4210	phenol	sugar	
382	480,1409	1,86	212,1594	784	1	149	5	528	816	1637	388	326	CSID23134182	M+K	C24H27NO7	96	-2,2436	phenol	acrylamide	
383	207,0642	5,16	135,4148	592	0	0	0	0	0	0	1	72	CSID23209631	M+H	C11H10O4	92,5	-4,7433	phenol	acid	
384	431,1171	4,70	187,9860	974	3	115	7	319	264	565	227	155	CSID23326458	M+H-H2O	C18H24O13	96,8	-2,9856	phenol	sugar	
385	417,1538	6,76	265,1324	1172	0	0	0	0	0	0	0	0	CSID23340712	M+H	C22H24O8	90,2	-1,4152	phenol		
386	659,2311	5,14	246,4053	125	28	1676	2	1193	15	59	9	5	CSID24645029	M+Na	C31H40O14	94,9	0,1088	phenol	sugar	
387	413,1559	6,30	284,1828	685	0	11	0	23	0	14	4	16	CSID24670996	M+Na	C21H26O7	91,3	-3,0046	phenol	cyclic	
388	491,1677	6,60	238,3402	831	0	157	0	168	0	30	0	73	CSID24700120	M+Na	C26H28O8	96,1	0,2033	phenol	tricyclo	
389	353,0840	4,25	184,8623	634	3	131	5	93	5	7	4	8	CSID24700703	M+Na	C14H18O9	92,2	-1,0012	phenol	sugar	
390	481,1499	0,69	197,8647	752	0	19	18	87	4	1	0	0	CSID24715727	M+H-H2O	C26H26O10	93,6	1,2421	phenol	trimer	
391	421,1640	6,06	225,5554	1251	0	185	0	195	0	4	0	10	CSID24842497	M+H	C25H24O6	92,9	-1,2545	phenol		
392	551,1574	2,89	222,0214	435	0	8	0	11	31	25	8	5	CSID24842659	M+H-H2O	C29H28O12	93,6	4,5966	phenol	sugar	
393	217,0697	3,54	188,7223	179	0	1	0	10	7	85	12	13	CSID25031688	M+Na	C8H10N4O2	98,4	0,2727	phenol	amide	
394	888,2933	7,31	276,0375	7	157	249	173	179	188	89	278	192	CSID25050706	M+NH4, M+Na	C42H46O20	90,9	1,4330	phenol	sugar	
395	293,1007	7,52	242,9207	592	26	46	27	33	26	10	40	34	CSID25054347	M+H-H2O	C15H18O7	95,1	-4,0197	phenol	quinone	
396	361,1272	6,58	187,3643	916	0	0	0	0	0	0	0	9	CSID25936979	M+H-H2O	C19H22O8	97,8	-2,6773	phenol	oleuropeine	
397	431,1312	4,57	193,5722	178	147	2302	111	1630	118	201	87	51	CSID26347909	M+H-H2O, M+Na,	C20H24O9	93,7	-0,1307	phenol	stilbene	
398	339,1212	6,10	182,5919	1526	0	39	0	81	0	43	1	487	CSID26369952	M+Na	C18H20O5	95,7	2,9980	phenol		
399	313,1422	6,00	183,6010	1227	0	76	0	26	0	1	0	5	CSID26386783	M+H-H2O	C19H22O5	91,4	-3,7951	phenol	cyclic	
400	167,0698	4,77	127,9134	463	0	12	0	29	0	1	13	4	CSID26607169	M+H	C9H10O3	91,8	-2,9311	phenol		
401	637,2246	6,53	268,2895	164	0	493	0	63	0	1	3	12	CSID26607197	M+Na	C32H38O12	95,5	-1,5795	phenol	lignan	
402	405,0797	3,17	185,9573	811	0	4	0	73	106	105	69	13	CSID26632517	M+H-H2O	C24H14N4O2S	98,8	-1,8775	phenol	pteridine	
403	605,2203	7,31	232,5857	67	403	651	509	457	474	222	767	486	CSID26632985	M+H, M+Na, M+K	C28H38O13	90,5	-0,2302	phenol		
404	397,1258	6,13	177,9301	1267	4	5452	2	4628	1	448	10	1003	CSID28643083	M+Na	C20H22O7	96,3	-0,0071	phenol		
405	701,2422	5,89	260,7814	78	0	122	0	85	1	21	478	75	CSID28661815	M+2Na-H	C31H44O15	95	4,6168	phenol	dimer	
406	871,2621	5,43	273,1985	34	0	0	0	0	2	15	0	0	CSID28663840	M+H	C42H46O20	90,4	-3,9226	phenol	trimer	

407	166,0857	2,09	130,5253	819	0	0	0	0	0	1	6	36	CSID29212142	M+H	C9H11NO2	94,9	-3,4144	phenol	amine
408	373,1259	5,09	192,5534	348	31	2163	1	472	3	47	45	160	CSID31107281	M+Na, M+K	C18H22O7	90	0,3685	phenol	stilbene
409	737,2689	5,86	263,1627	36	21	2677	2	1194	0	14	0	0	CSID31121492	M+H	C42H36N6O7	96,4	-3,9192	phenol	hexamer
410	357,1310	6,36	187,5033	1213	0	5	0	8	0	24	47	475	CSID31128872	M+Na	C18H22O6	96,1	0,5693	phenol	
411	720,5118	7,37	269,6636	4	51	82	68	56	63	27	100	56	CSID34999446	M+Na	C47H69O4-	96	3,4751	phenol	hydrocarbon
412	209,0802	2,37	140,4279	627	0	4	0	12	0	6	5	2	CSID35015217	M+H-H2O	C11H14O5	93,5	-2,5892	phenol	
413	296,1123	1,38	162,4755	462	0	0	0	0	0	66	0	62	CSID35516676	M+NH4	C14H14O6	93,6	-2,1020	phenol	chromene
414	581,1973	5,58	236,0879	309	0	85	0	64	0	4	3	4	CSID58859132	M+2Na-H	C27H36O11	92,6	0,6013	phenol	
415	539,1896	5,39	225,2337	579	4307	67985	2403	57763	462	1792	93	228	CSID58921311	M+H	C29H30O10	97,7	-2,9209	phenol	
416	931,2875	3,70	294,2611	8	0	1	0	4	30	29	0	0	CSID59006972	M+H	C44H50O22	94	0,9558	phenol	trimer
417	166,0857	0,96	130,5253	819	0	0	0	0	0	11	50	223	CSID60762937	M+H	C9H11NO2	94,9	-3,5144	phenol	amine
418	167,0699	4,54	127,9134	462	0	5	0	22	0	2	23	9	CSID62896357	M+H-H2O	C9H12O4	96,7	-2,2723	phenol	
419	329,1007	6,93	185,7477	1045	0	0	0	0	0	0	0	3	CSID74851995	M+Na	C16H18O6	94,1	3,5874	phenol	
420	537,1753	3,38	213,6319	447	0	6	0	17	4	2	1	1	CSID74886633	M+H	C29H28O10	98,7	-0,4844	phenol	
421	347,2009	1,52	174,0647	248	0	5	0	19	51	59	42	7	CSID76745261	M+H-H2O	C24H28O3	97,1	0,9650	phenol	stilbene
422	321,0940	4,66	164,1893	372	6	249	8	279	25	57	101	80	CSID90659494	M+Na	C14H18O7	95,3	-1,4456	phenol	sugar
423	163,0394	5,25	130,3656	211	0	71	0	119	3	64	12	37	CSID4451098	M-H	C9H8O3	95,3	-4,3470	phenyl	acid
424	295,1012	0,81	182,5521	431	0	0	0	0	0	0	0	0	CSID14950152	M-H	C15H20O4S	95,4	0,8507	phenyl	thio-sugar
425	265,0703	3,55	156,5043	70	0	0	0	17	2	21	32	49	CSID18540259	M-H2O-H	C9H12N6O5	90,3	4,2699	phenyl	acid
426	239,0550	0,99	146,9861	43	0	0	0	14	2	22	3	6	CSID20127257	M-H	C11H12O6	92	-4,7269	phenyl	acid
427	317,0655	6,61	168,0639	427	0	8	0	0	0	0	0	0	CSID23154097	M+FA-H	C15H12O5	90,1	-4,3280	phenyl	tricyclic
428	385,0917	6,89	193,5294	431	0	0	0	2	0	8	0	33	CSID23237714	M+FA-H	C19H16O6	96,7	-3,4849	phenyl	benzoic
429	395,1181	1,90	215,9188	677	0	0	0	2	18	58	2	1	CSID23297032	M+FA-H	C18H22O5S	91,4	3,0398	phenyl	thio-sugar
430	824,5869	6,27	306,2189	4	2	0	9	0	13	0	6	0	CSID24643366	M+FA-H	C45H81NO9	95	-3,0876	phenyl	amine
431	343,1170	5,26	186,4171	426	0	23	1	62	1	12	5	16	CSID24704446	M-H	C19H20O6	99,3	-4,9212	phenyl	
432	451,1041	0,68	194,6788	229	0	7	2	5	39	5	2	0	CSID24844358	M-H2O-H	C24H22O10	93,2	1,4390	phenyl	sugar
433	373,0911	5,25	191,0767	216	0	7	0	26	0	35	16	96	CSID30777034	M-H2O-H, M-H	C19H18O8	95,2	-4,6364	phenyl	
434	513,1759	5,99	210,2438	284	0	189	2	176	2	28	7	12	CSID58131499	M+FA-H	C26H28O8	94,7	-1,5753	phenyl	cyclic
435	653,1936	3,53	245,2913	53	0	0	0	0	0	0	2	0	CSID90659289	M+FA-H	C25H36O17	95,1	0,3046	phenyl	sugar
436	653,1920	5,62	269,1118	69	0	0	0	1	0	19	1	0	CSID58837450	M+FA-H	C25H36O17	93,3	-2,3787	phenyl	sugar
437	165,0540	4,23	130,6062	415	0	0	0	0	1	10	55	256	CSID67224	M+H-H2O	C9H10O4	92,8	-3,1790	phenyl	acid
438	175,1111	7,15	137,5244	640	39	52	51	36	48	22	66	40	CSID71995	M+H-H2O	C12H16O2	90	-3,3113	phenyl	acid
439	147,0437	1,75	132,1622	195	0	5	0	9	0	2	0	0	CSID133480	M+H-H2O	C9H8O3	91	-2,0504	phenyl	acid
440	148,0753	2,09	126,9587	743	0	0	0	0	0	0	7	70	CSID134096	M+H-H2O	C9H11NO2	91,9	-2,5630	phenyl	amide
441	193,0853	4,72	141,4297	799	1	70	0	18	1	6	9	44	CSID10528124	M+H-H2O	C11H14O4	97,1	-2,8866	phenyl	acid
442	149,0596	6,21	145,0162	403	0	0	0	1	0	0	0	0	CSID11410177	M+H-H2O	C9H10O3	96,4	-0,6665	phenyl	mandelic acid
443	474,1810	1,27	215,2121	1055	0	0	0	2	4	34	2	3	CSID13142646	M+K	C25H29N3O4	97,5	4,6298	phenyl	amide
444	146,0596	4,27	134,8369	386	0	0	0	0	0	0	15	60	CSID13413874	M+H-H2O	C9H9NO2	96,7	-2,6981	phenyl	amide
445	195,0647	3,44	138,7139	486	0	0	0	3	0	2	8	37	CSID16740223	M+H-H2O	C10H12O5	96,9	-2,0643	phenyl	
446	280,0964	0,01	163,1500	851	299	356	393	232	314	153	528	328	CSID17923124	M+H-H2O	C17H15NO4	94,1	-1,4198	phenyl	amide
447	210,1118	1,22	145,5570	1034	0	0	0	0	1	3	14	57	CSID20100682	M+H-H2O	C11H17NO4	97,4	-2,8531	phenyl	amine
448	337,1867	3,28	179,9007	82	0	0	0	0	3	19	140	638	CSID23201688	M+H, M+Na	C16H24N4O4	90,3	-0,9206	phenyl	amide
449	297,1124	5,87	165,1164	1154	0	1	0	0	0	0	0	15	CSID23226256	M+H-H2O	C18H18O5	93,9	0,7686	phenyl	
450	297,1111	5,09	170,5222	1220	0	3	0	2	0	0	0	9	CSID23226256	M+H-H2O	C18H18O5	914	-3,3364	phenyl	
451	667,2054	4,21	237,2543	113	0	11	0	24	76	109	2	0	CSID23228441	M+H-H2O	C35H32N4O11	90,7	2,7304	phenyl	purine
452	173,0588	6,57	137,6802	328	0	0	0	0	0	0	1	3	CSID23252884	M+H-H2O	C11H10O3	93,3	-4,7945	phenyl	naphtalene
453	224,0909	1,18	142,1639	717	0	0	0	0	2	11	17	52	CSID23262678	M+H	C11H13NO4	98,1	-3,5125	phenyl	amide
454	345,1319	5,18	185,1466	1086	0	8	0	17	0	6	2	22	CSID23320289	M+Na	C17H22O6	98,6	3,1092	phenyl	sugar
455	341,1374	5,83	190,8834	1392	0	108	0	59	0	9	0	62	CSID24620226	M+H-H2O	C20H22O6	90,9	-2,6529	phenyl	naphtalene
456	493,1674	4,64	278,2684	726	0	0	0	0	0	0	5	1	CSID24621638	M+Na	C22H30O11	97,3	-1,2588	phenyl	sugar
457	683,2006	3,88	245,9277	72	0	2	0	4	2	0	0	0	CSID24687274	M+K	C36H32N6O6	98	-1,4571	phenyl	adenosine
458	333,0939	6,68	166,4401	515	5	87	10	53	7	28	13	4	CSID24785656	M+Na	C15H18O7	96,6	-1,8829	phenyl	sugar
459	437,1938	7,39	207,5929	1150	825	0	59	0	8	0	92	0	CSID26402926	M+Na	C24H30O6	93,3	0,7478	phenyl	
460	179,0696	6,20	137,2317	318	0	188	0	278	1	230	142	462	CSID31107037	M+H-H2O, M+H	C10H10O3	91,6	-3,5257	phenyl	
461	230,0803	3,48	147,0367	697	0	0	0	0	0	0	43	238	CSID31116307	M+H	C13H11NO3	93,8	-3,6616	phenyl	naphtalene
462	258,1116	3,83	156,1508	923	0	0	0	0	0	0	15	128	CSID31116310	M+H	C15H15NO3	95,6	-3,2232	phenyl	naphtalene
463	272,1276	4,49	160,8265	1106	0	0	0	0	0	0	4	52	CSID31116311	M+H	C16H17NO3	92,2	-1,9972	phenyl	naphtalene
464	234,1844	6,93	173,6350	511	21	41	27	28	22	15	37	13	CSID32684962	M+NH4	C15H20O	92,2	-3,7301	phenyl	naphtalene
465	611,2098	6,05	247,4219	207	0	53	0	29	0	48	3	133	CSID34249053	M+K	C27H40O13	90,8	-0,3437	phenyl	sugar

466	175,0745	5,41	132,3944	509	0	0	0	0	0	0	31	58	CSID37692118	M+H-H2O	C11H12O3	94,5	-4,5077	phenyl		
467	463,1575	4,56	209,7341	723	13	425	23	545	154	147	290	122	CSID58163619	M+Na	C21H28O10	95,2	0,0306	phenyl		
468	189,0901	6,04	144,3066	680	0	2	0	7	0	13	3	130	CSID58876663	M+H	C12H12O2	92,3	-4,8987	phenyl		
469	399,1416	6,24	200,1809	1143	0	1236	0	643	0	210	80	760	CSID58917271	M+Na	C20H24O7	97,1	0,5299	phenyl		
470	611,1801	2,42	247,4226	24	20	1163	56	3131	4668	8230	2014	1412	CSID58971355	M+Na, M+K	C35H28N2O7	95,9	2,1167	phenyl	amide	
471	275,0901	6,05	166,0647	226	0	0	0	0	0	81	4	898	CSID90650077	M+H-H2O, M+H	C15H14O5	90,4	-4,6995	phenyl	pyranone	
472	329,1585	8,08	202,7084	310	233	265	244	194	239	103	372	188	CSID90660067	M+H	C16H24O7	92,5	-3,0732	phenyl	sugar	
473	179,0695	5,34	132,1079	684	0	0	0	0	0	2	49	225	CSID103870852	M+H	C10H10O3	93,2	-4,1372	phenyl	acid	
474	252,1225	2,80	153,7922	709	0	0	0	0	0	0	10	45	CSID103874408	M+NH4	C13H14O4	94,6	-2,0916	phenyl	acid	
475	250,1439	7,97	165,2359	288	64	147	124	84	193	42	284	54	CSID23223258	M-H2O-H	C14H23NO4	92,4	-3,6832	piperidine		
476	381,1914	8,94	202,0714	359	95	209	183	126	271	54	428	69	CSID30825595	M-H2O-H	C21H28N4O4	90,2	-4,6156	piperidine		
477	261,1229	4,17	158,6660	1162	0	0	0	0	1	1	24	101	CSID26355881	M+H	C14H16N2O3	91,3	-1,8708	piperidine		
478	197,1279	4,38	141,1648	1055	0	0	0	1	2	11	72	217	CSID28300990	M+H-H2O	C10H18N2O3	95,4	-2,7621	piperidine		
479	197,1279	4,45	143,7635	1055	0	5	0	21	19	52	112	267	CSID30541022	M+H-H2O	C10H18N2O3	95,4	-2,7249	piperidine		
480	295,1648	4,47	170,6039	729	0	3	0	11	28	56	256	801	CSID30839660	M+H	C15H22N2O4	95,3	-1,3807	piperidine	phenyl	
481	819,2741	4,17	260,6382	14	0	32	0	29	0	1	0	0	CSID10227312	M-H2O-H	C39H50O20	90,3	2,8239	polyphenol	sugar	
482	363,1070	4,35	183,0455	346	0	25	0	12	0	4	6	17	CSID10404377	M+FA-H	C17H18O6	94	-4,9208	polyphenol		
483	675,2426	6,14	256,7667	73	0	51	0	38	0	8	0	0	CSID23339930	M-H	C37H40O12	99,2	-3,1124	polyphenol	dimer	
484	355,1171	6,51	200,0369	523	0	45	0	44	0	36	87	297	CSID24691019	M-H	C20H20O6	96	-4,4606	polyphenol		
485	989,3160	1,68	282,6543	29	0	0	0	0	0	0	0	3	CSID24710568	M+FA-H	C42H56O24	90,4	1,7313	polyphenol	sugar	
486	549,0863	1,91	218,0962	61	0	0	0	1	0	3	0	0	CSID24844865	M-H	C24H22O15	96,4	-4,2347	polyphenol	isoflavone	
487	483,1644	5,01	216,5727	361	0	1	0	4	0	0	0	1	CSID24846348	M-H2O-H	C26H30O10	93,3	-3,2351	polyphenol	glucoside	
488	305,0808	6,86	182,1738	345	19	44	38	25	61	14	89	4	CSID30791352	M-H2O-H	C19H16O5	98,2	-3,4282	polyphenol		
489	599,1821	1,48	231,5957	86	0	0	0	0	0	5	3	0	CSID31128729	M+FA-H	C35H26N2O5	90,5	-0,5252	polyphenol	indole	
490	707,2005	4,38	242,4637	65	0	1	0	5	49	103	0	1	CSID23339500	M+H-H2O	C36H36O16	95,7	4,7439	polyphenol	phenyl	sugar
491	579,1511	3,22	218,4791	338	0	16	0	70	1	35	0	0	CSID24647781	M+H-H2O	C30H28O13	90	2,2772	polyphenol		
492	565,1665	6,10	233,4814	378	0	225	0	185	0	146	0	735	CSID24844468	M+Na	C28H30O11	91,2	-2,8416	polyphenol	sugar	
493	797,2290	3,84	274,4566	23	0	0	0	0	4	4	0	0	CSID26380317	M+H-H2O	C39H42O19	92	0,3380	polyphenol	sugar	
494	319,1181	6,92	229,5089	800	0	0	0	0	0	0	0	0	CSID34258914	M+H	C17H18O6	98,1	1,4866	polyphenol		
495	764,2106	1,77	262,6661	23	0	117	0	105	0	0	0	0	CSID35031951	M+Na	C33H41O19+	92	-3,0163	polyphenol	sugar	
496	806,2148	3,40	280,5532	16	0	0	0	6	2	0	1	0	CSID59052837	M+NH4	C36H36O20	97,4	1,2406	polyphenol	dimer	sugar
497	1067,3291	1,44	321,2419	4	0	2	0	76	256	473	32	2	CSID59696251	M+H	C48H58O27	90	4,9412	polyphenol	dimer	sugar
498	765,2727	6,00	271,9216	54	1	1465	1	1338	0	33	0	2	CSID78439059	M+Na	C38H46O15	94,6	-0,2371	polyphenol	sugar	
499	163,0393	4,70	127,7676	209	0	2	0	5	2	17	22	32	CSID99219	M-H2O-H	C9H10O4	92,6	-4,3417	pyranone	maltol	
500	239,0555	1,23	149,6326	173	0	6	0	23	7	39	12	16	CSID15367651	M-H	C11H12O6	97,3	-2,4693	pyranone		
501	177,0548	6,21	137,2244	142	0	21	0	28	4	21	50	49	CSID20037401	M-H2O-H	C10H12O4	95,6	-4,6481	pyranone		
502	255,0500	0,72	148,9386	90	0	7	0	40	0	2	0	4	CSID21378038	M+FA-H	C10H10O5	98	-4,8993	pyranone		
503	225,0396	0,99	142,3728	116	0	37	9	249	73	100	29	29	CSID24691928	M-H	C10H10O6	94,4	-3,6548	pyranone		
504	255,0500	0,80	148,9386	90	0	6	0	40	0	4	0	2	CSID24701096	M+FA-H	C10H10O5	96,7	-4,7004	pyranone		
505	191,0342	5,45	136,3354	122	0	12	0	52	40	198	358	537	CSID24701096	M-H2O-H	C10H10O5	90,4	-3,6092	pyranone		
506	419,1185	4,72	229,7119	649	0	0	0	3	22	39	5	1	CSID24783244	M+FA-H	C16H22O10	92	-2,6318	pyranone	sugar	
507	305,0667	0,75	165,7629	308	0	0	0	3	0	1	0	0	CSID28505061	M-H	C15H14O7	97,8	0,1099	pyranone	phenyl	
508	389,1230	5,61	201,8450	454	0	73	0	158	8	79	65	70	CSID28517153	M-H2O-H	C20H24O9	96,3	-2,9218	pyranone	phenyl	
509	419,1184	3,27	218,1261	646	0	0	0	4	53	46	8	1	CSID29420015	M-H	C17H24O12	93,2	-2,5993	pyranone	sugar	
510	269,0659	2,54	156,3444	77	0	0	0	86	10	67	14	13	CSID57482821	M-H, M+FA-H	C11H12O5	91,8	-3,4174	pyranone	acid	
511	239,0550	4,44	149,6327	43	0	0	0	0	0	1	0	1	CSID76759102	M-H	C11H12O6	98,8	-4,7364	pyranone	acid	
512	508,3650	9,34	200,0223	75	40	19	35	29	27	13	59	24	CSID23109981	M+NH4	C29H46O6	95,9	3,4998	pyranone	fatty acid	
513	443,1158	4,15	187,6584	838	0	9	7	234	64	98	14	2	CSID29420015	M+Na	C17H24O12	97,1	-0,5136	pyranone	sugar	
514	443,1161	4,96	198,8724	873	0	35	0	8	36	154	16	62	CSID29420015	M+Na	C17H24O12	97,7	0,2517	pyranone	sugar	
515	194,1170	2,52	141,3613	1274	103	136	120	75	113	25	204	199	CSID14649465	M+H	C11H15NO2	97,2	-3,1006	pyridine	fatty acid	
516	216,1013	3,60	147,8170	911	1	0	2	0	0	1	74	187	CSID24626615	M+H	C13H13NO2	93	-2,6441	pyridine	phenol	
517	166,0859	1,65	135,6472	820	0	2	0	0	18	89	464	882	CSID32780200	M+H	C9H11NO2	94,8	-2,3218	pyridine		
518	176,0701	4,53	137,4525	747	0	0	0	0	0	2	268	1108	CSID34210599	M+H-H2O	C10H11NO3	91,5	-2,6988	pyridine		
519	182,0804	0,70	200,2366	684	0	0	0	0	0	20	0	1	CSID34244927	M+H	C9H11NO3	94	-4,0200	pyridine		
520	558,2021	4,40	221,8592	414	0	2	0	28	27	224	22	12	CSID59001605	M+NH4	C22H28N4O12	93,1	-3,7836	pyridine		
521	343,1165	6,55	183,6469	171	0	4	0	6	0	37	109	432	CSID28520124	M-H2O-H	C15H18N6O5	98,6	1,3558	pyrimidine	sugar	
522	399,1412	5,81	197,3451	1141	0	432	0	158	0	28	14	201	CSID23271221	M+H	C17H22N2O9	91,1	3,4625	pyrimidine		
523	433,1477	3,85	204,8460	182	570	8423	364	3660	53	21	21	29	CSID25065916	M+Na, M+K	C21H22N4O5	91	-1,3334	pyrimidine	phenyl	

524	471,1475	3,50	203,7928	848	1	199	1	63	0	0	0	0	CSID26640812	M+Na	C20H24N4O8	91,2	-2,5798	pyrimidine		
525	695,2015	4,51	239,6975	56	26	1302	303	8602	11854	22710	6462	1171	CSID58837497	M+2Na-H	C25H38N4O16	97,5	3,2006	pyrimidine	sugar	
526	221,1535	7,14	183,3388	29	34	53	76	32	164	15	208	27	CSID8761515	M-H2O-H	C12H23N3O2	93,4	0,7322	pyrrol		
527	373,1259	5,22	189,7494	982	86	2701	4	347	3	9	10	88	CSID30971114	M+K	C16H22N4O4	96,8	-4,1584	pyrrol		
528	228,0866	0,62	144,5398	55	0	34	0	390	32	1239	177	392	CSID2055368	M+H-H2O, M+H	C10H13NO5	94,7	-0,0852	pyrrole		
529	193,0968	0,93	138,8420	1054	0	0	0	24	17	70	144	346	CSID4604185	M+H-H2O	C10H14N2O3	94,6	-1,7888	pyrrole		
530	612,1833	2,95	250,4297	157	3	262	22	608	1073	1342	370	197	CSID23156579	M+K	C29H35NO11	94,3	-1,5194	pyrrole	sugar	phenol
531	471,1626	5,48	221,1220	719	29	558	7	399	4	15	1	6	CSID23301119	M+NH4	C21H19N5O7	95,1	0,6353	pyrrole		

Acknowledgements

At the end of these three years of PhD project, I would like to thank Prof Augusta Caligiani, who accompanied me in this path with her great patience and support.

I would like to acknowledge Soremartec Italia S.r.l., which funded the present PhD project, for giving me the opportunity to work on such an interesting topic. I would like to thank in particular my external tutors, Ginevra and Franco, for their help and for being always available.

I also want to thank the Flemish Institute for Technological Research (VITO), for allowing me to conduct part of my research in their laboratories, especially my external supervisor, Dr. Winnie Dejonghe.

About the author

Andrea Fuso was born on November 6th, 1994, in Parma (Italy). He performed his academic studies at the University of Parma obtaining both bachelor and master's degree in Food Science and Technology at the Food and Drug Department. After one year as research fellow in Food Chemistry at the same University, he started in 2019 the Ph.D. within the same research group, under the supervision of Prof. Augusta Caligiani. From April 2022 to July 2022, he worked as visiting researcher at Flemish Institute for Technological Research (VITO), Belgium, under the supervision of Dr. Winnie Dejonghe. He is author of scientific articles, published in ranked journals.

List of publications:

- Barbi, S.; Macavei, L.I.; **Fuso, A.;** Luparelli, A.V.; Caligiani, A.; Ferrari, A.M.; Maistrello, L.; Montorsi, M. Valorization of seasonal Agri-food leftovers through insects. *Sci Total Environ* 2020, 709, 136209
- **Fuso, A**.; Barbi, S.; Macavei, L.I.; Luparelli, A.V.; Maistrello, L.; Montorsi, M.; Sforza, S.; Caligiani, A. Effect of the rearing substrate on total protein and amino acid composition in black soldier fly. *Foods* 2021, 10, 1773
- **Fuso, A.**; Risso, D.; Rosso, G.; Rosso, F.; Manini, F.; Manera, I.; Caligiani, A. Potential valorization of hazelnut shells through extraction, purification and structural characterization of prebiotic compounds: A critical review. *Foods* 2021, 10, 1197
- Luparelli, A.V.; Leni, G.; **Fuso, A.**; Pedrazzani, C.; Palini, S.; Sforza, S.; Caligiani, A. Development of a Quantitative UPLC-ESI/MS Method for the Simultaneous Determination of the Chitin and Protein Content in Insects. *Food Anal. Methods* 2022.
- **Fuso, A.**; Rosso, F.; Rosso, G.; Risso, D.; Manera, I.; Caligiani, A. Production of xylo-oligosaccharides (XOS) of tailored degree of polymerization from acetylated xylans through modelling of enzymatic hydrolysis, *Food Research International*, 2022, 162, Part A, 112019.
- **Fuso, A.**; Viscusi, P.; Larocca, S.; Sangari, F.S.; Lolli, V.; Caligiani, A. Protease-assisted mild extraction of soluble fibre and protein from fruit by-products: a biorefinery perspective. *Foods,* 2023, 12(1), 148.
- **Fuso, A.**; Bancalari, E.; Castellone, V.; Caligiani, A.; Bottari, B.; Gatti, M. Feeding lactic acid bacteria with different sugars: effect on EPS production and their molecular characteristics. *Foods,* 2023, 12(1), 215.

- **Fuso, A.**; Dejonghe, W.; Cauwenberghs, L.; Rosso, G.; Rosso, F.; Manera, I.; Caligiani, A. DPPH radical scavenging activity of xylo-oligosaccharides mixtures of controlled composition: a step forward in understanding structure-activity relationship. *Journal of Functional Foods,* 2023.
- **Fuso, A.**; Righetti, L.; Rosso, F.; Rosso, G.; Manera, I.; Caligiani, A. A multiplatform metabolomics/reactomics approach as a powerful strategy to identify reaction compounds generated during hemicellulose hydrothermal extraction from agro-food biomasses (SUBMITTED).
- **Fuso, A.**; Viscusi, P.; Rosso, F.; Rosso, G.; Pedrazzani, C.; Caligiani, A. Hydrothermal treatment of hazelnut shells: impact of temperature on degradation compounds and fibre's structure (SUBMITTED).

Oral communications at International Congresses

- **Andrea Fuso**, Vincenzo Castellone, Elena Bancalari, Augusta Caligiani, Benedetta Bottari, Monica Gatti. Molecular characterization of exopolysaccharides from wild lactic acid bacteria strains fed with different sugar sources. EPNOE JUNIOR Conference, 03-04/02/2021.
- Veronica Lolli, **Andrea Fuso**, Pio Viscusi, Francesca Bonzanini, Giulia Leni, Augusta Caligiani. Characterization and valorization of fruit side streams as unconventional sources of functional ingredients. RAFA Conference, 06-09/09/2022. Prague (Czech Republic).

Poster communications at International Congresses

- **Fuso**, **A.**; Risso, D.; Rosso, G.; Rosso, F.; Manini, F.; Manera, I.; Caligiani, A. Continuous production of xylo-oligosaccharides of tailored degree of polymerization from agro-industrial by-products through optimization of enzymatic hydrolysis and tangential ultrafiltration. EFFoST Conference, 01-04/11/2021. Lausanne (Switzerland).
- **Fuso, A.;** Rosso, F.; Rosso, G.; Risso, D.; Manera, I.; Cauwenberghs, L.; Dejonghe, W.; Caligiani, A. Modelling of enzymatic hydrolysis for production of tailored polymerization degree xylo-oligosaccharides, and their bio-functional properties. Dietary Fibre Conference 2022, 16-18/10/2022. Leuven (Belgium).

- **Fuso, A.**; Sadovskaya, I.; Cauwenberghs, L.; De Rechter, P.; Caligiani, A.; Timmermans, K.; Robbens, J.; Grard, T.; Dejonghe, W. Enzymatic hydrolysis of ulvan into (oligo)saccharides and determination of their functional properties. EFTA 2022 CONFERENCE, 17-21/10/2022. Rotterdam, Netherlands.